UNCLASSIFIED

CF-54-1-81

REACTORS—POWER

UNITED STATES ATOMIC ENERGY COMMISSION

U-233 POWER-BREEDER REACTOR

Reactor Design and Feasibility Problem

By
R. R. Halik
L. H. Beckberger
J. M. Haibeck
J. E. Mealia
W. A. Northrop
D. R. Rees
W. A. Robba

January 1954

Oak Ridge School of Reactor Technology
Oak Ridge, Tennessee

Technical Information Service Extension, Oak Ridge, Tenn.

UNCLASSIFIED

OAK RIDGE SCHOOL OF REACTOR TECHNOLOGY

F. C. VonderLage, Director

Reactor Design and Feasibility Problem

"U-233 POWER-BREEDER REACTOR"

(Employing Techniques of Fluidized and Moving Beds and the Transportation of Solids by Gases)

Prepared by:

R. R. Halik, Group Chairman

L. H. Beckberger

J. M. Haibeck

J. E. Mealia

W. A. Northrop

D. R. Rees

W. A. Robba

PREFACE

The authors of this report were students in the 1951-52 session of the Oak Ridge School of Reactor Technology. After nine months of formal study of reactor technology they undertook the preliminary design which is reported here. Its purpose was primarily that of an opportunity for each of them to apply in a specific but representative case the principles and technology which the Oak Ridge School of Reactor Technology attempts to impart.

Because this is a report made by seven people after ten weeks study (including time of preparation of the report), it can hardly be either complete or be guaranteed free of errors in judgment. Our knowledge of the authors allows us to judge that they would first insist on this as a condition under which the report is presented. Withal, the faculty here records its great pride in the authors.

As noted elsewhere, several members of the Oak Ridge National Laboratory gave valuable assistance. To the authors' gratitude for this the faculty would adjoin its own. In particular, the group's advisor, R. B. Briggs, gave sagacious counsel and welcome encouragement. The faculty herewith acknowledges its debt to him.

F. C. VonderLage

for

The Faculty of ORSORT

ACKNOWLEDGEMENT

The authors would like to take this opportunity to thank the various people at ORNL who kindly gave their advice and assistance during the preparation of this report. We would like to give special thanks to our group advisor, R. B. Briggs for his support throughout the summer and the ORSORT faculty for their general interest and encouragement. We would also like to express our appreciation to Dr. Visner for his assistance and guidance with nuclear calculations and F. L. Steahly, P. Agron, D. E. Ferguson, A. T. Gresky, R. E. Leuze, and R. W. Stoughton for their advice on chemical formulations and processing. In addition we would like to express our appreciation to Theodore Stern for his assistance with the reading of the report.

TABLE OF CONTENTS

LIST OF TABLES

LIST OF FIGURES

ABSTRACT

The fluidized solids technique, used so extensively in the petroleum and chemical industries, has been investigated for possible adaptation to nuclear power-breeder reactors. This report represents the first attempt to analyze such a system and, surprisingly, shows that the technique is extremely attractive.

The authors have looked at several designs and present detailed engineering and nuclear calculations on the design they consider to have the greatest promise as a breeder-reactor for a large electric power station. Basically, the design calls for the circulation of solid particles consisting of a fuel-moderator mixture, from the core to a separate heat exchanger vessel from which the solids flow freely to and through the core by gravity. Argon, at essentially atmospheric pressure is recommended as the gas to be used in circulating the solids and fluidizing them in the heat exchanger. The blanket, consisting of solid particles of moderator and fertile material (Th-232), is separated from the core region by means of a graphite shell and is fluidized by a separate gas stream.

Many advantages of this system over other existing or proposed systems are listed. Foremost among these are the high breeding gain obtainable, utilization of basic engineering principles presently in use in industry, and the ability to produce steam at pressures and temperatures comparable to those presently available to the power industry.

Nuclear calculations were made using an elaborate 2-group 2-region method. A typical system, operating at 250 MW (heat output) and producing over 80 MW electrical power, requiring a 10.5 foot (diameter) core, a 3-foot thick blanket, and 48 Kg. of U-233 in the core proper, is discussed.

Additional holdup of fuel in the heat exchanger and blanket brought the total fuel inventory to somewhat less than 200 Kg. Breeding gains of over + 0.2 were calculated even after consideration was given to the poisons, leakage, and core shell absorption.

The authors finally conclude that the fluidized solids reactor appears to be feasible and recommend that additional work be done, especially

(1) In obtaining pertinent experimental data

(2) In making a detailed cost analysis

(3) In investigating the nuclear aspects of this system

I. INTRODUCTION

1.0 Need for Power-Breeder Reactors

The future of the atomic energy industry beyond the realm of weapons appears to depend upon the development of nuclear reactors which simultaneously generate heat at thermodynamically efficient temperaturesand produce nuclear fuel more rapidly than they consume it. Such reactors are called "power converters" or "power breeders". A converter is a reactor which consumes one type of fuel and produces another, e.g. consumes U-235 to produce Pu-239. A breeder, on the other hand, produces the same type of fuel that it consumes. It is said to operate with a "positive breeding gain" if its net production exceeds its consumption.

The importance of breeders arises from the fact that of the three fissionable nuclides, U-233, U-235 and Pu-239, the only one occurring naturally is U-235 and it constitutes only0.7% of natural uranium. The remainder (99.3%)of natural uranium is U-238. The non-fissionable abundant isotope, Th-232, and the abundant isotope of uranium, U-238 can be converted by transmutation followed by two successive beta disintegrations into the fissionable isotopes U-233 and Pu-239 respectively. Breeders employing Pu-239 as fuel in combination with U-238 as fertile material can be used to convert all the U-238 to Pu-239 and hence ultimately to useful energy. Similarly, breeders employing U-233 as fuel with thorium as the fertile material can be used to convert the entire supply of thorium into a source of energy.

According to surveys made by the Atomic Energy Commission, there exists a world reserve of 25 million tons of uranium and 1 million tons of thorium recoverable for less than $100. per pound. Of this supply about one and

one-half million tons of uranium ore is recoverable at a cost of $50. per pound or less.[54] On this basis a production rate of 10,000 tons per year can be maintained for a few hundred years without exceeding the $50. a pound cost. Table I-1 lists the uranium resources available to the United States, as estimated by J. R. Menke.[55]

TABLE I-1

URANIUM RESOURCES AVAILABLE TO THE UNITED STATES[55]

CONCENTRATION	POUNDS	DOLLARS PER POUND	ENERGY AVAILABLE Q UNITS (10^{18} BTU)
1%	10^7	5	.3
.1%	10^8	10	3.3
.01%	10^9	50	33
.001%	10^{10}	500	330

The total U-235 content of the few rich deposits now known is of minor importance in relation to the total energy requirements of the world. This supply may be increased by a factor between 3 and 10 by the use of present day converters. On the other hand a successful breeder using Pu-239 and U-238 can make utilizable as fuel the entire available supply of natural uranium. This would result in an energy production 140 times that equivalent to the U-235 content of natural uranium. Similarly, a successful breeder operating with U-233 and Th-232 may effectively utilize as fuel most of the thorium available, requiring only the small amount of U-235 necessary to get the first plant(s) under way.

Figure I 1-1 illustrates methods for the production of fissile material.

Justification for Th-232 and U-238 breeders can readily be made on the basis of projected energy requirements for the United States and the world

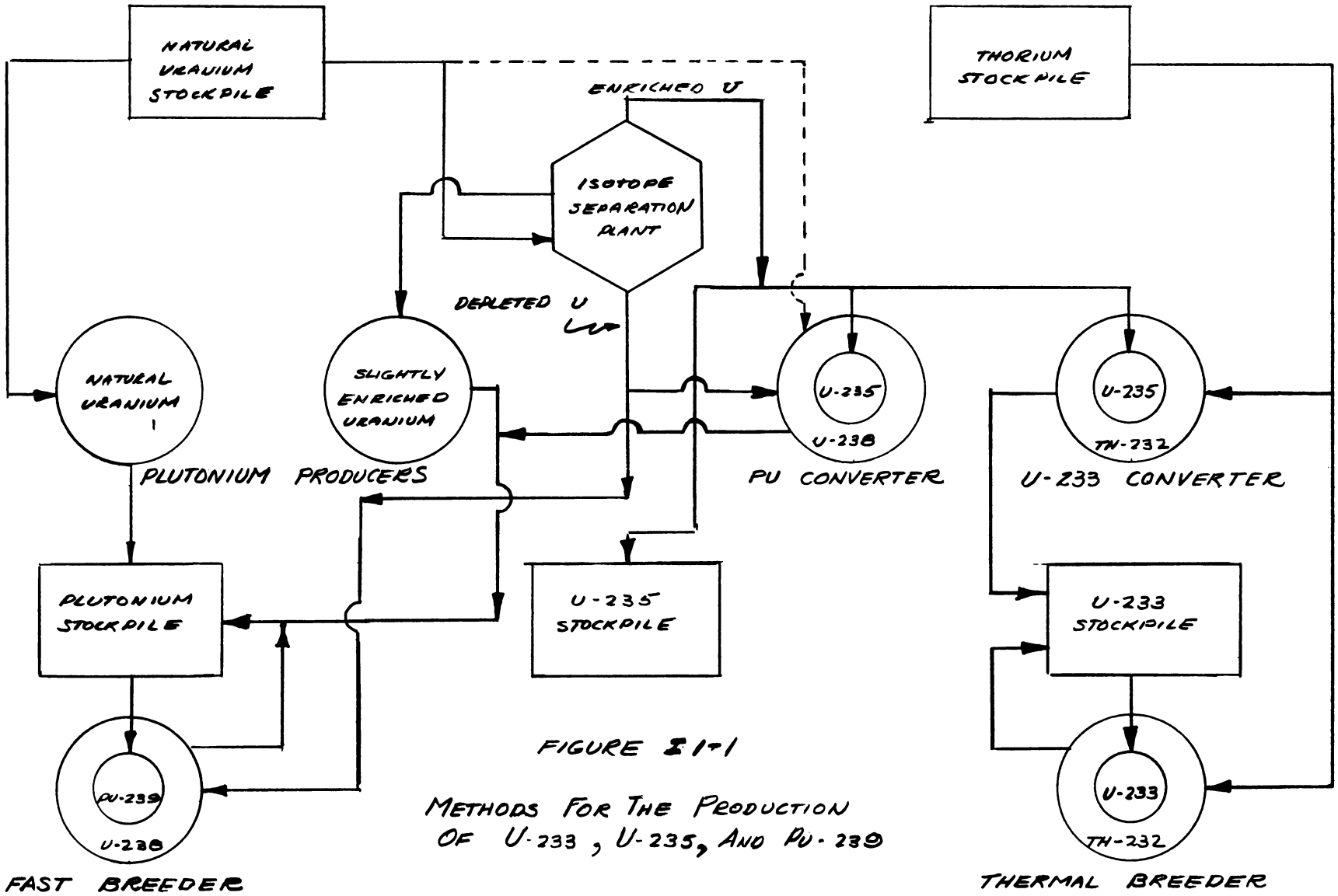

FIGURE II-1

METHODS FOR THE PRODUCTION OF U-233, U-235, AND PU-239

as shown in Table I 1-2 (54) it is apparent that atomic energy or some other yet undeveloped source of energy will be mandatory long before the year 2050 A.D. It appears probable that atomic energy can competitively be used for power generation even if one considers the present economics. Recent economic studies made for the AEC by the Dow-Detroit Edison team indicate that power breeders can be justified if the reactor and its accessories (exclusive of the power generating unit) require an investment no greater than $227. per kilowatt capacity. These figures were obtained by comparing a nuclear power plant to an existing 450,000 kilowatt plant using fuel costing 30.4¢ per million B.T.U.'s and representing an investment of $77. per kilowatt capacity, for the steam generating facilities. Furthermore, the above figures were based on the assumption that there were no credits available from sale of excess production of fissile material or from fission products. A successful breeder could thus require an investment figure higher than the $227. per kilowatt, quoted above, and still be competitive in present day economics.

TABLE I 1-2 (54)

Present and Projected Energy Requirements for the United States to the Year A.D. - 2050

	A.D. 1950	2000	2050
Population	154×10^6	315×10^6	500×10^6
Per capita outputs, Btu	68×10^6	340×10^6	1700×10^6
Efficiencies, %	29	40	45
Per capita inputs, Btu	230×10^6	850×10^6	3780×10^6
Total annual inputs, Btu	35×10^{15}	265×10^{15}	1890×10^{15}
Integrated inputs from 1950 (Q = 10^{18} Btu)	0	5.1 Q	44 Q

TABLE I 1-3 (54)

Present and Projected Energy Requirements for the World to the Year A.D. - 2050

	A.D. 1950	2000	2050
Population	2330×10^6	3880×10^6	7000×10^6
Per capita outputs, Btu	9×10^6	40×10^6	176×10^6
Efficiencies, %	23	35	36
Per capita inputs, Btu	40×10^6	115×10^6	490×10^6
Total annual inputs, Btu	93×10^{15}	450×10^{15}	3430×10^{15}
Integrated inputs from 1950 (Q = 10^{18} Btu)	0	10.7 Q	76 Q

TABLE I 1-4 (54)

Potential United States and World Energy Resources

Source	United States	World
Coal	7 Q	32 Q
Oil - Gas	0.9 Q	5.6 Q
Shale oil	1.2 Q	2.0 Q
Hydro	.05 Q	0.2 - 0.6 Q*
Wood	.05 Q	0.4 - 1.4 Q*
Total	9.2 Q	40.2 - 41.6 Q

* This is a continuing supply which increases with time. Values are for A.D. - 2000 and A.D. - 2050.

Palmer Putnam, a consultant to the AEC estimates that 18% of the total maximum energy produced in the United States in A.D. 2000, may be obtained from nuclear fuel.(54) Such a requirement for energy production from nuclear fuels corresponds to 1600 reactors each generating 1000 megawatts of heat.

As can be seen from the above discussion, most reactors will have to be breeders supplying enough fuel to keep themselves going with enough left over to start new breeders and to supply fuel for non-breeder reactors of special application.

Of the two types of breeders, Pu-239 and U-233, only the latter is considered in this report. From the engineering point of view the major consideration in this design is the heat removal problem. In addition to the usual engineering requirements for heat removal one must consider the nuclear aspects. From a comparison of the neutrons produced per fissionable atom destroyed (η), at various energies, as shown in Table I 1-5, it is evident that a U-233 breeder may be operated at thermal energy whereas a Pu-239 breeder could be successful only if operated as a fast reactor.

TABLE I 1-5

Fissile Material	Neutrons per Fission (ν)	Neutrons per destroyed atom (η)		
		0.025 ev	100 ev	1 Mev
U-233	2.57	2.33*	2.33	2.56
U-235	2.50	2.12	1.60	2.45
Pu-239	3.00	1.95	1.70	2.90

Assuming, thus, that one wishes to design a thermal breeder employing U-233 as the fissile material, one must then carefully consider both the engineering and nuclear aspects in selecting the moderator, fuel compound,

* More recent value for η_{23} is 2.30 ± 0.03.

coolant, and structural materials. To obtain the maximum gain, the coolant material must introduce a minimum interference with the heat producing nuclear reaction. This requires that the coolant have minimum possible volume and low neutron absorption cross section. Furthermore, power consumption in moving the coolant should be low.

Obviously, by moving the moderator and/or moderator plus fissile material from the reactor for cooling and replacing it for further heating in a continuous manner one can eliminate the need for a liquid coolant in the core.

For breeder applications, movement of liquid moderator alone would require the introduction of structural retaining materials into the core which would make it impossible to get a high breeding gain or might eliminate breeding possibilities entirely. For this reason, the scope of this study involves primarily the movement of solid moderator and fuel particles between the core and heat exchanger.

2. Industrial Application of Fluidization of Solids

Several industries are employing the processes which embody the principle of moving large quantities of heat by means of moving solid particles. The solids are usually transported by a gas.

In the petroleum industry, this system involves continually removing coke from a reaction vessel by means of a bed of solid particles carrying the adhering coke out of the vessel. The coke is then burned off in the second vessel, the heat given off being absorbed in the solid particles. The hot particles are then returned back to the reaction vessel wherein heat is extracted from the particles to provide the heat required for the endothermic reaction. The solid particles actually perform three useful

functions (1) continuously remove coke from the reaction vessel , (2) provide a mobile heat sink so that heat produced in the regenerator can be returned to the reaction vessel, and (3) catalyze or speed up the desired chemical reaction in the reactor.

Here a nuclear reactor has been conceived employing the gas-solid system wherein the solid acts as a heat sink and is transported by means of a gas. The transporting gas in such a system may be used to "fluidize" the solids in a heat exchanger. Fluidization of the solids involves passing the gas through the finely divided particles at such a rate that the solid bed behaves as an ordinary fluid. Thus, the bed seeks its own level and exerts a pressure on the retaining vessel equivalent to a hydrostatic pressure of an ordinary fluid. In a fluidized bed, the solid particles are in random motion. Because of this high degree of particle motion and the relatively small particle size, the particles transfer their heat very rapidly to the fluidizing gas. In turn, the fluidizing gas transfers the heat to exchanger surfaces rapidly since the particle motion reduces the exchanger surface gas film thickness. Therefore, the principle of fluidization as applied to heat transfer in a gas-solid system offers the advantages of attaining a high heat removal rate for a given amount of fissile material hold-up.

3. Advantages of a Moving Solids Nuclear Reactor

In general, it appears that application of the moving solids technique to a nuclear reactor results in the following advantages:

Advantages of a Moving Solids Nuclear Reactor

1. Most of the advantages of the homogeneous system are retained, e.g.:
   a) High specific power
   b) High power density
   c) High total power output
   d) Negligible radiation damage
   e) Continuous removal of gaseous fission products.
2. Extremely high neutron economy possible.
3. Chemical processing can be continuous and simplified. (e.g.: fluoride processing for U; chloride removal of Pu.)
4. No corrosion problem.
5. Reactor system can operate at atmospheric pressure.
6. Inexpensive structural materials possible.
7. Good heat transfer in heat exchanger.
8. Heat readily removable from blanket.
9. High pressure and temperature steam available.
10. Relatively simple controls possible.
11. Good (negative) temperature coefficient of reactivity.
12. Can start up at low temperatures.
13. Basic engineering principles based on established commercial practice.
14. Possibility of producing low cost power.

4. Objectives of the Present Report

The primary objectives of this report are to investigate the engineering and nuclear feasibility of the fluidized-solids nuclear power-breeder. Consideration will be limited mostly to the gas-solids techniques. An energy release of 250 megawatts in the reactor system will be used as the

basis and the total holdup of fissile materials will be limited to about 200 Kg. Additional objectives will include: maximum gain, simplest and cheapest engineering design, and serious consideration to fuel preparation and chemical processing. It is understood that overall optimization will be impossible in the time allotted for this survey. Consequently, calculations are to be made and results presented which cover a sufficient range to give the readers a clear picture of the effect of the many variables on the overall operation.

II. SELECTION OF REACTOR MATERIALS

1. Moderators and Fuel

The general problem of a moving bed reactor permits consideration of either a liquid or a gas as a fluidizing medium. A list of probable moderators should thus include both liquids and solids. Such a list is presented below:

Liquid Moderators	Solid Moderators
H_2O	Petroleum coke
D_2O	Graphite
NaOH (fused)	BeO
	BeC
	Various ceramics and ceramets containing beryllium or carbon

Fuel	Compound or Form
Fertile Isotopes	As metal, e.g. balls, chips, etc.
U^{235} partly or highly enriched	Oxide (UO_2 or U_3O_8)
U^{233} partly or highly enriched	Carbide (UC_2)
PU^{239}	Impregnation of uranium in BeO or graphite
	UF_6 (with a solid moderator only)

To retain one of the big advantages of the moving bed technique for a power breeder, it is desirable that the heat transfer (to the steam cycle) be done outside the core. This requires that the heat be carried out of the reactor with the solids or in a liquid stream. To remove the heat with D_2O or H_2O it would be necessary to operate at high pressures. With NaOH there would be no problem with high pressures, but expensive, corrosion resistant, high cross-section alloys would be required to contain the fused hydroxide. The other, and more attractive, alternative is to circulate the solids to an external heat exchange vessel. Most of the discussion to follow applies to the latter technique, using only the gas-solids system.

Preliminary calculations indicated that a much lower critical mass is obtained with all or most of the breeding outside the core. This condition requires the fissile material to be almost fully enriched. Thus, in order to attain sufficient heat capacity (per unit weight of fissile material) in the movable solids, it is necessary to introduce a non-fissile carrying material which is, preferably, also a moderator. Fortunately, materials such as BeO and graphite can serve the purpose not only of adding heat capacity, but also providing moderation with minimum neutron loss. After a general survey of possible moderators the field was narrowed down to graphite impregnated with uranium, and possibly BeO.

Impregnation can be readily accomplished using either an aqueous solution of uranium, preferably as $UO_2(NO_3)_2$, or using a dispersion of finely powdered oxide or carbide of uranium in a pitch or tar. Steele (42) describes in some detail the impregnation of graphite using a uranyl nitrate solution. Smith and Yound (40) report impregnation up to 0.35 grams of uranium per cc. Strength properties of the above impregnated graphite were

reported by Malmstrom and Miller (25). The results show no weakening effect of the impregnate on the graphite within the range of concentrations studied (up to 0.15 grams uranium per cc.)

The uranyl nitrate with which graphite is impregnated is converted to the oxide, U_3O_8, upon firing the graphite at about 1000° C. Above about 1500° C, the oxides are gradually converted to the carbides. Because of the tendency of the carbides to hydrolyze in water, only the oxides would be permitted using the D_2O or H_2O system. However, either the oxide or carbide can be used in the gas-solid system providing the gas is relatively inert. Thus, it is suggested that the graphite (after impregnation) be heated to about 1000° C. Under these conditions the uranium will exist primarily as U_3O_8. During operation some portion of this oxide will be converted to the carbide without any serious effect on the system.

Beryllium and its compounds were eliminated in the present analysis as moderators for systems wherein the uranium is homogeneously mixed with the moderator because of greater chemical processing difficulties. Using uranium as the gaseous UF_6, however, beryllium oxide might be desirable if it shows sufficient chemical stability. Since most of the fission products would remain in the gaseous UF_6 stream and would be removed as such, one would need to process only a small amount of the beryllium compound.

A reactor system employing the gaseous UF_6 both as a fuel and a fluidizing gas has been proposed (Figure II-1). This system has not been carefully analyzed for gain or chemical stability of probable moderators. Nuclear calculations, however, did show that the reactor can readily be made critical using BeO as the moderator.

Dwg. 15936

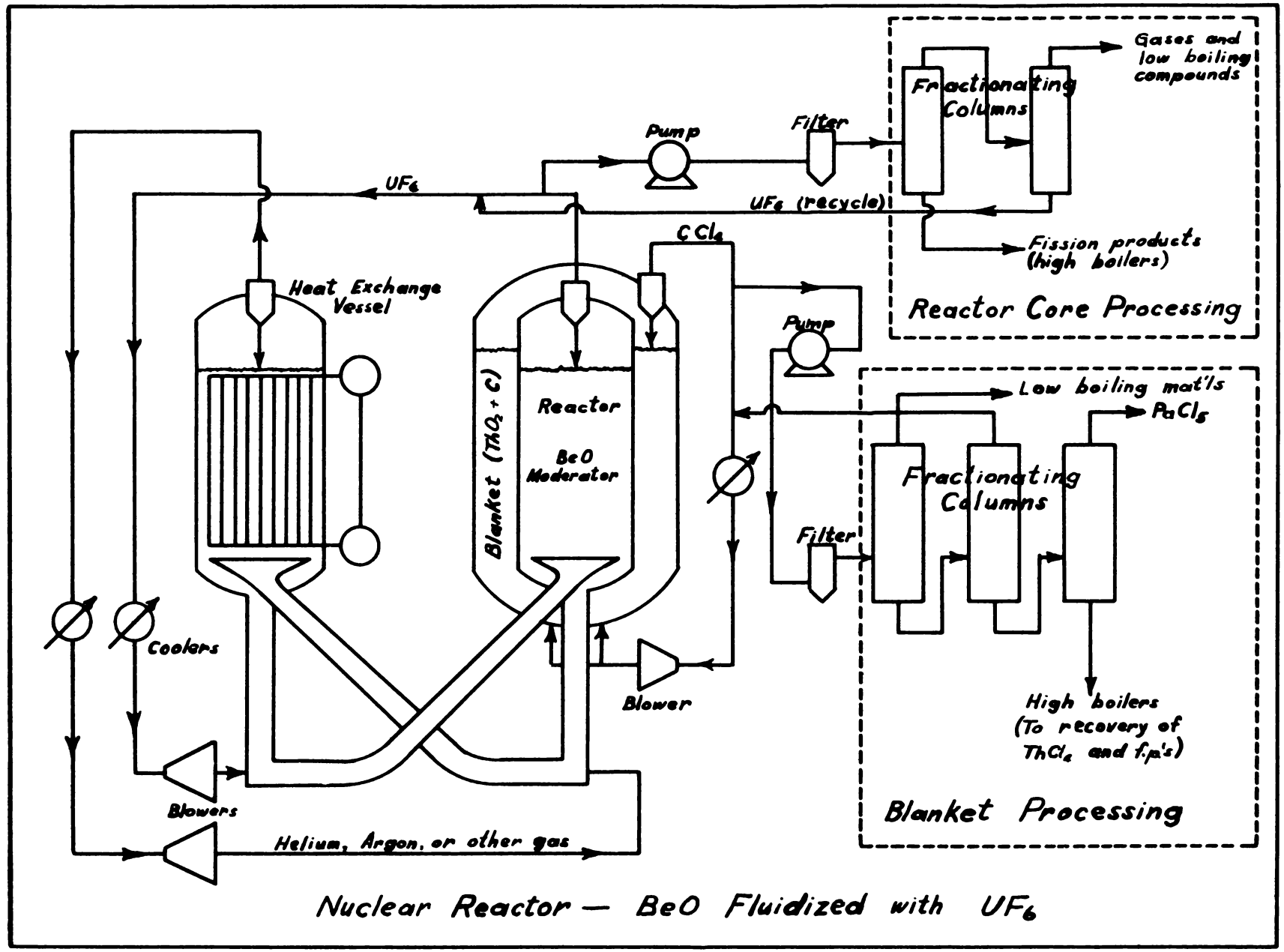
Gases and low boiling compounds
Fractionating Columns
Pump
Filter
UF6
UF6 (recycle)
CCl4
Fission products (high boilers)
Reactor Core Processing
Heat Exchange Vessel
Pump
Low boiling mat'ls
PaCl5
Reactor
BeO Moderator
Blanket (ThO2 + C)
Fractionating Columns
Filter
Coolers
Blower
High boilers (To recovery of ThCl4 and f.p's)
Blowers
Helium, Argon, or other gas
Blanket Processing
Nuclear Reactor — BeO Fluidized with UF6

2. Blanket Materials

The blanket for a breeder reactor necessarily contains a fertile material. Only thorium and its compounds have been considered in this report. The three compounds most likely to be useful in the present reactor design are ThO_2, ThC_2, and ThF_4. It seems preferable to include in the blanket more moderation than is obtained from the above compounds. This becomes even more important as greater fractions of the total number of fissions occur in the blanket. Just as in the core, graphite becomes a convenient moderator to use. It is proposed that the ThO_2 or ThC_2 be incorporated in the graphite by impregnation, although a properly prepared physical admixture of the graphite and the thorium compound particles may be used.

The ThF_4 would probably be considered only in conjunction with the fluoride process for removal of the uranium. Although the thorium could be charged as the ThO_2 (this would be converted to ThF_4 in the blanket) it is suggested that the initial charge be ThF_4. This should be prepared in the desired particle size to permit fluidization with helium or argon containing 1% F_2. It has been found (1) that the optimum operating temperature would be about 1100° F. At this temperature the ThF_4 particles slowly break up and must be "rejuvenated" periodically. Agron (1) states that the rejuvenation should not be considered a serious disadvantage since this can be carried out merely by hydrolyzing the fluoride, drying, and then fluorinating the resulting oxide or fluoride.

3. Fluidization Fluids

Liquids, such as H_2O or D_2O, as well as gases may be used to fluidize the solids in the system. The liquids have several advantages and should

be evaluated in a more complete examination of the fluidized solids reactor. In the work covered in this report, the authors limited their activity to the gas-solids systems except for the brief survey presented in section IV on the use of D_2O.

Table II - 1 presents a list of some of the gases considered by the authors and shows some of the pertinent properties of these gases.

TABLE II - 1

Properties of Gases for a Fluidized Solids Nuclear Reactor

Gas	Mol. Wt.	Specific Heat Btu/lb/° F @ 1500°F	Thermal Conductivity Btu/hr/ft/°F @ 212° F
H_2	2	3.5	.115
He	4	1.25	
CH_4	16	1.5	.022
H_2O(steam)	18	.55	.014
N_2	28	.28	.018
Air	29	.28	.018
Argon	40		
CO_2	44	.38	.013
CCl_4	154	.4	.005
UF_6	352		

Argon and helium have the very attractive property of being, chemically, entirely inert. Hydrogen and helium have good heat capacity and thermal conductivity. The solids carrying capacity of these two gases is, however, so low that their use would be limited to those designs wherein little or no solids are being transported by the gas from one vessel to another.

Thermodynamic (14) and kinetic data indicatesthat steam may react quite rapidly with graphite at temperatures above about 1200° F and could be used with a graphite moderator only at somewhat lower temperatures.

Gulbronson and Andrew (14) have presented data indicating that CO_2 may be used with pure graphite up to temperatures of about 1500-1800° F before the reaction rates become appreciable. However, although the authors found no data on the catalytic effect of the fission products on the reaction at high temperatures, they believe that this effect would be very pronounced. It should be noted that the use of a CO_2 - CO mixture would retard, but not prevent, the reaction. The equilibrium concentrations are sufficiently different at the two extreme temperatures that one could get a "burning up" of the graphite in the hot zone and redeposition of the graphite in the cold zone, probably on the water tubes. Thus, in view of the probable reactions of steam or CO_2-CO gases with graphite at the elevated temperatures, neither gas was considered further in the present report.

Methane has several desirable features, but may be subject to radiation damage, and its low molecular weight gives it a low solids carrying capacity. Nitrogen does not seem to have sufficient advantages over argon to overcome its greater reactivity. The choice was thus narrowed down to argon, not because the other gases were impractical, but rather that insufficient information was available on the behavior of many of these gases in the proposed reactor.

III Gas-Solids System

1.0 Engineering

1.1 Heat Transfer in A Gas-Solid System

Two methods are widely employed in industry for the removal of

heat from moving solid particles, namely

(1) Submerged tubes in a fluidized bed.

(2) Submerged tubes in a moving bed of solids in which the particles move in one direction (rod-like flow).

The relative merits of these two systems have been based primarily on their obtainable specific power, defined as the kilowatts of heat removed per kilogram of U-233. To attain a high specific power it is necessary to obtain high overall heat transfer coefficients. With the tubes submerged in a gas-solid mixture, the gas film heat transfer coefficient will control the rate of heat transfer in both the preheater and boiler tubes. However, in the superheater tubes both the steam side and gas-solid side heat transfer coefficients are important in determining the overall heat transfer coefficient.

In addition to high heat transfer coefficients, a large temperature difference between the fuel and coolant is required to obtain high specific power. This temperature difference, for the most part, depends on the temperature limitations of the fuel and moderator and the creep characteristics of the submerged heat transfer tubes. As a design point this study is based upon a 2000° F average solids temperature entering the heat exchanger, although it is believed that higher temperatures are worthy of consideration.

HEAT TRANSFER IN A FLUIDIZED BED

A literature survey on fluidized heat transfer revealed that the Gamson (9) correlation predicts most accurately commercial experience (39). Table III 1-1 shows a comparison of predicted heat transfer coefficients and those observed in commercial fluid beds (39).

TABLE III 1-1

Convective Heat Transfer Coefficients in Gas Fluidized Solids Beds

Correlation	Solid-Gas Film Coefficient Btu/(hr)(sq ft)(°F)	
	Calculated	Experimental
Gamson (9)	100	125-150*
Jakob (6)	29	
Miller (30)	69	
Modified Gamson	135	

* 125 near center of 20 ft. diameter bed
150 near periphery of 20 ft. diameter bed

If the heat transfer coefficient, calculated on the basis of an empty tube and the average fluid properties, is denoted by h and the actual heat transfer coefficient in the presence of particles as h_T, the incremental change in heat transfer coefficient can be defined as:

$$h_p = h_T - h \qquad (1)$$

Gamson (9) relates the parameters of heated fluidized beds according to the manner of heating:

Externally heated:

$$h_p = \frac{2.18 \; C_p \; G}{\left(\frac{C_p \mu}{k}\right)^{2/3} \left(\frac{6\,G}{\mu\, a}\right)^{0.72} \left(1 - E\right)^{0.30}} \qquad (2)$$

Internally heated:

$$h_p = \frac{2.80 \; C_p \; G}{\left(\frac{C_p \, \mu}{k}\right)^{2/3} \left(\frac{6\,G}{\mu\, a}\right)^{0.84} \left(1 - E\right)^{0.30}} \qquad (3)$$

Gamson's correlation is based upon Miekley and Trilling (29) heat

transfer studies in fluidized beds of spherical particles ranging in size from 0.0016 to 0.0178 inches in diameter. The particles were scotchlite glass beads having absolute particle densities of 151-177 lb/cu. ft. Fluidization occurred in an air stream and in vertical beds 1 to 4 inches in diameter and 4 to 8 feet high. Heat was transferred by means of electric energy through the tube walls or through the wall of a cylindrical heating element inserted axially in the bed. The solids concentration was varied from a minimum of 1.6 % to a maximum of 52 %. Special attention was given, in the design of the experimental equipment, to eliminate radiation to the particles from the heat exchange surface. In view of this, the heat transfer may be considered as typical of convective transfer only.

The coefficient of equation (2) has been modified in order that the calculated heat transfer coefficients will agree with commercial performance as shown in Table III 1-1. The modified equation becomes:

$$h_p = \frac{2.94\ C_p\ G}{\left(\frac{C_p\ \mu}{k}\right)^{2/3} \left(\frac{6\ G}{\mu\ a}\right)^{0.72} \left(1 - E\right)^{0.30}} \qquad (4)$$

The commercial data (39) which are the basis for the modification of equation (2) were taken in a fluid bed with widely spaced horizontal tubes. An additional correction to the Gamson correlation may be necessary for the closely-spaced tube arrangement proposed in this report. It will be necessary to obtain experimental data on the proposed design for precise heat transfer coefficients. It is anticipated that the same grouping of variables will correlate the data. The modified equation should predict the convective heat transfer coefficients for vertical tubes in the heat exchanger and blanket within $\pm$ 20%.

In addition to convective heat transfer coefficient, h_c, the effect of radiative transfer has been considered. The total heat transfer coefficient for exchanger surface to fluid is expressed as follows:

$$h_T = h_c + h_r \qquad (5)$$

Kent states,

$$h_r = \frac{\epsilon_1 \epsilon_2}{(T_1 - T_2)(\epsilon_1 - \epsilon_1 \epsilon_2 + \epsilon_2)} \left\{ 0.174 \left[\left(\frac{T_1}{100} \right)^4 - \left(\frac{T_2}{100} \right)^4 \right] \right\} \qquad (6)$$

where ϵ_1 and ϵ_2 are the emissivity constants for the radiating and receiving surfaces. Table III 1-2 shows typical radiant heat transfer coefficients for the design temperatures chosen.

TABLE III 1-2

Radiant Heat Transfer Coefficients In A Gas Fluidized Solid Bed

Receiver	Average Temperature	h_r at 1500° F Btu/hr -sq ft-°F	h_r at 2000° F Btu/hr-sq ft - °F
Preheater	300° F	11	38
Boiler	600° F	14	45
Superheater	800° F	16	50

where $\epsilon_1 = 0.95$

$\epsilon_2 = 0.55$

To determine the effect of percent solids in the fluid bed upon heat transfer it is necessary to establish a relationship between percent voids and gas velocity. This relationship between voids and gas velocity is dependent on the nature of both the gas and solid particles. Leva's (23) correlation for predicting the percent voids in a fluid bed has been employed in this study. Figure III 1-1 shows the maximum bed density for

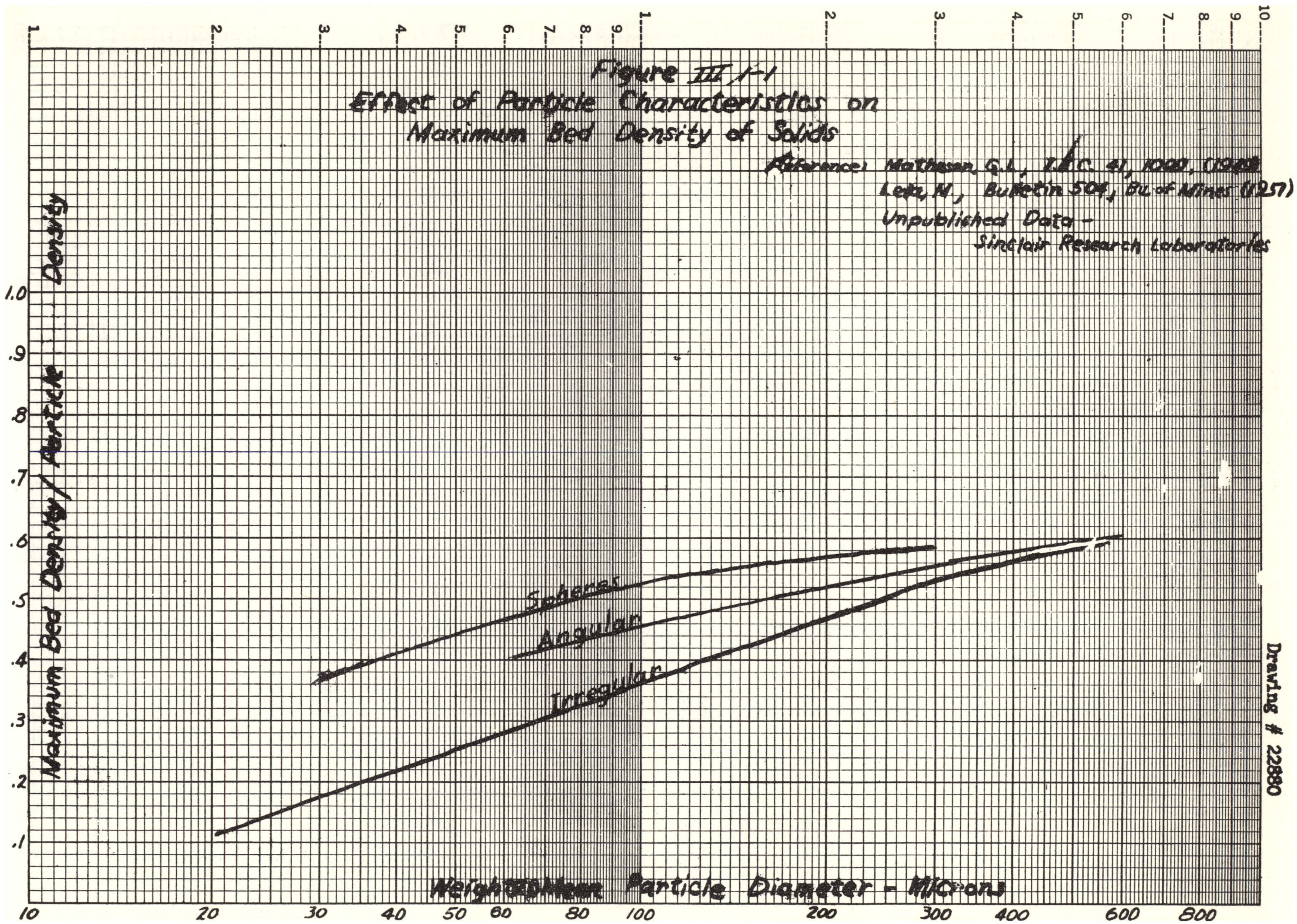
Figure III I-1
Effect of Particle Characteristics on
Maximum Bed Density of Solids
Reference: Matheson, G.L., I.&E.C. 41, 1000,
Leva, M., Bulletin 504, Bu. of Mines
Unpublished Data -
Sinclair Research Laboratories
Spheres
Angular
Irregular
Maximum Bed Density / Particle Density
Weight Mean Particle Diameter - Microns
10
20
30
40
50
60
80
100
200
300
400
600
800
.1
.2
.3
.4
.5
.6
.7
.8
.9
1.0
Drawing # 22880

Dwg. 22881

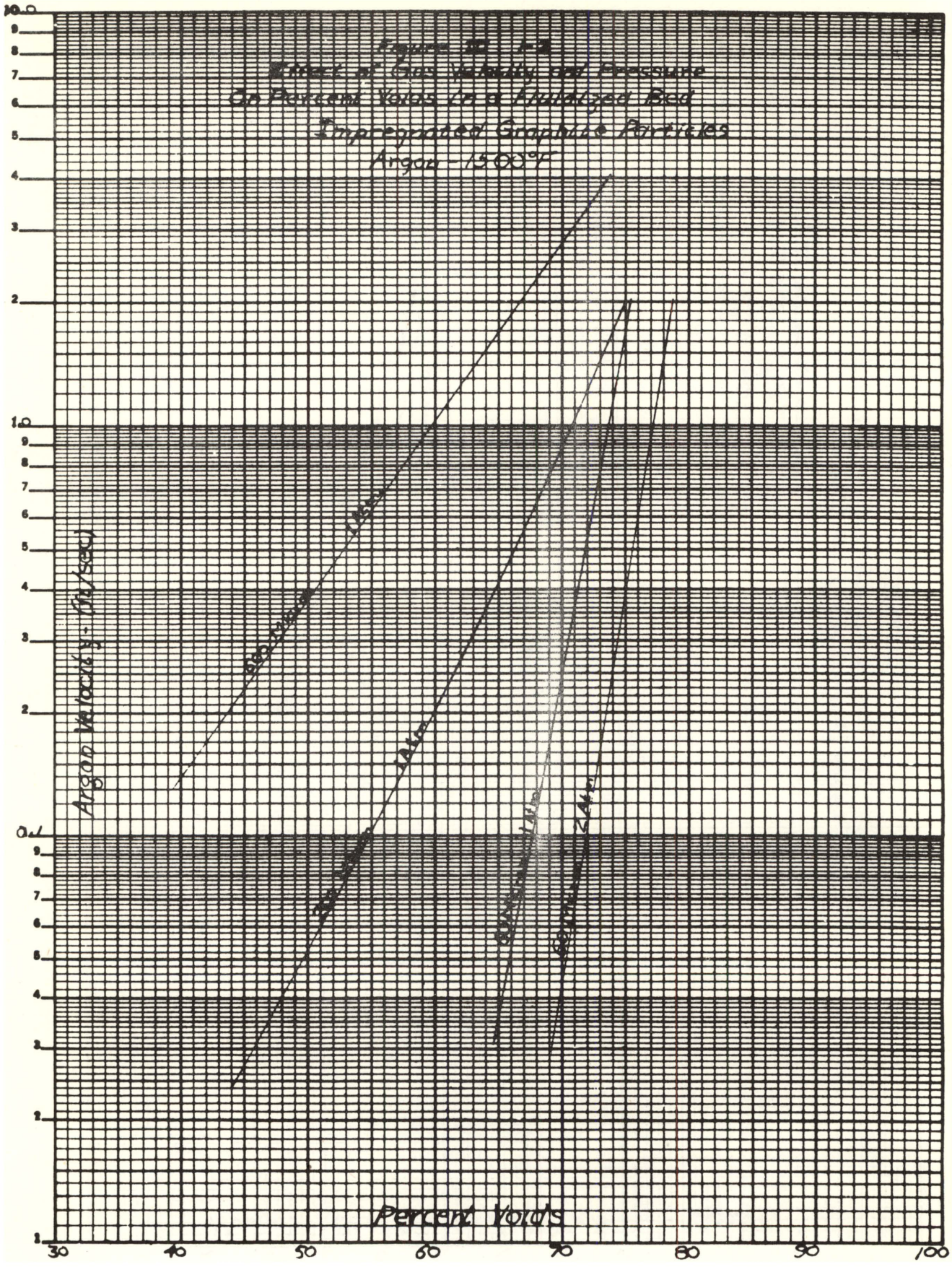
Figure 12-12
Effect of Gas Velocity and Pressure
On Percent Voids in a Fluidized Bed
Impregnated Graphite Particles
Argon - 1500°F
Argon Velocity, ft/sec
Percent Voids
30
40
50
60
70
80
90
100

for powdered materials. It is apparent from the experimental curves of Figure III 1-1 that the maximum bed density is for the most part dependent upon particle diameter and shapes. Other factors not shown in Figure III 1-1 are particle size distribution and nature of particle surface. In this study the line, drawn midway between the experimental curves for round and irregularly shaped particles shown on Figure III 1-1, has been assumed representative of the behavior of the core and blanket material.

The effect of argon gas velocity at 1500° F upon percent voids for weighted average particle diameters of 60, 200 and 600 microns have been evaluated. Leva's correlation described in Appendix VIII 2 gave the relationship between gas velocity and percent voids shown in Fig. III 1-2. From the standpoint of obtaining optimum heat transfer it is apparent from equation (4) and Figure III 1-2 that for given materials in a fluid bed one must optimize between particle diameter, gas velocity and solids entrainment.

Typical particle, gas composition, and operating conditions for a commercial fluid catalytic cracking regenerator vessel are shown in Table III 1-3.

Although Figure III 1-10 indicates a marked increase in heat transfer coefficient for particle sizes below 60 microns, it has been shown by Mickley (29) that 40 micron particles behave the same as larger particles. Gamson (9) accounted for this effect by introducting a shape factor into his correlation which, in effect, accounts for the agglomerating tendencies of the particles. In this report, a shape factor of 1.0 has been assumed. In addition to the agglomerating tendency, which causes a reduction in heat transfer as the particle size is decreased, the percent solids in the fluid bed at a given gas velocity decreases as the particle size is decreased. This effect tends to reduce the heat transfer coefficient. Furthermore, as particle

TABLE III 1-3

Typical Commercial Fluid Bed Operating Conditions

A. Regenerator Gas Composition

Component	Mol %
N_2	71
O_2	3
CO_2	9
CO	7
H_2O	10

B. Particle Size (Roller Screen)

Size (microns)	Wt. %
0 - 10	4.2
10 - 20	9.0
20 - 40	16.6
40 - 80	16.5
80 +	53.7
67	Mean weighted average

C. Miscellaneous (in Regenerator)

Temperature	10 75° F
Pressure	10 psig.
Gas Velocity	1.5 ft. per sec.
Loose Bed Density	0.643 gr. per cc.
Packed Bed Density	0.83 gr. per cc

size is decreased the entrainment rate of solids increases in the gas leaving the fluid bed. The increased entrainment rate increases solid holdup in cyclones and filters. For these reasons the fluid bed design studies have been restricted to a 60 micron minimum particle size.

Figure III 1-3 shows the effect of velocity and disengaging height upon solid entrainment for a 60 micron weighted average particle size. The unpublished correlation (39) indicates that the rate of solids entrainment

Dwg. 22882

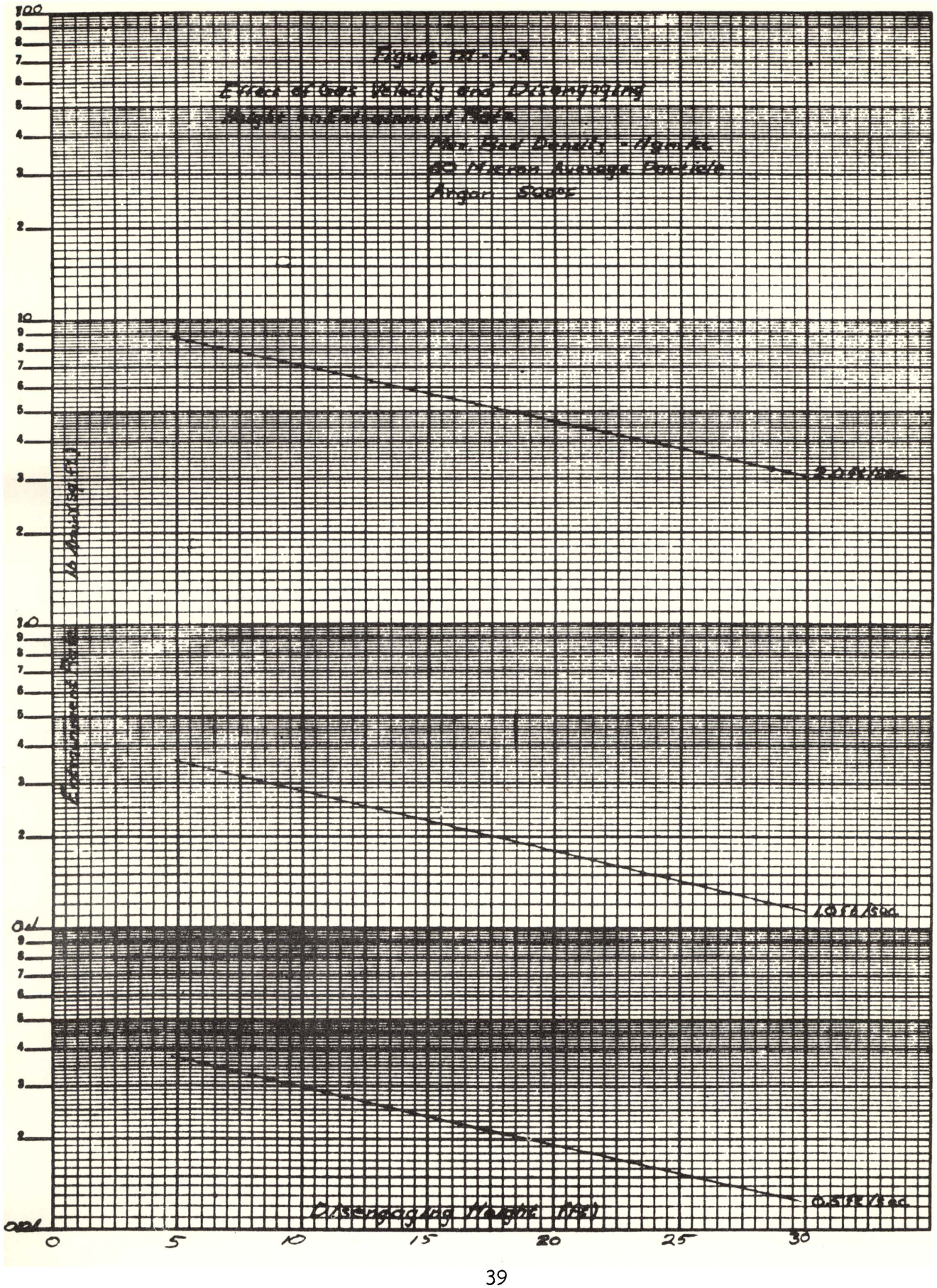
Figure 22-2-3
Effect of Gas Velocity and Disengaging Height on Entrainment Rate
Min. Bed Density = 19 pcf
60 Micron Average Particle
Angora Shale
200 ft/sec
100 ft/sec
50 ft/sec
Disengaging Height (ft)
0
5
10
15
20
25
30

increases with decrease in disengaging height. Disengaging height is that distance above the top of the bed in which solids may settle out. Furthermore, the correlation indicates the entrainment rate; (1) increases with increasing gas velocity, viscosity and density, (2) increases with a decrease in particle size. The effect of particle shape, surface roughness and particle density were not investigated. Since the effect of particle density has not been reported it has been assumed, in the proposed design, that the entrainment rate decreases linearly with an increase in average particle density. The validity of this assumption is dependent largely upon the particle size distribution. It is believed that the entrainment rates reported for 60 micron material are reasonably accurate since the original correlation is based upon 70 to 100 micron weighted average particles from a fluid catalytic cracking unit. The entrainment rate for 200 and particularly 600 micron particles will be less than predicted by Figure III 1-3.

Summarizing it appears desirable and feasible to employ a particle size and gas velocity in a fluid nuclear reactor and/or its associated heat exchanger which are similar to those now used in commercial fluid catalytic cracking practice. A gas velocity between 1 and 2 ft/sec. is indicated for a 60 to 200 micron average particle size.

HEAT TRANSFER IN MOVING BED(not fluidized)

Correlations, on the heat transfer coefficients from a continually moving bed of solids to normal stationary solid surfaces, were not found in the open literature. However, it is generally known that such coefficients are lower than from fluidized solids by as much as a factor of 10 to 20.

An attempt has been made to analyze the correlations which were found

in the literature for somewhat related conditions. Heat transfer for three conditions are considered: (1) gas flowing normal to heat exchanger tubes, (2) granular solids transferring heat to tubes by conduction through solid particles and stationary gas filling the void space of the bed, (3) granular solids transferring heat to tubes where gas is flowing through the bed.

Spiers (41) has analyzed the system of non-moving solids transferring heat to tubes with a non-circulated gas filling up the void spaces. He states that a bed of granular solids conducts heat partly through the solid particles and partly through the intervening gas. The thermal conductivity, k, of the combined system depends on the thermal conductivity of the gas, k_g, the thermal conductivity of the solid, k_p, and on the fractional voids, ϵ, occupied by the gas. k/k_g is a function of k_p k_g and of ϵ.

The relationship which best satisfies the experimental data is given in Table III 1-4.

TABLE III 1-4

Effect of Thermal Conductivity and Per Cent Void on Heat Transfer in Granular Bed With Interstitial Gas Stationary

ϵ \ k_p/k_g	20	50	100	500	1000	2000
			k/kg			
0.60	2.3	2.5	2.8	5.0	8.0	13.2
0.55	2.4	2.7	3.0	5.2	8.2	13.6
0.50	2.6	3.0	3.3	5.6	8.5	14.4
0.45	3.8	4.1	4.5	6.9	9.6	16.2
0.40	7.0	7.3	7.7	10.0	12.7	19.4
0.35	12.0	12.4	12.8	15.0	18.2	23.9
0.30	19.3	19.6	20.1	22.3	25.6	31.4

Based upon 3 inch staggered tube heat exchanger with 1 inch tubes Table III 1-5 shows the heat transfer coefficient of conduction. Comparison

of convective heat transfer coefficients in Table III 1-1 with conductive heat transfer coefficient in Table III 1-5 shows a fifteen fold increase in heat transfer for fluidized bed. Furthermore, the greater per cent voids in the fluid bed of the heat exchanger reduces the amount of fissionable material holdup outside the core.

TABLE III 1-5

Conductive Heat Transfer in Moving Granular Bed With Stationary Interstitial Gas

3 inch Staggered - 1 inch tubes

Gas	Temp.	Particle Diameter	Heat Transfer Coeff.
Argon	1500° F	60 microns	8.2 Btu/hr -ft^2-°F
Argon	1500° F	200 microns	10.1 Btu/hr -ft^2-°F
Argon	1500° F	600 microns	12.0 Btu/hr -ft^2-°F
Helium	1500° F	60 microns	16.8 Btu/hr -ft^2-°F
Helium	2000° F	60 microns	17.3 Btu/hr -ft^2-°F

A granular bed with gas flowing through the interstices would be expected to give somewhat higher heat transfer than if the gas were stationary. The magnitude of the increase in heat transfer for a given tube spacing, tube diameter, and particle diameter, depends upon gas velocity. Colburn (4) compares heat transfer coefficients for packed tubes and empty tubes for a given mass velocity based on the gross cross section. For air mass velocities from 0.25 to 4.0 lb/sec-ft^2 in 1 inch inside diameter tubes the transfer rates for the packed tubes are from 5 to 10 times the empty tube rates. McAdams(26) gives heat transfer coefficients for gases flowing outside and normal to staggered tubes as,

$$h = \frac{0.133\, C_p\, G_{Max}^{0.6}}{D^{0.4}} \qquad (7)$$

Heat transfer coefficients calculated from equation (7) for 3 inch spaced staggered tubes are shown in Table III 1-6.

TABLE III 1-6

Gas Heat Transfer Coefficients in Staggered Tube Heat Exchanger With Normal Flow

Gas	Pressure (atm.)	Velocity (ft/sec)	h (Btu/hr-ft^2-°F
Argon	1.0	1.0	1.0
Argon	1.0	2.0	1.5
Argon	2.0	1.0	1.5
Helium	1.0	1.0	10.0

If the heat transfer coefficients in Table III 1-6 are multiplied by a factor of 10 as indicated by Colburn (4) the resulting heat transfer coefficients for tubes submerged in a granular bed with normal flow of Argon are similar to those in a granular bed with stationary argon.

Summarizing, it is apparent from equation (7), modified for the effect of solids, and Table III 1-1 that mass velocities of over 100 times the fluid bed mass velocities are required in order to obtain heat transfer coefficients in the moving bed which are comparable to those for the fluid bed. A comparison of heat transfer coefficients for various heat exchanger conditions is shown in Table III 1-7.

TABLE III 1-7

Comparison of Heat Transfer Coefficients in Fluidized and Non-Fluidized Solid-Gas Beds.

1 atm. - 1.0 ft./sec. Argon - 1500° F - 60 Micron Graphite Particles

Solid and Gas Conditions	h (Btu/hr - ft^2 - °F)
No solid-Gas flow	1.0
Solid flow(non-fluidized)-No Gas Flow	8.2
Solid flow(non-fluidized) -Gas flow	10.0
Fluidized gas-solid system	109

The excessive mass velocities required for a non-fluidized bed in order to obtain heat transfer rates equivalent to a fluidized bed necessitates larger particle sizes (about 1/8 inch diameter) to avoid excessive pressure drop. In turn, large particles cause an increase in temperature gradient within the particle. Such temperature gradients tend to increase spallation and particle cracking.

In conclusion, the low heat transfer for non-fluidized gas-solid beds increases the fissile material hold-up to such an extent that it is believed to be impractical to consider a non-fluidized heat exchanger.

III 1.2 Vessel Arrangement

Three vessel arrangements have been considered which employ gas fluidization of finely divided solid particles. Compared to a solid-gas system without fluidization the heat transfer coefficients with fluidization are 10 to 100 times greater. Therefore, it is expected that relatively high specific power is obtainable from the fluidized system. Table III 1-8 lists the vessel arrangements considered.

TABLE III 1-8

Vessel Arrangements

Figure	Core	Location of Heat Exchanger	Blanket
III 1-5	Fluidized Moving Bed	Fluidized Moving Bed Outside of Core	Fluidized Fixed Bed
III 1-6	Fluidized Fixed Bed	Periphery of Core	None
III 1-7	Moving Bed	Fluidized Moving Bed Outside of Core	Fluidized Fixed Bed

Fluidized Moving Bed Core and Heat Exchanger

Figure III 1-5 shows a fluidized core and heat exchanger arrangement. With a graphite wall separating the core and blanket, calculations show that a high breeding gain may be obtained. However, with a gas fluidized core which is subject to slugging the control of the reactor was questionable. A literature search did not reveal the seriousness of this question. However, preliminary nuclear calculations indicated that a 4 inch drop in bed height (3%) increased its reactivity with a δk of 2.7 per cent.

Ever since fluidization was considered as a possible operation by which solid catalysts may be contacted effectively by gases or fluids in general, the phenomenon of slugging has received much attention. The reasons for this consideration were simply,
that in slugging beds the contact between the solid phase and the fluid is not as effective as would be desirable, primarily because of poor dispersion. There are, of course, other features, primarily mechanical in nature, that render excessive slugging in a fluidized bed undesirable.

Because it appears that experimental work is required to analyze the controllability of this reactor, this arrangement did not receive further consideration.

Fluidized Fixed Bed Core

Figure III 1-6 shows a fluidized fixed bed core in which slugging may be minimized because large quantities of gas are not required to transport the solid from one vessel to another.

If thorium is distributed evenly along with fissile material in the moderator this system entails a large U-233 hold-up and low breeding gain when compared with a two region reactor. The neutron absorption of thorium

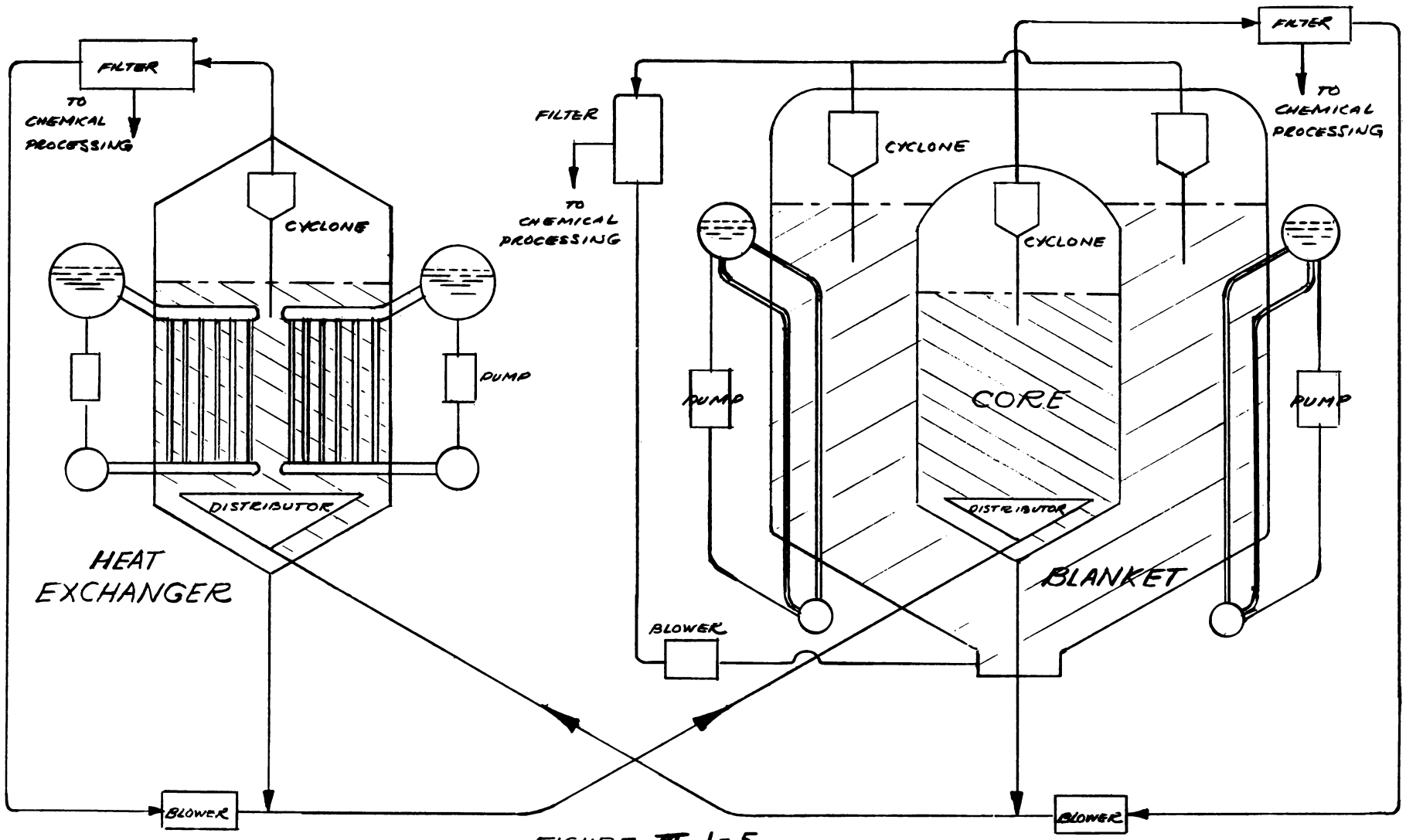

FIGURE III 1-5

FLUIDIZED MOVING BED CORE - FLUIDIZED NON-CIRCULATING BLANKET
FLUIDIZED MOVING BED HEAT EXCHANGER OUTSIDE CORE

accounts for this large holdup and low breeding gain.
To minimize the hold-up thorium rods or tubes containing thorium slugs or compounds should be located near the periphery of the fluidized bed.

In this report further consideration was not given to this arrangement because of its lack of positive flow distribution of solids and gases and its control problem. Experimental work is required to obtain flow patterns for a design of this type in order to avoid channeling. Channeling would cause hot spots and reduce the specific power. The channeling referred to may be defined as that condition that exists when fluids are flowing through beds of fixed or fluidized solids in such a manner that the rate of flow is not constant over the cross section of the bed.

However, a further study involving this vessel arrangement appears in order because of its inherent simplicity. The problems of erosion and attrition are minimized since transfer of solids from one vessel to another is not required.

Moving Bed Core and Fluidized Heat Exchanger

Figure III 1-7 shows a moving bed core with a separate fluidized heat exchanger. As compared to Figures III 1-5 and III 1-6 this arrangement offers these advantages:

(1) Reactor control easier. Core not subject to slugging or channeling
(2) Higher breeding gain. Maximum density of solids occurs in core
(3) Higher specific power. Maximum density of solids occurs in core
(4) Positive solids flow distribution in core. Multiple inlets may be required to obtain proper solids flow distribution.
(5) Engineering design of reactor simplified. Eliminates problems associated with removing entrained solids from core fluidizing gas. Eliminates problems of designing reflector for disengaging area above core.

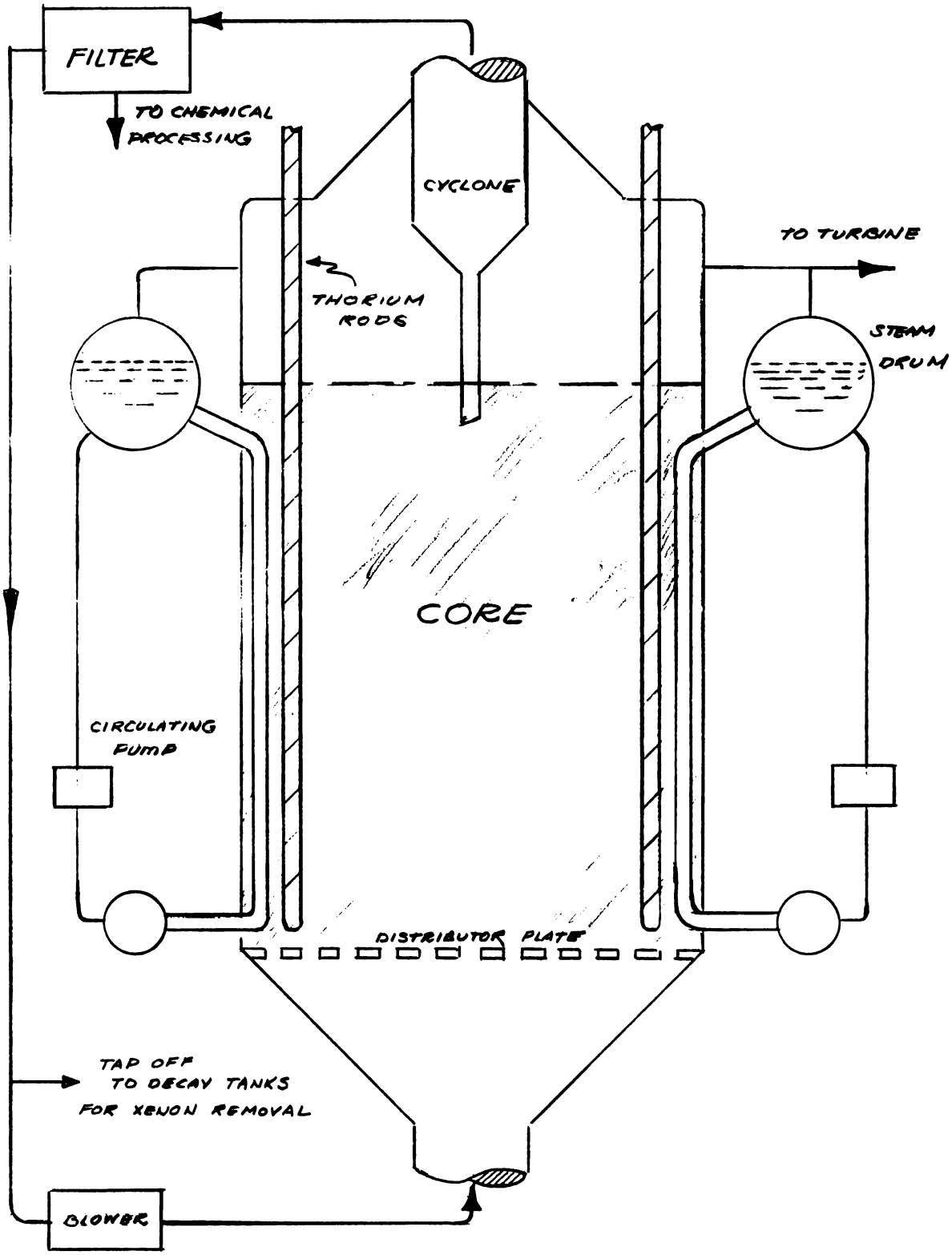

FIGURE III 1-6

FLUIDIZED FIXED BED CORE
INTERNAL HEAT EXCHANGER

Dwg. 15999

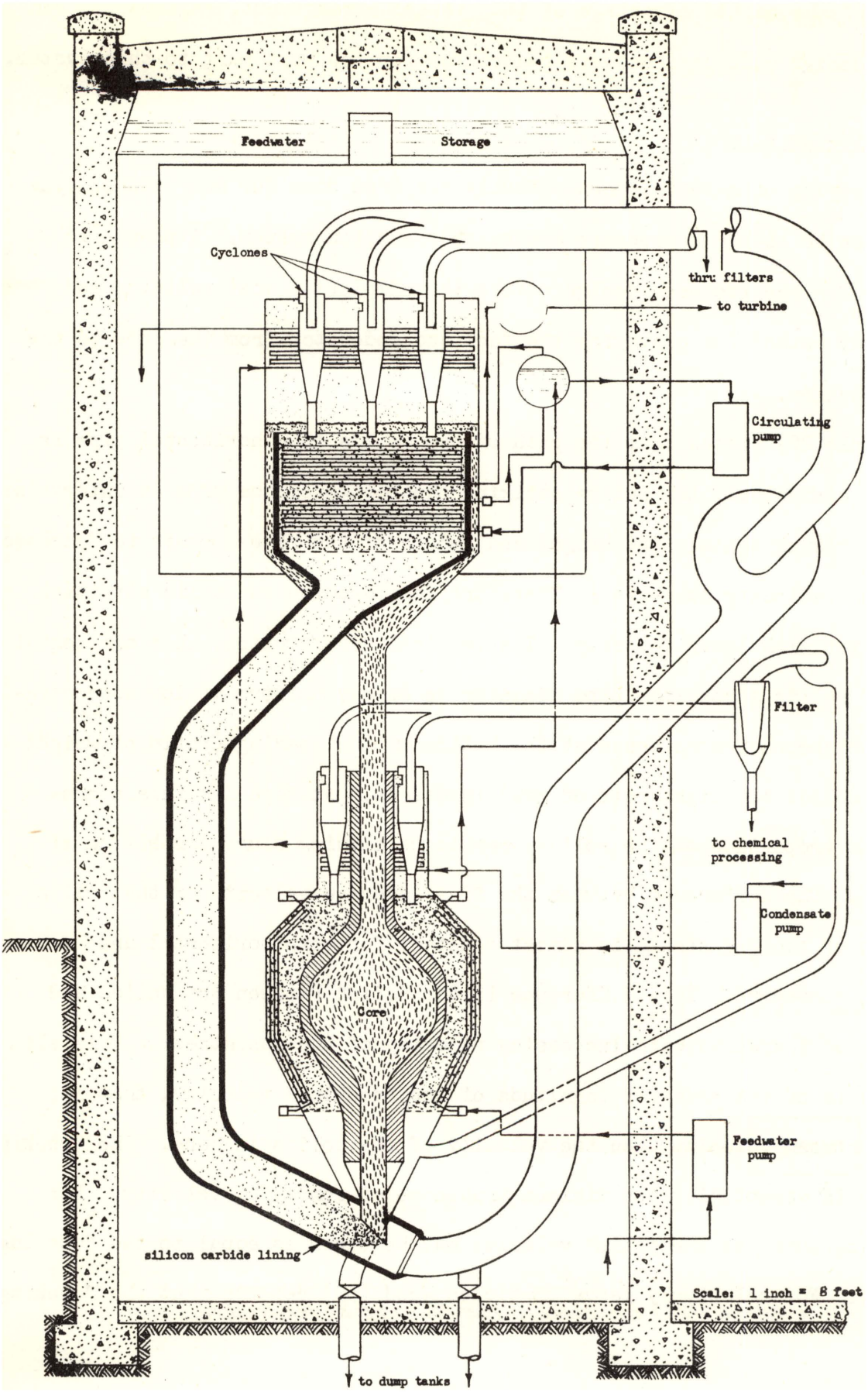

Figure III 1-7

DESIGN FOR A FLUIDIZED-SOLIDS POWER BREEDER REACTOR
MOVING BED CORE, FLUIDIZED HEAT EXCHANGER

Because of the marked advantage of this vessel arrangement, engineering and nuclear design calculations were restricted for the most part to this system.

1.3 Solid-Gas Flow

Conveying of material pneumatically has been done for many years. The system can be either a pressure system or a suction system. A pneumatic conveyor for the proposed design offers the simplest, most reliable and convenient method for conveying the fuel and moderator from the core to the heat exchanger.

Lapple(20) states that the path of the solids in a horizontal pipe is somewhat sinusoidal, the solids striking the bottom of the pipe at intervals and then rising again. The height and length of the rise appears to decrease as the gas velocity decreases. Therefore less erosion and solid attrition is expected with lower velocity. The vertical distribution, in a horizontal pipe, of solids across the pipe diameter is fairly uniform at low concentrations, but becomes more dense at the bottom as the loading (ratio of weight rate of solids to weight rate of gas) increases. At high loadings a considerable proportion of the solids seem to be sliding along the bottom of the pipe. The difference between the final average velocity of the solids and that of the gas stream is almost constant for both horizontal and vertical conveyors. This difference is the "slip" between the solids and the gas and increases with increasing velocity of the gas stream. This slip velocity is of the order of magnitude of the "choking" velocity, that is, the gas stream velocity when the velocity of the solids is zero. The "choking" velocity is essentially the minimum transport or conveying velocity. For estimating purposes the "slip" velocity may be taken as equal to the "choking" velocity. For relatively large particles Wood (53) reports that the "choking"

velocity is independent of loading.

The minimum transport velocities for a material can be estimated by testing the solids in horizontal and vertical transparent quartz tubes. The transport velocity for the horizontal pipe can be determined by measuring the minimum gas velocity at the proposed operating conditions necessary to convey the solids in a horizontal tube. The transport velocity for vertical pipes can be determined by measuring the minimum velocity necessary to just suspend the solids in a vertical tube. The minimum transport velocity of the solids may be several times the free falling velocity. Table III 1-9 shows free falling velocities for various particle sizes of graphite in argon at 1500° F and 1 atmosphere.

TABLE III 1-9

Effect of Particle Size on Free Falling Velocities
In Argon at 1500°F and 1 Atmosphere

Particle size (micron)	Particle Shape	Free Falling Velocity ft/sec
60	sphere	1.8
200	"	6.4
600	"	10.1

TABLE III 1-10

Typical Fluid Catalytic Cracking Transfer Line Conditions

Transfer Line	Velocity (ft/sec)	Solid Loadings (lb solid/lb gas)
To reactor	15-25	15-25
To regenerator	25-45	40-60
To recycle cooler	20-35	40-60

Temperature	950 to 1050° F
Pressure	2 to 20 psig

Velocities in transfer lines are kept to a minimum to avoid excessive erosion of the line and attrition of the particles. Stokes (43) has shown that erosion is proportional to the cube of velocity. He also demonstrates how critical is the angle of impingement at low angles. It is apparent from these studies that sharp bends are to be avoided in solid-gas transfer lines. Erosion resistant linings are employed in commercial solid transfer lines at locations which are susceptible to erosive action.

Based upon 25 feet per second transport velocity and an allowable solid loading of 60 lbs. of solids per lb. of gas, the effect of type of gas, temperature, and pressure, upon transport line diameter, are illustrated in Table III 1-11.

TABLE III 1-11

Effect of Gas Properties on Transfer Line Diameter
(710 lb. solid per sec flow)

Gas	Temperature (°F)	Pressure (atm)	Diameter (ft)
Helium	2000	1	17.3
Argon	2000	1	5.5
Argon	2000	2	3.9
Argon	1500	1	4.9

The comparison of helium and argon on transfer pipe diameter requirement neglects the effect of gas viscosity since their viscosities are nearly equal. In a design in which solids transport is not required such as is shown in Figure III 1-6 further consideration should be given to helium because of its high heat capacity which will increase the convective heat transfer coefficient in the fluidized bed.

III 1.4 Dust Collection

In the proposed nuclear power plant provision must be made to remove the solids entrained in the gas leaving the heat exchanger for several

reasons; namely

(1) Reduce erosion of blower blades.

(2) Provide a means of removing fines resulting from the attrition of solid particles.

(3) Minimize fissile material hold-up outside of heat exchanger and reactor.

(4) Lower radioactivity in cells housing the blower.

Fly ash particles greater than 10 micron size must be removed from the flue gas in order to avoid excessive turbine blade erosion according to Bradley and Buckley (1A). However, their studies do not indicate the effect of pounds of solid per cu.ft. gas. In their powdered-coal, steam power plant they have demonstrated nearly 100% collection efficiency for 10 micron and larger fly ash particles by means of Dunlab cyclones.

A dust collection system has been proposed for the nuclear power plant in this report based upon the following particle size distribution:

Solid Particle Size	Weight Percent
0-10 Micron	4.0
10-20	11.5
20-40	20.7
40-80	33.0
80-104	20.4
104-147	10.4
	100.0

Average weight mean particle size = 59 microns.

The weight of production of fines (0-10 micron) depends primarily upon the nature of the individual particles. Forsythe (8) states that the presence of fines has shown to reduce the severity of attrition of coarse particles in two ways; by a cushioning effect which limits the force of collision impact between coarse particles, and by dilution which reduces the number of coarse particles available for attrition.

In fluid catalytic cracking practice one to five tons per day catalyst losses are quite common. With a 30 day chemical processing cycle for the core an attrition rate of one ton per day would constitute a proper balance for the proposed nuclear plant. This assumes that the attrition rate of the fresh fuel is less than the attrition rate of the spent fuel. With a higher attrition rate it would be necessary to use a shorter chemical processing cycle, which may lower the net gain from the proposed U-233 breeder. Studies should be made to compare the attrition rate of the proposed fuel and moderator with fluid catalytic cracking catalysts for which considerable commercial data is available. (39)(8).

The force or mechanisms utilized for dust collection are classified by Lapple (14) as:

(1) Gravitational
(2) Inertial
(3) Filtration
(4) Electrostatic
(5) Physical Chemical
(6) Thermal
(7) Sonic

Most dust collection systems utilize more than one of these factors.

The performance of a dust collector is termed collection efficiency and is generally expressed as a weight ratio of dust collected to dust entering the apparatus. Typical fractional efficiency curves (39) for various particle sizes are shown in Figure III 1-8 for commercial cyclone and electric precipitators. From these curves it is evident that cyclones alone are not adequate for reducing the solid content of the gas entering the blower. Comparison of curves A and B indicates the effect of gas viscosity upon cyclone efficiency. Hence, by cooling the argon entering the cyclone improvement in efficiency is attained. The gases and entrained solids

Dwg. 22883

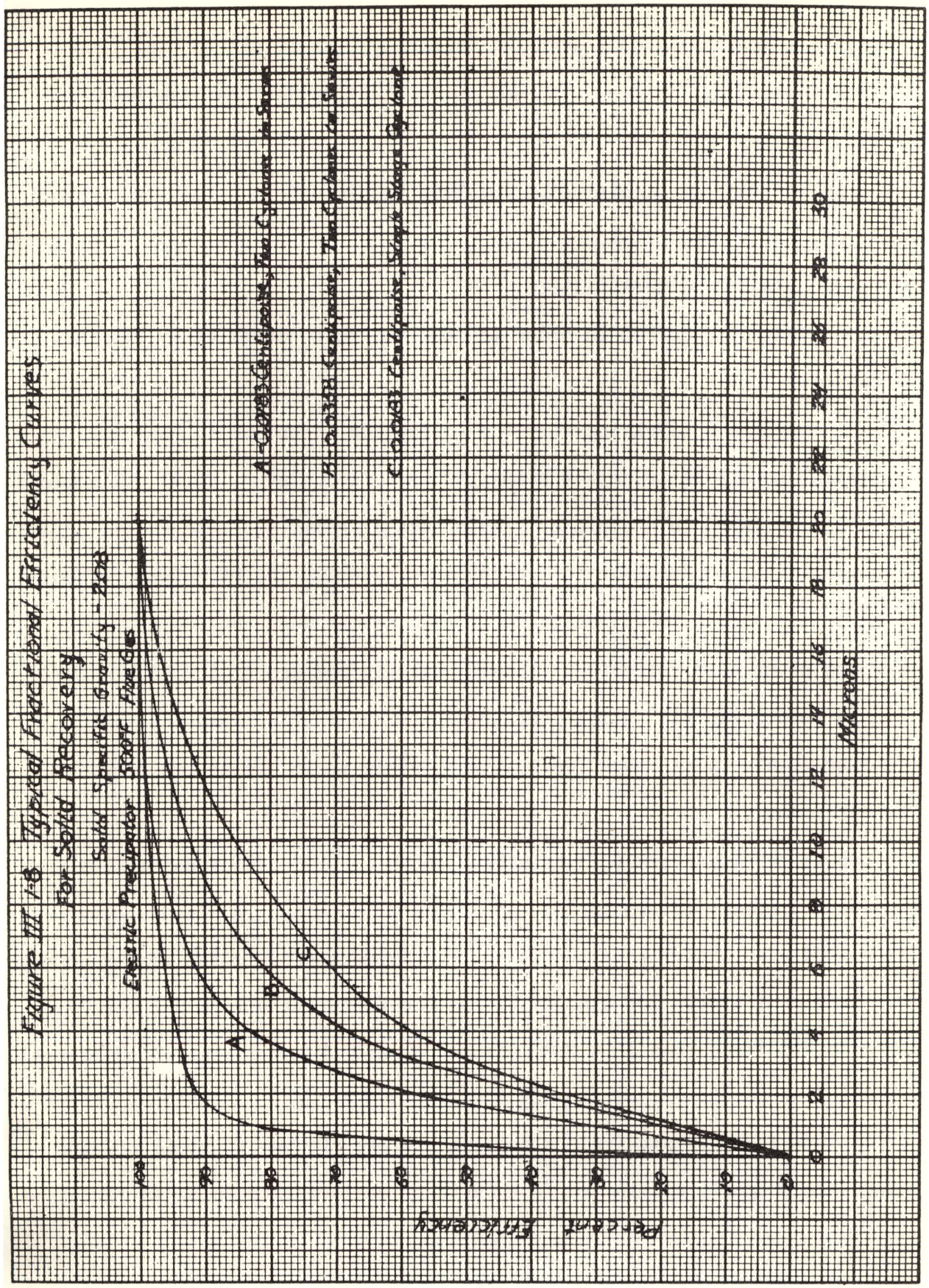
Figure III-8 Typical Fractional Efficiency Curves
For Solid Recovery
Solid Specific Gravity - 2.08
Electric Precipitator Room Fine Ore
A-Conventional Cyclone, Two Cyclones in Series
B-Cottrell Precipitator, Two Cyclones in Series
C-Cottrell Precipitator, Single Cyclone Overload
Percent Efficiency
Microns

entering the two stage cyclones at the top of the heat exchanger are cooled to 500° F.

To reduce the solids loading of primarily 0 to 10 micron particles in the gas leaving the cyclones, three dust collection devices have been considered namely;

(1) electrical precipitator followed by cyclones

(2) sonic precipitators.

(3) stainless steel filters.

Further study is required in order to make the most economically feasible selection.

In the carbon black industry the collection is unique in that the electrical precipitator serves primarily as a flocculator, final collection being accomplished in a cyclone. The effect of gamma and beta radiation and high electrical conductivity of graphite in reducing the efficiency of the precipitator should be investigated if this device were considered for the proposed plant dust collection system. Largely because of the high maintenance associated with electrical precipitators in the fluid catalytic cracking plants it is deemed desirable to avoid their use in the proposed nuclear plant.

Sonic precipitators (43) have been shown to give efficiencies similar to electric precipitators in the carbon black industry. A disadvantage associated with their operation is the requirement of dilution gas to operate the sound generator. For example Ultrasonic Corporation type U-2 sound generator (43) requires 1850 CFM measured at 450° F and 1 atm. which represents 15% of the total gas flow in the proposed design. Additional experimental work and cost studies are required before the use of sonic precipitators are properly eliminated from further consideration in a gas fluidized

solid nuclear reactor.

Experience (39) with Micrometallic Corporation stainless steel filters leads the authors to choose this type of collector for 0-10 micron particles. To avoid excessive pressure drop these filters require periodic blow-back to release the filter coke. This is accomplished by admitting high pressure gas to the outlet side of the filter element. The primary advantages of this filter system are low maintenance, simplicity of operation, and ease of decontamination. The filters may be decontaminated with acid wash solution. Graphite plugs may be removed from filters by combustion with hot air.

A major portion of the 0 to 10 micron material is released from the filters into a duct which carries them to the chemical processing plant. The remainder of the 0 to 10 micron particles are returned to the reactor.

III 1.5 Power Cycle

One of the important advantages of the fluidized system being studied is that the reactor materials used are capable of withstanding high temperatures, and therefore, a high temperature, high efficiency power cycle can be utilized. On the other hand from an economic standpoint the lower temperature and pressure conditions may result in a lower overall investment per kilowatt. The effect of temperature and pressure on the overall cost per kilowatt of the plant is apparently not too well known and is a deciding factor in this comparison. One study (38) that was made on this effect shows that the cost per kilowatt increases with temperature, whereas a more recent study being made by J. Maloney at ORNL shows just the opposite effect. A study of this nature can hardly be made from existing cost data because of the many variables such as location, type of plant, company engineering

standards, plant capacity, and many others. It would seem that the only reliable study of this kind would be one made by a large consulting firm which specializes in building power plants. Such a firm would have the wealth of information and talent required to make such a study. Even then many estimates would have to be made since data on low pressure high capacity plants are non-existent.

In order to evaluate the effect of the steam cycle on the system fissionable material holdup, five standard steam conditions from 600 psi. to 1800 psi were selected. A simple cycle without feedwater heaters was selected with the belief that the fissile material holdup would be a minimum for this type of cycle. Further calculations (See appendix VIII 2) showed that this is not quite true. A cycle without feedwater heaters would have approximately six and one-half % more holdup per kilowatt than a cycle with feedwater heaters. This would amount to $260,000 in investment based on a 100 kilogram holdup and a U-233 cost of $40,000 per kilogram. It seems doubtful that five feedwater heaters and the additional building space required would cost over $260,000. It is obvious that a more detailed study would be required before a decision could be made on the advisability of installing a regenerative cycle.

Table III 1-12 shows the heat absorbed in each section of the plant and the generator output for the five steam conditions mentioned. It will be noticed that the heat absorbed in the superheater increases with temperature and pressure while the heat absorbed in the boiler decreases. This has the effect of increasing the total heating surface required and therefore the total holdup. Table III 1-13 shows the heating surface required for each steam condition and the resulting investment cost per kilowatt of capacity.

The base cost for this study was obtained from the Detroit Edison-Dow Chemical Study (5) made for the AEC. It was assumed that the volume would vary directly with the area and it will be noticed that there is a considerable increase in area with pressure and temperature. It will also be noticed though, that this increased cost is more than offset by the increased output and that the overall cost per kilowatt goes down. The increased cost per kilowatt due to increased temperature was obtained from Sidney Siegel's study (38) and as mentioned earlier may not be correct. Also any investment effect caused by temperature and pressure would not necessarily be the same for both a conventional plant and a nuclear plant. In fact this effect may not be as pronounced in a nuclear plant since both the superheater section and the steam generating section will be much smaller than for a conventional plant.

It is apparent that the variation in investment cost per kilowatt of capacity for different pressures and temperatures is small and a more detailed study would have to be made before selecting a particular set of steam conditions. If there is no difference or a negligible difference in cost between the high pressure and low pressure, the low pressure cycle should be favored because of lower maintenance cost and better reliability.

Figure III 1-9 shows a typical cycle. The pressure and temperature conditions of 850 psi and 900° F, respectively, are merely typical values and are not to be construed as the cycle recommended for this type of reactor plant. With a regenerative cycle, the superheater would preferably be placed in the blanket. The additional heat transfer area required, in replacing the preheater (as planned for the non-regenerative cycle) by a superheater, can be installed in the blanket without any increase in fissile material holdup. On the other hand, the corresponding decrease in heat

transfer surface required in the heat exchange vessel would greatly reduce the holdup in that vessel and thus in the entire plant. A second, but less important advantage that could be gained by having the superheater in the blanket is that the steam will not become nearly as radioactive in this high neutron flux region as a corresponding volume of feedwater. With this arrangement an insulation would be required outside of the tube wall to prevent boiling of feedwater serving as gamma shield around the blanket. There are disadvantages in using heating surface in the blanket but the advantage of savings in holdup should outweigh these disadvantages. One disadvantage is that it will take several months for U-233 to build up in the blanket and bring the power in the blanket up to the design value of 13 percent. During this period it will be necessary to operate at ten to fifteen per cent reduced power.

In the cycle using the blanket as a preheater, it will be necessary to design the steam connections for thermal shock caused by the relatively cold water being fed directly into the boiler.

Another advantage of this type of reactor plant is that a superheater does not increase the holdup nearly as much as it does with many of the homogeneous liquid fuel reactors. The reason for this is that the ratio of the overall heat transfer coefficient for the boiler to that of the superheater is around 1.5 to 1 whereas it is several times higher in a homogeneous liquid metal type reactor. The higher superheat possible eliminates the erosion problem on the last stage blades of the turbine and eliminates the necessity of having a moisture separator. Typical calculations for overall heat transfer coefficient are included in Appendix VIII 2-2.

TABLE III 1-12

Steam Cycle Data for Various A.S.M.E. - A.I.E.E. Preferred Standard Steam Conditions

Pressure at throttle	psia	600	850	1250	1450	1800
Temperature at throttle	°F	825	900	950	1000	1100
Condenser Back pressure	In. Hg.	1	1	1	1	1
Heat input to reactor	Meg.	250	250	250	250	250
Temperature to preheater	°F	79	79	79	79	79
Drum pressure (10% S.H. drop)	psia	660	935	1375	1600	2000
Saturation temperature	°F	497	536	585	605	621
Feedwater temperature to drum	°F	447	486	535	555	571
Heat absorbed in preheater	%	27.6	30.2	34.8	35.4	35.6
Heat absorbed in boiler	%	56.5	51.5	46.6	42.1	37.5
Heat absorbed in superheater	%	15.9	18.3	18.6	22.5	26.9
Heat absorbed in preheater 10^8	Btu/hr	2.35	2.58	2.96	3.02	3.04
Heat absorbed in boiler 10^8	Btu/hr	4.81	4.38	3.97	3.58	3.20
Heat absorbed in superheater 10^8	Btu/hr	1.36	1.56	1.59	1.92	2.29
Throttle flow	1000 lb/hr	622	605	614	593	572
Generator output	Meg.	79	82.7	85.2	87	90.2
Thermal efficiency	%	31.6	33.1	34.1	34.8	36.1
Heat rate	Btu/kwh	10800	10300	10010	9815	9450

TABLE III 1-13

Heat Exchanger Surface Required For Various Steam Cycles

Based on Solids To Wall Film Coefficient of 100 Btu per Hr.-Sq. Ft.-°F

Pressure	psia		600	850	1250	1450	1800
Temperature	°F		825	900	950	1000	1100
Surface required in 1000 Sq. ft.							
Preheater			2.12	2.30	2.69	2.77	2.8
Boiler			5.08	4.99	4.77	4.40	4.0
Superheater		*	2.08	2.74	2.97	3.87	5.05
Total			9.28	10.03	10.43	11.04	11.85
Relative Surface Required			1	1.081	1.126	1.150	1.277
Overall Inv. Cost Per KW Assuming a base of $310./KW at $40.00 per gram for U^{235}							
50 Kg holdup			$310.00	$298.00	$290.50	$286.00	$277.50
100 Kg holdup			335.50	325.00	318.00	313.50	306.00
150 Kg holdup			361.00	350.00	343.50	341.00	334.00
**Increased Cost per Kw Due to Temp.			----	13.00	20.00	28.00	42.00
Total Plant Cost per Kw							
50 Kg holdup			310.00	311.00	310.00	314.00	319.50
100 Kg holdup			335.00	338.00	338.00	341.50	348.00
150 Kg holdup			361.00	363.00	363.50	369.00	376.00

* Based on low carbon steel tubing

** See Fig. 3, p. 69, TID-72, Sidney Siegel, "AHigh Temperature Reactor for Power Breeder Application" Report NAA-SR-147

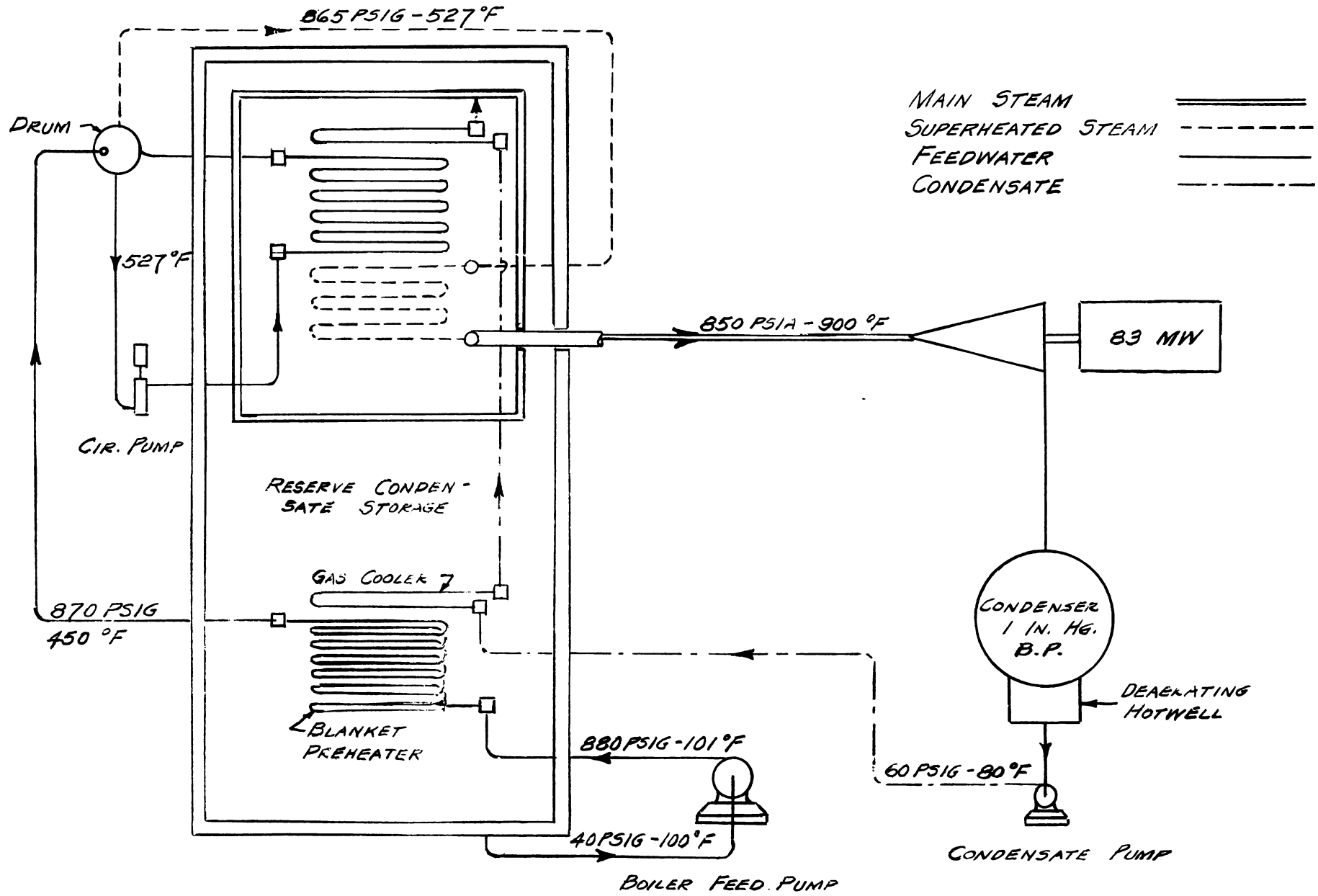

FIGURE III 1-9 TYPICAL STEAM & WATER CYCLE

III. 1.6 Heat Exchanger

The heat exchanger for this reactor plant must satisfy the requirements of a steam generator and superheater as well as the requirements for fluidization. In many respects these requirements are in conflict.

Since highly enriched uranium will be used, the holdup will be one of the major design factors. The smallest holdup can be obtained by using small diameter closely spaced tubes, small particle size, high gas velocity through the bed, and high bed temperature. These parameters have to be balanced against such things as strength of materials at high temperatures, solids carryover from the bed, solids attrition rate, pressure drop, and pumping power.

The small particle diameter and high gas velocity are desirable in order to obtain the highest possible heat transfer coefficient. Figure III 1-10 shows heat transfer plotted against particle size at four different gas conditions. Table III 1-14 gives all the physical constants and the correlations used for obtaining these heat transfer coefficients. It will be noted that these heat transfer coefficients are for a bed temperature of 1500 degrees fahrenheit. Heat transfer does increase slightly with temperature and this is shown in Table III 1-14. The 200 micron size at one foot per sec. was calculated for both 1500 degrees Fahrenheit and 2000 degrees Fahrenheit. The heat transfer coefficient was increased by about six per cent. The main advantage of higher bed temperature is the higher temperature differential between the fluidized solids and the heat transfer surface. The effect of particle size and bed velocity are discussed in more detail in the section on Heat Transfer in a Gas-Solid System. Three particle sizes 60, 200, and 600 microns and two bed velocities one ft. per sec. and two ft. per sec.,

TABLE III 1-14

Typical Convective Heat Transfer Data For Graphite Particles Fluidized with Argon

D_p x 10^4 ft.	Velocity Ft/Sec.	Temperature °F	G $\frac{\text{Lb.}}{\text{Ft}^2\text{-Hr}}$	μ $\frac{\text{Lb.}}{\text{Ft-Sec x } 10^5}$	$\frac{D_pG}{\mu(1-\epsilon)}$	j_{ht}	h_t	h_{tc}
1.97	1	1500	101	3.82	.575	4.43	81.0	109
6.56	1	1500	101	3.82	2.83	1.63	30.4	41
6.56	1	2000	80.4	4.44	1.83	2.21	32.2	43.5
19.68	1	1500	101	3.82	4.12	1.03	18.9	25.5
1.97	1-2 Atm.	1500	202	3.82	1.3	2.63	97.5	131
6.56	1-2 "	1500	202	3.82	7.15	.93	34.7	46.8
19.68	1-2 "	1500	202	3.82	8.91	.62	23.0	31
1.97	2	1500	202	3.82	1.31	2.60	97.0	130
6.56	2	1500	202	3.82	8.71	.855	31.9	43.1
19.68	2	1500	202	3.82	11.0	.756	20.9	28.2
1.97	.0033	1500	.334	3.82	.0012	270	16.35	22.1
6.56	.0238	1500	2.40	3.82	.022	33.9	14.75	19.9
19.68	.132	1500	13.35	3.82	318	5.14	12.41	16.80
	For Fluidized Graphite and Thorium Carbide Particles							
6.56	.137	2000	11.1	4.44	.091	13	26.2	35.4
19.68	1.42	2000	11.5	4.44	2.81	1.18	24.5	33.1

Reference: W. B. Gamson, Chemical Engineering Progress 47, 19 (1951)

D_p = Particle diameter

G = Mass flow of gas

μ = Viscosity

C_p = Specific heat of argon=.126 for all temperatures

h_t = Film coefficient

h_{tc} = Film coefficient corrected to commercial data

Equations Used

$$j_{ht} = 2.00 \times \left[\frac{D_p G}{\mu(1-\epsilon)}\right]^{-.69} \times (1-\epsilon)^{-.3}$$

$$h_t = j_{ht} \times C_p \times G \times \left(\frac{C_p \mu}{k}\right)^{-.67} \qquad \frac{C_p \mu}{k} = .58$$

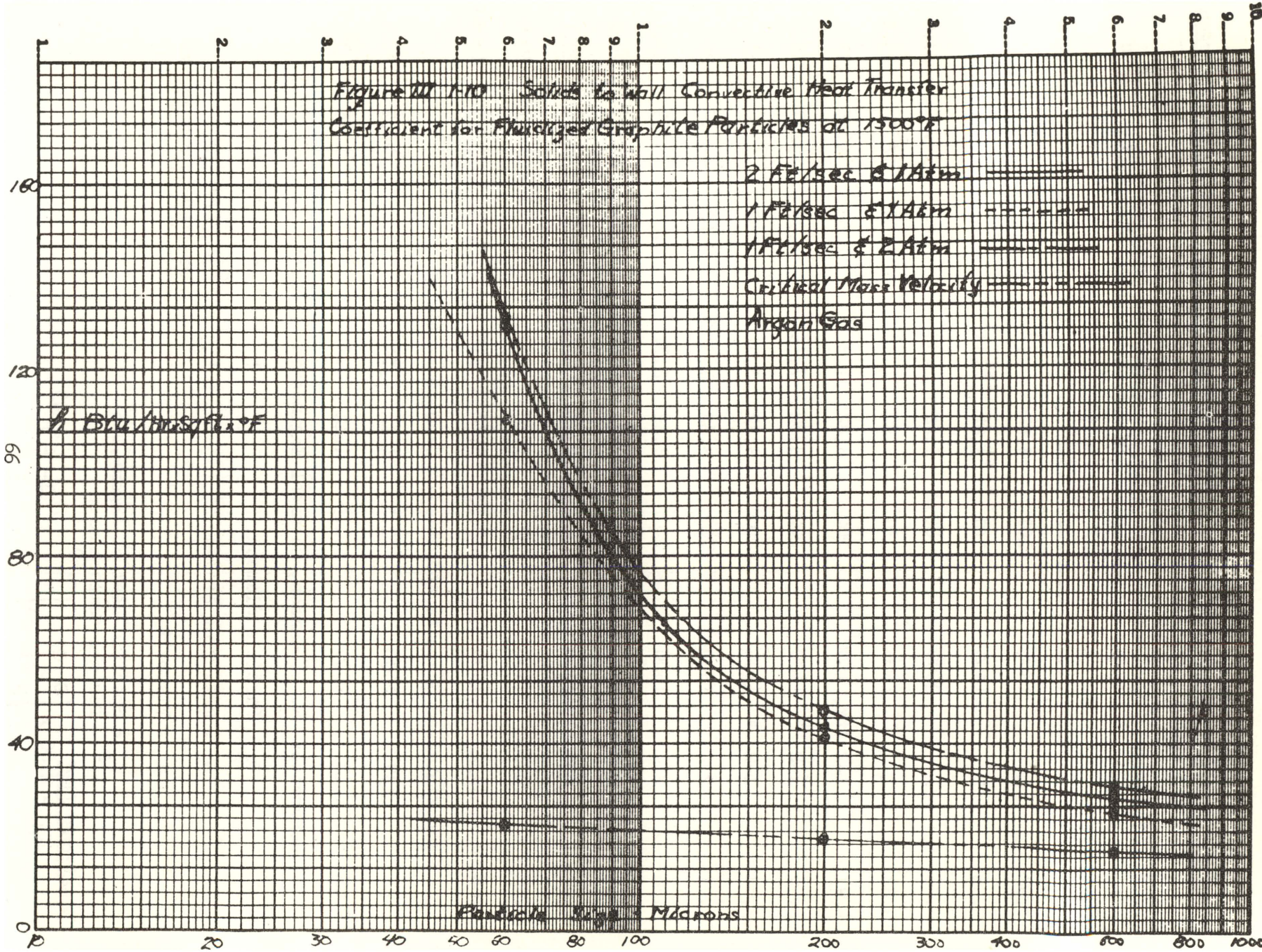
Figure III 1-10 Solids to Wall Convective Heat Transfer Coefficient for Fluidized Graphite Particles at 1500°F
2 Ft/sec & 1 Atm
1 Ft/sec & 1 Atm
1 Ft/sec & 2 Atm
Critical Mass Velocity
Argon Gas
h Btu/hr-sq ft-°F
Particle Size - Microns
0
40
80
120
160
10
20
30
40
50
60
80
100
200
300
400
600
800
1000

Dwg. 22884

which bracket the range of commercial fluid catalytic working vessel operating conditions, were used for evaluating the holdup in the heat exchanger and the total system.

As mentioned in the section on fluidization, the effect of close tube spacing and tube arrangement in the bed on fluidization is unknown and special studies will be required. Three inch and five inch tube spacings were arbitrarily selected as being the minimum spacings for which fluidization might be possible. Table III 1-15 shows the results of a total core and heat exchanger holdup evaluation for these tube spacings for a 600 psi steam cycle and 1500 degree fahrenheit bed temperature. This bed temperature is based on a minimum temperature drop across the heat exchanger of 500 degrees and an arbitrarily selected maximum core temperature of 2000 degrees Fahrenheit. Figure III 1-11 shows a plot of the data in Table III 1-15.

A one inch O.D. tube was also arbitrarily selected for these studies as the minimum size tube satisfactory from a structural stand point. Further study might prove that a smaller size could be used, However, it believed that tubes supports would then become quite a problem. From the standpoint of economy the smallest tube diameter structurally possible is the optimum.

Pressure drop and pumping power in the steam and water sections are not important factors. The heat transfer coefficient can be varied considerably on the water side of the preheater and boiler tubes without appreciably affecting the overall heat transfer coefficient. Since this is true, a velocity as low as one ft. per sec. can be used in the preheater section, and the resulting pressure drop is almost negligible. This is not true however, in the boiler section where a higher velocity is required in order to keep the tube wet at all times and prevent scaling. With one inch tubes

TABLE III 1-15

Heat Exchanger Hold-up Volume For Various Particle Sizes

D_p Microns	Gas Velocity Ft/Sec.	1 In. Dia. Tube Spacing Inches	Flow Area Sq.Ft.	Heating Surface Sq. Ft.	Height. Feet	Volume Cu.Ft.	Gas and Solids Volume Cu. Ft.	Solids Volume Cu. Ft.
60	1	3	423	24	3.06	1760	1605	401
200	1	3	423	24	7.5	4320	3940	710
600	1	3	423	24	11.75	6760	6160	2160
60	2-1Atm. 1-2Atm.	3	211	17	5.2	1500	1370	301
200	"	3	211	17	13.25	3830	3490	454
600	"	3	211	17	19.5	5640	5140	1665
60	1	5	423	22.5	9.7	4900	4750	1190
200	1	5	423	22.5	24.1	12200	11800	2120
600	1	5	423	22.5	37.5	19000	18400	6440
60	1-2Atm	5	211	16	16.4	4190	4050	890
200	"	5	211	16	41.0	10500	10200	1325
600	"	5	211	16	61.0	15600	15100	4900

Core Hold-up

D_p Microns	Core Radius Feet	Core Volume Cu. Ft.	PerCent Voids	Solids Volume Cu. Ft.	Critical Mass KG
60	5.25	626	60	242	46.8
60	5.66	759	60	303	48
200	4.26	322	48	167	26.5
600	4	205	40	123	19.5

Above data based on steam cycle for 600 psia at 825° F

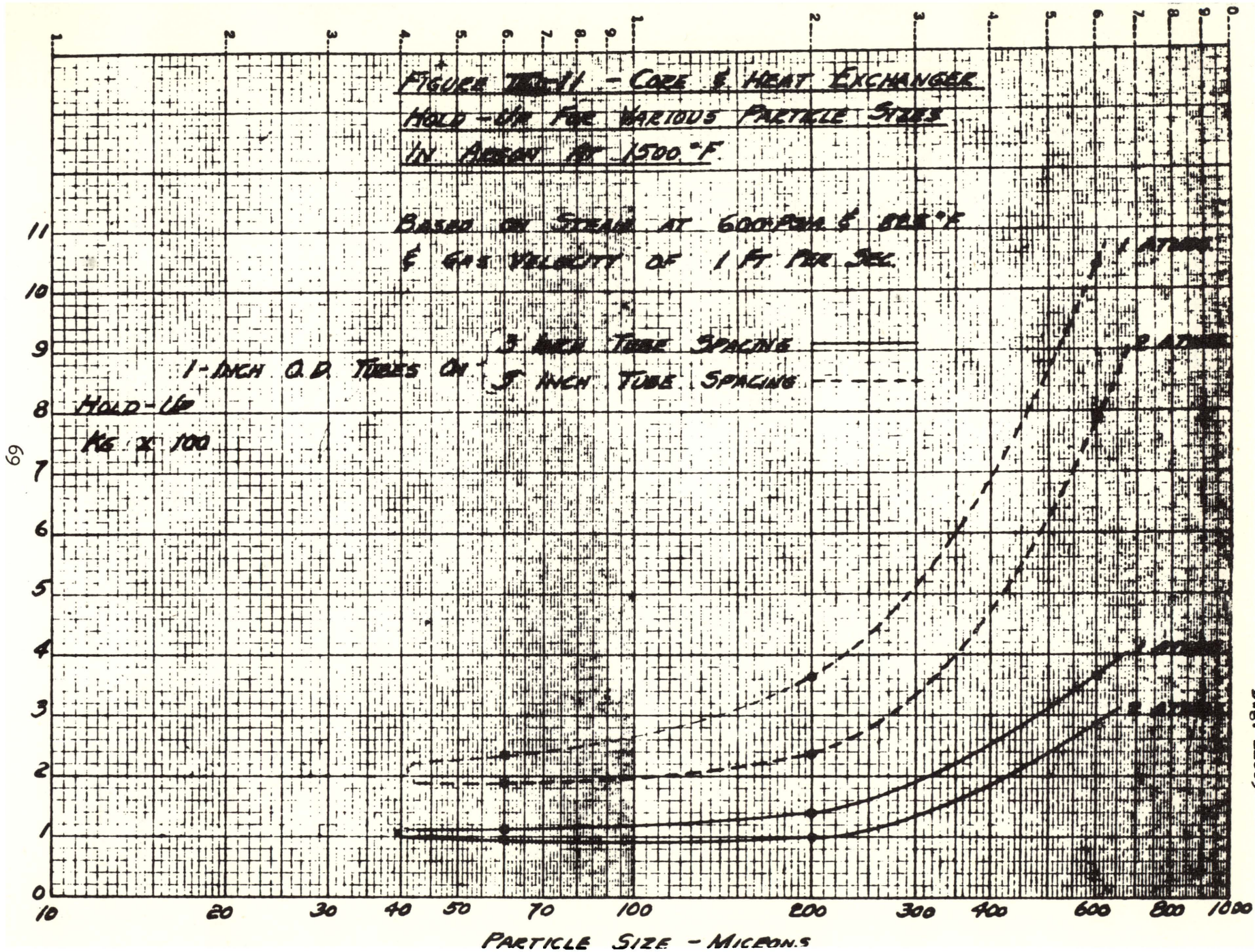
FIGURE IV-11 - CORE & HEAT EXCHANGER
HOLD-UP FOR VARIOUS PARTICLE SIZES
IN AGESA AT 1500°F
BASED ON STEAM AT 600 PSIA & 850°F
& GAS VELOCITY OF 1 FT PER SEC.
1-INCH O.D. TUBES ON
3 INCH TUBE SPACING
3 INCH TUBE SPACING
HOLD-UP
KG X 100
1 ATMOS.
2 ATMOS.
PARTICLE SIZE - MICRONS

Dwg. 22885

natural circulation will not be satisfactory and it will be necessary to use controlled circulation. With this type of circulation there is an orifice and strainer assembly at the entrance to each tube, and this orifice accounts for most of the pressure drop in the system. The heat flux in this type of boiler would be several times higher than in a conventional boiler, and therefore the number of tubes and the pressure drop might be less. This does not mean however that the pumping power would be less since a higher circulation rate will probably be required for this boiler design. In any event it does not appear that the pumping power for this boiler would be any higher than for a conventional boiler.

The velocity in the superheater has a more pronounced effect on the overall heat transfer coefficient and will have to be kept fairly high. At 70 ft. per sec. this pressure drop is not appreciable since the superheater elements will be quite short compared with conventional superheater elements. The effect of higher heat flux on size is more pronounced in the case of the superheater than it is for the boiler since the heat flux for this superheater is 10 to 15 times higher than for a conventional superheater.

For minimum holdup and minimum resistance to the flow of gas required for fluidization, it appears necessary that the tubes be placed in a horizontal position. This arrangement is suitable for the superheater elements, but is not considered good practice for steam generating tubes. It is difficult to keep the top of the tube wet and as a result the water is evaporated to complete dryness and a film of scale is deposited on the tube. This film raises the tube metal temperature and may thus cause a tube rupture. The Navy has an experimental boiler with horizontal tubes in operation and while the results of this experiment are not known, it is believed that with high enough tube velocities this type of tube

arrangement can be made to operate satisfactorily. A higher recirculation ratio would be required and this would increase the pumping power required by the circulation pump. This increased pumping power will e asily be offset by the savings in holdup of this arrangement over a vertical tube arrangement if the tubes could then be placed only around the periphery of the heat exchanger. This latter tube arrangement would probably require a number of smaller heat exchangers in order to get in all the heating surface, and this would further complicate the operating and design problems. Approximately 300 horse-power will be required for the boiler circulating pump.

The present design has been based on an arrangement such that the heat exchanger will be box shaped with one inch tubes forming water walls in the fluidized bed area. A water wall design now being used by the Combustion Engineering - Superheater Inc. is proposed. The Combustion Engineering design employs 1-1/4 inch tubes with 3/8 inch rods welded in between to form a pressure tight wall, while the wall for this heat exchanger would use 1 inch tubes with 1/4 inch rods as spacers. This type of wall is fabricated in sections so that there is a minimum of welding to be done in the field. This vessel would be fairly complicated since all the 1 inch boiler and superheater elements in the bed would have to pass through the water wall. This type of vessel can be fabricated, though, since the same problem is encountered in a conventional steam boiler and these walls have been constructed to withstand a positive pressure of 16 inches of water.

Table III 1-15 gives the vessel dimensions for several different conditions. The width is dictated by the gas flow area required. While calculations were also made for a gas pressure of two atmospheres, this condition does not seem to be practical because of the reinforced construction

that would be necessary to withstand this pressure. These latter results are, however, almost directly applicable to the case employing a two foot per second gas velocity at one atmosphere except for the greater particle entrainment at the higher velocity and the resulting greater load on the cyclones.

Many of the bed heights shown in Table III 1-15 would probably not be practical because of the high pressure drop across the bed. It would be very desirable to keep the entire gas system below atmospheric pressure to prevent outward leakage that would create a hazard to personnel. This becomes very difficult to obtain because of the very low pressure which would be necessary on the suction side of the blower. The vessels for either the 9.7 ft. or preferably the 3.1 ft high beds for 60 microns particle size and one ft. per sec. velocity could probably be fabricated without an excessive amount of reinforcing.

One of the most difficult problems in the heat exchanger design is the distribution plate support. This support must extend across almost the entire width of the vessel. It is in a high temperature zone (about 2000°F). The distribution plate has many small holes in it for distributing the flow of gas and solids into the bed. Since the gas velocities through this plate will be extremely high there will be an erosion problem. Silicon carbide has been proposed as the material for this plate since it has excellent resistance to erosion at high temperatures. The plate support problem can probably be solved by using a water cooled grid formed out of two or three inch O.D. tubes. The distribution plate could be formed out of silicon carbide bricks anchored to the tube grid or suitably shaped to fit around the tubes. Feedwater may be used as the coolant. The heat transfer is expected to be poor in this so the thermal stress in the tube wall should

be small. Thermal stress calculations were made and the total stresses obtained for the various section were found to be within the allowable stress for the material being used. The worst conditions would be in the superheater elements where an alloy steel would be required at 900°F and 1000° F. The thermal stress was also calculated for the transport line and feed line which are surrounded by approximately 100° F water and these stresses were within the allowable limit for low carbon steel.

III 1.7 Gas Blower

Since it appears desirable that the gas cycles be operated at a negative pressure of a few inches of water, a conventional type fan or blower can be used. It will be necessary, however, to supply gas to the shaft seals to prevent inward leakage of air along the shaft. This can be done by maintaining a small differential in pressure between the sealing gas and the gas on the inside of the blower casing. The amount of gas leaking in along the shaft will have to be removed at another point in the cycle to keep the system in balance and under a negative pressure at all times. This leakage can be held to a minimum by close clearances and packing, and the gas bled off the cycle can be sent to a chemical processing cycle for the removal of the gaseous fission products. See Fig. III 3-1.

A total of four half-capacity blowers should be used so that there would always be two in reserve. These blowers could be located in a separate shielded room adjacent to the heat exchanger shield or core shield. With this arrangement it is conceivable that by using temporary shielding between the blowers they could be inspected periodically and minor maintenance work could be performed.

All the piping in this room and the blowers would have to be heavily

insulated to keep down the ambient temperature. In addition to this it would probably be necessary to have a forced ventilating system exhausting to a stack through filters. Conventional induction type electric motors could be used for the blowers. It will be necessary to provide a water cooled heat exchanger for each motor coil and a cooling water supply for a lubricating oil system for both the motor and blower bearings.

Each blower will have to handle approximately 6200 cfm. of 500 degree Fahrenheit argon and develop a total head of approximately 5 psi. for a 10 foot bed depth. For this service each blower would require 170 shaft horsepower and a 200 horsepower motor could be used. This is based on a mechanical efficiency of 80 per cent for the blower.

A Roots-Connersville positive rotary type blower would probably be best suited for this application. Erosion will be a serious problem for these blowers and the impellers may have to be replaced frequently. A hard surface material could be applied to these impellers although this would introduce another maintenance problem if these materials contain elements that become very radioactive.

The above mentioned blowers are for fluidizing the heat exchanger bed. The core blanket will also be a fluidized bed and will require blowers. The same set of blowers could supply gas to both the heat exchanger and core blanket. However, a separate set of blowers should be more desirable both from the standpoint of safety and maintenance. The gas velocity in the blanket is quite low (.14 ft. per sec.) in order to maintain a high bed density, and therefore these blowers will be relatively small compared to the heat exchanger blowers. Each of these blowers will have to handle 550 cfm. of 500 degree Fahrenheit argon against a head of approximately 8 psi. A 25 horsepower motor will be required.

From the standpoint of safety it would be desirable to have the controls for these blowers arranged so that a spare unit would start up automatically in case of failure of one of the running units.

III 1,8 Core Shell Structure

Graphite was chosen as the material of construction for the core because of its engineering as well as nuclear advantages over metals at high temperatures. Graphite can be molded into various shapes and can be easily machined. It is (presently) being fabricated into cylinders greater than 2-feet diameter and it seems reasonable that a custom order for a 10-12 feet diameter unit could also be filled.

The tensile strength of graphite, as shown in Figure III-1-12 is over 3000 psi and increases as the temperature increases. Thus a 1-piece shell, 10 1/2 feet in diameter can withstand an internal pressure of about 50 psi for each inch of thickness. It has been felt that a 1-piece unit may not be possible and that the core shell may have to be made of overlapping and interlocking slabs or bricks. Consequently, for nuclear calculations, the thickness was arbitrarily chosen as 10 cm (about 4 inches).

The erosion resistance of the graphite is not too high. Thus it is recommended that all surfaces subject to wear be coated with silicon carbide.

III 1-9 Blanket Wall

The blanket has been designed for the presence of a tube wall at the periphery of the blanket. It has been suggested that the outermost layer of tubes be welded together to form a solid wall which should be capable of holding the solids. A supporting shell can then be placed outside of the tube wall and contain the entire reactor core-blanket vessel. Since this shell will not be directly exposed to any of the hot solids and since

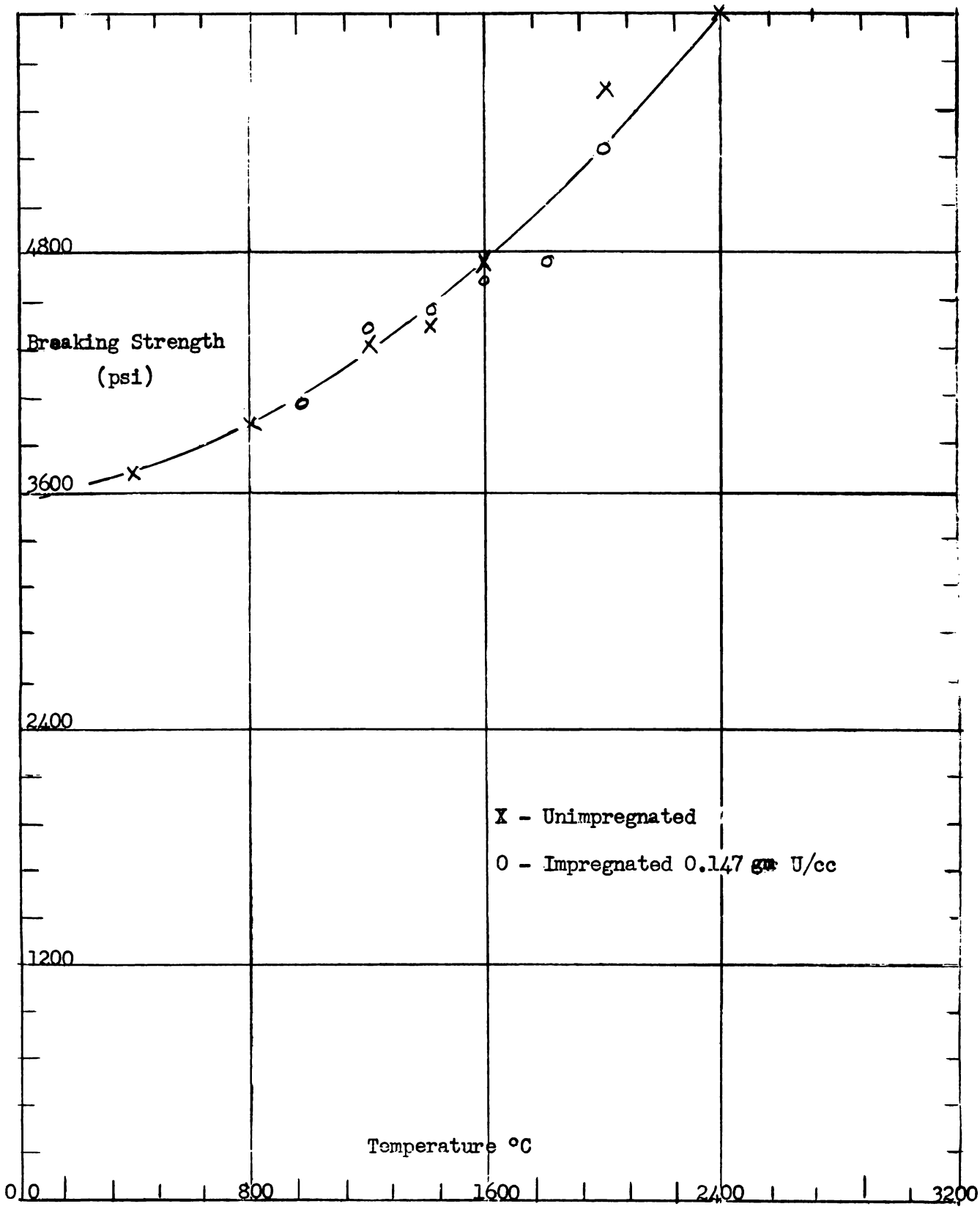

Figure III 1-12

Short Time Breaking Strength of Unimpregnated And Impregnated Grade E.C.A. Graphite (Copied from NAA-SR-151)

it is expected that the shell will be surrounded by a water shield, the temperature of the shell wall will be low. Thus, any available, low cost steel material may be used for this purpose.

III 1-10 Flow Pattern Through The Core

It has been recognized that the most desirable flow pattern of the solids through the core would be one such that all the solids leave the core at exactly the same temperature. This equalization would be approximated if the average velocity of the particle through any given path of travel were directly proportional to the average flux integrated over the same travel path.

In a fairly long, cylindrical core reactor, the above requirement would be fairly closely achieved. The solids flow then approaches a parabolic distribution (measured radially), with the maximum velocity in the center. Similarly, the flux approaches a cosine distribution, also with the maximum at the center. Since the core design proposed in this report is more nearly a sphere or at best a short cylinder, experimental data on flow or temperature patterns would be required to get the optimum design to permit evaluation of a suitable distributor. It may be pointed out that considerable information has already been obtained industrially on the control of flow patterns in moving beds in reaction vessels using special draw off plates at the bottom of the vessel.

III 2 Nuclear Calculations

2.1 General Comments

Though the actual shape of the proposed reactor is cylindrical with approximately conical entrance and exit sections all nuclear results were obtained assuming a spherical homogeneous system.

The fundamental object of this project was to investigate the feasibility of a reactor employing the transportations of solids by gases. Thus two alternatives were available for passing solids into and out of the core. One of these, that of employing a fluidized bed, was investigated from the standpoint of controlability by the simple Fermi Age Theory. The reactivity was found to be very sensitive to the bed height, which is related to voids. A four inch change in bed height, produced by varying the bed density while holding the mass constant, was approximately equivalent to 2% δ K. This sensitivity combined with the doubtful stability of fluidized beds made control of such a reactor questionable, if not impossible. Thus the second alternative, that of a moving bed, was adopted. Such a bed would occupy the whole volume of the reactor core and would be incapable of large changes in density. It is more compact than the fluidized bed and thus requires less fissile material to attain criticality.

Uranium-impregnated-graphite was chosen as the fuel moderator combination. The bed was estimated to have a net density 60% of that of the graphite particles necessitating that 40% of the total volume (termed"voids") be occupied by the gas medium. The blanket consists of a mixture, of thorium carbide and graphite, which occupies 55% of the blanket volume, the other 45% being argon. The core operates at 2000° F and the blanket at 1500° F all absorption cross sections were corrected to these temperatures by the 1/v law. The core and blanket are separated by a graphite shell 10 cm thick. This shell was ignored in all but the final calculations where its absorption was accounted for. The fuel was assumed for cases of calculations to be 100% U-233 in all cases.

2.2 Description of Calculation Methods

Calculation of critical mass and gain was accomplished for numerous systems using the following four methods:

.1 Fermi Age Theory for bare homogeneous reactors and one group of neutrons.

.2 A simplified two group two region method devised by Dr. T. A. Welton (46) but modified to account for the thorium resonance absorption in the blanket. See Appendix (VIII 3.2) for the details of this method.

.3 The standard two group method modified for the thorium resonance absorption in the blanket. See Appendix (VIII 3.2) for the modification.

.4 A two group method worked out by Dr. S. Visner (50) which is similar to the standard two group method but incorporates the effect of thorium resonance absorption , fissioning in the blanket due to uranium buildup, higher isotope buildup, fission product poisons and shell absorption. The method is described in full including derivations in Appendix (VIII 3.2).

2.3 Results And Conclusions of Fermi Age Theory, Welton Method, and Standard Two Group Calculations

2.3.1 Fermi Age Theory - A minimum in the critical mass versus radius curve was observed at about six feet. However, at this radius the thermal utilization was only 88.4 % and the maximum potential breeding gain only 0.20.(Potential breeding gain is here defined as the gain possible assuming that all leakage from the core is captured in fertile material). These figures indicated that it would be necessary to go to a smaller core in order to increase thermal utilization. An alternative to decreasing core size would be to put some thorium in the core and do part of the breeding there. The strong thorium absorption, however, increases the critical mass considerably. A large critical mass in the core did not appear advisable

in this system because of the large holdup outside the reactor in transfer lines and heat exchangers. Therefore the possibility of core breeding was not evaluated further. Putting heat exchange tubes in the core was contemplated but the idea was abandoned for reasons of neutron economy.

2.3.2 Modified Welton Method - Computations were carried out using this method for three different thorium concentrations in the blanket, namely;0.5, 1, and 2 gm. per cc, and the reactor in "startup" condition. "Startup" condition implies that the reactor is at operating temperature but has no fissioning in the blanket, no poisons, and no higher isotope buildup. A blanket thickness of 100 cm, was selected in the belief that it would absorb practically all the core leakage. Curves in Visner's Report (50) indicated that little was to be gained by going beyond a 90 cm blanket with a thorium concentration of 1 gm/cc. In view of the smaller scattering power of this blanket compared to the one on which the curves above were based, there was the possibility that there would be some advantage in going beyond 90 cm. Hence 100 cm was chosen as a convenient figure.

In spite of the highly absorbing blanket, critical masses were found to be considerably less than these calculated by the Fermi Theory. This is not unreasonable since the albedo of the blanket which contains considerable carbon, cannot fail to be larger than the albedo of zero which is an assumption one makes in using the previous method. Other effects noted were a general flattening of the mass-radius curves, a considerable shift of the mass minima to smaller radii of about four feet and a decrease in thermal utilization and potential breeding gain for any given radius. This latter observation led to removal from consideration, at least temporarily, any core greater than four feet in radius.

These calculations also resulted in the selection of 1 gm. per cc. as the thorium concentration in the blanket. It was seen that increasing the concentration to 2 gm/cc increased gain very little but added approximately 15% to the critical mass and, of course, doubled the already large thorium holdup. Dropping the thorium concentration to 0.5 gm/cc decreased the thermal utilization in the core and blanket appreciably and introduced the possibility of considerably more leakage, while decreasing the critical mass less than 10%. Figures III 2-1 and III 2-2 show the effect of thorium concentration on gain and mass respectively. The nuclear constants used in this section are listed in Table III 2-1.

Results of additional calculations made using this method are presented under "Nuclear Calculations For Low Density Beds", later in this report.

2.3.3 Modified Standard Two Group Method - Calculations by this method were completed for the one thorium concentration selected above and with the reactor in "startup" condition. The results were quite close to those obtained by the modified Welton method and hence justified the use of the latter in selecting thorium concentration and in narrowing down the possible radii. The minimum critical mass calculated by this method also occurred at a radius of about four feet. Comparisons of the results discussed thus far are found in Figures III 2-3 and III 2-4. Nuclear constants employed are those for the 1 gm/cc thorium concentration in Table III 2-1.

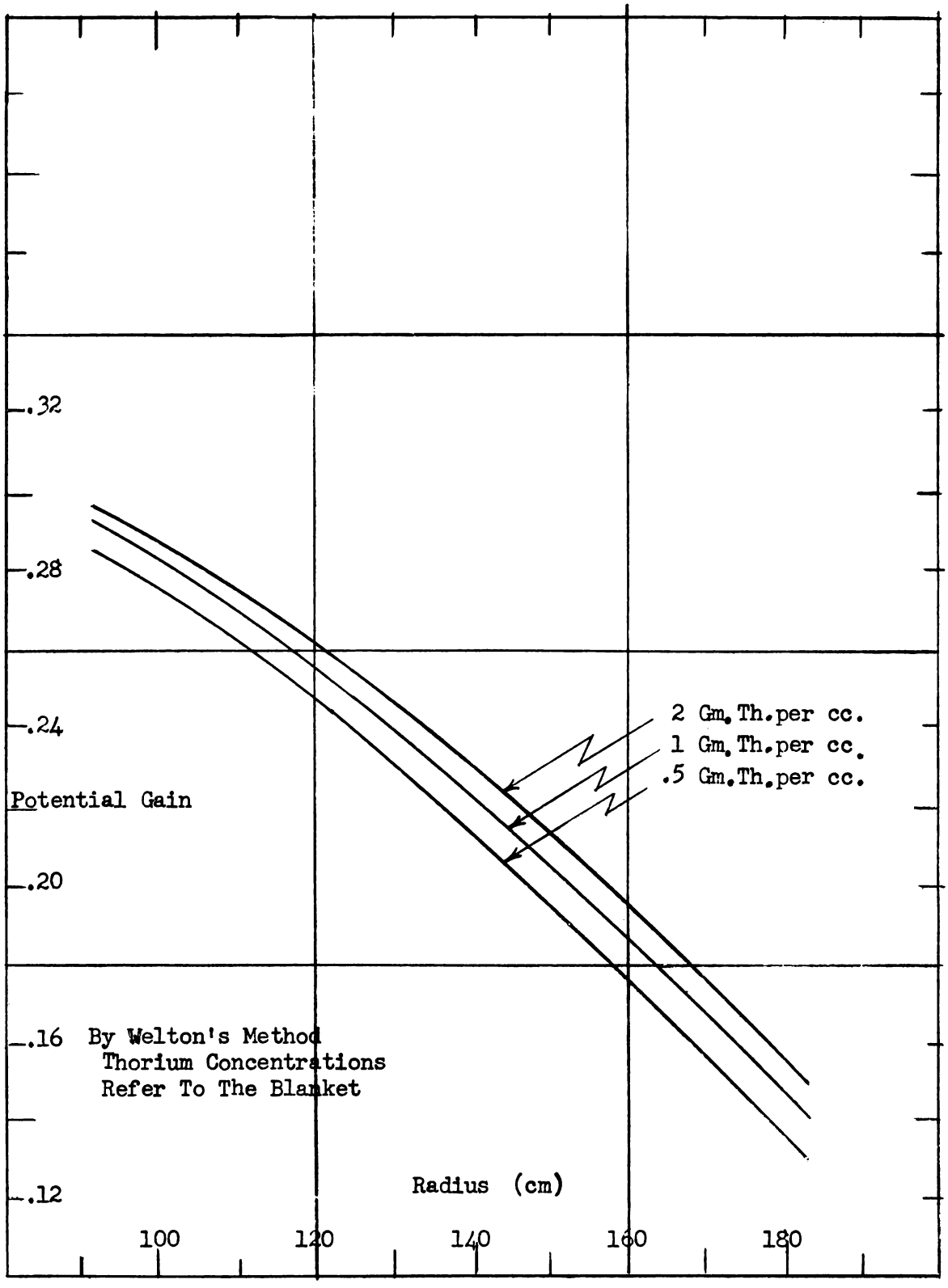

Figure III 2-1

Potential Gain vs. Radius

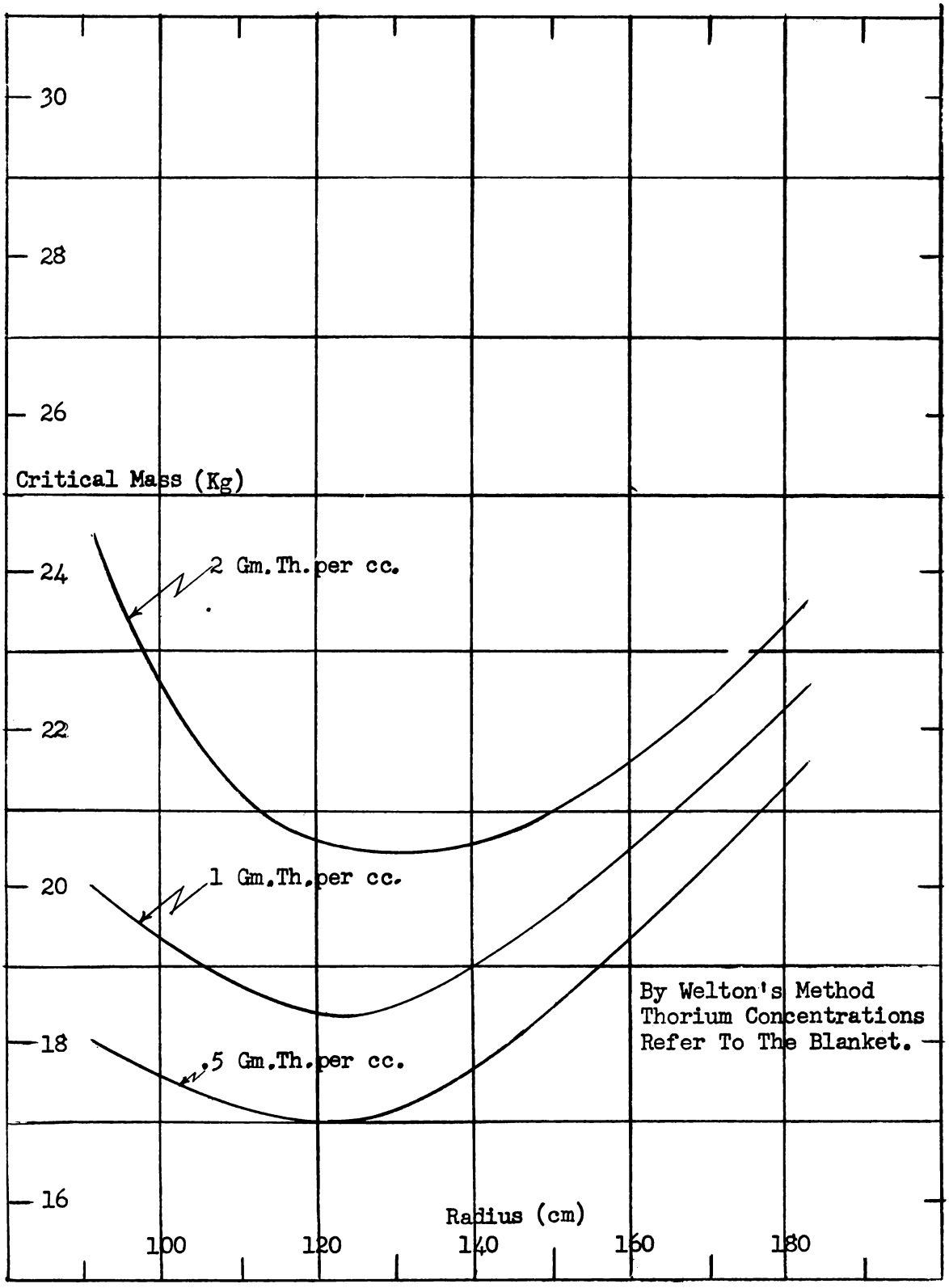

Figure III 2-2
Critical Mass vs. Radius

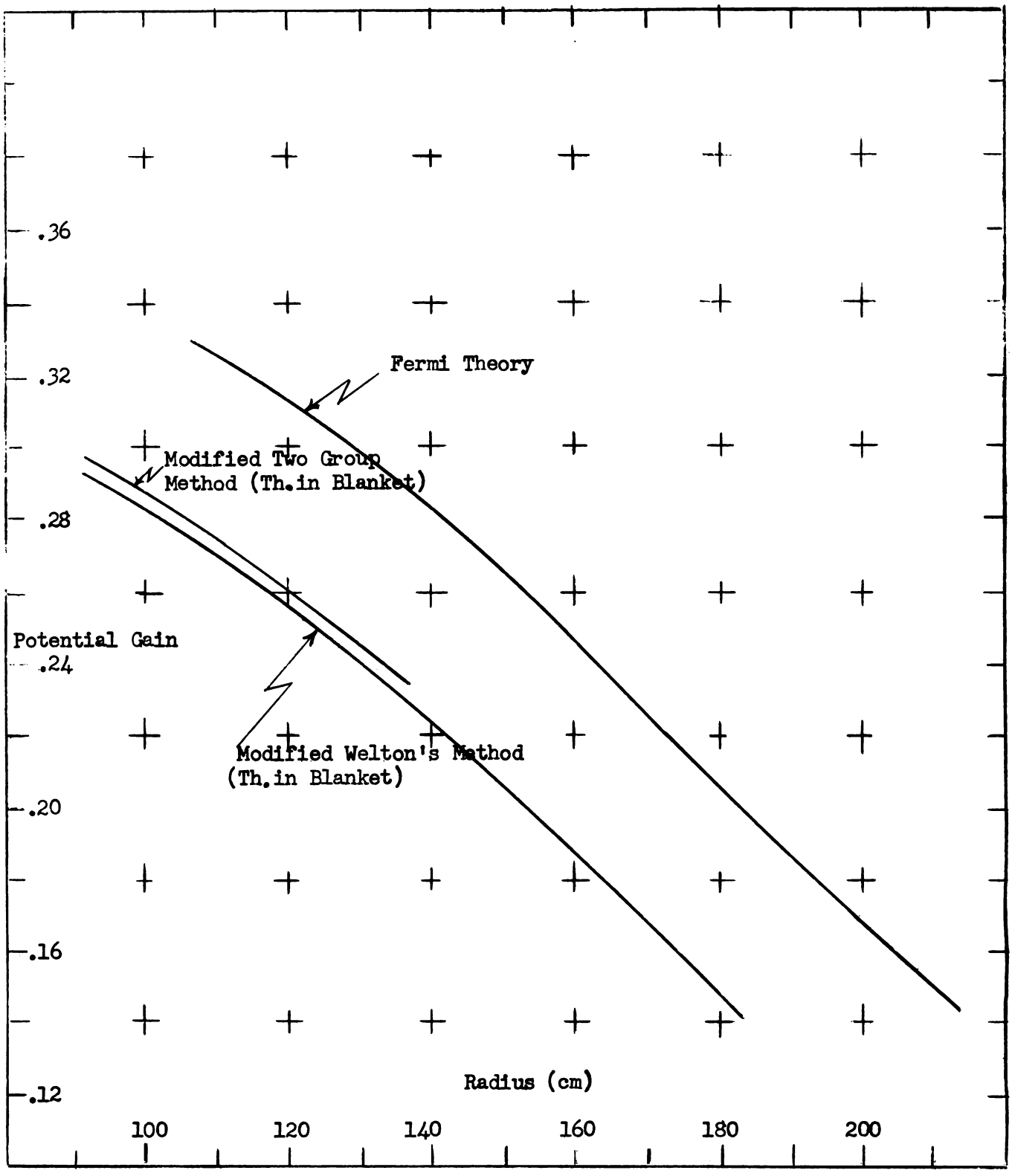

Figure III 2-3
Potential Gain vs. Radius

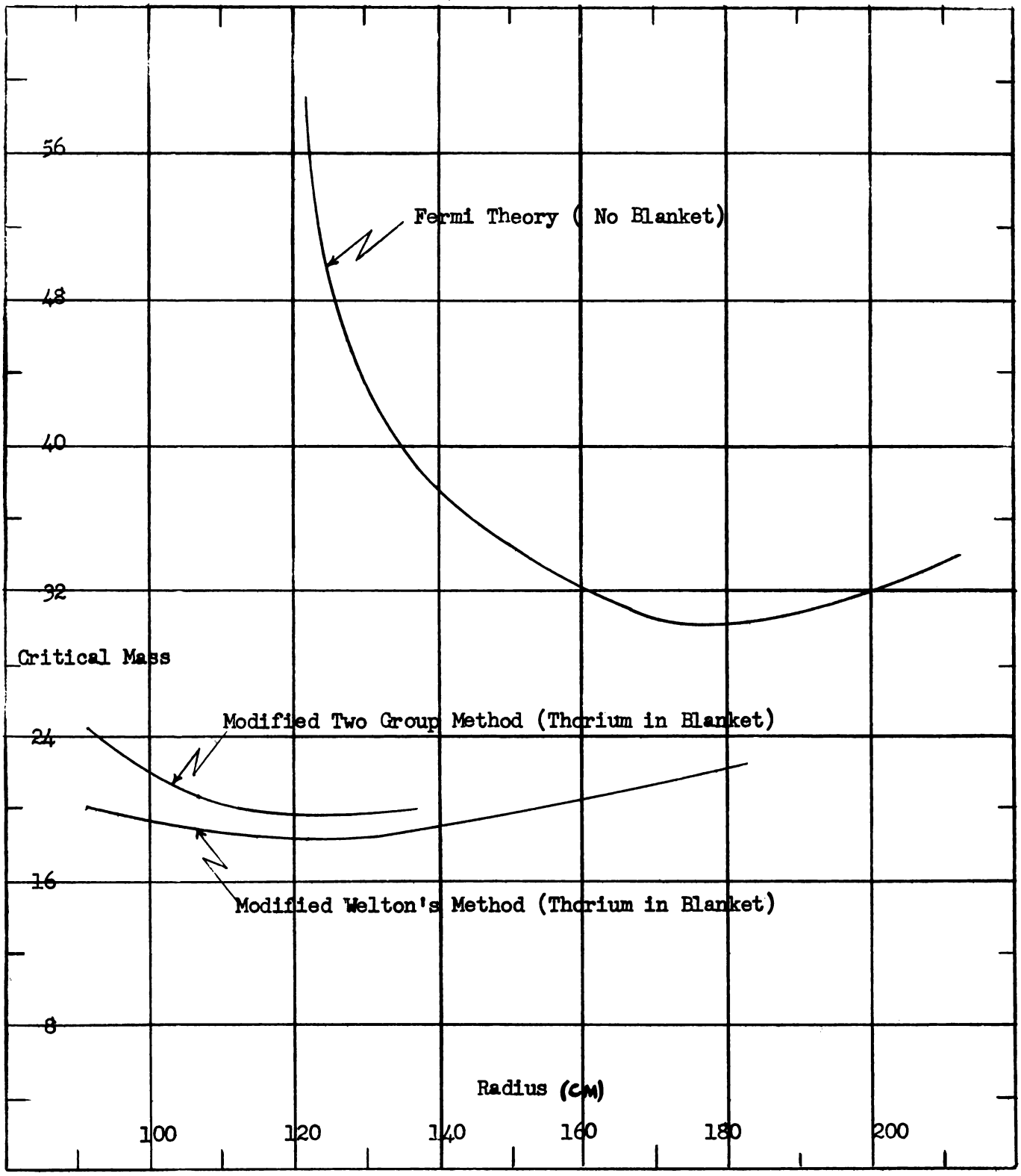

Figure III 2-4

Critical Mass vs Radius

TABLE III 2-1

Nuclear Constants

Welton Calculations on 40% Voids In Core, 45% Voids in Blanket

	Core	Blanket		
		.5 gm.Th/cc.	1 gm.Th/cc.	2 gm.Th/cc.
η	2.33	2.33	2.33	2.33
τ	958	552	379.4	251.2
L_o^2	16,220	345.8	183	78
P	1.0	.295	.1166	.0155
D_s cm	1.488	1.612	1.547	1.478
D_f cm	2.153	2.37	2.193	2.103

2.4 Results of the Visner Method Calculations

2.41 General Comments - Since none of the aforementioned methods were adaptable to calculation of the reactor while in operating condition, the Visner method was applied. The results of calculations by this method are deemed accurate and useful and an attempt has been made to include the effect, on gain and mass, of all the pertinent factors except the moderating effect of the shell. The shell absorption is accounted for in the boundary condition concerning the slow neutron current at the core-blanket interface. The moderating effect,however, is ignored since a three region calculation would be necessary to account for it. Instead, the 10 cm. shell was assumed to be part of the core and the fuel concentration calculation was made on this basis. Since the graphite shell is such a good reflector it was further assumed that the reflector savings of the shell was equal to the thickness of the shell. Hence the fuel concentration above

need not be changed when the shell is considered and a saving in fuel is effected with the shell replacing some core material. A more complete analysis of the shell effect will be found in Appendix VIII 3.2

In the absence of final values for the flux in the core and blanket the fission product poisoning was taken as 2% in the core and 1% in the blanket. Percent poisoning is defined as one hundred times the neutron absorption in poisons per neutron absorbed by the fuel. The values for poisoning vary with four factors, namely, flux, processing cycle, time, ratio of total to core holdup, and cross sections of the poisons consumed. The figures quoted above were based on our best estimates of these variables. Xenon poisoning was not included since it has been assumed that the xenon escapes from the fuel and is removed continuously from the gas or allowed to decay outside the core.

The effect of higher isotopes was assumed to be the same for core and blanket. The equilibrium value of 0.0013 neutrons net loss to higher isotopes per neutron produced in the core, was taken from Visner's Report (2). This equilibrium value is attained in the core in about 2×10^{23} nvt where nv is flux and t is time in seconds. Hence, at a flux of 10^{15} the equilibrium is reached in 2×10^{8} seconds or 2,080 days. The value of .0013 multiplied by η (2.33) gives the neutrons lost per absorption in the core or $\frac{\Sigma_{H.I.}}{\Sigma_{a}^{(28)}}$. This loss amounts to 0.303 %. A more complete treatment of higher isotope buildup is presented in section III 3.2 of this report.

A neutron loss to protactinium was also included though it amounts to as little as 0.15% of the thermal thorium absorption. The above figure corresponds to a flux of $3. \times 10^{13}$ and a process cycle time of 300 days. (See Section III 3.5)

2.4.2 Basis for Calculations

Several systems were investigated making use of the Visner method. The initial work was done on systems specified as follows.

Thickness of Blanket	100 cm.
Temperature of core	2000° F
Temperature of Blanket	1500° F
Thickness of graphite shell	10 cm
Concentration of Thorium in blanket	1 gm/cc
Percent voids in core	40%
Percent voids in blanket	45%
Fission product poisoning - Core	2%
Fission product poisoning - Blanket	1%
Net loss to higher isotopes in core and Blanket	0.303%

With all the factors listed above fixed, there remained only two variables which could affect critical mass; breeding gain, and fraction of power produced by fissioning in the blanket. These variables were the radius of the core and the amount of uranium allowed to buildup in the blanket. Critical conditions were determined for cores of 90, 105, and 120 cm. radii and for 0, 50, and 100 Kg. of U-233 buildup in the blanket. Gains were found for the 120 cm. core with 0, 50, and 100 Kg. buildup. In addition, gains were calculated for the three different radii with 100 Kg. of fissionable material in the blanket. at startup.

2.4.3 Effect of 23 Buildup in Blanket On Critical Mass

Figure III 2-5 shows the effect, on critical mass in the core, of increasing 23 buildup in the blanket for three radii. It is interesting

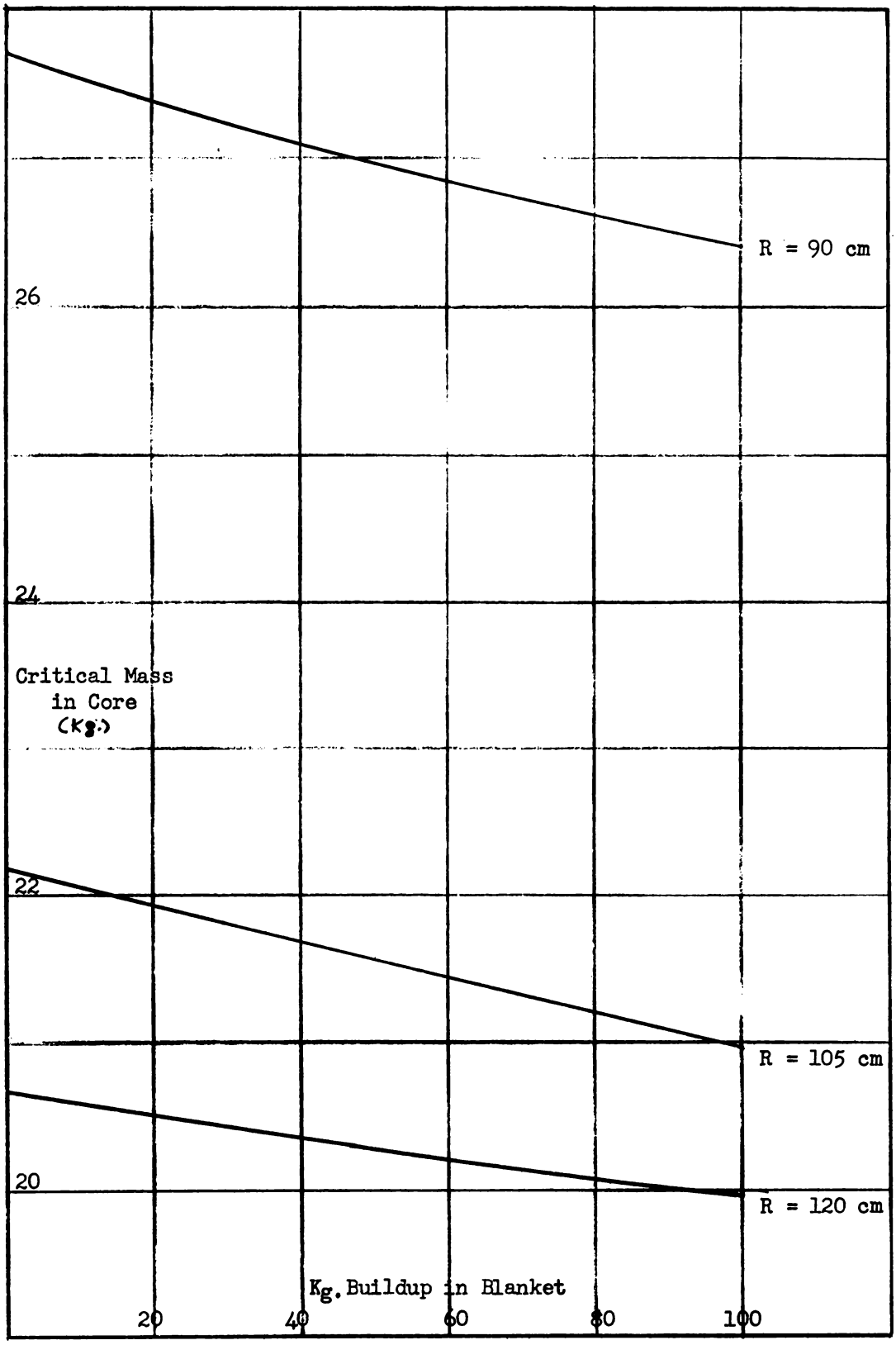

Figure III 2-5

Critical Mass in Core
vs
Kg. Buildup in Blanket

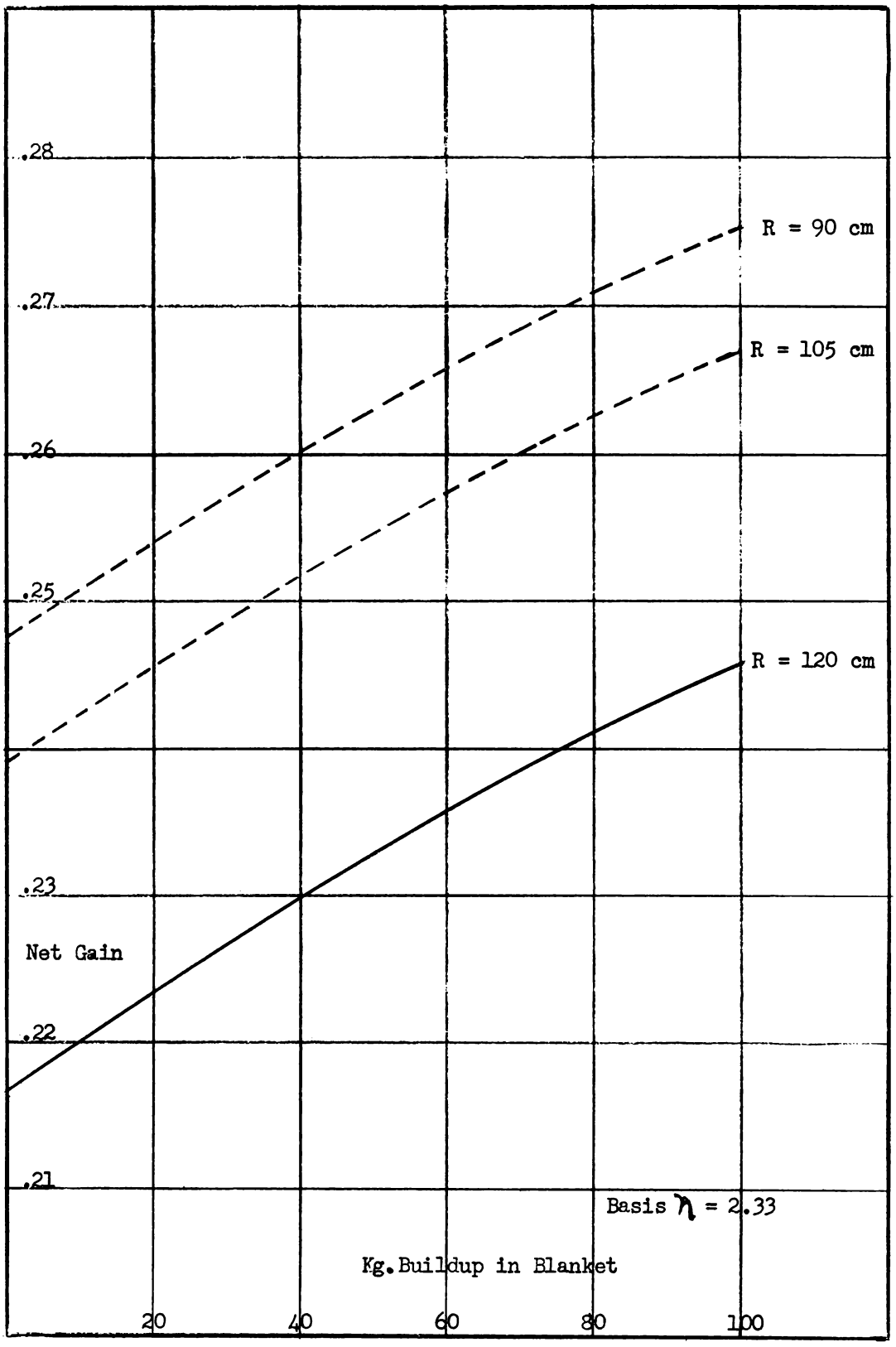

Figure III 2-6

Net Gain vs Kg. Buildup in Blanket

to note that allowing 100 Kg to accumulate in the blanket has the effect of reducing the necessary mass in the core by approximately a kilogram. Such a small change is due to the very low average flux in the blanket relative to the core.

Though having little effect on the critical condition of the reactor, the amount of buildup in the blanket has a pronounced effect on net gain and power produced by fissioning in the blanket. It has, however, only a small effect on "breeding gain." The distinction between "net gain" and "breeding gain" is as follows: Net gain is defined as

$$\frac{\Sigma_a(\text{Th}) - \Sigma_a(P_a) - \Sigma_a(23)\ (\text{Blanket Only})}{\Sigma_a(23)\ (\text{core only})} - 1$$

Breeding gain is defined as:

$$\frac{\Sigma_a(\text{Th}) - \Sigma_a(P_a) - \Sigma_a(23)\ (\text{Blanket Only})}{\Sigma_a(23)\ (\text{Total}) + \Sigma_a(P_a)} - 1$$

Obviously the above definitions do not include chemical losses. The net gain increases appreciably with build-up in the blanket due to an additional source of neutrons in the blanket, against which no destruction of fissionable material is charged in the definition. Figure III 2-6 shows this effect on net gain for the 120 cm. core. (Curves for the 105 cm. and 90 cm. cores are dotted in through one calculated point.) Breeding gain exhibits a slight decrease as uranium is built up in the blanket. Fissions occurring in the blanket result in the production of neutrons in the region where they can be readily absorbed in the fertile material. This alone would enhance the breeding gain were it not for the more than compensating increase in leakage, mostly fast, due primarily to fissions near the perimeter of the blanket. Figure III 2-7 compares breeding gain, net gain, and a modified net gain which assumes that 40% of the calculated leakage from the blanket is actually returned by the shield. Realistically, the advantage

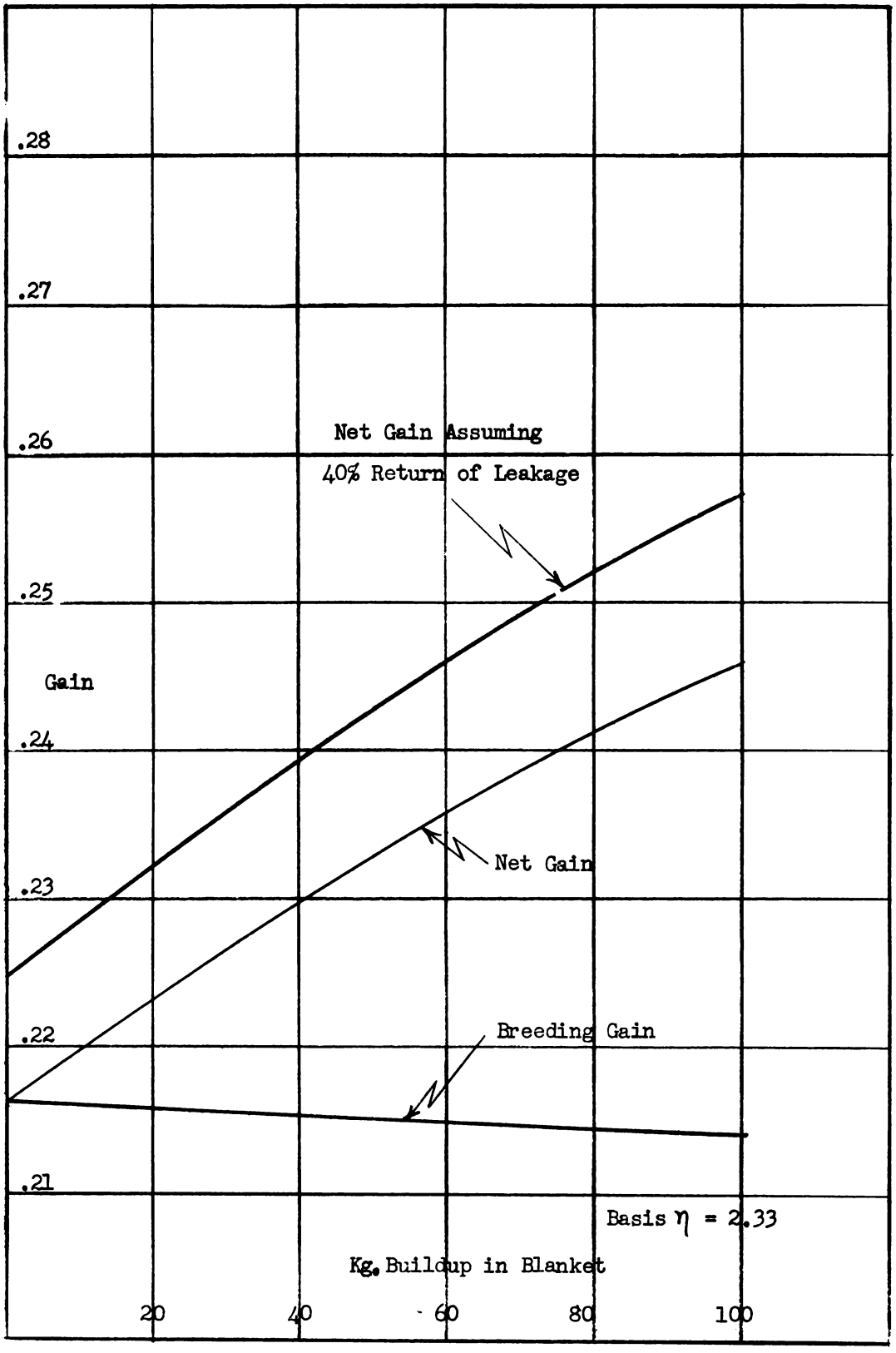

Figure III 2-7

Gain vs Kg. Buildup in Blanket

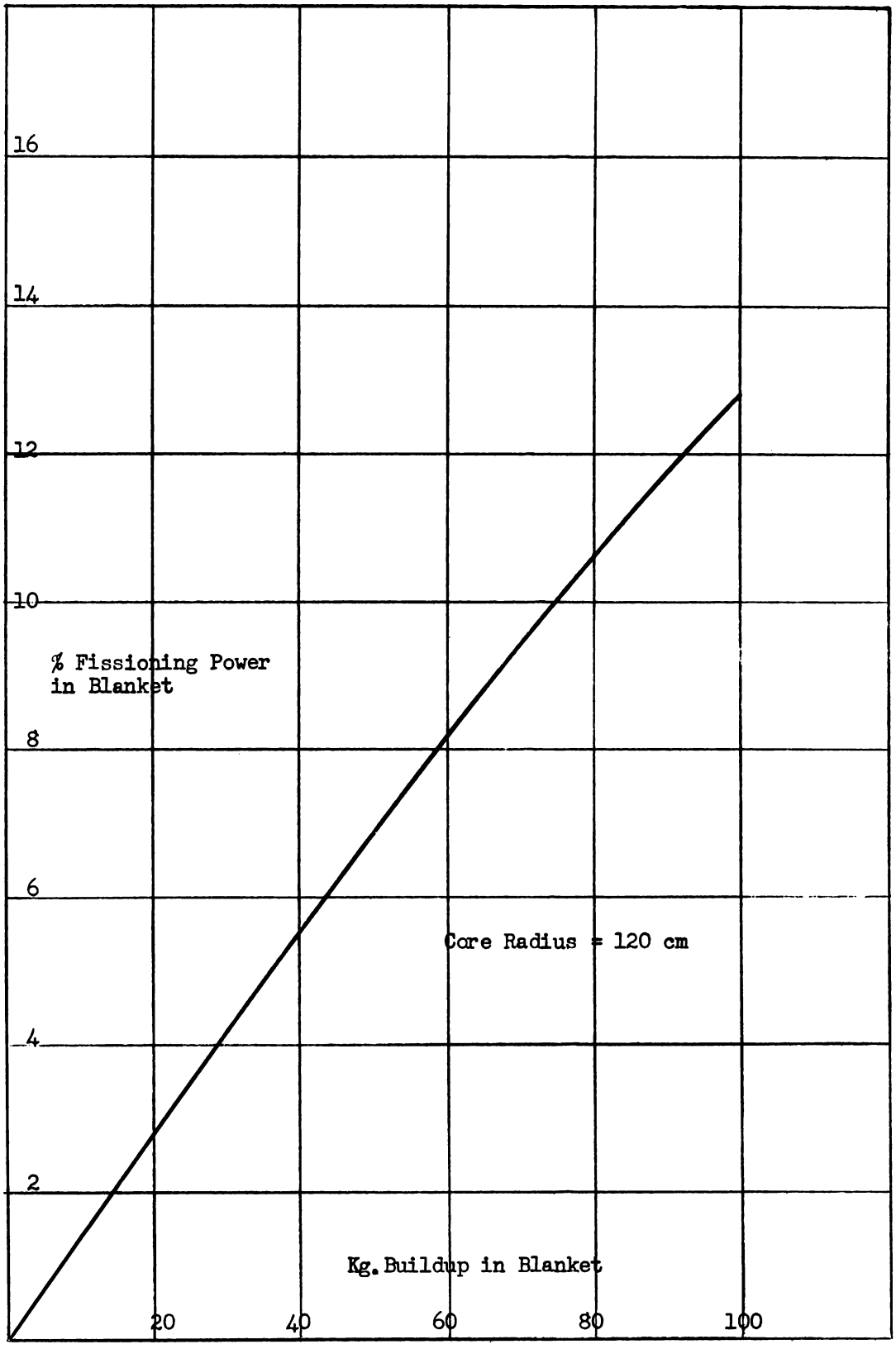

Figure III 2-8

% Power Due to Fissioning in the Blanket
vs
Kg. Buildup in Blanket

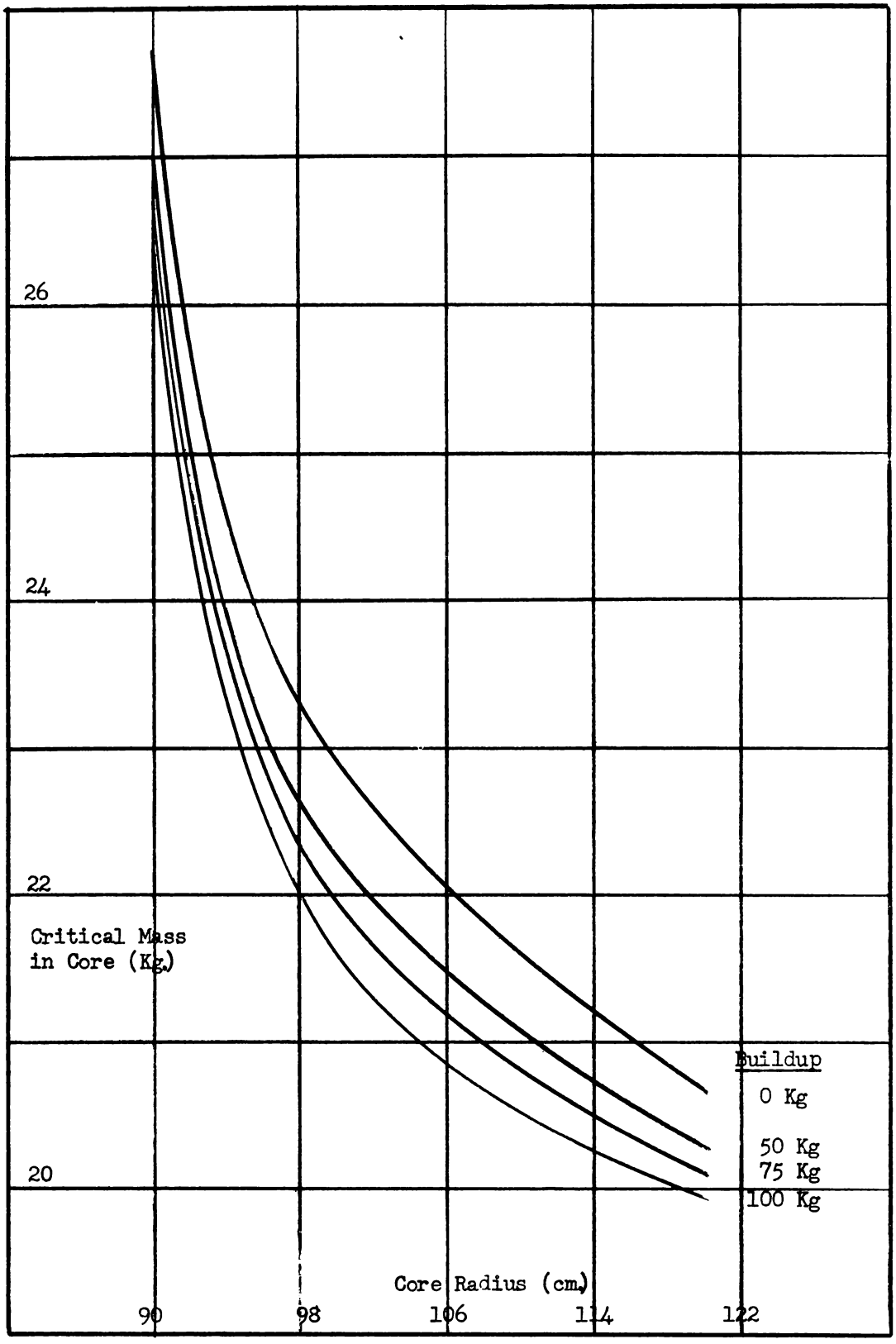

Figure III 2-9

Critical Mass in Core vs Core Radius

gained from return of neutrons from the shield should be neglected in view of the unknown losses of neutrons such as leakage through unblanketed areas of the core and absorption in what little structural material there is in the core.

On Power Production in The Blanket

The production of power by fissioning in the blanket increases almost linearly with buildup. The increase would be linear except that the ratio of integrated thermal flux in the blanket to integrated thermal flux in the core decreases as the buildup increases. This decreasing ratio is the result of increased thermal absorption in the blanket by the uranium while the production of thermal neutrons increases only slightly. The thermal absorptions in the uranium result in production of fast neutrons, a very large percentage of which never reach thermal energies but are absorbed in the thorium resonance. Figure III 2-8 shows the above results in graphical form.

2.4.4 Effect of Core Radius on Critical Mass

Critical mass, gain, and power production by fissioning in the blanket were quite noticeably affected by changes in core radius. Critical mass in the region of interest was nearly at a minimum at 120 cm.but increased rapidly with diminishing radii. The rapid increase is due to the rather considerable leakage from such small cores into the absorbing blanket. Of course, high leakage from core to blanket is a necessary condition for a two region breeder. Figure III 2-9 describes the influence of core size on mass for fissionable material buildup in the blanket of 0, 50, 75 and 100 kilograms.

On Gain

Net gain shows a marked improvement with the smaller core sizes. This

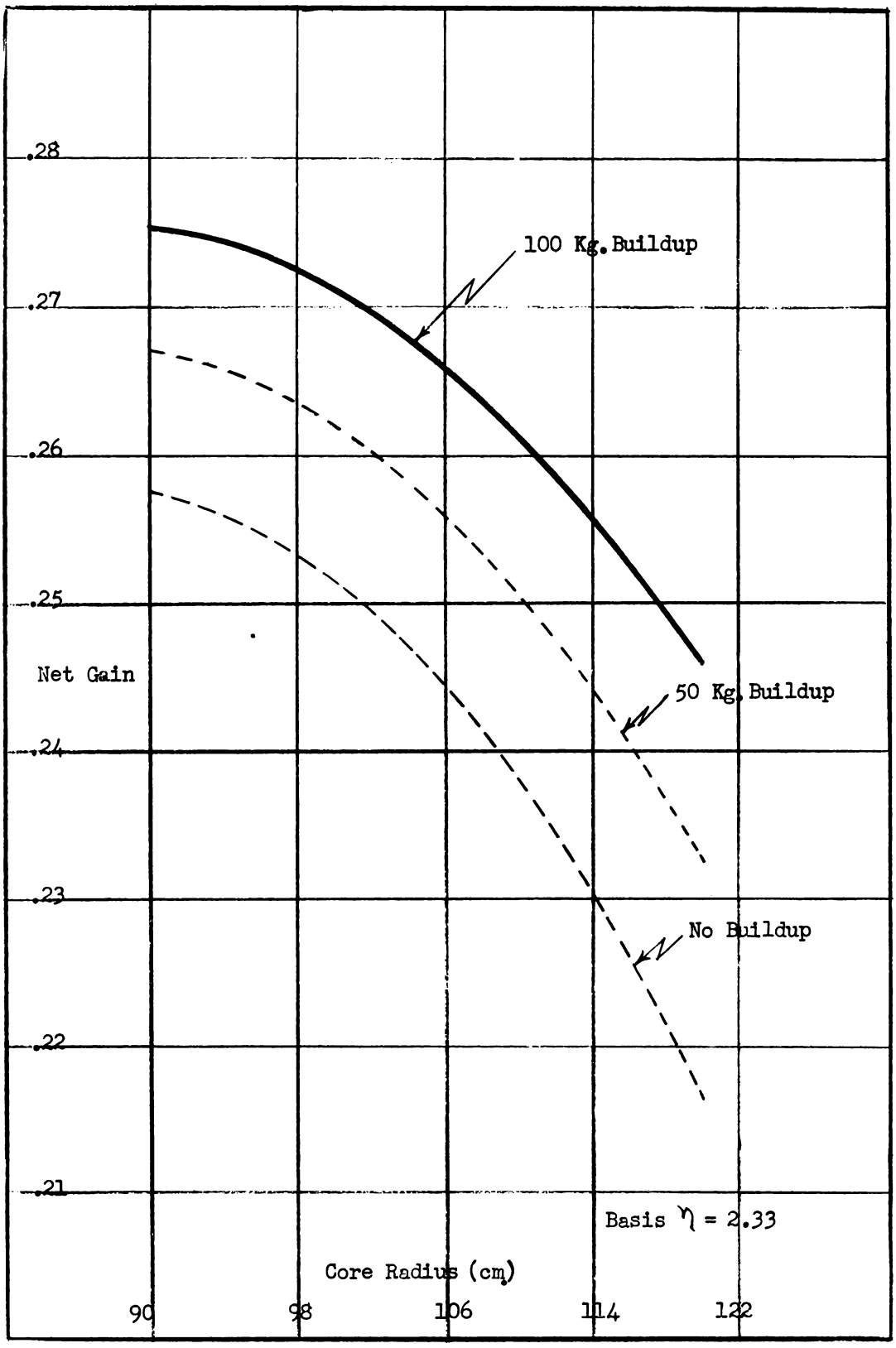

Figure III 2-10

Net Gain vs Core Radius

arises from the better thermal utilization in the core due to higher fuel concentrations. The higher fuel concentration is required to attain criticality in the smaller cores. Figure III 2-10 represents the effect of radius on net gain for the system containing 100 kilograms of 23 in the fertile region. Curves for buildup of 0 and 50 kilograms are dotted in to complete the family, although net gain was calculated only for the 120 cm. core. Net gain is compared as before with breeding gain, and modified net gain which assumes 40% return of blanket leakage, in Figure III 2-11.

It should be pointed out that the gain appears to be approaching a maximum as the radius decreases. At the maximum gain a further decrease in core size would increase the leakage more than would be compensated for by improved thermal utilization in the core. These are not the only factors involved but are the major ones. Changes in poisoning and fissioning in the blanket might well play a role but it is difficult to separate their effects.

On Power Production In The Blanket

If the mass of 23 in the blanket is fixed, a slight increase in the fraction of fissions occurring in the blanket is noticed for core of smaller radii. Since the mass of fissile material is the same in each case the greater power production can result only from an increased ratio of the thermal flux in the blanket relative to the core. Since the major portion of the thermal flux in the blanket comes from core leakage of thermal neutrons, the smaller core radius results in a higher slow flux in the blanket. Very little of the blanket slow flux arises from slowing down because of the strong thorium resonance. Figure III 2-12 shows the variation of

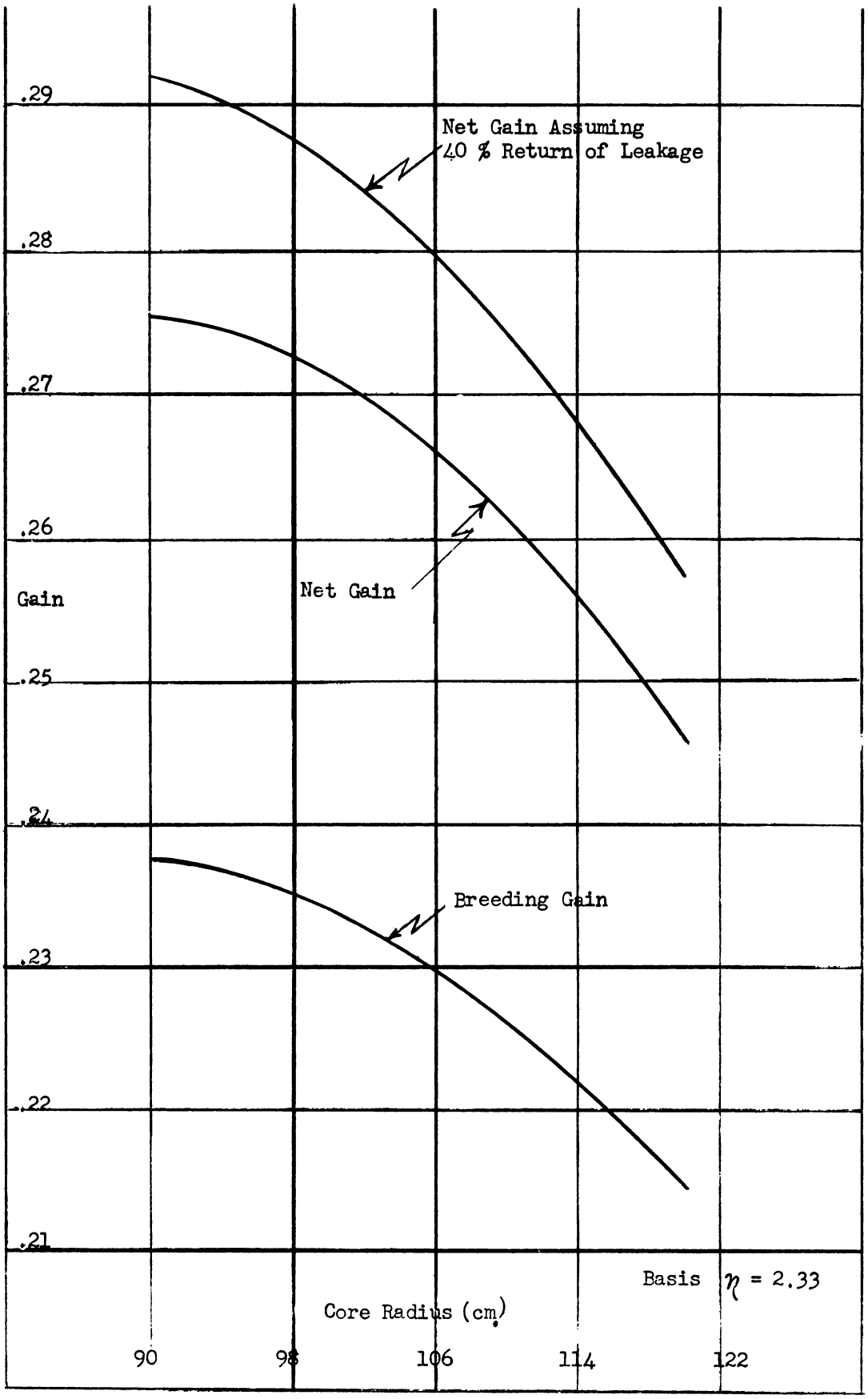

Figure III 2-11

Gain vs Core Radius

blanket power with radius.

2.4.5 A System With High Fission Product Poisoning

Additional results were obtained for a system with 10% core poisoning, a core radius of 120 cm., and a 100 kilogram buildup of fissile material in the fertile region. All other factors were the same as those for the previous set of calculations. This system was evaluated as an extreme case which might arise if either there were no removal of Xenon, if the flux were much higher than originally estimated, or if the chemical processing rate were decreased appreciably. Under the conditions above, gain, of course, suffered badly. Net gain was reduced to 0.1908 compared to 0.2459 with 2% poisons and breeding gain was reduced to 0.1676 from 0.2144. The critical mass was also affected quite noticeably, increasing from 19.95 kilograms to 25.82 kilograms.

2.5 Nuclear Calculations For Low Density Beds (60% Voids)

2.5.1 Modified Welton Method - Investigations of heat transfer in the fluidized bed heat exchanger showed that to get very high heat transfer coefficients from solids to tubes it was necessary to employ very small particles, probably as small as 60 microns. With much larger particles the heat exchanger volume by present calculations would be so large as to make the external holdup of fissionable material prohibitive. However, it is impossible to compact the small particles beyond about 60% voids. Hence the moving bed in the core would have to be 60% voids rather than the 40% originally assumed, which corresponded to much larger particles (600 microns). If one is to use the same particle size in the fluidized, hence less compact, blanket the voids must be raised to about 65%. The results to be reported are for these void percents; all other conditions are the same as those for the first set of calculations by this method, with the investigations

* Direct results of calculations are reported. Their absolute accuracy should not be inferred from the number of significant figures.

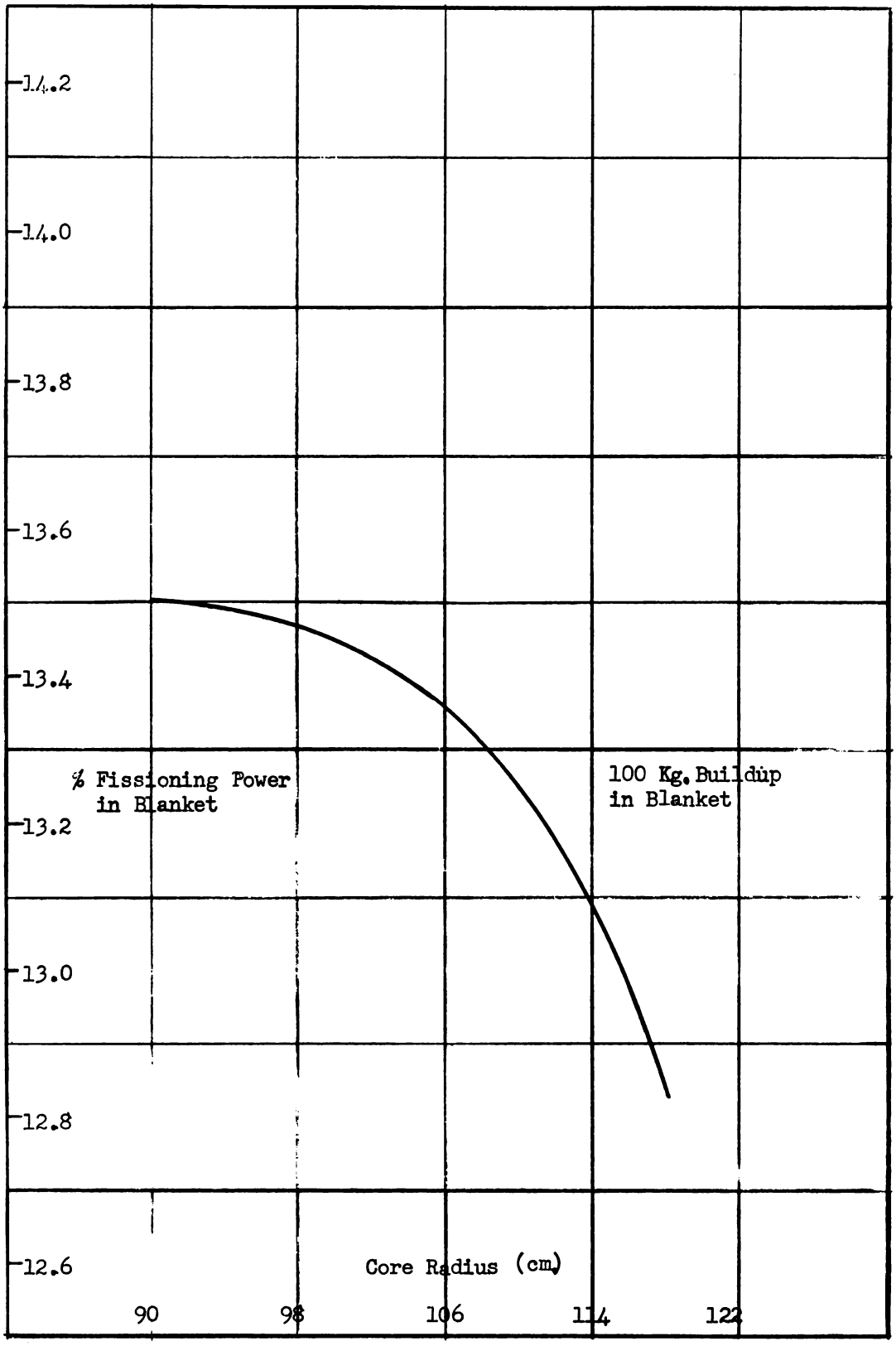

Figure III 2-12

% Power Due To Fissioning in The Blanket

limited to the case of 1 gm/cc. of thorium in the blanket. The large increases in Fermi Age and diffusion length brought about drastic changes in critical mass, location of the critical mass minimum, and thermal utilization for a given core radius. These changes revolutionized thinking on the system. The minimum critical mass was raised from 18.35 to 45.3 kilograms yet the total holdup was much smaller because of the considerable saving in external holdup. The critical mass minimum was shifted from about 4' to around 6 1/2'. Acceptable thermal utilizations were now obtainable at radii up to six feet whereas previously any core over four feet was considered to have too poor a thermal utilization. One would expect that the leakage from the blanket would be appreciably increased due to the decrease in blanket moderating power. The new mass-radius curve appears in Figure III 2-13.

2.5.2 The Visner Method - Partially on the basis of the preceeding calculations a system was chosen around which the preliminary design of the reactor has been chosen. It is not proposed that this is the optimum system though it is indeed an attractive one. The conditions imposed on the final nuclear calculations were as follows:

Radius of core	150 cm.
Thickness of blanket	100 cm.
Temperature of core	2000° F
Temperature of blanket	2000° F
Voids in core	60%
Voids in blanket	50%
Thorium conc. in blanket	1 gm/cc.
Mass buildup in blanket	100 Kg.
Poisoning in core	2%

Poisoning in blanket 1%

Higher isotope loss in core and blanket 0.303%

Some of the above conditions represent changes from the conditions for the Welton calculations. The drop in percent voids in the blanket was considered necessary to prevent excess leakage from the blanket. Decreasing percent voids was accomplished by employing larger particles which in turn caused a decrease in the heat transfer coefficient between the fluidized blanket and the peripheral tubes. To remove the necessary amount of heat from the blanket, with this lower coefficient, it was neceasary to increase the mean temperature drop between the solids and the water flowing in the tubes. This was accomplished by raising the blanket temperature to 2000° F. The radius was selected on the basis of the thermal utilization and critical mass predicted by Welton's method, which has previously been shown to be reasonably accurate. The results of calculations adhering to the above stipulations, are reproduced in Table III 2-2. The nuclear constants employed are listed in Table III 2-3.

TABLE III 2-2

Mass of U-233 in core	46.81 Kg.
Mass of U-233 external to core (approximate)*	58.2 Kg.
Total burnup of U-233 per day	313 gm.
Total production of U-233 per day	381.7 gm.
Net Production of U-233 per day	68.7 gm.
Net gain	.2448
Breeding gain	.2179
Doubling time-on basis of total original holdup	1330 days
Doubling time- on basis of original charge plus outside purchased make-up	2460 days
% Power due to fissioning in blanket	10.90 %
Thorium inventory	56,381 Kg.
Average slow core flux	3.08×10^{14}
Maximum slow flux	7.08×10^{14}

* Based on approximate ratio of solids in core to solids in external system. See Table III 1-15

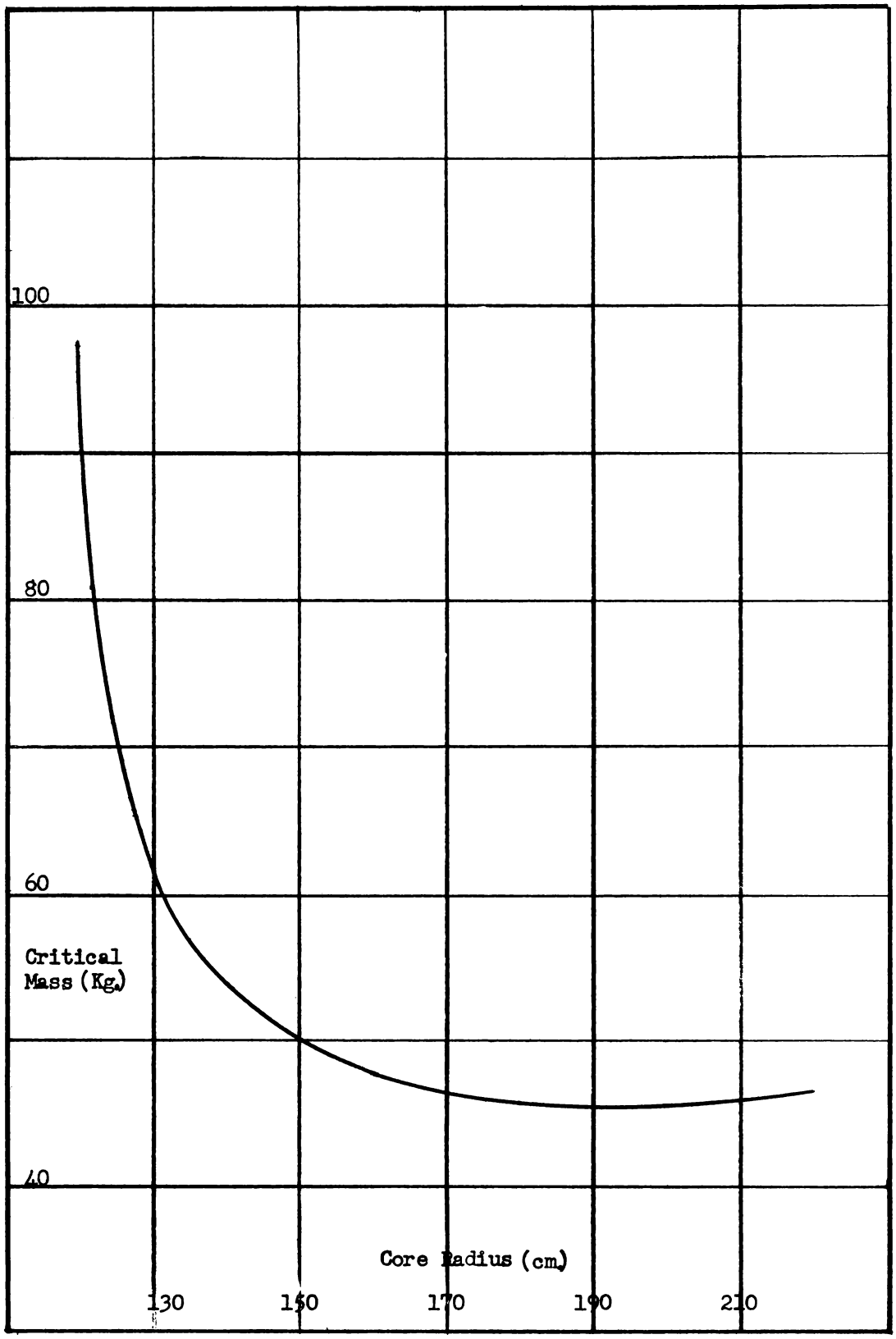

Figure III 2-13

Critical Mass vs Core Radius

The mass of U-233 in the core quoted above is based on the full size core and does not take advantage of the reflector savings of the shell. The total burnup per day is based on a utilizable energy release of 184 Mev. per fission and an η/γ ratio of 0.906.

TABLE III 2-3

NUCLEAR CONSTANTS
(Final Visner Calculation)

	Core 60% Voids	Blanket 50% Voids
η	2.33	2.33
τ_{cm}	2156.25	1476.33
$L_o^2{}_{cm}$	26,524	222.70
$L^2{}_{cm^2}$	1302.486	185.84
K_∞	2.196328	0.38566
P	1.0	0.0957
D_s cm	2.2341	1.6958
D_f cm	3.2309	2.4523

Figure III 2-14 shows the variation of the fast and slow fluxes with core radius. The customary buildup of slow flux in the neighborhood of the core-blanket interface is not observed since the absorption cross section in the blanket is much greater than for the core and thus no build-up is possible.

The fluxes are represented by the following equations:

$$\phi_{sc} = \frac{1}{r} \left(A \sin B_{ic} r + C \sinh B_{rc} r \right)$$

$$\phi_{fc} = \frac{1}{r} \left(\alpha_{ic} A \sin B_{ic} r + \alpha_{rc} C \sinh B_{rc} r \right)$$

$$\phi_{SB} = \frac{1}{r} \left(E \sinh B_{ib} (a_2 - r) + G \sinh B_{rb} (a_2 - r) \right)$$

$$\phi_{FB} = \frac{1}{r} \left(\alpha_{ib} E \sinh B_{ib} (a_2 - r) + \alpha_{rb} G \sinh B_{rb} (a_2 - r) \right)$$

With the constants:

$A = 4.218 \times 10^{16}$
$C = -7.715 \times 10^{12}$
$G = 7.080 \times 10^{12}$
$E = 2.510 \times 10^{14}$

$B_{ic} = .01678$
$B_{rc} = .03889$
$B_{ib} = .04333$
$B_{rb} = .08704$

$\alpha_{ic} = 1.564$
$\alpha_{rc} = -1.111$
$\alpha_{ib} = 3.576$
$\alpha_{rb} = -.4097$

$a_2 = 260$ cm

The two major losses of neutrons in the system are, as seen in Table III 2-4, non-productive capture in the core and leakage from the blanket. Little can be done to reduce core losses since the absorptions are in poisons which cannot be removed rapidly enough and in moderator which, of course, must be present. A smaller core would necessitate higher fuel concentration and hence relatively less moderator absorption would occur but the saving would probably not be worth the extra fuel inventory. The high blanket leakage of 4.68%, compared to the 2-3% for previous systems studied, is the result of two changes. First, the blanket temperature was increased causing all cross sections in the blanket to become smaller. Secondly, the bed density was reduced and consequently values for Fermi Age and diffusion length were much greater since they depend on the reciprocal of the density squared. Since neither temperature or bed density can be altered there are three courses left open to decrease leakage: (1.) increase the blanket thickness (2.) increase the thorium concentration (3.) surround the blanket with a strong reflector. The first two seem most likely to produce results and the easiest alterations to make.

TABLE III 2-4

Neutron Accountability

(Normalized to one neutron absorption in the core fuel)

Absorptions in core	
23	1.00000
Graphite	.03783
Poisons	.02000
Higher Isotopes (net)	.00303
Total in core	1.06086
Absorptions in Blanket	
23	.12231
Graphite	.00544
Poisons	.00122
Higher Isotopes (net)	.00037
Thorium	1.36798
Protoactinium	.00090
Total in Blanket	1.49822
Absorption in Shell	.00594
Leakage	.04687
Total Consumption in Reactor	2.61189

Production $2.33\ (\ 1 + .12231) = 2.6150$

Net Gain $1.36798 - .12231 - .00090 = .24477$

Breeding gain $\dfrac{.24477}{1 + .12231 + .0009} = .21792$

% Power due to fissioning in blanket $\dfrac{.12231}{1.12231} = 10.898\ \%$

2.6 Multi-Group Calculations

In addition to the one and two group calculations, two multigroup analysis by the D. K. Holmes (17) method were completed for bare cores operating at 2000° F. The main purpose of these calculations was to determine at what energies the majority of fissions occur and to estimate the effect of epi-thermal fissioning on the necessary critical mass.

The first results were obtained for a reactor of seven feet (213 cm) radius, 45% voids and 35.7 kilograms of U-233. 35.7 Kilograms is the mass required to make the system critical according to the Fermi Age One Group Theory. This multi-group computation indicated an effective multiplication factor of 1.25 and showed that 8.1 % of all fissions were occurring above the thermal range. The fact that k_{eff} is greater than unity is due primarily to the epi-thermal fissions which cannot be accounted for in the Fermi Theory.

The second calculation of this type was made on the core of the reactor system which has been proposed in this report. The core has a radius of 160 cm, operates at 2000° F, and contains a moving bed with 60% voids. The neutron spectrum under these conditions is much faster than the spectrum for the first system, due to the lower bed density. 41% of all fissions occur above the thermal range, yet the mean energy of fission is only 0.6 ev. Since the mean energy of fission is so near thermal the slowing down length is not considerably different from the slowing down length to thermal energy. Thus the use of the Fermi Age from fission to thermal, in the two group Visner method quite likely results in only a small error. The mass of U-233 assumed in this multi-group calculation was 46.81 Kg, the amount calculated by the Visner method as being required to make the same system critical while surrounded with a breeder blanket. The resulting K_{eff} of 0.932 indicates that the epi-thermal fissioning is sufficient to bring the

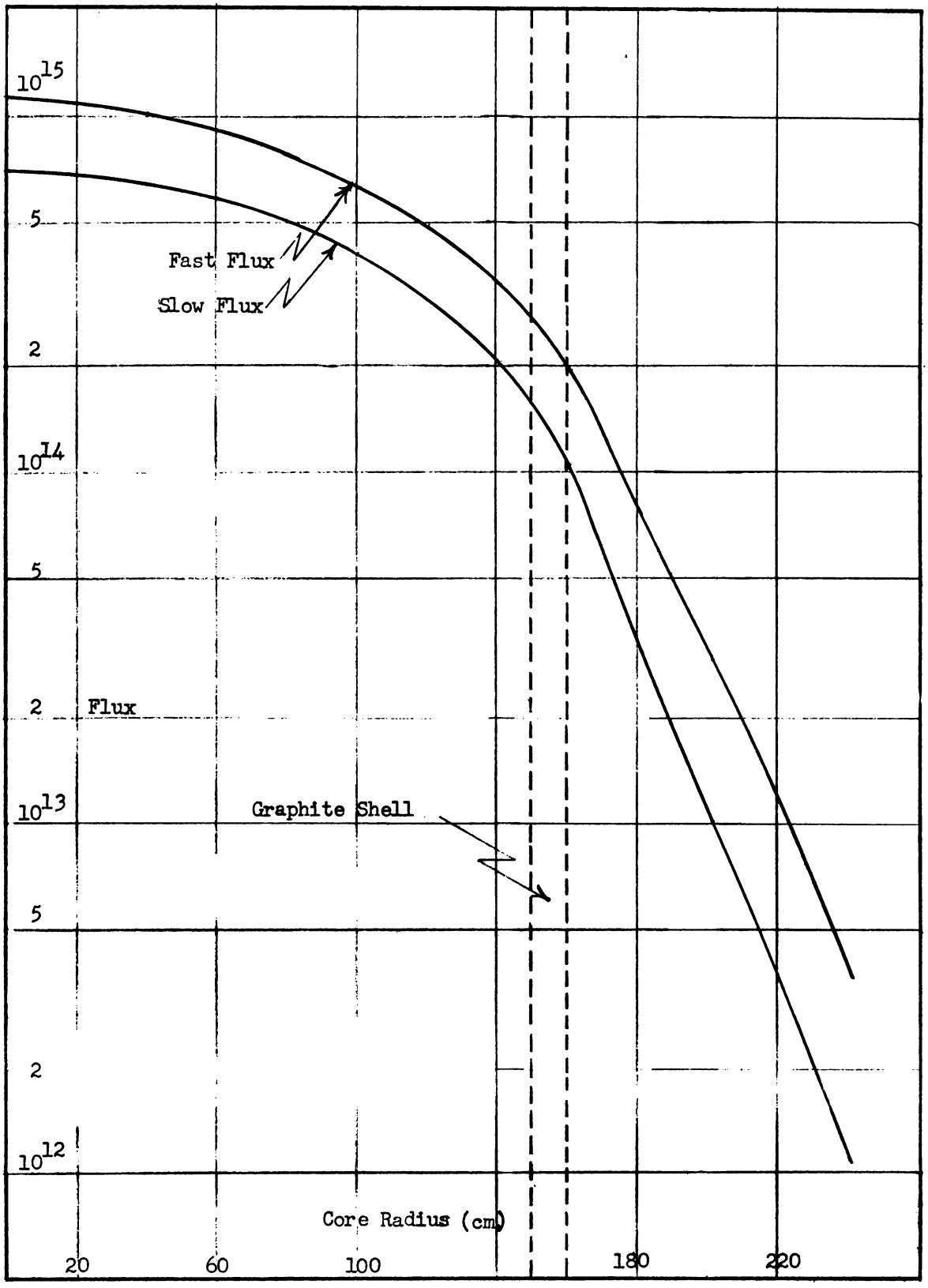

Figure III 2-14

Fast and Slow Fluxes vs Core Radius

bare core fairly near criticality with the mass required for a blanketed core. Hence the conclusion is that less than 46.81 Kg are actually required in the blanketed core. This results in a favorable decrease in total fuel holdup but at the same time results in an unfavorable decrease in thermal utilization unless the radius is also decreased. The fission absorptions in the epi-thermal range, where there is little moderator absorption, may help to counteract the detrimental change in thermal utilization. A reduction in core size would force an increased fuel concentration and, therefore, restore the high thermal utilization, while still retaining some of the saving in total fuel holdup.

There was insufficient time to carry the multigroup calculations far enough to obtain the critical mass which would actually be required for the proposed reactor. However, the figures on mass, gain etc. which came from the Visner calculations are believed to be consistent within themselves to present a good picture of the variation of these properties with variations in core radius, mass of 23 in the blanket, etc. The actual values should be slightly more favorable indicating that the correlation presented in the earlier sections of this report are somewhat on the conservative side.

3.1 Chemical Processing

3.1.1 General

One of the many advantages of the fluidized solids reactor system is simplicity in processing the fuel or blanket materials. Unfortunately, those schemes which seem to be the best suited for the fluidized-solids reactor are not conveniently applicable to the existing reactor systems and have not yet been thoroughly studied in the research laboratories. The authors wish to propose in the pages to follow, several plausible schemes to give the readers a better idea of the flexibility of the fluidized

solids system. It is probable that none of the schemes shown will accompany the final reactor design but each one was chosen after a careful analysis of the classified information now available. The processing plant will be required to handle three separate, continuous streams:

1) The fuel-moderator mixture from the core.

2) The blanket material.

3) The fluidization gas.

3.1.2 The Fuel Moderator Mixtures

After seriously considering the overall design of a fluidized solids reactor, the authors concluded that the most favorable fuel-moderator mixture would be graphite impregnated with uranium. The uranium would be present (after treatment of the mixture in a high temperature kiln) mostly as the oxide (U_3O_8) and partly as the carbide (UC_2) dispersed throughout the graphite particles. The alternative of binding together (using a pitch or tar and then firing in a kiln) separately formed U_3O_8 or UC_2 and graphite would not seriously change the processing required.

It is planned that the solids would be removed continuously, preferably by means of a cyclone or other fines-removal device installed in the circulating gas stream. This plan has the advantage of removing from the system the very fine products of attrition and also those particles most severly broken up by the radiation effects.

If, thus, we hypothesize that the finest particles are preferentially removed, that an abnormally high concentration of fissioning in a particle tends to accelerate its breakage into extreme fines, and that all particles contain fission products in a concentration proportional to the number of fissions previously occurring in that particle, we thus have a system for removing preferentially those particles having an abnormally high concentration

of the fission product poisons.

The treatment of the solids after withdrawal from the reactor system will depend on the method chosen for the separation of the uranium from the fission products. The author feels that all of the cycle may be carried out behind shielding and thus there is no need to cool the solids for more than the 1-3 day holdup planned in the surge hopper.

The first processing proposed is the "acid leach; solvent extraction" design. The solids are charged batch wise to a vessel along with the required quantity and strength of nitric acid. The mixture is digested for several hours; steam can be used satisfactorily for agitation as well as heating. If most of the graphite will later be recycled to the reactor, it will not be necessary that all of the uranium be removed at this time. The slurry is then left to settle (an acid-stable, organic coagulant may be added to speed up the process). The solution, containing the dissolved uranium and fission products, is decanted off, cooled and filtered.

The above filtrate is sent to a surge and feed-adjustment vessel wherein it is prepared for the extraction step. The solvent extraction proposed employs the T.B.P. process which has been studied in great detail at ORNL (2,7, 13). In the present design, it is contemplated that the product $UO_2(NO_3)_2$ will be re-impregnated on fresh or recovered graphite and will thus not require an extremely high decontamination factor. Thus a simple 2 - column, 1-cycle extraction is all that is proposed. The $UO_2(NO_3)_2$ is thus adjusted to the proper concentrations required for impregnation (of graphite) and sent to the proper surge or storage tank. The fission products leaving the first tower in the aqueous layer are to be sent to waste or may be processed for whatever market they may have.

The filter cake, produced in the last section, should consist of the smallest graphite particles removed from the system. This may be either:

(1) Discarded directly, if the uranium content is negligible

(2) Leached further to remove the last traces of uranium and then sent to waste

(3) "Recovered" by drying, treating with a suitable binder, re-graphitizing in a suitable kiln, and crushing for reuse, or

(4) Burned to reduce the solids waste handling problem.

In the last case, the product gas can be scrubbed with a suitable liquid such as the aqueous waste stream from the extraction towers to concentrate all the remaining fission products into a more easily handled waste stream.

The thick graphite slurry remaining in the original solution tank should be washed by slurrying with fresh acid solution and then decanting off the liquid layer. This acid solution can be recycled to the first solution step but may first be used to scrub the side stream of the fluidizing gas (to be discussed later.) The remaining graphite (left in the thick slurry in the vessel) can now be treated with the processed and/or makeup $UO_2(NO_3)_2$ solution for impregnation. Fresh, makeup graphite can be added at this point.

The impregnated graphite can then be dried and heated in a kiln (to about 1000° C) to drive off all the nitrogen compounds and to convert the uranium to the oxide. If, during the cycle, the graphite fines had agglomerated to sizes larger than desired in the reactor, the product is then ground to size and sent to the reactor-makeup feed tank.

An alternate scheme for processing the core materials is shown in Figure III 3-2. The basic principle of this plan is the utilization of the "fluoride volatilization" technique (2,21). Graphite reacts very

readily with both hydrogen fluoride and fluorine (1). Consequently, any graphite thus processed will not be recoverable as such but must be replaced with fresh material. As shown in the flow sheet (Figure III 3-2), it is suggested that the solids be passed into the upper of two towers or vessels in series. HF is introduced into the bottom of this vessel and fluorinates most of the graphite (into CF_4), some of the fission products, and some of the uranium. The residue from the above tower can then be dropped into a second tower or vessel where it is treated with F_2 to convert the uranium to the volatile UF_6. The stream from both of the above mention towers are then fractionated to separate the UF_6 from both the lower boiling and the higher boiling compounds. The UF_6 is then converted to the uranyl nitrate and sent back for reimpregnation on fresh graphite.

The residue obtained from the second of the fluorination stages may or may not contain additional uranium. If uranium is present, the residue should be processed further, probably by dissolving in nitric acid and purifying in a small laboratory size, solvent extraction process.

The fluorination may be conducted either continuously or batch-wise. In the latter case, only one fluorination vessel is required, being operated first with the HF treatment and them F_2. Similarly, the same train of fractionating columns could then be used for both steps.

The fluorination can also be carried out in either a fluidized solids bed or in a fixed or moving bed.

The fluoride process, since it requires "burning up" all the graphite, suggests that variation be made in the fuel-moderator preparation.

1. The uranium fuel may be prepared as the oxide or carbide and then mixed physically with the graphite particles. The particles containing the uranium (and most of the non-gaseous fission products)

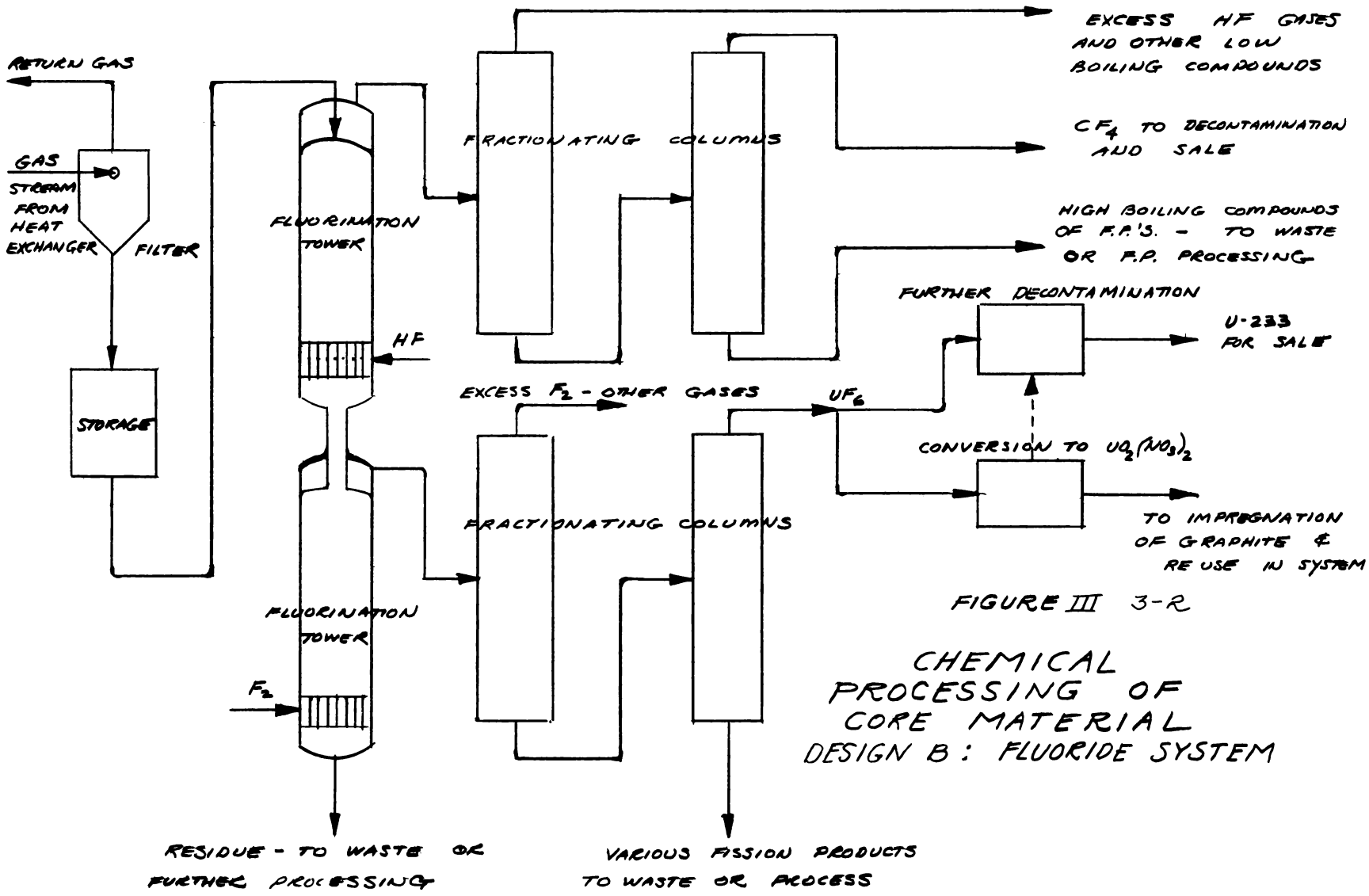

FIGURE III 3-2

CHEMICAL PROCESSING OF CORE MATERIAL
DESIGN B : FLUORIDE SYSTEM

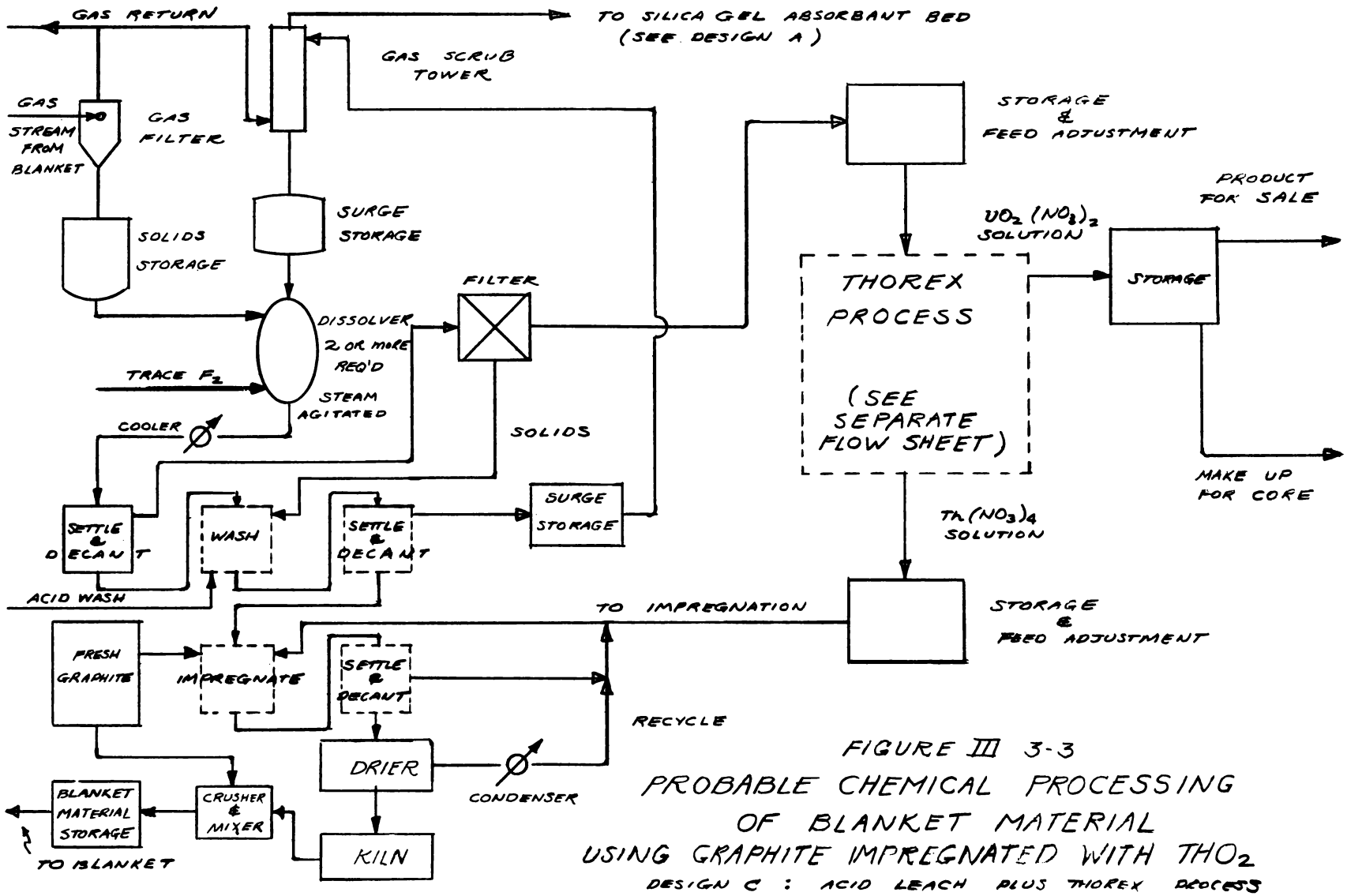

FIGURE III 3-3

PROBABLE CHEMICAL PROCESSING OF BLANKET MATERIAL USING GRAPHITE IMPREGNATED WITH THO_2

DESIGN C : ACID LEACH PLUS THOREX PROCESS

would be heavier than the graphite and could be separated from the graphite in an external vessel using either gas elutriation or liquid flotation. Thus only a small part of the graphite would be lost through fluorination.

2. It may be preferable to use B_eO as the moderator-carrier.

A third proposal for processing the fuel requires an entirely different reactor system. This scheme employs UF_6 as the fuel and fluidizing gas and a solid moderator as the movable solids. With a slight amount (probably under 0.1%) of free fluorine in the UF_6 stream and at high reactor temperatures essentially all the fission products will be volatilized and can be removed merely by continuous fractionation of a portion of the UF_6 stream. This is briefly illustrated in Figure II-1.

3.1.3 Processing Blanket Materials

The fluidized solids technique also permits consideration of many possible processing schemes for the blanket. In each case, the objective is to separate uranium and/or protoactinium from the thorium and to separate both from the fission products.

Figure III 3-3 illustrates a design for solution of the blanket materials in acid, and purification by solvent extraction. This process is almost identical to the discussed "processing of core materials" except that the extraction requires 3 towers (first cycle) and some of the uranium must be decontaminated very carefully since it will be withdrawn as saleable product. Figure III 3-4, obtained through the courtesy of the Chemical Technology Division at ORNL, shows the most recent recommendations for the specific concentrations and rates employed in the Thorex Process.

DWG. 14511A

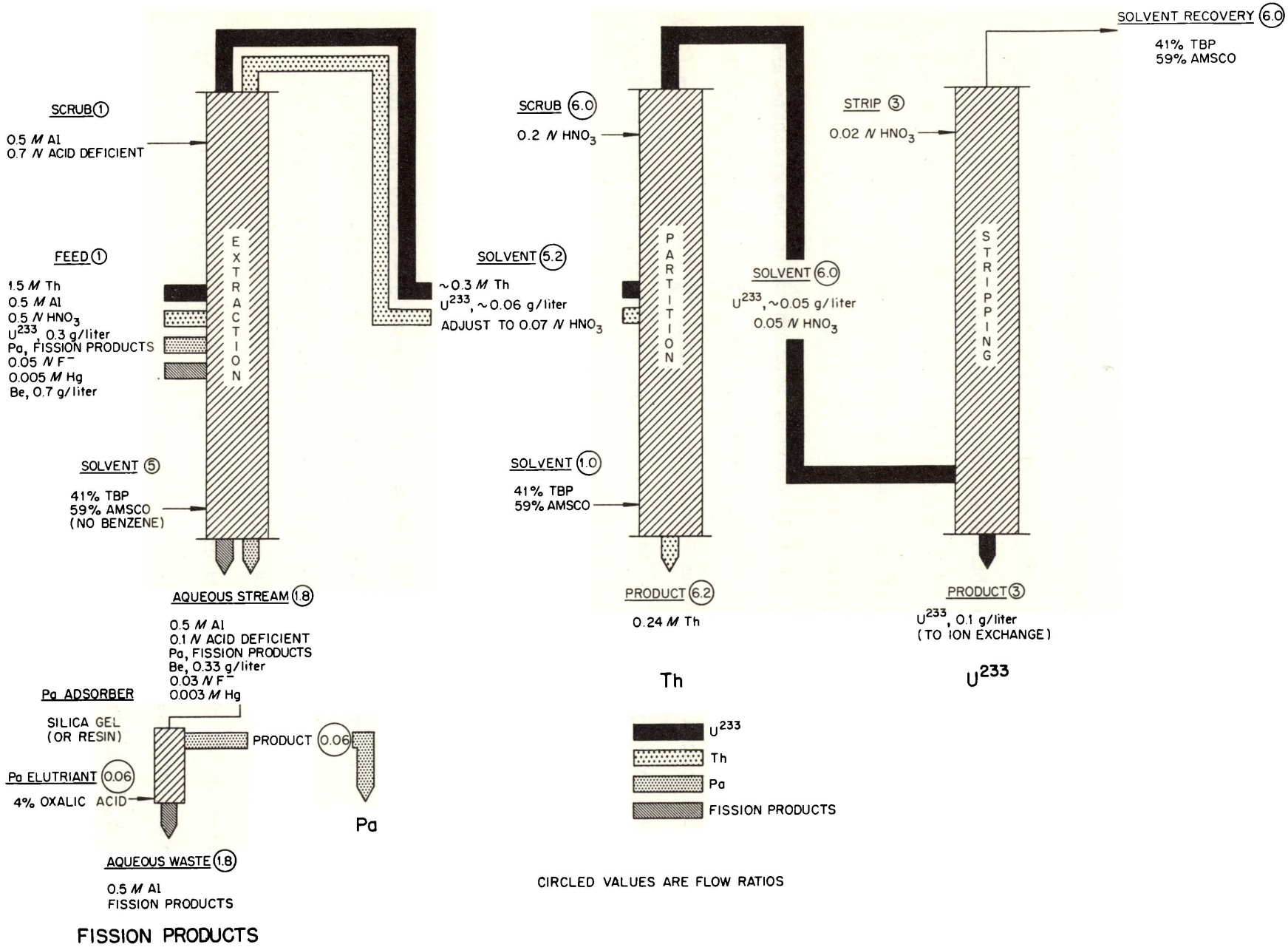

117

Instead of impregnating the thorium uniformly on all the graphite particles, it is possible to introduce the thorium as the oxide or carbide particles of such size that when mixed with plain graphite, stratification will not occur in the blanket. The thorium-uranium rich particles may thus be separated from the graphite by processes taking advantage of the large difference in gravity. Figure III 3-5 illustrates a process employing the sink-float principle to obtain a rough separation between the graphite and thorium-rich particles. Thus most of the graphite bypasses the chemical processing plant reducing both the load on the chemical plant and also the loss of graphite from the system. An entirely different approach is illustrated in Figure II-1. In this scheme, thorium oxide and graphite are fluidized in the blanket with carbon tetrachloride. The $C Cl_4$ reacts with the freshly formed protactinium forming the volatile $Pa Cl_5$. J. G. Malm (24) shows that recovery of over 95-98% is possible. Actually, the authors feel that fissioning in the blanket is desired. Thus it would not only be acceptable but may even be preferable (excluding the existance of a premium market for pure Pa-233), to operate in such a way that 10-15% of the Pa decays to U-233 within the blanket.

The fluidized solids system lends itself extremely well to the fluoride system. In this process, thorium is charged as the fluoride particles. The bed would then be fluidized with helium containing about 1% fluorine (1). Most of the uranium (as well as many fission products) would be quickly volatilized as the fluoride and could readily be removed from the system by continuously processing a portion of the helium stream.

3.1.4 Fluidization Gas

The objectives of processing the fluidization gas are three fold:

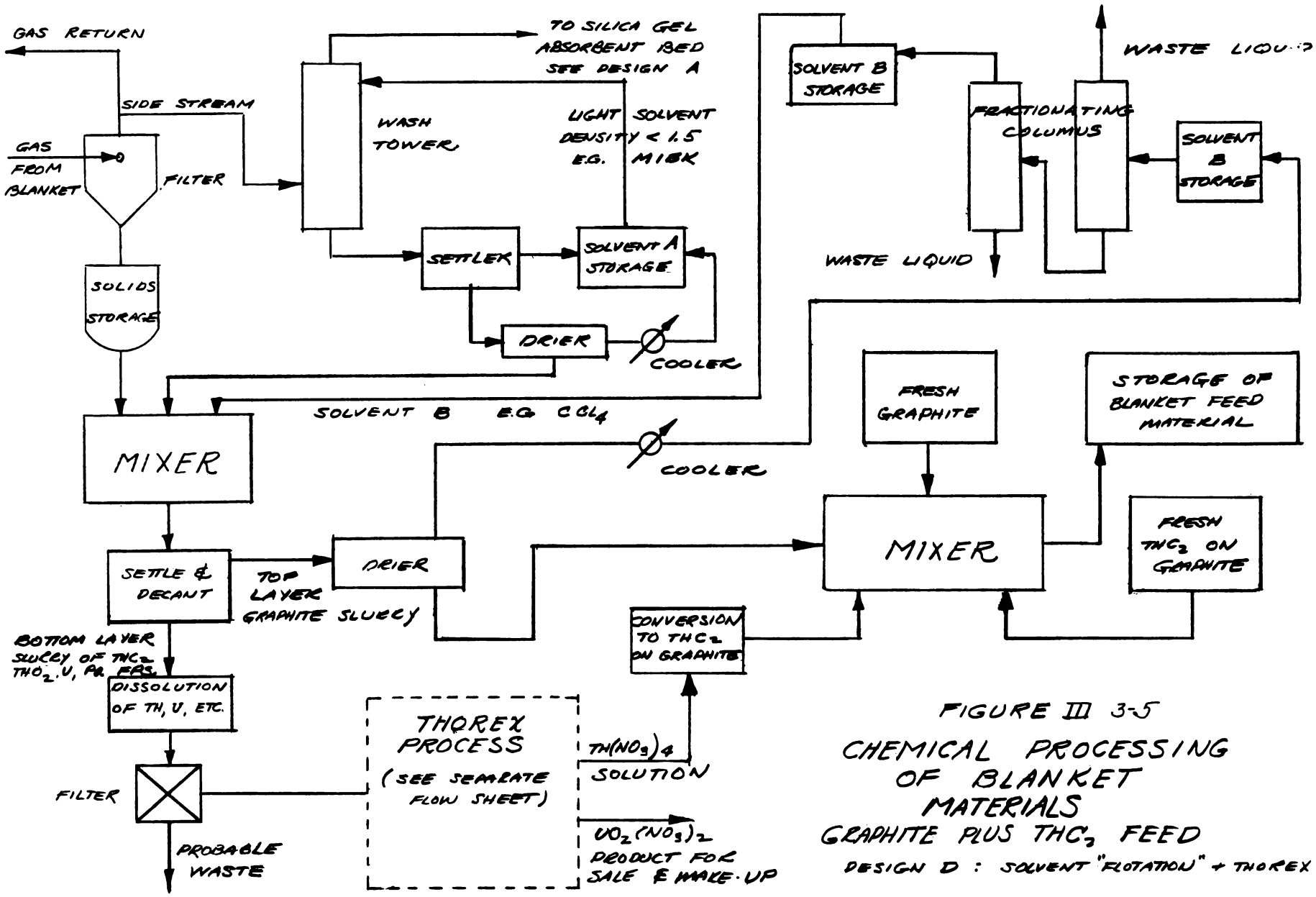

FIGURE III 3-5

CHEMICAL PROCESSING OF BLANKET MATERIALS

GRAPHITE PLUS ThC_2 FEED

DESIGN D : SOLVENT "FLOTATION" + THOREX

(1) Removal of the very small particle fines (graphite, fuel, and fission products) which would accumulate in the system if not continually removed.

(2) Provision for sufficiently large holdup volume for the gas to permit decay of most of the Xe-135 outside of the core.

(3) Maintenance of suitable purity in the gas stream, especially in regards to I_2, CO_2 (and CO), H_2O and other such chemically reactive compounds or elements.

Basically, the proposed processing cycle can be extremely simple. A relatively small portion of the gas is withdrawn, cooled (if necessary), and then scrubbed in a waste tower to remove all entrained solids. The scrubbed gas is then sent into the bottom of a large holding tank partly filled with an adsorbent such as silica gel or activated carbon. The adsorption could be carried out in a tower with the spent adsorbent continually being discarded. It is believed, however, that the volume of materials to be adsorbed is so small that one could bury a large tank partly filled with the adsorbent and then operate for years without reactivating or replenishing the adsorbent. It is expected that very little of the Xenon as such would be removed by adsorption. The bed would, however, remove from the gas stream all ot the I-135, precursor of Xe-135. Thus with a sufficiently large tank holdup, most of the Xe would in itself decay (to Cs-135) before it could diffuse into the gas stream and be returned to the core. A preliminary estimate indicated that an inexpensive tank (about 50-75% full of adsorbent) having a volume of about 800-1000 cubic feet could be very effective. For the above design, a side gas stream of only about 200-500 standard cubic feet per day might be satisfactory.

The gas leaving the large tank may then be fractionated if greater purification is desired of the gas before recycling it back to the reactor system.

3.2 Optimizing Chemical Processing Rate

In the present report, the term "Process Cycle Time" is used to indicate the time required to reprocess an amount of solids equal in weight to the entire holdup of those solids in the reactor system. In considering the core materials, the holdup in the transfer lines and heat exchanger, as well as in the core proper, is used as the basis. Thus if the total holdup in these units were 60,000 pounds of moderator-fuel, a "30-day processing cycle time" requires the processing of 2,000 pounds or 1-ton per day.

It is expected that the blanket materials would be processed independnetly of the core materials. The rate would then be regulated by the concentration of uranium in the blanket since the daily removal (of U-233) rate must just equal daily production. A typical case is one with 100 Kg of 23 in the blanket and a net production rate of 350 grams U-233 per day (equivalent to a breeding gain of about 0.18). The process cycle time would thus be 100/0.350 or 286 days; i.e. processing 0.35% of the blanket volume per day. Corresponding chemical losses of 23 from processing this blanket material would be 0.35 grams per day for a yield of 99.9% and 0.175 grams for a 99.95% yield.

The processing rate for the core materials can be optimized for the minimum loss, in gain, due to fission products poisoning on one hand and chemical processing losses on the other. More information is available on the solvent extraction methods than any other possible processing schemes. For the T.B.P. processes, pilot plant runs with losses down to 0.01% have

been obtained. Losses as low as 0.03% to 0.05% appear to be feasible and values as high as 0.1% appear to be very conservative. The fluoride volatilization process has not been investigated as thoroughly. However, results indicate that losses can be kept well under 0.2% and probably under 0.1%.

It thus seems reasonable to optimize the processing rate assuming processing losses at 0.05% to 0.10%. Figure III 3-6 shows the loss in net production of 23 as a function of process cycle time. Figure III 3-7 shows the sum of the chemical losses and the losses to fission products, at an average core flux of 5×10^{14}. Chemical processing losses necessarily decrease rapidly with increase in processing cycle time, but losses to fission products poisoning increase quite rapidly. The operating optimum should include also a consideration of processing operating costs, increased critical mass with increased fission products poisoning, and similar cost analyses. If overall economics rather than U-233 production rate, is the chief concern, the optimum would lie well to the right of the minimum loss obtained from Figure III 3-7. However, for purposes of standardization, a 30-day processing cycle time for the core materials and a 300-day cycle time on the blanket had been chosen in evaluating the various poisons which must be considered in nuclear calculations.

3.3.1 Buildup of Higher Isotopes of Uranium in The Blanket

The concentrations of the various isotopes of uranium are dependent on the (1) concentration of U-233, (2) flux, (3) processing rate, and (4) time of operation, as well as the non-variable properties such as absorption cross section and normal decay rate (See appendix VIII 3.3). For a processing cycle time of 1 year or less , the poisoning effect of U-234 is quite small, and of the higher isotopes (e.g. U-235 and U-236) practically negligible. Figure III 3-8 shows the cummulative poisoning effect of these

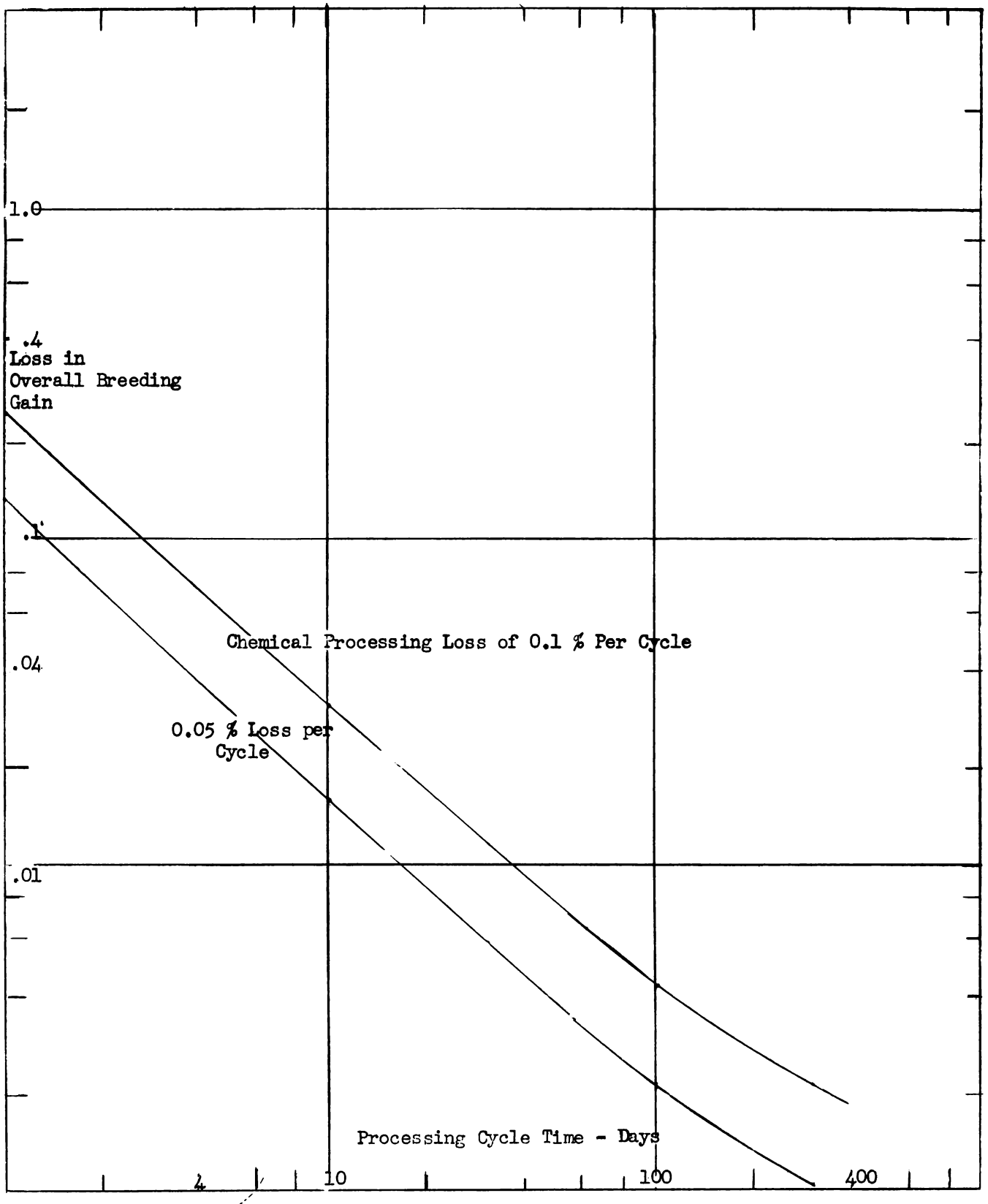

Figure III 3-6

Loss in Overall Gain Due to Chemical Processing Losses

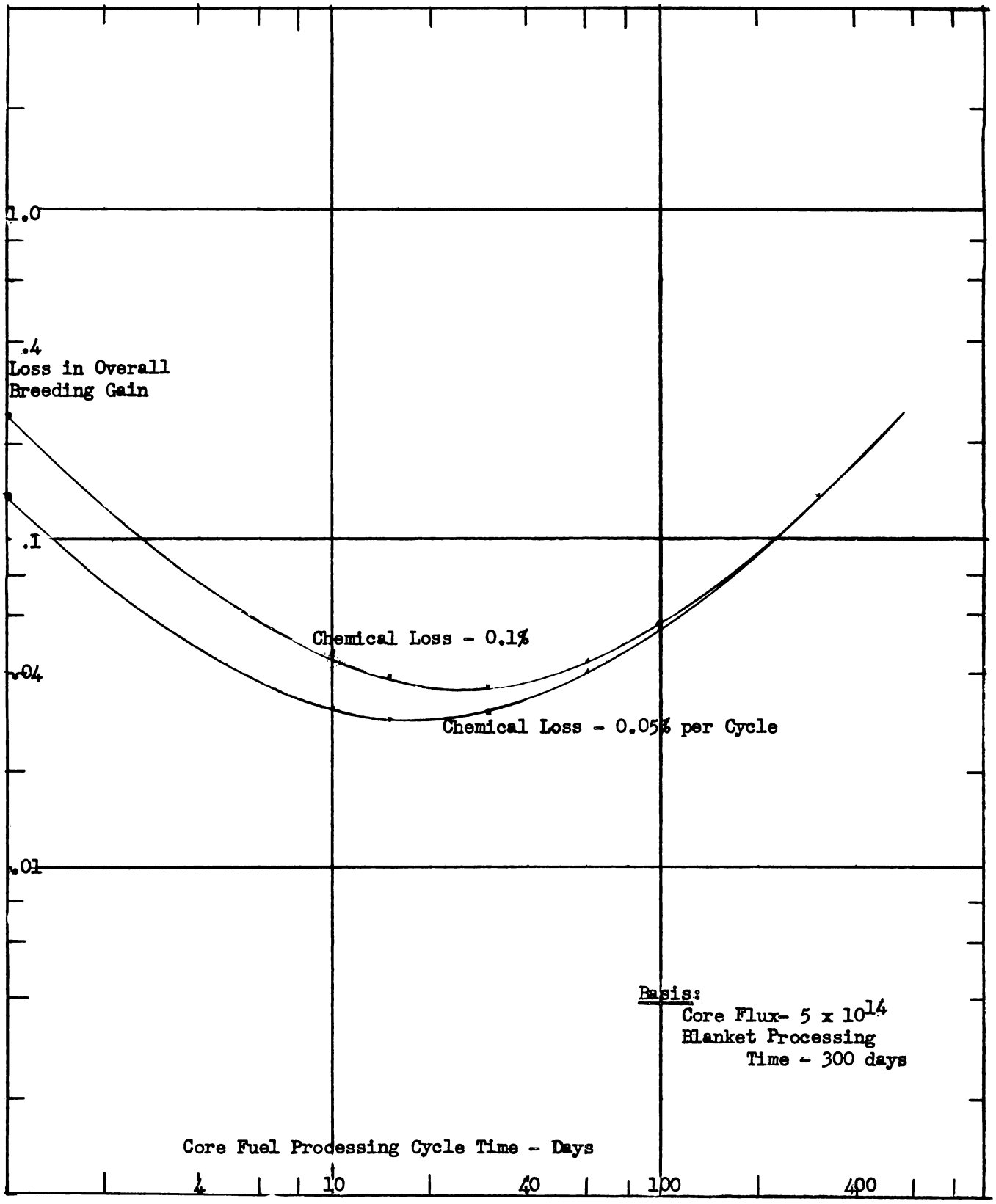

Figure III 3-7

Loss in Overall Breeding Gain From Chemical Processing
Losses Plus Fission Products Poisoning

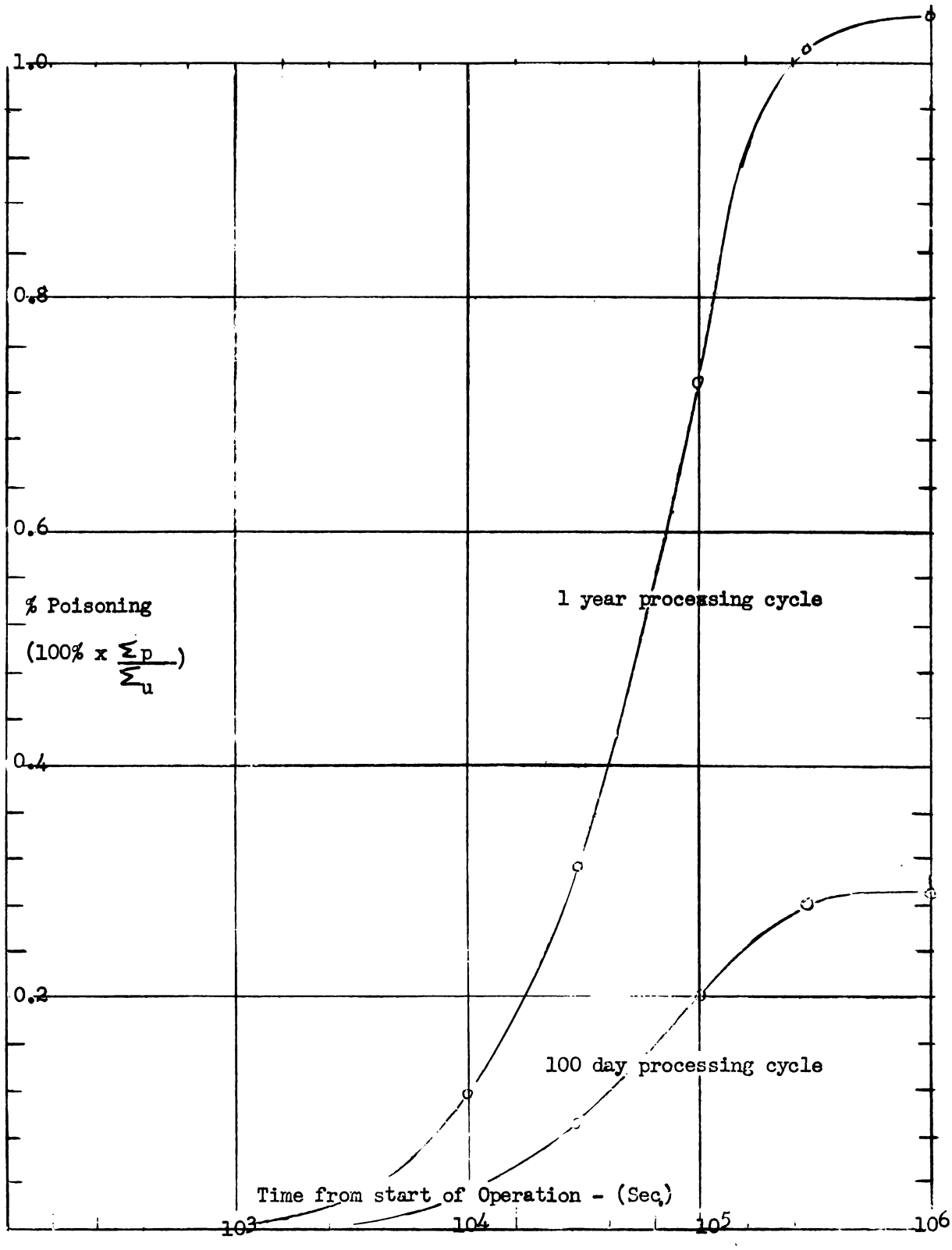

Figure III 3-8

Poisoning Due To Higher Isotopes Buildup In Blanket

— Relative to U-233 In Blanket

higher isotopes at a flux of 10^{13} and for both a 100-day and a 1-year processing cycle. In deriving these results, it was assumed that pure U-233 was charged to the blanket at the start of operation and was then removed in processing as fast as more was produced. Note that the maximum poisoning in the blanket, $\Sigma(HI)/\Sigma_a(23)$, is 0.0029 for a 100-day processing cycle and 0.0105 for a 1-year cycle.

The contribution to U-234 buildup from the neutron capture by Pa is small for the present system of breeding outside the core proper. A typical value for this effect is 2% of the U-234 produced from the neutron capture by the 23

3.3.2 Buildup of Higher Uranium Isotopes in The Core

The higher isotope buildup in the core, similar to the discussion for the blanket, depends on the fissionable material originally charged. The charge for this reactor could be either U-233 or U-235. Additional U-235 could be added to replenish the burnup until sufficient U-233 is produced in the blanket to supply replacement material.

Visner (1) and Ott (2) have evaluated in some detail the higher isotopes buildup for the case where U-233 is originally charged to the core and is continually replenished with pure U-233. Visner's results show that equilibrium poisoning effect, $\Sigma(HI)/\Sigma(23)$, is approximately 0.003 for U-235. The maximum poisoning effect is considerably greater. Thus charging U-235 initially. and then replenishing with U-233 one gets a poisoning peak earlier than predicted by Visner for 23. For the purposes of nuclear calculations, the estimated equilibrium poisoning of 0.003 was used.

3.4 Fission Products Poisoning

In evaluating the fission products poisoning in the H.R.E. reactor,

Stoughton (45) grouped the fission products (as obtained from U-235) into three groups: Group 1 of 1.5% yield and average cross section of 50,000 barns; group 2 of 158.5% yield and average thermal cross section of 50 barns; and group 3 of 40% yield comprising the gaseous (at 250° C) products whose cross section could be neglected. U-233 gives somewhat different yields (e.g. see KAPL-634 (36) or Appendix VIII 3.3) In this report, it was assumed that Stoughton's average figures were also applicable to U-233, but that the cross section for group 2 followed the 1/v rule, thus averaging 25 barns at the proposed operating conditions. Figures III 3-9 and III 3-10 show the total calculated fission product poisoning for the blanket and core, respectively, as a function of the flux and processing rate. These curves show that for a 30-day process cycle time and for a core average flux of 10^{14} and of 5×10^{14}, the core poisoning effects are 1.3% and 2.4 % respectfully. Similarly, for the probable operating conditions in the blanket of a 3×10^{12} flux and a process cycle time of 300 days, the poisoning effect is approximately 1.4 %. Similar results are shown in Figure III 1-11 assuming a higher cross section and lower external holdup.

Figure III 3-12 shows the relative effects of group 1 and of group 2 on the total poisoning as a function of flux. At flux values below about 10^{13}, group 1 is predominant, reaching over 80% of its equilibrium value at the flux of 10^{13}. Above 10^{14} flux, group 2 becomes the most important.

Protactinium Losses

Protactinium losses can occur in two ways: in chemical processing and in neutron capture in the blanket. The former would be about 0.1% of the Pa entering the processing plant. Since this is essentially the same as for the 23, this loss will be lumped in with the 23.

The neutron capture losses will be between 0.01% and 0.05% of the total

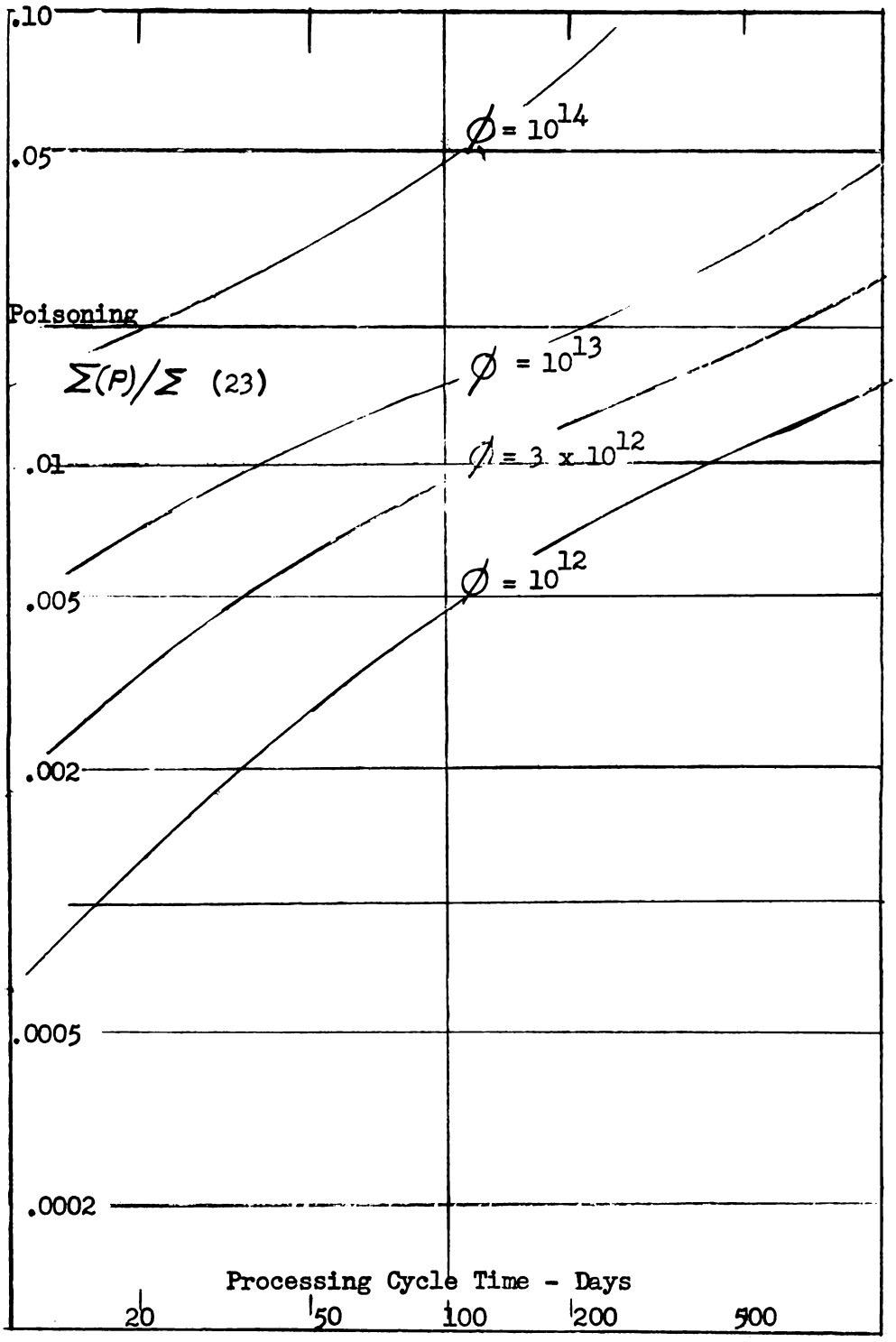

Figure III 3-9

Fission Products Poisoning
in Blanket

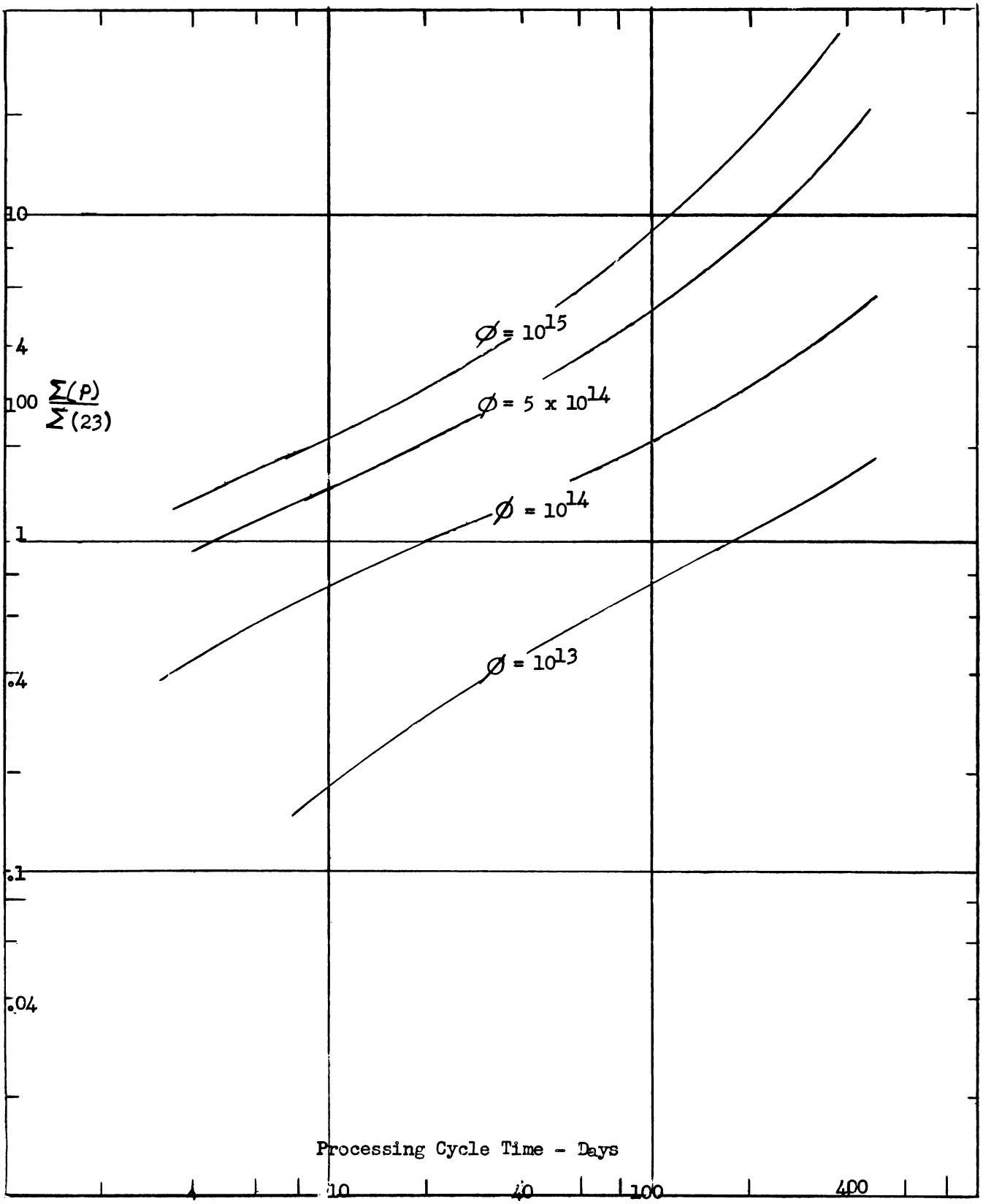

Figure III 3-10

Fission Products Poisoning in Core
(Case-1 ... σ_2 = 25 barns at 2000 °F ; $V_I = 4\ V_c$.)

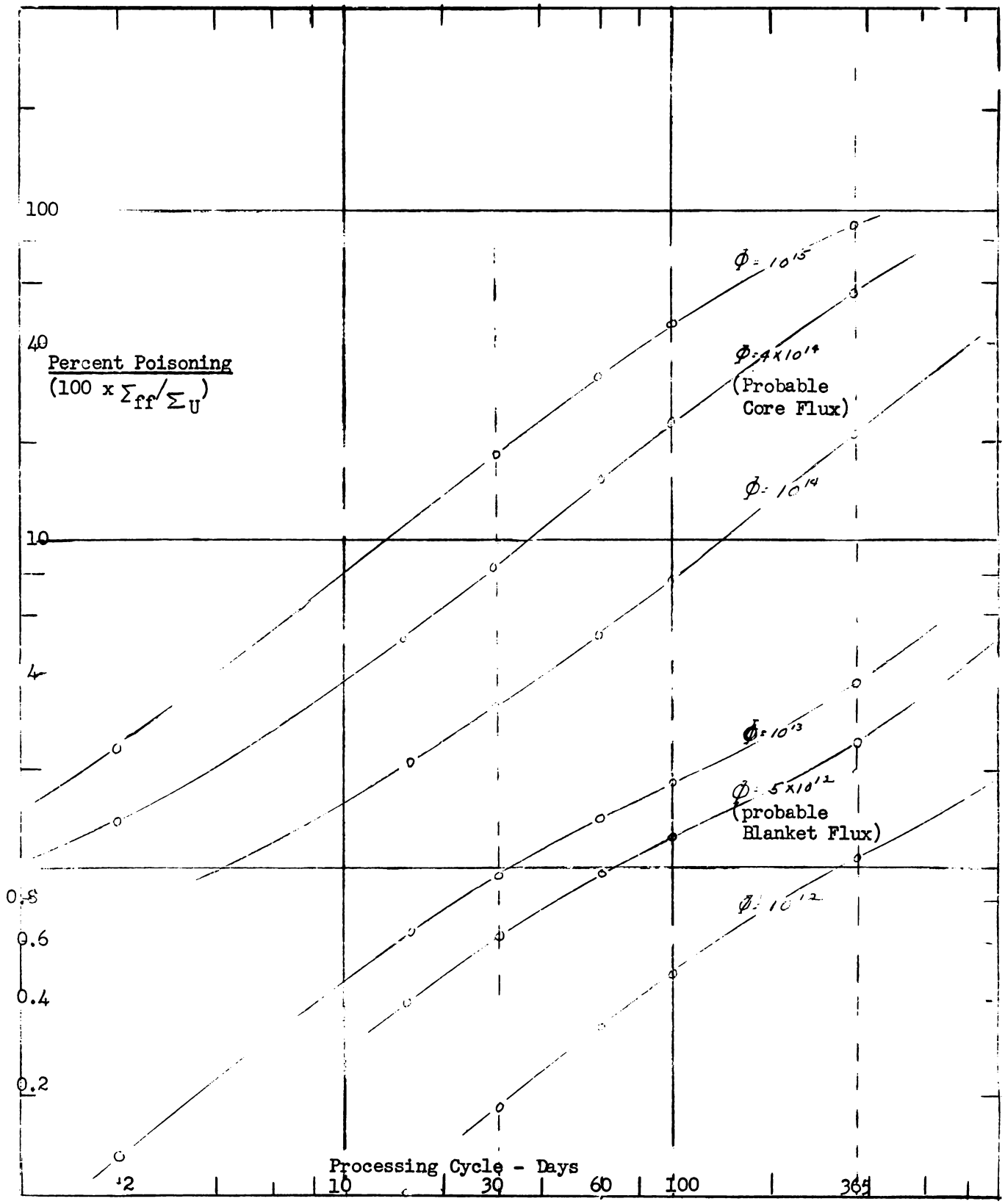

Figure III 3-11

Poisoning In The Core And Blanket Due To

Fission Products At Equilibrium

(Case 2 - σ_2 = 50 barns $V_t = V_c$)

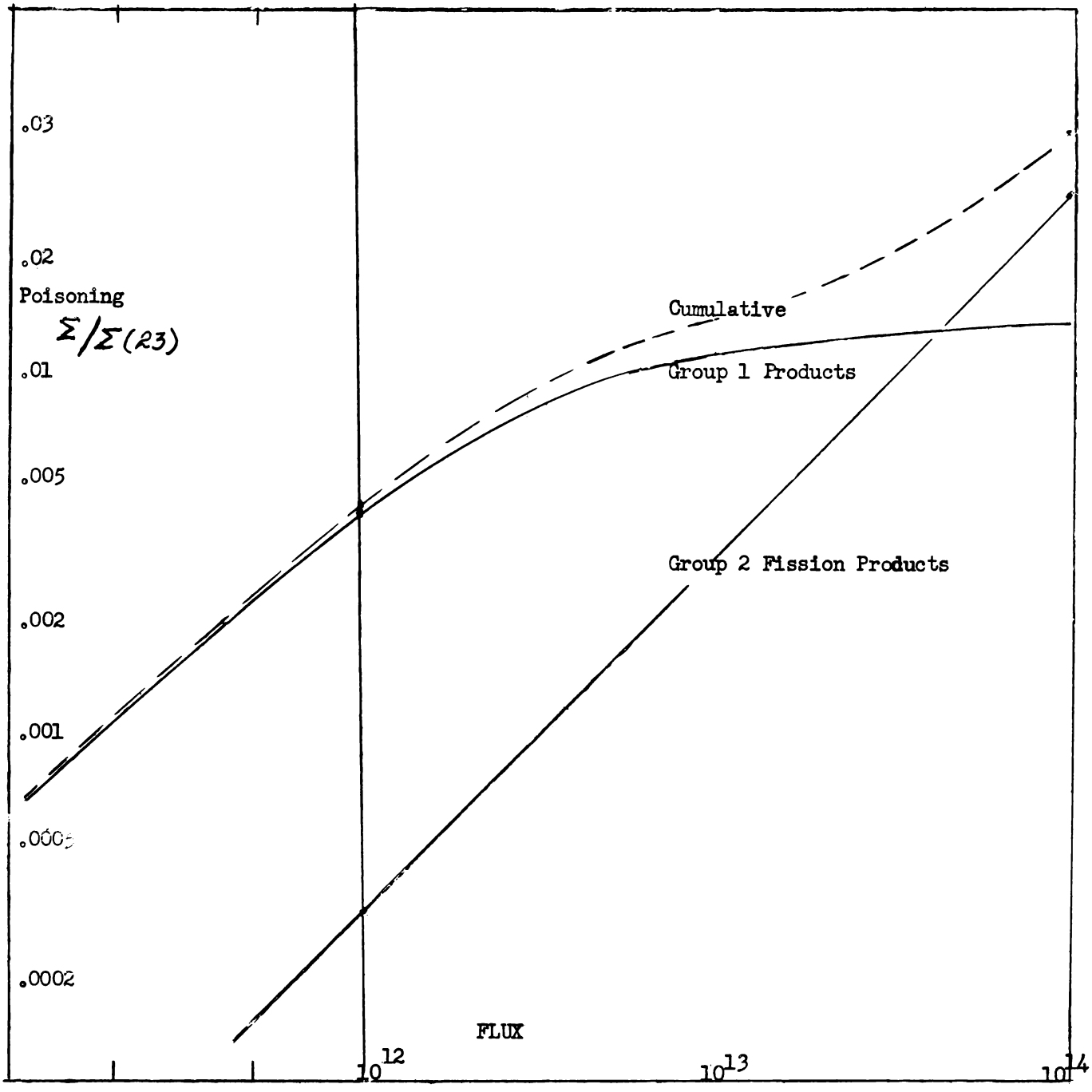

Figure III 3-12

Effect of Each Fission Product Group
On Total Poisoning

Pa produced. (See Appendix VIII 3.3), being 0.020% at a flux of 4×10^{12} and a 300 day processing cycle. For the latter case, the "poisoning" effect, $\Sigma(13)/\Sigma(Th)$, is approximately 0.00024

III- 4 Reactor Control and Safety

4.1 Start-up (Initial)

From the view point of instrumentation, start up of the reactor is simplified in that criticality can be attained with the entire system at room temperature. It is thus unnecessary to develop low flux detecting instruments to operate at high temperatures. Standard fission chambers can be used until criticality is reached and can then be withdrawn. Gamma compensated ion chambers exterior to the blanket indicate neutron flux after the critical point is attained.

The general procedure in starting up is as follows:

The blanket is filled and fluidized with the proper concentrations of thorium and graphite (also U-233 if so desired). All the fine control rods are at maximum withdrawal. The core-heat exchanger system is then nearly filled with the graphite-uranium fuel mixture containing less than the critical concentration of U-233 (or U-235). Circulation of the solids is then started and the concentration of U-233 is then gradually built up until the critical condition is reached and several kilowatts of power are being generated. At this point of the start up the temperature-sensitive, low flux instruments are withdrawn from the blanket and core surface and the exterior higher flux instruments take over. However the reactor system is still essentially at room temperature so that an attempt to increase the power will be accompanied by an increase in temperature and a resulting loss of criticality. Thus it is now necessary to further increase the fuel concentration in increments within control of the control plates. In this

manner a gradual build up to power is reached. If no U-233 is in the blanket, then the operating power of the reactor at this time would be about 225 MW, with a gradual buildup to 250 MW as U-233 is produced in the blanket.

Start-Up (General)

It is assumed here that the reactor has been running for a considerable length of time and is now shut down. Start up in this case is accomplished by controlling the blanket level. This can be done because we know that the core material has the critical concentration of fissile material for the operating temperature and that with no blanket present this concentration is sub-critical at room temperature. Thus, the procedure for initial start-up is now reversed in that the core is filled first, and the blanket materials containing operating concentrations of thorium and uranium, is then gradually introduced. If residual activity is high, it should be possible to reach criticality in a matter of minutes. However, if the reactor has been shut down for a considerable length of time, care must be exercised in the return to the critical condition. The fear in this case as in the initial start up is not that the reactor will "run away", for its high negative temperature coefficient (VIII 3.4) will hold it, but rather that a compression wave might be generated which in the most extreme case could rupture the graphite core shell. It is assumed that interlocks in the safety circuit will prevent such a condition.

Shut-Down

The reactor is shut down by a two-fold procedure. First the control plates move in and the reactor immediately becomes sub-critical. However, the control plates will only keep the reactor sub-critical during the first 100° C temperature drop. Therefore it is necessary that, to obtain a complete shut down, a simultaneous dumping of the blanket take place. It

should be kept in mind, however, that the core material should continue to circulate so that the heat from the exponentially decreasing power can be removed in the heat exchanger.

4.2 Control

4.2.1. Fine Control

Continuous fine control of the reactor on the order of one to two percent δk can be achieved by the use of movable thorium plates within the blanket. Maximum effectiveness occurs when all plates are approximately flush on the outer surface of graphite core shell. Calculations were made on the basis of a 120 cm radius core and a coverage of between 10 to 20% of the core surface area. It was found that a thorium plate 7.3 cms. thick is 50% effective in cutting the thermal neutron intensity and 20% effective in cutting the fast neutron intensity. The surface area of the core is 181,000 cm^2 so that 5 plates 61 cm square yields 18,605 cm^2 or 10% coverage with a maximum δk of 1%. Since the delayed neutron contribution of U-233 is 0,00242 we have then approximately $4.00 worth of fine control. Figs. III 4-1 and III 4-2 show plots of neutron intensity versus thickness and variation of δk with area coverage. Provision can be made for the withdrawal of the plates from the blanket so that they may be processed for the U-233 which will be produced within them. No special provision for cooling the control plates has been considered necessary since they are "immersed" in the fluid bed of the blanket and thus will transfer heat freely to the bed. Since the melting point of thorium is approximately 3000° F and the bed temperature 1500° F to 2000° F no difficulty is anticipated from overheating in the plate. The method used in calculating the effectiveness of the control plates is shown in Appendix VIII 3.4.

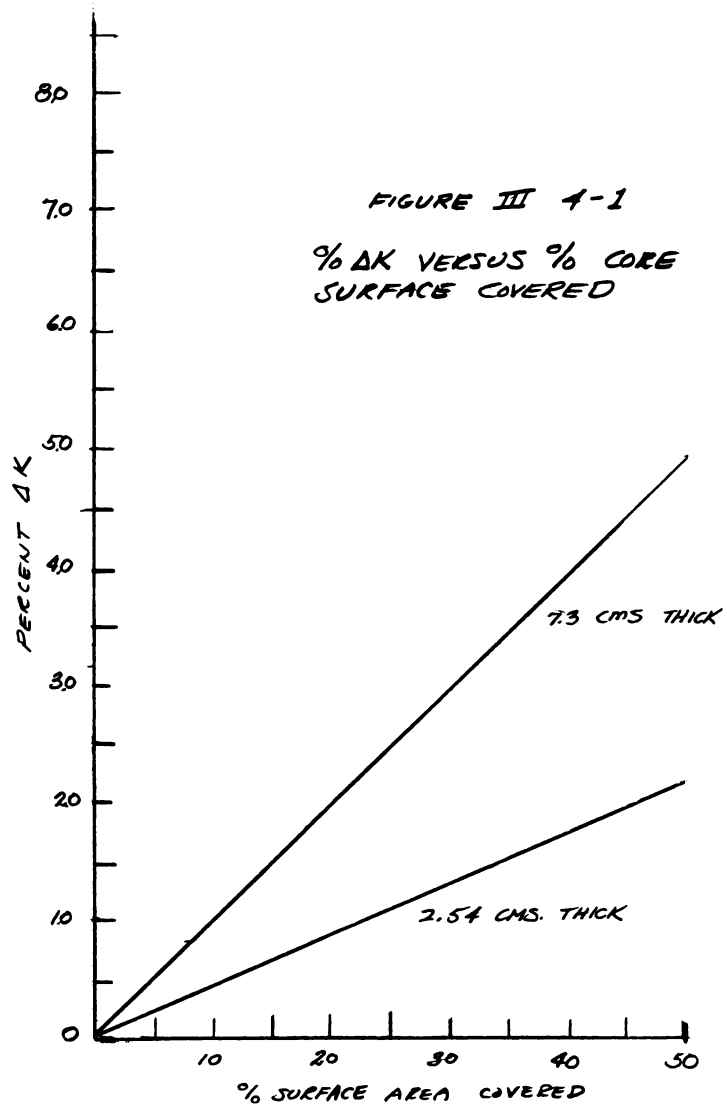

FIGURE III 4-1

% ΔK VERSUS % CORE SURFACE COVERED

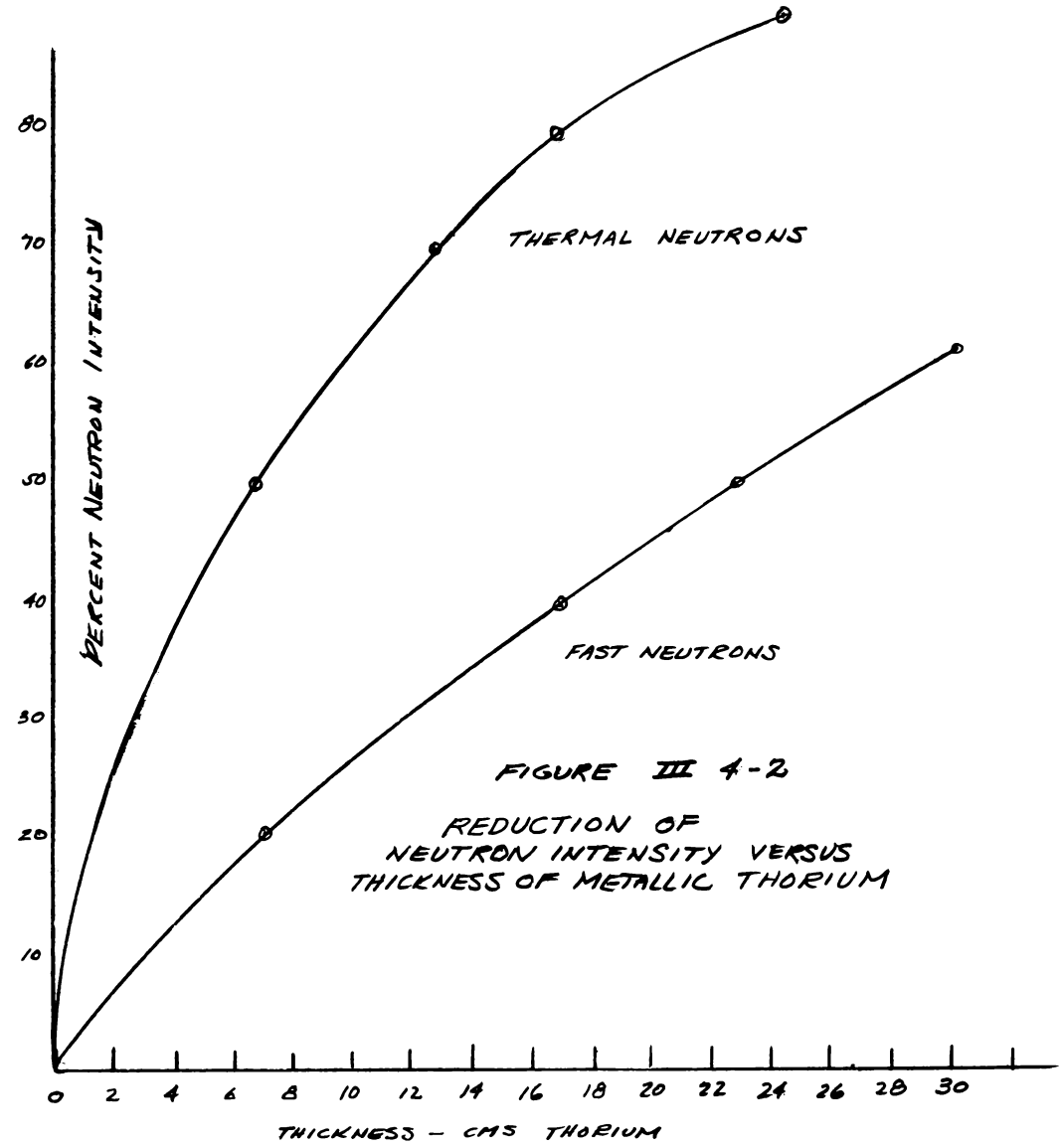

FIGURE III 4-2

REDUCTION OF NEUTRON INTENSITY VERSUS THICKNESS OF METALLIC THORIUM

4.2.2 Course Control

This type of control can be achieved in three independent ways, all three of which may be combined or used separately as the situation demands.

The first and most useful for slow, gradual changes in reactivity is control of the U-233 concentration in the circulating fuel system. This is accomplished by withdrawing a stream of fuel material and at the same rate returning either graphite particles for a reduced concentration effect or enriched particles for a higher concentration. Since there is a continuous side process stream to and from the reactor system for chemical processing, concentration control could be made simultaneously at these points.

The second method of control is primarily a scram, and thus falls under the category of safety control. This method consists in purging all or part of the core material into the heat exchanger. With a flow rate of over 11 ft^3/sec through the core, a 250 ft^3 vessel can be emptied in less than 23 seconds.

The third and last method consists of a variation of blanket density by the regulation of the percent voids in the fluidized solids. This can be achieved by varying the gas velocity through the bed. It might be noted that the decrease in k due to increase in voidage in the blanket is effected through increased leakage of neutrons from the blanket. Since this results in a loss in gain, this type of control is recommended only for temporary use.

Provisions can also be made for dumping the blanket. This method of control can keep the reactor sub-critical even when the core is cooled down to room temperature. If the entire contents of the blanket are dumped, the resulting δk obtained is -30% while the cooling of the core increases k by only 18%. Moreover, such a system could be "gravity operated" and

could thus be made to "fail safe".

Control of Power

It is assumed that drastic changes in power will not be demanded of the power plant and that large reductions will not extend over periods greater than a few days. Such changes can be handled by increasing the bed voidage, operating at a lower temperature, and accepting the resulting loss in gain. Long term change in power level can be handled by varying the concentration of U-233 in the core.

4.3 Safety

As stated previously in the section on control, the reactor fails safe in an emergency. This is accomplished by the gravity dump system incorporated in the blanket. There should be provision for a tandem blower system in both blanket and core system, the secondary blower in each case being connected to a standby power supply such that failure in either the primary electrical supply or the primary blower will not necessarily require that the reactor be shut down.

Monitoring the off gases of both the blanket and core-heat exchanger systems will give indication of leaks in steam tubes of either blanket or heat exchanger vessel by detecting the presence of water vapor, hydrogen and excess carbon monoxide.

The probability of erosion failure in core shell, cyclones and transfer lines has been lessened by arbitrarily overdesigning these members by factors of 5, 2, and 2 respectively. Transfer lines and cyclones must stand the worst erosive conditions but the silicon carbide liner specified has stood up remarkably well for several years in existing systems under similar conditions. Thus it is anticipated that the yearly shut-down inspection will detect excessive wear before it can become a hazard.

Consider now the very remote possibility that the core materials jam in the core thus preventing circulation. If it is assumed that the reactor has been running at full power for a considerable time prior to this emergency then the delayed power at time t after shutdown is given by

$$* \quad P \simeq 0.0325 \; P_o \; t^{-1/5}.$$

where P_o = operating power

t = seconds ; with 10 sec $<$ t $<$ 10 days.

* Note that since the total volume of the fuel material will be at least 2 times the core volume, the overall power density will be approximately 1/2 of the power density based on the core alone. Hence the constant of 0.0325 rather than the 0.065 normally recommended.

The 5.25 foot radius reactor core contains 32,200 lbs. of solids with a heat capacity of 0.5 Btu/lb - °F so that the total heat capacity is 16,100 Btu/°F. The power P_o in the core at the instant of shutdown is 2.13×10^5 Btu/Sec. (90% in core, 10% in blanket). The temperature rise at full power is therefore,

$$\frac{2.13 \times 10^5}{16{,}100} = \frac{\text{Btu/Sec}}{\text{Btu/ °F}} = 13.2 \text{ °F/Sec.}$$

Integrating the power equation and assuming somewhat pessimistically that no heat is removed from the core the core temperature after 5 hours will be,

$$2000° \text{ F} + 0.536 \left[t^{4/5} \right]_{t_1 = 10 \text{ sec}}^{t_r = 18{,}000 \text{ sec}}$$

$$= 3{,}365° \text{ F}$$

Now as far as the graphite shell and core material are concerned this is not a dangerous temperature and the writer feels justified in assuming that in 5 hours a method (such as blowing argon gas through the core) can be found to keep the temperature from rising even to the value just calculated. Figure III 4-3 shows a graph of this rise versus time after shutdown. * (47)

FIGURE III 4-3

CORE TEMPERATURE V.S. TIME AFTER SHUTDOWN

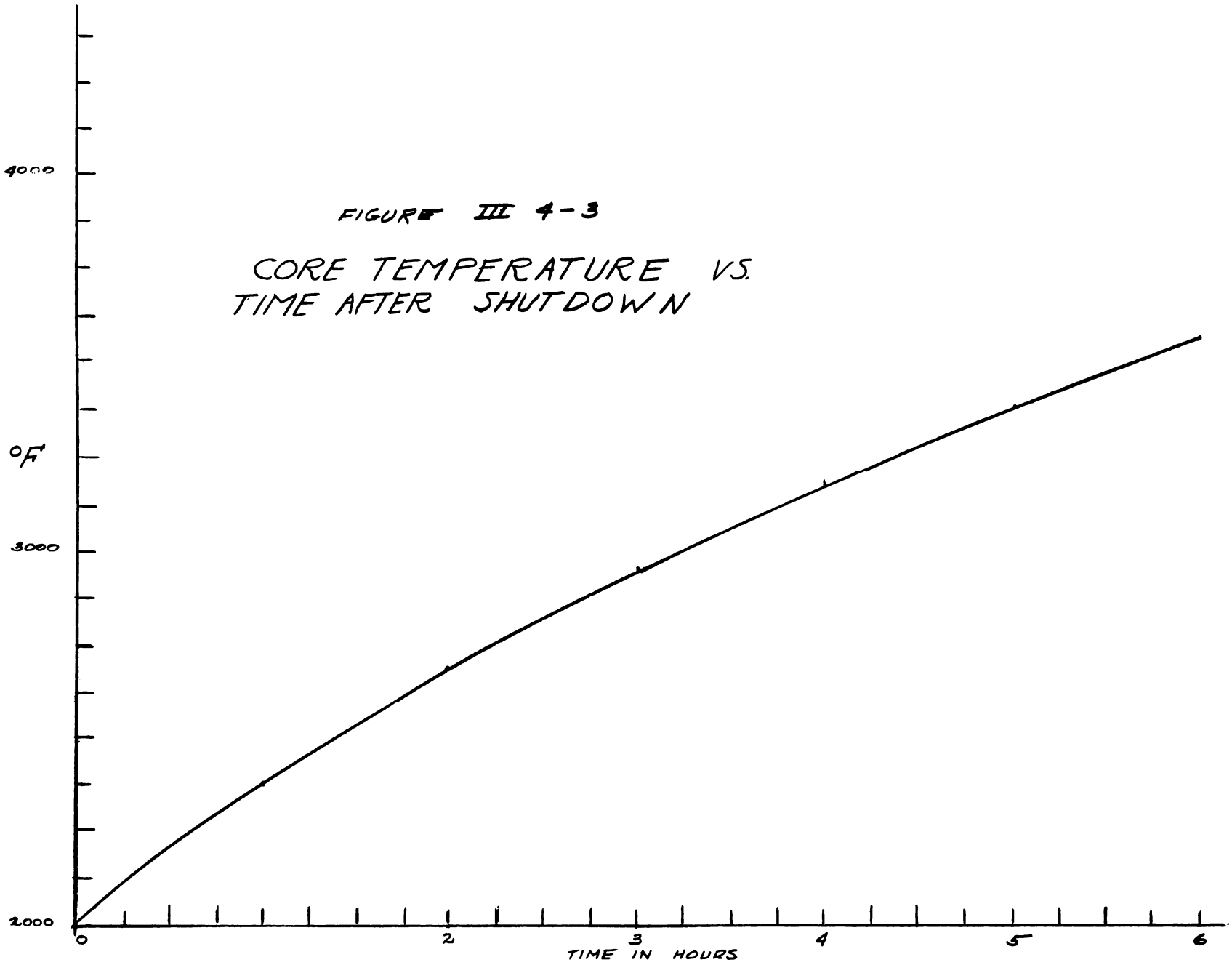

Calculations on the possibility of a critical condition existing in either transfer lines or heat exchanger are shown in Appendix 3-4. It is found that both are sub-critical under the worst possible conditions with one exception, the highly improbably condition that the vessels are flooded with liquid water. Should such a situation occur, the vessel would become critical and the water begin to boil. The system would then operate either as a low temperature boiling reactor until the water boiled off or upon boiling would become sub-critical again and then oscillate between critical and sub-critical. Occurrances such as these are only listed so that the evaluation of the reactor safety is complete.

One further topic will be discussed and this is the possibility of a leak in the gas-solids system. Since the reactor operates in the region of atmospheric pressure it would be relatively simple by means of a blower to have a slightly higher pressure within the shield compartments so that any leak that occurred would be into, rather than out of, the system. The monitoring system that is used to detect water tube leaks would also detect air leaks so that no additional instrumentation is required.

III - 5 Shielding

In order to include shielding calculations in this feasibility study it was necessary to base these calculations on what appeared at the time, to be the most likely final design. Although the final design may be somewhat different than that assumed in this section,

these differences are not expected to greatly affect the shielding requirements.

The following calculations will be based on the assumption that the reactor consists of a spherical core of 120 cm. radius surrounded by a blanket 100 cm. thick. The core will contain graphite particles impregnated with U-233, and 40% of the core volume will be voids. About 87% of the fission power will occur in the core. The blanket will consist of a fluidized bed of Th C_2 and graphite particles and 100 Kg of U-233.

250 Megawatts is to be released in the reactor as heat. Assuming 195 Mev is released for each fission of a U-233 nucleus, of which 11 Mev disappear with neutrinos and 184 Mev per fission will appear as heat.

Thus:

$$250 \times 10^6 \text{ watts} \times \frac{1 \text{ erg}}{10^{-7} \text{ watt-sec}} \times \frac{1 \text{ Mev}}{1.6 \times 10^{-6} \text{ ergs.}} \times \frac{1 \text{ fission}}{184 \text{ Mev}} = 8.5 \times 10^{18} \text{ fiss/sec}$$

$$\text{No. of fissions/sec in core} = N_c$$

$$N_c = (8.5 \times 10^{18})(\% \text{ of fissions in core})$$

$$= \frac{(8.5 \times 10^{18})(87)}{100} = 7.4 \times 10^{18} \text{ fissions/sec.}$$

$$\text{No. of fission/sec in blanket} = N_6$$

$$N_6 = (8.5 \times 10^{18}) \left(\frac{\% \text{ of fissions in blanket}}{100}\right)$$

$$= \frac{(8.5 \times 10^{18})(13)}{100} = 1.1 \times 10^{18} \text{ fissions/sec.}$$

Although a constant power density will probably not be achieved, such an assumption can be justified for the purpose of these calculations on the basis of giving a conservative answer for the shielding requirements, the power distribution that will be finally obtained will not greatly affect these requirements, and the shielding calculations will be somewhat simplified.

No. of fissions/cm^3 - sec in core = n_c

$$n_c = \frac{N_c}{V_c}$$

V_c = core volume = $\frac{4}{3} \pi R_c^3$

R_c = core radius = 120 cm

$$n_c = \frac{(7.4 \times 10^{18})(3)}{(4)(3.1416)(120)^3} = 1.02 \times 10^{12} \text{ fissions/cm}^3\text{-sec}$$

No. of fissions/cm^3 - sec in blanket = n_b

$$n_b = \frac{N_b}{V_b}$$

Vb = blanket volume = $\frac{4}{3} \pi (R_b^3 - R_c^3)$

$$n_b = \frac{(1.1 \times 10^{18})(3)}{(4)(3.1416)\left[(220)^3 - (120)^3\right]} = 2.94 \times 10^{10} \text{ fiss/cm}^3 \text{ - sec.}$$

Gamma Production in Core

Fission capture in U-233

Assume 5 - 1 Mev instantaneous γ's per fission

$$\gamma \text{ production} = 5\, n_c$$
$$= (5)\ (1.02 \times 10^{12})$$
$$= 5.1 \times 10^{12} \text{ 1 Mev } \gamma\text{'s/cm3-sec}$$

Non-fission capture in U-233

Assume 1 - 7 Mev γ per capture

For U-233: $\nu = 2.57$

$\eta = 2.33$

$$\text{i.e. } \frac{2.57 - 2.33}{2.33} = \frac{.24}{2.33} \quad \frac{\text{non-fission captures}}{\text{fission capture}}$$

$$\gamma \text{ production} = n_c \left(\frac{.24}{2.33}\right)$$

$$= \frac{(1.02 \times 10^{12})\ (.24)}{2.33}$$

$$= 1.05 \times 10^{11} \text{ 7 Mev } \gamma\text{'s/cm}^3 - \text{sec}$$

Capture in carbon

Assume 1 - 5 Mev γ per capture

$$Z = \frac{\text{absorptions in U-233}}{\text{absorptions in carbon}}$$

$$\gamma \text{ production} = \frac{\text{abs. in U-233}}{z}$$

(probable value of z about 20)

$$\gamma \text{ production} = \frac{(1.02 + .105)\ 10^{12}}{20}$$

$$= 5.63 \times 10^{10} \quad 5 \text{ Mev } \gamma\text{'s/cm}^3\text{-sec}$$

Fission product gammas

Assume 2 - 2.5 Mev γ's per fission

$$\gamma \text{ production} = 2\ n_c$$

$$= (2)(1.02 \times 10^{12})$$

$$= 2.04 \times 10^{12} \quad 2.5 \text{ Mev } \gamma\text{'s/cm}^3\text{-sec}$$

Gamma Production In Blanket

Fission capture in U-233

Assume 5 - 1 Mev γ's per fission

$$\gamma \text{ production} = 5\ n_b$$

$$= (5)(2.94 \times 10^{10})$$

$$= 1.47 \times 10^{11} \quad 1 \text{ Mev } \gamma\text{'s/cm}^3\text{-sec}$$

Non-fission capture in U-233

Assume 1 - 7 Mev γ per capture

$$\gamma \text{ production} = n_b\left(\frac{.24}{2.33}\right)$$

$$= \frac{(2.94 \times 10^{10})(.24)}{(2.33)}$$

$$= 3.03 \times 10^{9} \quad 7 \text{ Mev } \gamma\text{'s/cm}^3\text{-sec}$$

Fission product gammas

Assume 2 - 2.5 Mev γ per fission

$$\gamma \text{ production} = 2\ n_b$$

$$= (2)\ (2.94 \times 10^{10})$$

$$= 5.88 \times 10^{10} \quad 2.5 \text{ Mev } \gamma\text{'s/cm}^3\text{-sec}$$

For the subsequent calculation of gamma production in the blanket the following constants will be assumed as being representative of the final

design:

Σ_a (carbon) = .000842

Σ_a (thorium) = .008355

Σ_r (thorium) = .003963 (resonance absorption)

Σ_f (U-233) = .0017877

Capture in carbon

Assume 1 - 5 Mev γ per capture

$$\gamma \text{ production} = n_b \frac{\Sigma a \text{ (carbon)}}{\Sigma_f \text{ (U-233)}}$$

$$= (2.94 \times 10^{10}) \frac{.000842}{.0017877}$$

$$= 1.38 \times 10^{10} \quad 5 \text{ Mev } \gamma\text{'s/cm}^3\text{-sec}$$

Thermal neutron capture in Th-232

Assume 1 - 5 Mev γ per capture

$$\gamma \text{ production} = n_b \frac{\Sigma a \text{(thorium)}}{\Sigma_f \text{(U-233)}}$$

$$= \frac{(2.94 \times 10^{10})(.008355)}{.0017877}$$

$$= 1.37 \times 10^{11} \quad 5 \text{ Mev } \gamma\text{'s/cm}^3\text{-sec}$$

Resonance capture in Th-232

Assume 1 - 5 Mev γ per resonance capture

$$\gamma \text{ production} = n_b \frac{\Sigma r \text{ (thorium)}}{\Sigma_f \text{ (U-233)}}$$

$$= \frac{(2.94 \times 10^{10})(.003963)}{.0017877}$$

$$= 6.52 \times 10^{10} \quad 5 \text{ Mev } \gamma\text{'s/cm}^3\text{-sec}$$

Source	γ- energy (Mev)	γ production (γ's/cm^3 - sec)	
		Core	Blanket
Fission capture in U-233	1	5.10×10^{12}	1.47×10^{11}
Non-fission capture in U-233	7	1.05×10^{11}	3.03×10^{9}
Fission product gammas	2.5	2.04×10^{12}	5.88×10^{10}
Capture in carbon	5	5.63×10^{10}	1.38×10^{10}
Thermal capture in Th	5	---------	1.37×10^{11}
Resonance capture in Th	5	---------	6.52×10^{10}

Radiation at Reactor Surface From Core Gammas

Mass absorption coefficients*

Absorber	μ_m (cm^2/gm)			
	1 Mev γ's	2.5 Mev γ's	5 Mev γ's	7 Mev γ's
Carbon	.063	.039	.027	.022
Thorium	.082	.044	.045	.048

* CF 51-10-70 Part 1, pages 39 and 40

Absorption coefficients for reactor

μ (cm-1) = $\mu_m \rho$

Assuming: .704 gm carbon/cm^3 in blanket

1.0 gm thorium/cm^3 in blanket

$$(1.65)\ 1 - \frac{\%\text{voids}}{100} = (1.65)(0.6)$$

= .99 gm carbon/cm^3 in core

Absorber	ρ	μ (cm^{-1})			
		1 Mev γ's	2.5 Mev γ's	5 Mev γ's	7 Mev γ's
Carbon in core	.99	.062	.039	.027	.022
Carbon in blanket	.704	.044	.027	.019	.015
Thorium in blanket	1.0	.082	.044	.045	.048

Since the reactor core is large nearly all the radiation that leaks out does so from near the core periphery. Simple exponential attenuation becomes a good approximation in this case for replacing the volume distributed source by an equivalent surface distributed source. If a is the volume source, γ's/cm^3-sec., and λ_c is the core relaxation length, it can be shown that a good approximation of an equivalent surface source, σ (γ's/cm^2-sec), is given by:

$$\sigma = \lambda_c \, a \qquad \text{(See CF 51-10-70, Part 2, page 86)}$$

$$\lambda_c = \frac{1}{\mu_c}$$

where μ_c is the absorption coefficient for carbon in the core

γ - energy	μ_c (Cm^{-1})	λ(Cm)	a(γ's/cm^3-sec)	σ (γ's/cm^2-sec
1 Mev	.062	16.1	5.10×10^{12}	8.21×10^{13}
2.5 Mev	.039	25.6	2.04×10^{12}	5.23×10^{13}
5 Mev	.027	37.1	5.63×10^{10}	2.09×10^{12}
7 Mev	.027	45.5	1.05×10^{11}	4.78×10^{12}

Attenuation of core gammas through blanket

It is desired to find the number of γ's per cm^2 per sec. at the surface of the reactor due to the source calculated above, distributed on the surface of the reactor core. To obtain this result the following formula will be used:

$$\sigma(R_b,R_c) = \frac{R_c}{R_b}\left[\sigma_{pl}\,(R_b - R_c, \infty) - \sigma_{pl}(R_b + R_c, \infty)\right] \quad (1)$$

where R_b = radius of reactor = 220 cm.

R_c = radius of core = 120 cm

$\sigma(R_b,R_c)$ = No. of γ's/cm^2-sec at R_b due to a surface distributed source, σ, on a sphere of radius, R_c, imbedded in an isotropic medium.

$\sigma_{pl}(R_b - R_c, \infty)$ = No. of γ's/cm^2-sec. at $R_b - R_c$ cm from a surface distributed source, σ, on an infinite plane in an isotropic medium.

$$= \frac{\sigma}{2} e^{-\mu_b (R_b - R_c)}$$

(assuming linear build-up)

μ_b = absorption coefficient for blanket

$$\sigma_{pl}(R_b + R_c, \infty) = \frac{\sigma}{2} \left[e^{-\mu_b (R_b + R_c)} \right] (2)$$

$$\sigma(R_b, R_c) = .272 \sigma \left[e^{-100\mu_b} - e^{-340\mu_b} \right]$$

μ_b = μ(carbon in blanket) + μ(thorium in blanket)

Because R_b and R_c are so large, the exponential factor $e^{-340\mu_b}$ becomes negligibly small.

γ-energy (Mev)	μ_b (cm^{-1})	σ (γ's/cm^2-sec)	$e^{-100\,\mu_b}$ A	$\sigma(R_b, R_c)$ (γ's/cm^2-sec)
1	.126	8.21×10^{13}	3.39×10^{-6}	7.57×10^{7}
2.5	.071	5.23×10^{13}	8.26×10^{-4}	1.17×10^{10}
5	.064	2.09×10^{12}	1.67×10^{-3}	9.51×10^{8}
7	.063	4.78×10^{12}	1.84×10^{-3}	2.39×10^{9}

Radiation at Reactor Surface from Blanket Gammas

Because R_b and R_c are so large, the blanket will be treated as an infinite self-absorbing slab source. With this assumption the volume distributed source in the blanket, a_b(γ's/cm^3-sec) can be replaced by an equivalent source at the reactor surface, σ_b(γ's/cm^2-sec), by the following formula: (assuming exponential attenuation with linear buildup).

$$\sigma_b = \frac{a_b}{2\,\mu_b} \qquad \left[\text{CF 51-10-70, equation 49} \quad z = 0 \right]$$

(1) CF 51-10-70 equation 32
(2) CF 51-10-70 equation 45

γ-energy (Mev)	μ_b (cm^{-1})	a_b (γ's/cm^3-sec)	σ_b (γ's/cm^2-sec)
1	.126	1.67×10^{11}	6.63×10^{11}
2.5	.071	5.88×10^{10}	4.14×10^{11}
5	.064	2.16×10^{11}	1.69×10^{12}
7	.063	3.03×10^{11}	2.40×10^{10}

Source Strength of γ-rays at Reactor Surface

Source strength = γ's/cm^2-sec x $\frac{Mev}{\gamma}$ = Mev/cm^2-sec

Source	Energy	σ	Source Strength
Core	1	7.57×10^{7}	$.008 \times 10^{10}$
	2.5	1.17×10^{10}	2.925×10^{10}
	5	9.51×10^{8}	$.475 \times 10^{10}$
	7	2.39×10^{9}	1.672×10^{10}
Blanket	1	6.63×10^{11}	66.3×10^{10}
	2.5	4.14×10^{11}	103.6×10^{10}
	5	1.69×10^{12}	845×10^{10}
	7	2.40×10^{10}	16.8×10^{10}
		TOTAL	1036.8×10^{10}

The γ radiation at the surface of the reactor can be taken as 10^{13} Mev/cm^2/sec. It will be necessary to reduce this radiation by a factor of 10^{11} to give an acceptably low dose at the shield surface. Bulk shielding tests in pure water indicate that 21.2 ft. of water will give the required attenuation. If the present plan to submerge the reactor in water is found to be feasible γ radiation will be adequately reduced by absorption in the feedwater and concrete shield wall.

Neutron Leakage

Calculations indicate the following neutron leakage from the reactor

Fast neutrons $4.08 \times 10^{11}/cm^2/sec.$

Thermal neutrons $7.53 \times 10^{10}/cm^2/sec.$

Assuming that water surrounds the reactor, bulk shielding tests show that 6' of water for the fast neutrons and 4' of water for the thermal neutrons will be required to reduce the dose from these radiations to acceptably low levels.

Heat Exchangers

According to present plans the heat exchanger compartment will also be surrounded by water, as well as a concrete wall. The radiations from the compartment will be the same as from the reactor but the amount of radiation will be considerably less. The heat exchanger will be quite conventional and should present no unusual problems. It is desirable for maintenance reasons to have such pieces of equipment as air blowers, pumps, dust filters, etc outside the shield which contains the reactor and heat exchanger. Radiation hazards will result from the radioactive "fines" collected in the filters and from the "fines" which are not removed in the filters and carried through the gas lines and blowers.

Since about 5 Mev are released per fission as delayed gamma's, and the fission rate in the core is 7.4×10^{18} fissions per sec, $(7.4)(5)\ 10^{18} = 37 \times 10^{18}$ Mev/sec is released as delayed gammas. The core will contain some 16 tons of solid material and a study of the efficiency of the cyclones and filters in removing the fine particles in the gas stream indicates that 2.42×10^{-5} lbs. of this material per cu. ft. will be carried through the blower and gas lines. Thus.

$$(37 \times 10^{18}) \frac{2.42 \times 10^{-5}}{(16 \times 2000)} = 2.8 \times 10^{10} \text{ Mev/cu ft/sec}$$

will radiate from the gas lines and blowers between the filters and the point at which the lines reenter the reactor shield. The filters themselves will collect some 5 lbs. of the radioactive material per min. As a result of this γ-activity, all equipment in the gas transfer system must be heavily shielded and cannot be worked on during reactor operation except by remote control. In the above calculation the decay of the fission products in the heat exchanger has been neglected and also the induced activity in the gas, probably Argon.

III-6 Maintenance

Introduction

If a nuclear power plant is to be economically feasible the unit will have to remain in operation over a considerable period of years. It seems reasonable therefore, that one of the important problems to investigate in determining the feasibility of any nuclear power plant is the possibility of prolonging the life of the plant by the application of inspection and maintenance procedures. Although this would also apply to conventional power plants it is especially important in connection with a plant employing nuclear reactions as a source of power because the additional hazard of radioactivity greatly increases the difficulty of repairing faulty equipment located behind cumbersome shields. It seems highly improbable that a reactor system could be designed for the generation of useful power which would not be subject to some unforeseen failures in equipment. To minimize this possibility, considerably more emphasis has been attached to the design of individual components in a reactor system than is the usual industrial practice. In addition, duplication of certain critical units has been used as an insurance measure in many existing and proposed

reactor systems. However, past experience indicates that contingencies still arise despite all precautions and eventual access to the shielded equipment is required to repair or replace faulty equipment.

One of the principle advantages of the fluidized reactor design as illustrated in Figure III 6-1 is that if a failure does occur despite all precautions it should be possible to gain access to all parts of the system. An additional advantage of this particular layout of equipment is that installation or replacement of equipment can be accomplished if it becomes apparent after the system has been operating that improved performance is possible with a modified design.

Facilities can be provided in the layout of the plant for the storage of replaced equipment. A flooded compartment can be constructed below or adjacent to the reactor chamber as a storage site for dismantled radioactive equipment.

Accessibility to Reactor Compartment

In addition to the biological shield of concrete constructed around the reactor compartment, it was decided to flood the entire chamber with water. This has two advantages; first, an additional storage facility for the feed water supply need not be provided, and second, it will be possible to maintain a sufficient depth of water so that the upper concrete shield can be removed to provide access to the reactor compartment during actual operation. In case of failure in the reactor compartment equipment the following procedure can be employed to gain access to the faulty equipment despite the presence of residual activity.

(1) After shutting down the reactor, the level of activity in the chamber can be considerably reduced by dumping the contents of the system into the storage facilities provided for this purpose.

(2) To remove any residual activity due to the adherance of the fuel mixture particles to various surfaces the system can be flushed out by circulating throughout the system, some fertile material that will eventually be charged to the blanket.

(3) The above step can be followed by flushing again, this time with an inexpensive carbon product such as petroleum coke. After discharging these materials, the bulk of the remaining activity in the chamber will be due to the induced activity in the materials of construction and to the presence of fission products which have impregnated the walls of the vessel with fission products.

(4) After monitoring the chamber and allowing a suitable decay period for the tolerance level to be attained, a shielded mechanism containing an operator can be submerged into the water. The mechanism will be equipped with remote control apparatus capable of performing the desired operations at safe distances. Shielding properties of the water are to be utilized to further attenuate the residual activity in the chamber.

Inspection

Since the equipment in the reactor compartment is to be submerged in water it should be possible to design remote controlled equipment to inspect the system. Because of the proposed layout, external inspection should be possible using telescopic devices, lowered into the chamber. Inspection of the interior of the equipment should also be possible but only after dumping the contents. The size of the equipment will enable such devices to be lowered into the interior for inspection.

Drawing #22896

FIGURE III 6-1

LAYOUT ILLUSTRATING ARRANGEMENT
OF EQUIPMENT TO FACILATE MAINTENANCE

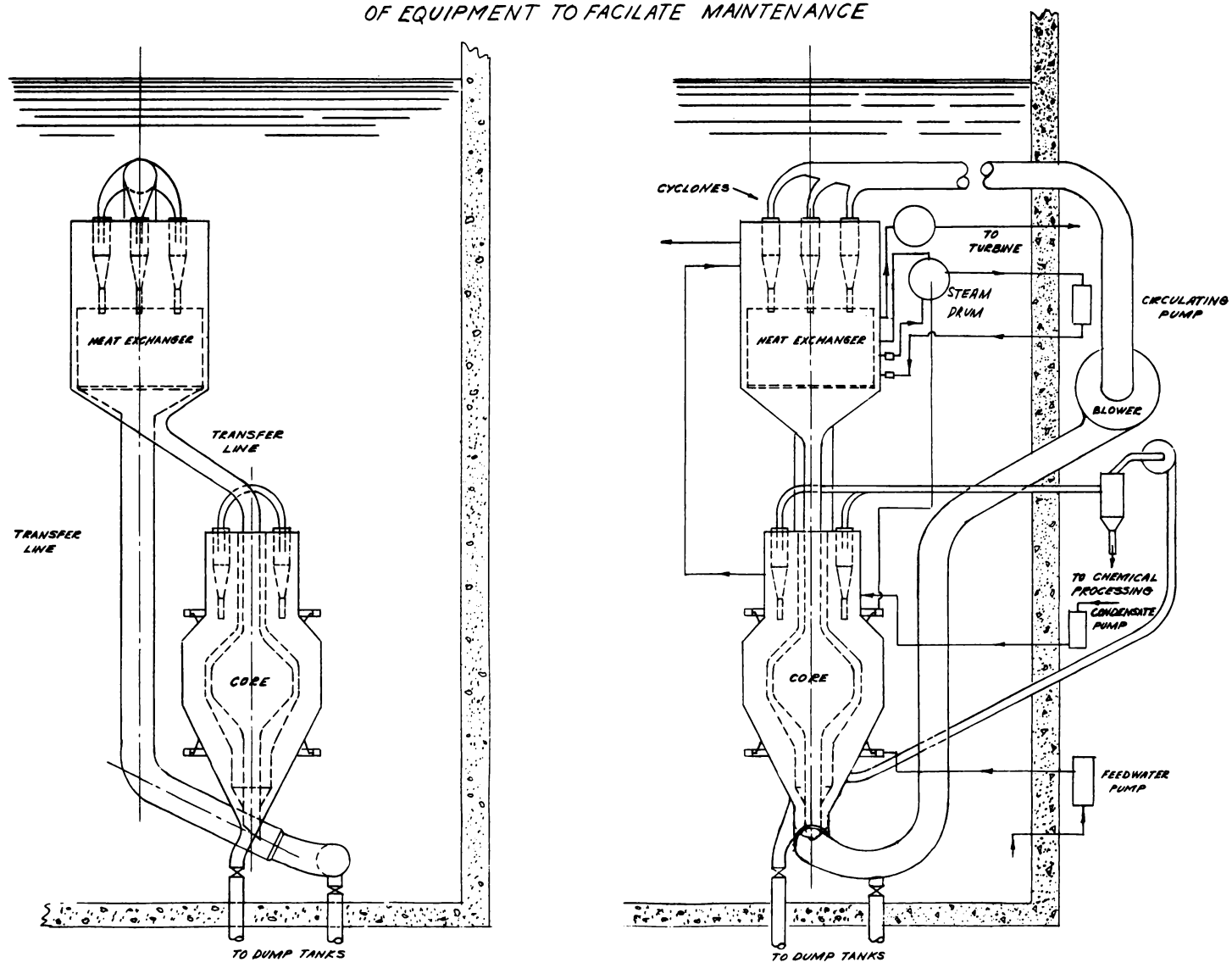

FRONT VIEW

SIDE VIEW

Arrangement of Reactor Compartment Components

The problem of maintenance on this system is greatly simplified by arranging the equipment as indicated in Figure III 6-1. Access to the main heat exchanger and the reactor can be obtained by remote controlled equipment lowered from above the compartment. This proposed layout affords excellent access to the cyclones and heat exchanger tubes, two items which are anticipated to require maintenance. All heat exchangers are so located and so constructed that the tubes will be readily accessible in case of tube failure. If, after considerable operation, it becomes apparent that the erosion of the core shell is greater than anticipated, a new shell can be installed since sufficient clearance can be provided. All pumps, and blower equipment is located in separate shielded compartments to simplify maintenance on this equipment.

Reactor Maintenance

Because of the simplicity of the reactor core design it is expected that the maintenance required will be negligible. However, if it develops that the core shell has been subjected to more severe erosion than anticipated, provisions can be incorporated in the layout of the equipment for its replacement. At points in the core shell where it is found by experiment that erosion is most severe, a lining of silicon carbide can be installed. If a failure occurs in the blanket heat exchanger tubes, the tube can be disconnected at the headers. This procedure is simplified by having the tubes terminate in the headers external to the reactor proper.

Heat Exchanger

Access to the interior of the main heat exchanger can be obtained by removing the upper assembly with a crane operated from above the water

shield. Burnt-out tubes can be cut out of service since each tube terminates outside the heat exchanger proper. The distributor plate at the entrance to the fluidizing section of the heat exchanger may require maintenance because of erosion due to the circulating solids. It is conceivable that a mechanical design can be incorporated in the equipment at this point so that replacement of this plate would be possible using remote control equipment. Accessibility to all parts of the main heat exchanger system should simplify to some extent the replacement of this distributor plate if it becomes necessary.

Transfer Lines

To reduce erosion, the transfer lines are to be lined with silicon-carbide. Maintenance on the lines can be reduced to a minimum by designing the lines so that the maximum erosion occurs in removable sections. Since most of the erosion will occur in the curved sections, these sections are located for maximum accessibility.

Cyclone

Industrial experience with cyclones similar to those contemplated for this design have operated satisfactorily at 850° F which is a more severe design condition than the 500° F temperature proposed in this system. This lower temperature is accomplished by using a heat exchanger to cool the gases before they reach the cyclone. Layout of the equipment is such that all cyclones are readily accessible.

Blowers

To simplify the maintenance that may be necessary due to erosion associated with circulating a particle-laden stream of gas, the blowers will be located in a separate compartment. Modifications in conventional blower design can be incorporated to enable removal of the complete

impeller assembly. The possibility of constructing silicon carbide coated impellers should be investigated. To minimize erosion of the blowers, separators are to be installed to remove all dust particles greater than 10 microns in size. Duplication of this equipment can be provided to insure operation in case there is a failure in one of these units.

Pumps

All pumps can be of conventional design; the only difficulty associated with maintenance will be the induced radioactivity of the water. Locating the pumps in a separate compartment will insure conventional maintenance procedures after the water is allowed to decay to a tolerable level.

Power Plant Equipment

Exclusive of the reactor compartment, no special problems will be encountered in the maintenance of the power plant equipment since standard steam conditions are used in this design. The maintenance procedure will be similar to that which is employed in present power generating installations. The only complication associated with the maintenance of this equipment will be the induced adtivity of the steam and condensed water. However, this condition can be remedied by allowing the activity to decay to a tolerable level before entering the shielded locations.

Chemical Processing Plant Equipment

The equipment used in the chemical processing plant for this reactor will be similar to equipment in operation at present at existing AEC installations. It is anticipated that there will be no special problems peculiar to the processing of this reactor fuel and therefore, adequate

data on this phase of maintenance should be available.

Summary of the Effects of Radioactivity on Maintenance

The problem of radioactivity associated with this nuclear power plant will complicate but not prevent maintenance and inspection of all equipment. After removing the radioactive contents of the system and circulating the charging material to remove the residual fuel materials, the following sources of radioactivity will remain:

(1) The induced activity of the water and steam will be appreciable during operation, but this is not too serious since the system can be shielded and entered only after the activity decays to a tolerable level. Calculations for experience with the naval reactors indicates that the half-life of this activity is short and the equipment can be approached after approximately fifteen (15) minutes.

(2) A more serious problem is the induced activity built-up in the materials of construction; this hazard can be minimized by special emphasis in the design of the components for correct selection of materials. In a similar category would fall the activity due to the impregnation of various components with fission products. It is difficult to estimate what the level of activity from these possible sources would be. However, the distance from which the operator in the submerged remote control equipment operates is extremely flexible because the water will be the principal shielding material.

Mechanical Joint for Removable Sections

Cutting heat exchanger tubes out of services with torches that operate under water is not a major problem since conventional equipment is presently available. However, welding new sections under water is a problem;

therefore, where it is presumed that removal and replacement of a section will be necessary a mechanical joint capable of being connected and disconnected by remote control equipment should be used. The design of this joint will be simplified by the fact that the system operates at atmospheric pressure. However, no leakage into the reactor system can be tolerated.

Quoting from page 25 of ORNL-730, "Homogeneous Reactor Experiment Feasibility Report":

> "Standard oval ring joints have been tested at 1000 psi and 285° C and are leak tight. This modified unit has provisions for leak detection between the sealing edges and is slotted for spring action to insure positive pressure on the contact surface at all times."

It appears that it would also be preferable to retain continuity in the lining material to prevent favorable conditions for the onset of erosion at the joint. This could be accomplished by providing a slight clearance and using a plastic graphite pitch mixture to seal the joint in the lining material where the ends are brought together.

Radiation Damage

One obvious advantage of the reactor design presented in this report is the absence of structural material other than graphite in regions of high flux. This eliminates the uncertainties associated with the effects of radiation damage on the engineering properties of the system. The only structural material in this design that is subjected to a high neutron flux (approximately 10^{14} neuts/cm^2/sec) is the graphite cone shell. Because of the wide use of graphite in the AEC program considerable research has already been done on the effect of reactor radiation on the physical properties of graphite. The effects of radiation on such properties as

thermal resistivity, breaking strength, and dimensional stability have been correlated by Tucker and Brooks (48), who state:

> "most, but not all, of these effects may be removed by annealing at 1000° C."

Since this reactor is to operate at 1500-2000° F it is anticipated that the effects of neutron bombardment or graphite will be continually removed by annealing during the actual operation.

III-7 Costs

It has been impossible to make a meaningful cost analysis for the fluidized solids reactor within the time available after a suitable reactor design had been completed. However, it is felt that some qualitative statements concerning the probable costs are in order.

The power generating part of the plant will be almost identical to a conventional design. The small amount of biological shielding required around the steam system may add no more than about $160,000 to the normal investment or an equivalent of about $2.00 per Kw added on to the $90 which may be required in a conventional plant. Thus, the total cost of this part of the plant may be about $7,700,000 equivalent to about 1.8 mils per Kw-Hr.

The reactor and its various accessories may be considered in five sections:

(1) The fuel-moderator and blanket materials inventory;

(2) The structural members in the core, blanket, heat exchangers, and transfer lines;

(3) The heat transfer surfaces or boiler system;

(4) Controls, pumps, and similar accessories;

(5) The chemical plant.

Evaluating fissile material at $50 per gram, the item (1) would total about 10 million dollars. If this is "charged" at 16% per year and if one assumes an 0.8 load factor, the equivalent unit cost becomes about 2.9 mils per kw. hr. A rough analysis of items (2), (3), and (4) indicate that these may cost about 5-8 million dollars. If these were written off in 10 years and if one uses normal rates for taxes, insurance, etc., the equivalent cost of this investment becomes about 1.5 to 2.4 mils per kw-hr.

Costs for the chemical processing are very questionable. It is claimed that since a high decontamination of the fuel is not desired except for the small fraction being prepared for sale, one may use the cheapest suitable means. Thus, for instance, cost figures on the purex process will indicate future probable costs of $5 -$10 per gram of the plutonium but only $2-5 per kilogram of uranium. If one were to assume that the latter were low by a factor of 10, one would get processing costs no greater than about $50. per kilogram of core uranium and $25. per kilogram of blanket thorium processed, one gets a total chemical plant operating cost of about $4850 per day or 2.0 mils per Kw. This assumes 30 day processing of core and 300 day processing of blanket. Thus if we total up the cost which have been so roughly estimated in the preceding paragraphs we get a probable cost of 8-9 mils per Kw-hr before taking any credit for the U-233 or Pa-231 produced. If one then assumes a gain of 0.2 and a net sale value on the U-233 of $40 per gram-($50 market value $10 processing costs), one gets an added income of $2500 per day or a credit of 1.3 mils per Kw-hr bringing the final power cost down to about 7 mils.

It should be repeated that the preceeding cost analysis has been estimated very roughly and may be greatly different from a carefully

prepared, detailed cost analysis.

IV. Liquid-Solid Fluidized System

1.0 General Discussion

This system was investigated as part of the preliminary analysis of the feasibility of the fluidized solids system. These calculations, as summarized below, show the system to be quite promising.

It employs heavy water as the liquid phase and uranium impregnated graphite as the solid-fuel bearing phase. The core is assumed to consist of a cylinder containing graphite pebbles which are fluidized by upwardly flowing D_2O. The blanket would be composed of either a fluidized or slurry system of D_2O and ThO_2.

The system briefly described above has several advantages and also some disadvantages compared with the gas-solid system. The primary advantage is that all of the heat may be easily removed from the core without transferring any of the solid material. This means a tremendous saving in initial fuel holdup since there is none outside the reactor. The critical mass is less to begin with, because of the better moderating properties of the system. The D_2O now occupies the so-called void spaces. Calculations have been made to show that the system has the advantage and interesting characteristic of very slowly changing reactivity with changes in bed height. Thus the system has good nuclear stability which is a questionable point of the fluidized core in a gas-solid system. Figure IV-1 shows the effect of bed height (or % voids) on the effective multiplication factor.

One of the disadvantages of the D_2O system is that it must be pressurized to obtain acceptable steam conditions. The pressurization requires

that a zirconium shell be used to separate the core and blanket. Though the shell may be made thin by pressurizing core and blanket equally, it will still be so thick that it will have a very detrimental effect on breeding gain. The low temperature steam available from the system is a second factor decreasing its attractiveness. There is a difference of about 7% in thermal efficiency between the two systems which amounts to more than 20% difference in usable power output.

2.0 Engineering:

The calculation of reactor core size was governed mainly by engineering considerations. Design limitations were: (1) the amount of heat to be removed, (2) the allowable liquid velocity through the core, (3) the attainable temperature rise across the core.

The amount of heat to be removed was, by the original specification, 250 megawatts. The maximum liquid velocity possible depends on several characteristics of the fluid bed such as: percent voids, density and diameter of solid particle, density and viscosity of fluid. In order to operate the system with the height of the bed fairly stable it was thought advisable to limit the voids to a maximum of 50%. A particle diameter of 1/4" was chosen as satisfactory from an engineering standpoint on the basis of some work by Wilhelm and Kwauk (52) on fluidization with water. With these selected values for percent voids and particle diameter, a superficial fluid velocity of 0.57 feet per sec was calculated making use of Wilhelm and Kwauk's data as correlated by Rollin D. Morse (31), who plotted the two dimensionless groups, $\frac{g_c \Delta P. \rho_F \cdot 6 \cdot \varepsilon^3}{L_F \quad G^2 \quad a}$, $\frac{6G}{\mu a}$, versus each other and obtained the curve in Figure IV-2 which is reproduced from I.E.C. June 1949. The symbols are defined in Table IV-1 and the

value of the constants used in calculating the fluid velocity found in Table IV-2. The reactor outlet temperature was limited to about 600° F since a higher temperature would require pressurization in excess of 2000 psi. Exit and entrance steam conditions at the turbine were chosen according to standard practice and the remainder of the power cycle designed around these conditions and the reactor outlet temperature. The idealized cycle, ignoring pressure drops through the boiler etc. called for a reactor inlet temperature of 314° F and therby a Δh across the reactor of 327 Btu/#. The complete power cycle appears in Figure IV-3. The diameter of the reactor, subject to the above conditions, was calculated to be 6.15 feet.

Some investigations were made into the compatibility of D_2O and graphite at the temperatures involved. It was concluded that there was no apparent reason for concern at the temperatures under consideration.

3.0 Nuclear Calculations:

The critical mass for the 6.15 foot diameter cylinder of minimum critical volume was calculated to be 8.83 Kg by the Fermi Age Theory for bare homogeneous reactor. For a reflected reactor this figure would, of course, be appreciably reduced. Absorption cross sections used were corrected for the high temperature of operation by applying the 1/v law. The curve in Figure IV-1 of effective multiplication factor verses bed height, alluded to previously was obtained considering a 6 foot diameter reactor operating at "thermal" energy and just critical with 50% void spaces, corresponding to a bed height of 5.54 feet. The curve shows that the reactor is very slightly supercritical at a slightly greater bed height and subcritical at all other heights.

1. Chemical Engineering Progress 1948, p. 203
2. IEC June 1949, page 1117 to 1124

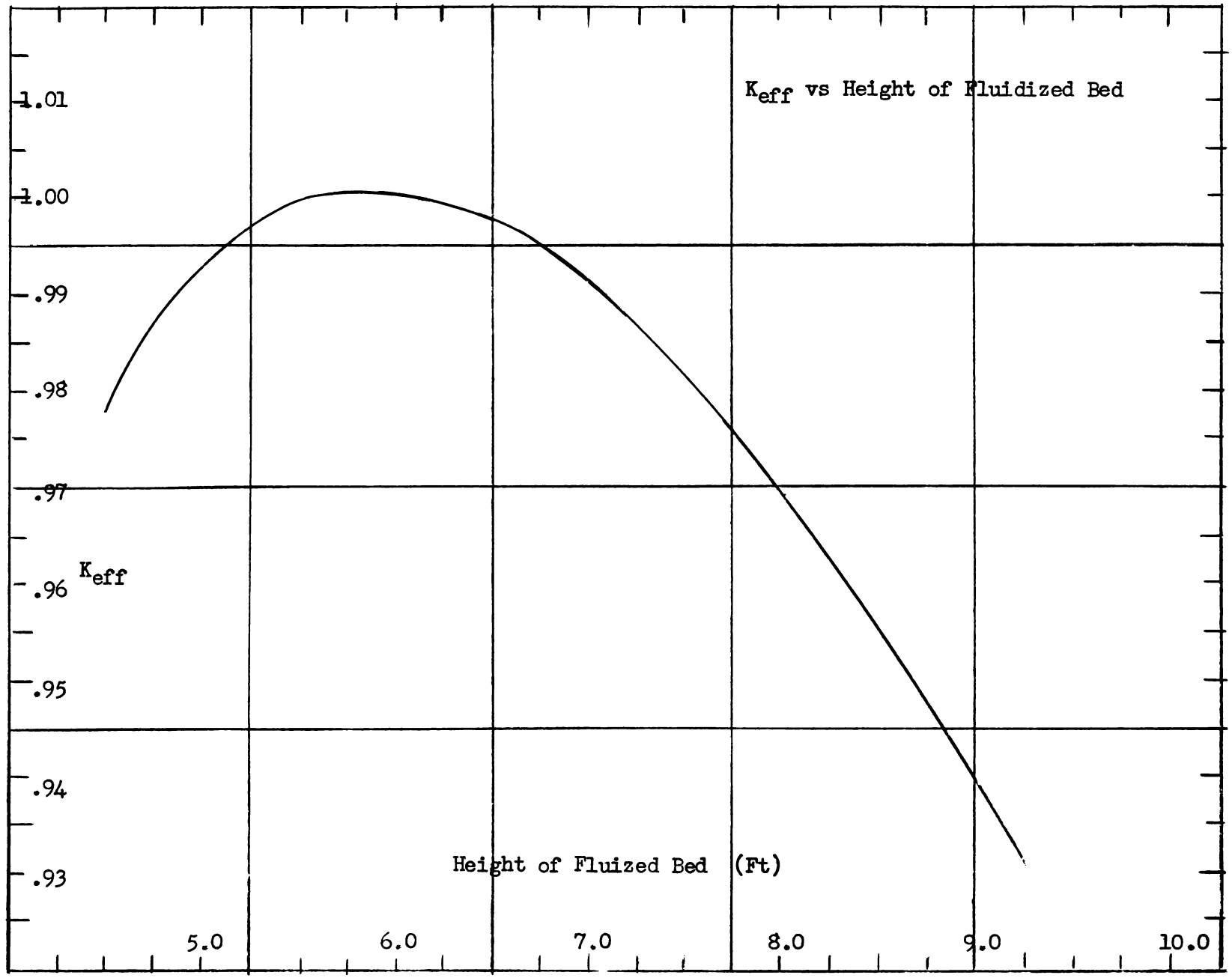
K_{eff} vs Height of Fluidized Bed
1.01
1.00
.99
.98
.97
.96
.95
.94
.93
K_{eff}
Height of Fluized Bed (Ft)
5.0
6.0
7.0
8.0
9.0
10.0

Figure IV - 1

TABLE IV - 1

Symbol	Definition	Units
g	Acceleration due to gravity	ft/sec^2
ΔP	Pressure drop across fluid bed	$\#/ft^2$
L_f	Height of fluid bed	Ft.
P_f	Density of fluid	$\#/ft^3$
G	Mass-velocity of fluid	$\#/ft^2$-sec
ϵ	% of void space	dimensionless
a	Surface area of solids per cubic foot of bed	ft^2/ft^3
u	Viscosity of fluid	#/ft-sec
ρ_s	Density of solid particles	$\#/ft^3$

TABLE IV - 2

Engineering Specifications

Diameter of Reactor	6.15 feet
Height of Reactor	5.54 feet
Outlet Temperature	600° F
Inlet Temperature	314° F
Fluid velocity	0.57 feet/sec
Flow rate	725 #/sec
Pressure drop across bed	1.8 $\#/in^2$

TABLE IV - 2 (Con't)

Data

Particle diameter	.25 in.
Particle density	137 #/ft^3
Fluid density	42.8 #/ft^3
Voids	50%
Pressure drop per unit length = $(1-\epsilon)(\rho_s-\rho_f)$	47 #/ft^3
Viscosity	5.86 x 10^{-5} #/ft-sec
Surface area of solids per cubic foot of bed	144 ft^2/ft^3
Dimensionless group $\frac{\Delta P\ g\ \rho_f\ G\ \epsilon^3}{L\ G^2\ a}$	.566
Dimensionless group $\frac{6\,G}{\mu a}$	17,350

V. Application to Systems Other Than A U-233 Breeder

Considering the breeding gain alone, the best thermal system is obviously the U-233 breeder. However, the inherent flexibility of this reactor will allow for many possible changes in design. These will be discussed briefly below.

It is obvious that, the first large U-233 producer will have to be started using U-235 as the fuel. Thus the fluidized solids reactor could be started by charging the fuel U-235 to the core and running the pile in this manner until sufficient U-233 has been produced in the blanket. There would be an accompanying loss of gain during this period but this is at least, partly offset by the savings on initial fuel investment.

Conversion ratio's have not been calculated but it is certainly feasible that the reactor could produce plutonium from natural uranium in

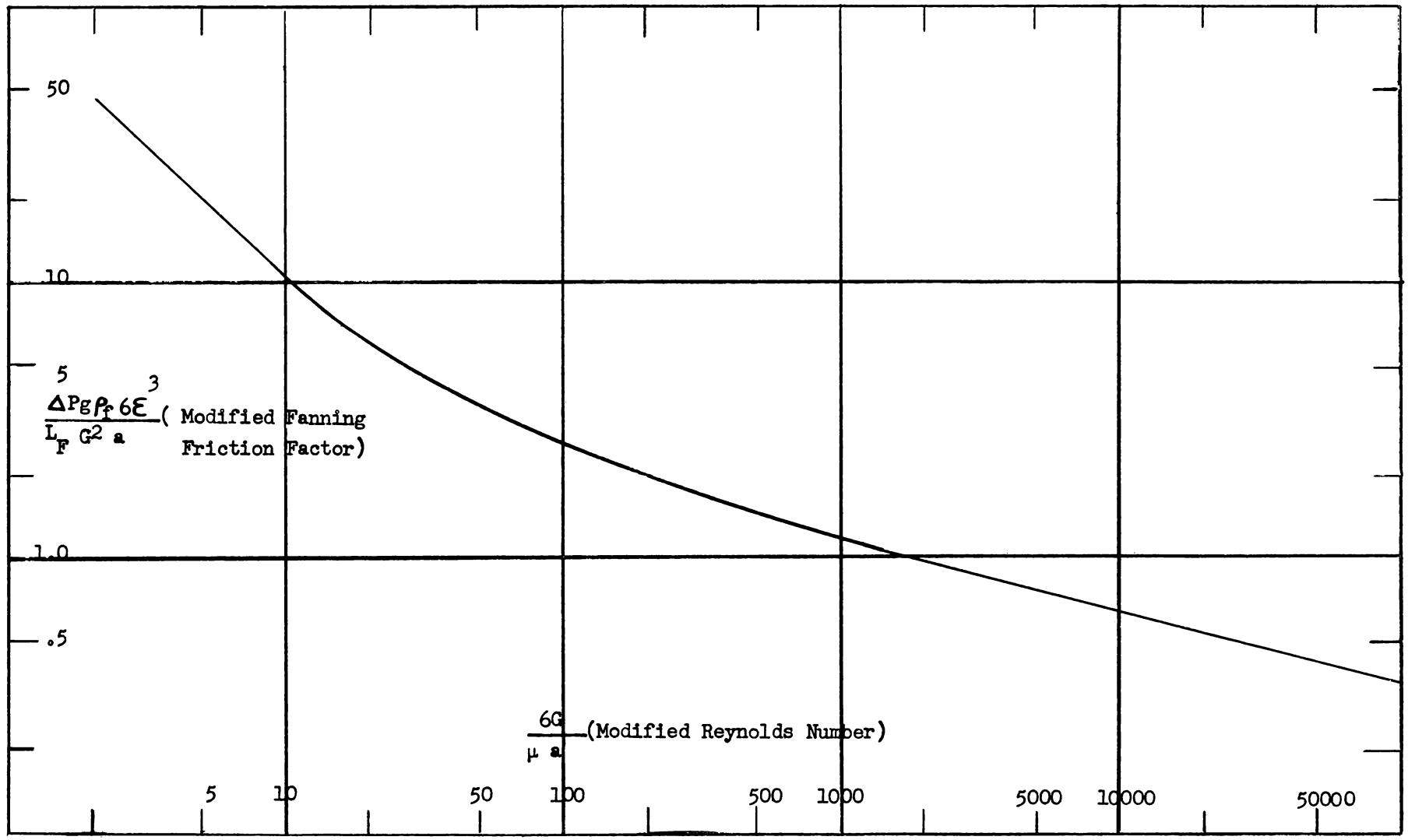

Figure IV - 2

Correlation of Wilhelm and Kwauk Data by Morse

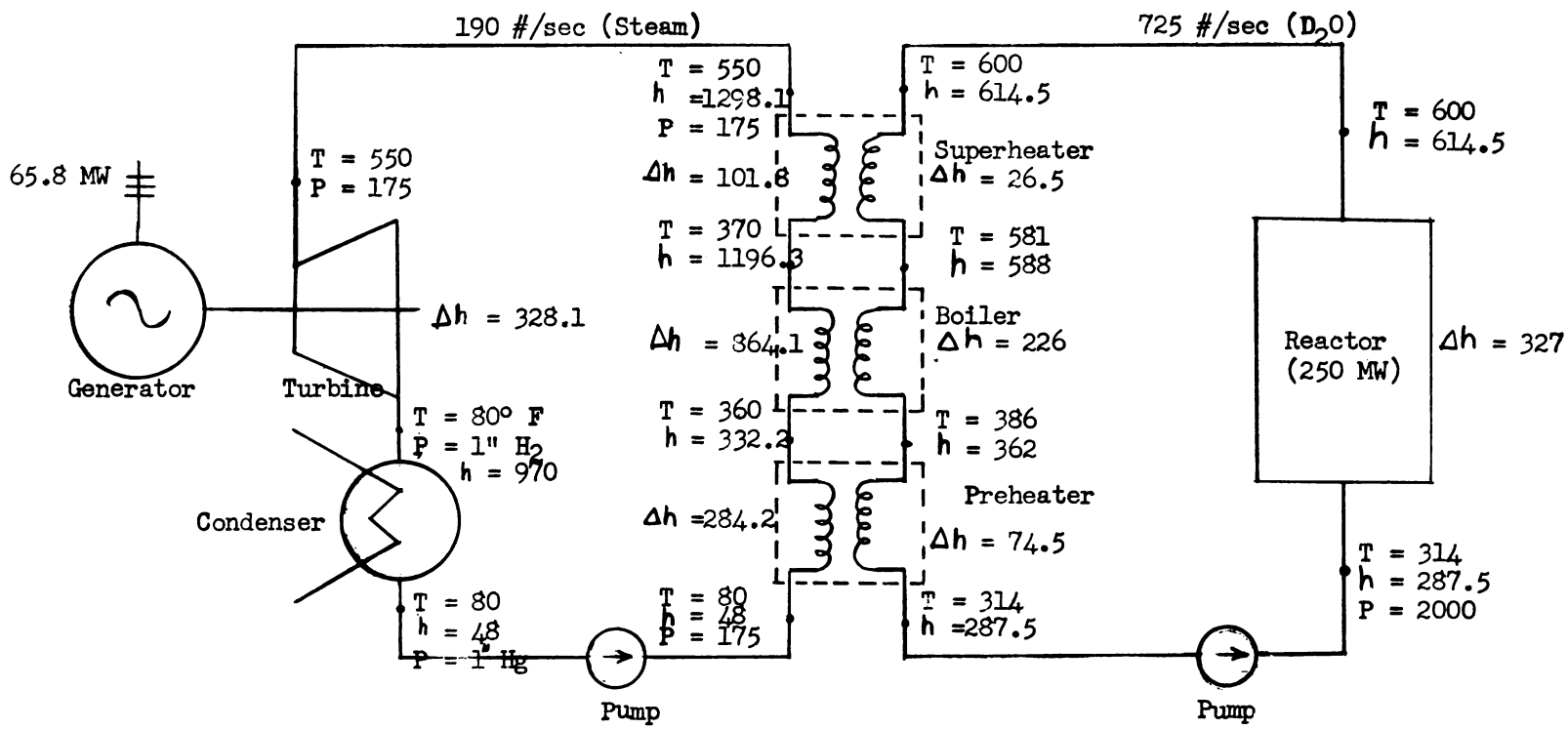

Figure IV - 3

Idealized Power Cycle for Liquid-Solid Fluidized System

the blanket. The fuel could be U-233 if available at a reasonable cost. Most probably it would be U-235 with an estimated conversion rates of unity.

The reactor can also be designed to be used only as a power producer. In this case the blanket becomes a pure reflector and need no longer be fluidized, but still must be cooled. The core could be smaller and part and perhaps all of the heat exchange could take place there. Although this new system would be considerably smaller and more compact the basic principle of operation demands that the reactor system be a stationary one.

As a final possibility, a fast plutonium power breeder may be briefly discussed. The writer believes that such a reactor system, retaining many of the advantages of the proposed thermal reactor, may therefore prove equally as attractive. The voidage inherent in such a design would surely increase leakage from the system so that a reflector or blanket is essential.

If uranium and plutonium were used in a metallic form under an inert atmosphere, core temperatures would be limited to about 1200° F. Since thermal absorption is no longer of any importance, part of the heat generated could be removed from the core vessel, using a suitable internal heat exchanger. The size of the core would probably be smaller than that of a thermal reactor. Power output might also be lower. In any event it is felt that such a system merits further study.

VI Conclusions

It has been concluded that unless further research and experimentation uncover unforeseen difficulties, a reactor system employing the principle of transfer of solid particles by gases is feasible. The reactor in this

system would be of the thermal, homogeneous type producing both power, and fissionable material in excess of that consumed.

Heat transfer calculations have shown that it is possible to remove a considerable amount of heat from the reactor core by carrying the heat in solid particles. These particles also act as a carrier for the fissionable material and as the moderator for the core.

Nuclear calculations of a rather detailed nature have predicted breeding gains in excess of +.2 and it is believed that such gains are readily obtainable in this system since nearly all possible neutron losses have been accounted for.

Some questions regarding the engineering and physics of this reactor have been left partially or wholly unanswered. A list of these is given in Section VII on "Recommendations for Future Work".

The reactor as proposed is semi-spherical in shape, employs graphite as a moderator in both active regions, burns U-233 as a fuel and makes use of thorium carbide as the fertile material. The core is operated as a moving bed, i.e., the solid particles flow into and out of the core by gravity and at nearly their settled density. The blanket is a fluidized bed of low void content, relatively speaking.

Some of the more important specifications of the reactor and related equipment are listed below in Table VI - 1.

TABLE VI - 1

Reactor heat output	250 MW
Generator output	85.2 MW
Reactor core radius	160 cm - 5.25 ft.
Blanket thickness	100 cm
Power density	12 watts/cc
Specific power	1300 watts/gm of U-233
Temperatures - Core	2000° F
Blanket	2000° F
Heat exchanger	1500° F
Steam to turbine - Temperature	950° F
Pressure	1250 psi
Steam load	7.0 lb/Kwh
Heat transfer surface - Blanket periphery	2690 sq. ft.
Heat exchanger	7740 sq. ft.
Voids - Core	60%
Blanket	50%
Heat exchanger	82%
Particle size - Core and heat exchanger	60 microns
Blanket	200 microns
Solids circulation rate	25 short tons/ min.
Solids hold-up time in core	30 seconds
Graphite core shell thickness	10 cm.
Mass of U-233 - Core	46.8 Kg
Heat exchanger and transfer lines	58.2 Kg*
Blanket	100 Kg
U-233 burn-up per day	313 gm.
U-233 net production per day	68.7 gm
Gain - per gm. of U-233 destroyed in core	.245 gm
per gm. of U-233 destroyed in core and blanket	.218 gm
Concentration of thorium in blanket	1 gm/cc

* Calculated on the basis of the ratio of solids in the core to solids in the heat exchanger as given in Table III 1-15.

VII Recommendation for Future Studies

Because of the shortage of time available for analysis of the Fluidized Solids Reactor, many questions that arose during the investigation were left unanswered. The authors have prepared the list given below of recommendations for future work on this system. It is hoped that the list will serve as a useful guide to other groups interested in carrying on the studies of the work originated in this report.

Nuclear

In order to evaluate more fully the nuclear characteristics of this reactor, the following course of action is suggested:

1. Analyze proposed systems using a multigroup, two region method.
2. Make some 3-region calculations (2 or more groups) to evaluate the full effects of the graphite shell.
3. Evaluate the effect of blanket thickness.
4. Evaluate holdup and gain as a function of percent breeding in core.
5. Evaluate, over a suitable range, the gain and holdup as a function of poisons due to fission products, higher isotopes, and structural materials.
6. Evaluate, and correct for, saving due to reflection from water tubes and shield; correct for added leakage through inlet and outlet lines.
7. Make a more intensive examination of the control problem. Especially, determine controllability of a fluidized core.
8. Evaluate variation in core material, e.g.: ThO_2 or ThC_2 in blanket with no added graphite, ThF_4 in blanket, UF_6 (as a gas) plus BeO (if stable) in core, etc.
9. Design and perform a critical experiment.

Engineering

There are several features of the engineering design of the proposed reactor which are questionable because of the uniqueness of the design or materials recommended in this report. Hence it is felt that certain

experiments or other investigations are needed. To fulfill this need, it is recommended that:

1. The feasibility of constructing a graphite shell of the required size and shape is investigated.

2. It be determined whether there is any tendency for graphite particles to fuse at elevated temperatures.

3. Experiments be conducted on the erosion in blowers, cyclones and transfer lines.

4. Specific heat transfer experiments be performed with the materials likely to be employed as a function of gas velocities, particle sizes, % voids and type of bed (Fluidized or Moving).

5. Fluidization characteristics in a heat exchanger with closely spaced tubes be observed by experiment.

6. Experimental work be done concerning solids-carrying capacity of various gases.

7. The temperature limitations imposed by materials in the system be determined.

8. The characteristics of the possible fluidizing gases be more fully evaluated to assure a proper choice. This would specifically include an investigation of the reaction of CO_2 (and CO) with graphite in the presence of the fission products.

9. The practicality of fabricating the proposed blanket and core solids be demonstrated.

10. Beryllium oxide be examined as a possible alternate for graphite as a moderator in core and blanket, especially for a reactor employing gaseous UF_6 as the fuel.

Cost Analysis

A fairly detailed cost estimate of the system should be made to permit optimization of operating conditions and to indicate probable power costs.

APPENDIX

VIII - 1 Nomenclature

1.1 Nomenclature for Engineering Calculations

h = Heat transfer coefficient Btu/hr-sq.ft. - °F

h_c = Convective heat transfer coefficient Btu/hr-sq.ft. - °F

h_p = Particle surface heat transfer coefficient Btu/hr-sq.ft. - °F

h_r = Equivalent radiant heat transfer coefficient Btu/hr-sq.ft. -°F

h_T = Total heat transfer coefficient Btu/hr - sq.ft.- °F

C_p = Specific heat Btu/lb. -°F

G = Superficial mass velocity of gas based upon total cross-sectional area lb/sq.ft. - hr

a = Effective area of heat transfer per unit volume

μ = Viscosity of gas lb/ft-sec

ϵ = Void fraction, dimensionless

k = Overall thermal conductivity of granular bed Btu/ft - hr -°F

k_g = Gas thermal conductivity Btu/hr - ft - °F

k_p = Solid particle thermal conductivity Btu/hr-ft - °F

D_T = Heat exchanger outside tube diameter (ft.)

D_p = Equivalent particle diameter (ft.)

$\left(\frac{C_p\mu}{k}\right)_f$ = Prandtl number evaluated at average gas film temperature (dimensionless)

e_1 = Emissivity for radiating surface (dimensionless)

e_2 = Emissivity for receiver surface (dimensionless)

T_1 = Radiating absolute temperature (°R)

T_2 = Receiver absolute temperature (°R)

g = Gravitational constant ft/sec-sec

G_{max} = Superficial mass velocity of gas based upon net cross-sectional area. When net cross sectional area is equal to gross area minus maximum heat exchanger tube cross sectional area. lb/sq.ft - hr

ρ_p = Solid particle density lb/cu.ft.

ρ_g = Gas density lb/cu.ft.

v = Gas velocity ft/sec.

1.2 Nomenclature for Nuclear Calculations:

a_1	-	Radius of core	cm
a_2	-	Radius of blanket	cm
V_c	-	Volume of core	cu. cm.
V_B	-	Volume of blanket	cu. cm.
t'	-	Thickness of blanket	cm
t	-	Thickness of core shell	cm
Kc	-	Infinite multiplication factor - core	--
K_B	-	Infinite multiplication factor - blanket	--
P_c	-	Resonance escape probability - core	--
P_B	-	Resonance escape probability - blanket	--
D_{SC}	-	Slow diffusion coefficient - core	cm
D_{SB}	-	Slow diffusion coefficient - blanket	cm
D_{FC}	-	Fast diffusion coefficient - core	cm
D_{FB}	-	Fast diffusion coefficient - blanket	cm
τ_c	-	Fermi Age - core	cm^2
τ_B	-	Fermi Age - blanket	cm^2
L_c	-	Diffusion length - core	cm
L_B	-	Diffusion length - blanket	cm
$L_{graphite}$	-	Diffusion length -in graphite as employed in system	cm
$L_{moderator}$	-	Diffusion length - in moderator	cm
L(M+Th+Pa)	-	Diffusion length - in moderator containing Pa and Th	cm

Σ_{sc} - Macroscopic absorption cross section - core cm^{-1}

Σ_{sB} - Macroscopic absorption cross section -blanket cm^{-1}

Σ_{RC} - Macroscopic resonance absorption cross section-core cm^{-1}

Σ_{RB} - Macroscopic resonance absorption cross section-blanket cm^{-1}

Σ_{sa} - Macroscopic shell absorption cross section cm^{-1}

Σ_{a} (23) - Macroscopic absorption cross section - U-233 cm^{-1}

Σ_{a} (Pa) - Macroscopic absorption cross section -Protactinium cm^{-1}

Σ_{a} (Th) - Macroscopic absorption cross section - Thorium cm^{-1}

Σ_{a} (C) - Macroscopic absorption cross section -Graphite cm^{-1}

Σ_{a} (F.P.)- Macroscopic absorption cross section -Fission Products cm^{-1}

Σ_{a} (H.O.)- Macroscopic absorption cross section -Higher Isotopes cm^{-1}

ϕ_{SC} - Slow flux - core neuts/cm^2-sec

ϕ_{SB} - Slow flux - blanket neuts/cm^2-sec

ϕ_{FC} - Fast flux - core neuts/cm^2-sec

ϕ_{FB} - Fast flux - blanket neuts/cm^2-sec

J - Neutron current neuts/cm^2-sec

VIII - 2

2.1 Calculation of Percent Void in Gas-Fluidized System

Leva (23) and Miller (30) investigated the effects of gas and solid properties upon the minimum gas mass velocity required to impart motion to solid particles. Leva defined and related this critical mass velocity to the gas and solid particles by the following equation:

$$G_{mf} = C D_p^2 g \rho_p \frac{\rho_g}{\mu} \qquad (1)$$

The equation is only applicable to solid-gas systems for modified Reynolds numbers that are smaller than 10.

Miller's empirical equation for critical mass velocity is expressed as follows:

$$G_{mf} = \frac{0.00125\, D_p^2\, (\rho_p - \rho_g)^{0.9}\, \rho_g^{1.1}\, g_c}{\mu} \qquad (2)$$

This equation is limited to 60 to 200 micron size particles.

Agreement between these two correlations is quite good. Table VIII 2-1 shows calculated argon minimum mass velocities for impregnated 60, 200, and 600 micron graphite particles.

For iron Fischer-Tropsch catalyst and sand particles ranging in size from 40 micron to 600 micron Leva (23) has shown the effect of particle size upon percent voids in a gas fluid bed. A log-log plot of mass velocity versus a void function expressed as:

$$\frac{(1 - \text{void fraction})^2}{(\text{void fraction})^3}$$

TABLE VIII 2-1

Argon Critical Mass Velocities
Impregnated Graphite

D_p Micron	$D_p \times 10^4$ (ft)	Temp. (°F)	ρ_g (lb)(cu ft)	ρ_p (lb)(cu ft)	$\mu \times 10^5$ (lb)(ft)(sec)	*C $\times 10^3$	$G \times 10^3$ (lb)(sq ft)(sec)	$v \times 10^3$ (ft)(sec)
60	1.97	1500	0.028	101	3.82	1.00	0.093	3.32
200	6.56	1500	0.028	101	3.82	0.65	0.667	23.8
600	19.7	1500	0.028	101	3.82	0.40	3.71	133

*Leva et al, Bulletin 504
Bureau of Mines pg. 77

Dwg. 22888

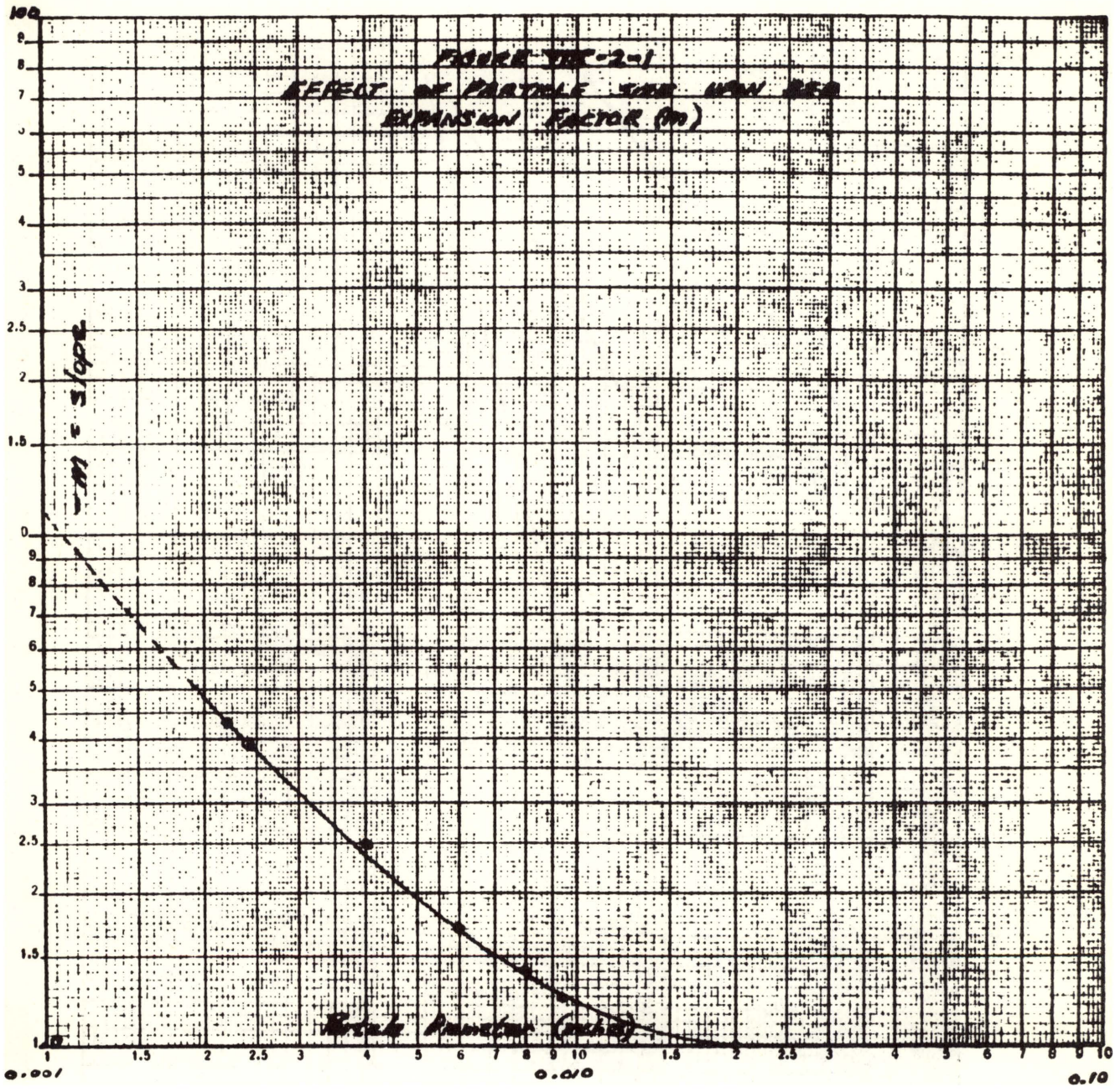
FIGURE NO. 2-1
EFFECT OF PARTICLE SIZE UPON BED
EXPANSION FACTOR (m)
Slope = m
Particle Diameter (inches)
0.001
0.010
0.10

Dwg. 22889

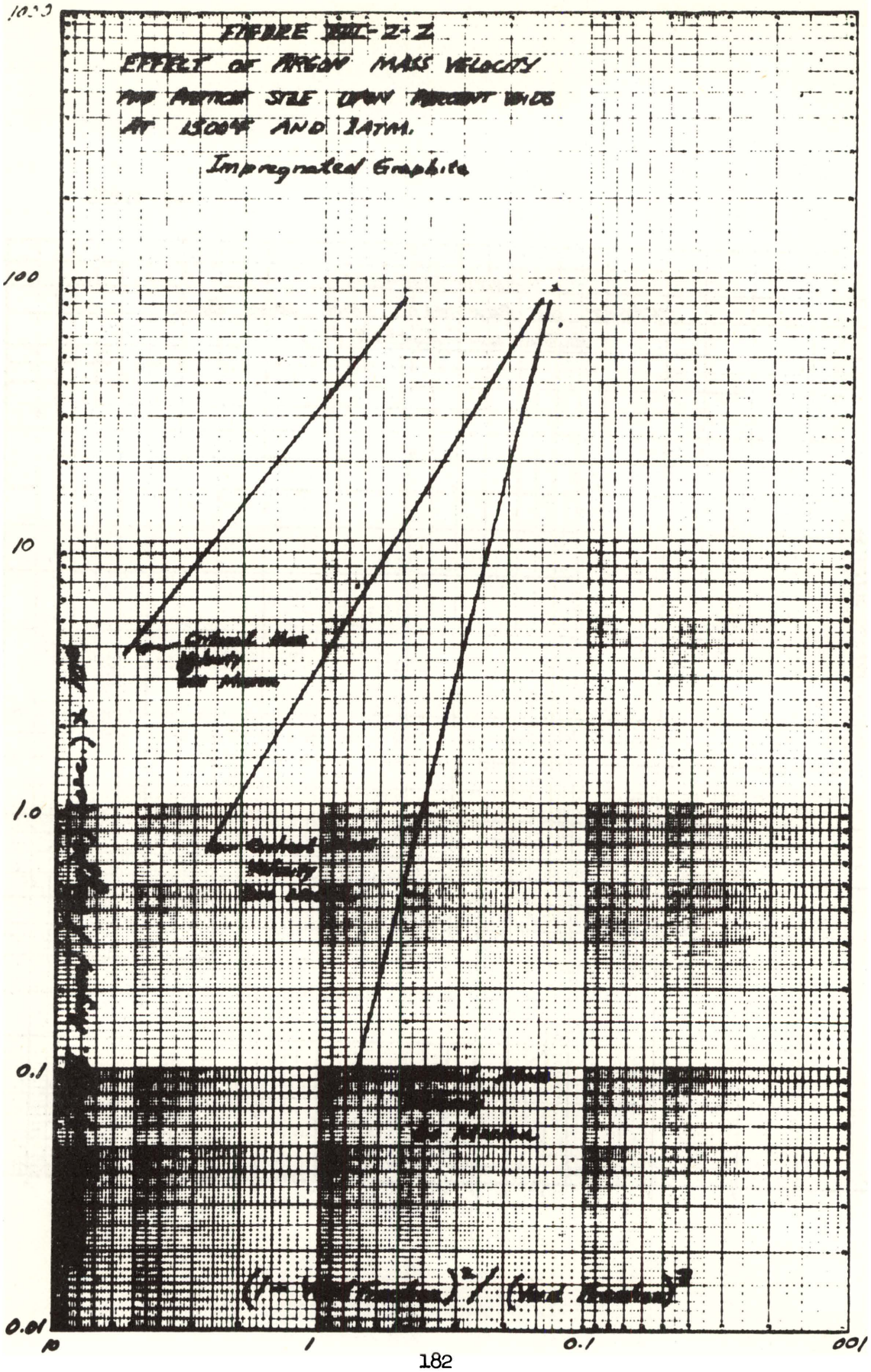
FIGURE XXII-2-2
EFFECT OF ARGON MASS VELOCITY
AND ARGON SIDE GAS PERCENT WIDE
AT 1500°F AND 3 ATM.
Impregnated Graphite
100
10
1.0
0.1
0.01
1
0.1

yields a straight line. The slope of this straight line is determined by the mean particle diameters. Figure VIII 2-1 shows the slope for various mean diameters. Therefore, by determining the minimum mass velocity by equation (1) and the minimum percent voids from Figure III 1-1 a point is established on a log-log plot of mass velocity versus the void function. From Figure VIII 2-1 the slope of a line originating at the minimum percent void point establishes the relationship between mass velocity and percent voids for a given average particle diameter for Reynolds numbers of less than 10. Figure VIII 2-2 shows such a plot for impregnated graphite in Argon at 1500° F and 1 atm. From this plot and the gas density a velocity versus percent void curve for various particle sizes is constructed as shown in Figure III 1-2.

To accurately evaluate the relationship between bed density and velocity for a given particle size experimental data are required. However, the Leva correlation is consistent with experimental data (39) and it is believed predicts fraction of voids within $\pm$ 20% in the range 0.5 to 2.0(ft)/(sec) for the particle sizes considered.

2.2 Typical Calculation for Overall Heat Transfer Coefficients for Argon At 1 Ft/Sec and 60 Micron Particles

Heat Exchanger

Based on 1-in O.D. .095 wall thickness tubes
Low carbon steel tubes
Boiler Tubes

$$\frac{1}{U} = \frac{1}{h_1} + \frac{1}{h_2} + \frac{1}{h_3}$$

where h_1 = water side film

h_2 = coefficient for wall thickness

h_3 = gas-solid film

$$\frac{1}{U} = \frac{1}{2500} + \frac{1}{3300} + \frac{1}{130}$$

$$U = \frac{3300}{27.52} = 120 \text{ Btu/hr. sq ft. } ^\circ\text{F}$$

Superheater Tubes

h_1 = Steam Film

$$\frac{1}{U} = \frac{1}{400} + \frac{1}{3300} + \frac{1}{130}$$

$$U = \frac{3300}{34.45} = 96 \text{ Btu/hr. sq ft. } ^\circ\text{F}$$

Blanket - same tubes as above

Preheater $\frac{1}{U} = \frac{1}{1000} + \frac{1}{3300} + \frac{1}{70}$ $U = 64.3$

Superheater $\frac{1}{U} = \frac{1}{400} + \frac{1}{3300} + \frac{1}{70}$ $U = 58.5$

2.3 Feedwater Heater Calculations

2.3.1 Case I Without Feedwater Heaters for 850 psi - 900° F

Heat Rate 10300 Btu/Kw

Steam Rate $\frac{10300}{(1454 - 69)} = 7.44$ lb./Kw

Output $250{,}000 \times \frac{3414}{10300} = 82{,}800$ Kw

Heating surface required - 1000 sq. ft.

Blanket	2.09 S.H.(U = 58) + .43 Pre-Htr.	(U= 70)
Boiler		4.99
Superheater		1.80
	Total	6.79

Specific Area = $\frac{67900}{82800} = .082 \frac{\text{sq. ft.}}{\text{Kw}}$

2.3.2 Case II With Feedwater Heaters for 850 psi and 900° F

5 Heaters raising temperature T_o 486° F

Max. possible enthalpy rise 472 Btu

Actual Enthalpy Rise 425 Btu

Percent of possible rise 90

Theo. Res. in St. Cond. St. Rate 13.8 %

Corr. for No. of Htrs. and Enthalpy Rise .79

Corr. Factor for actual Reg. Cycle $1 - \frac{13.8}{100} \times .79 = 891$

Reg. cycle Ht. Rate $10300 \times .891 = 9150$

Output = $250{,}000 \times \frac{3414}{9150} = 93{,}300$ Kw

Heating surface required - 1000 sq. ft.

Blanket (Sup)	2.98 (U = 58)
Boiler	7.17
	10.15

Special Area = $7170 \div 93{,}300 = .077 \frac{\text{sq. ft.}}{\text{Kw}}$

2.4.1 Properties of Graphite

Listed below are some properties of AGOT graphite as reported by R. G. McPherson (28).

Thermal expansion at 60° C $1.1 - 3.8 \times 10^{-6}$ per °C

Thermal conductivity at 0° C 0.29 - 0.56 Cal/cm sec -°C
70 - 135 Btu/ft hr -°F

Variation of Thermal Conductivity with temperature

Temperature	0°C	200°C	400°C	600°C
Kt/Ko	100	75	60	55

Modulus of elasticity $6 - 12 \times 10^6$ psi

The high temperature mechanical properties are given below as reported by Malmstrom, Keen, and Green (25A):

Temperature	0°C	800°C	1600°C
Tensile strength	3100 psi	3400 psi	4000 psi
Young's modulus	1.0×10^6 psi	1.1×10^6 psi	1.3×10^6 psi

2.4.2 Structural strength

Based on the preceeding figures an allowable stress of 300 psi was taken for the graphite shell. For a core radius of 160 cm or 5.25 feet the necessary thickness for a given internal pressure is calculated from the formula for a cylindrical or spherical vessel:

$$P = \frac{2 S t}{D}$$

P - pressure - psi

S - stress - psi

t - thickness - in.

D - diameter - in.

$$P = \frac{2 \times 3000\ t}{2 \times 5.25 \times 12} = 47.6\ t$$

Thus 47.6 psi of internal pressure can be withstood for each inch of shell thickness. Since the core shell should never be subjected to a pressure gradient more than a few psi, the 10 cm or 4 in. shell proposed introduces a large safety factor to cover possible shock loads.

3. Nuclear

3.1 Nuclear Data:

3.1.1 Graphite:

All of the nuclear properties of graphite were taken from a compilation of moderator constants prepared By the Oak Ridge School of Reactor Technology The data are consistent and represent reasonably accurate values of the parameters. Following are the properties of graphite for a Maxwell-Boltzmann flux distribution with its maximum at .025 electron volts.

Density, ρ	1.65 gm/cc
Microscopic absorption cross section, σ_a	.004 barns

Macroscopic absorption cross section, Σ_a	3.31×10^{-4} cm^{-1}
Macroscopic scattering cross section, Σ_s	.395 cm^{-1}
Macroscopic transport cross section, Σ_t	.373 cm^{-1}
Diffusion coefficient, D	.894 cm
Diffusion length squared, L^2	2700 cm^2
Average logarithmic energy decrement, ξ	.158
Fermi Age (Fission to .025)	345 cm^2

3.1.2 Thorium

The absorption cross section for thorium listed below is for .025 ev.

Density, ρ	11.2 gm/cc	(16) Handbook of Chemistry and Physics
Microscopic absorption cross section, σ_a	7.0 barns	(15) ORNL-86 Pomerance page 10
Microscopic scattering cross section, σ_s	12.7 barns	(15) ORNL-86 Page 10
Density of ThC_2, ρ_{ThC_2}	8.96 gm/cc	(16) Handbook of Chemistry and Physics
Average logarithmic energy decrement, ξ_{Th}	.0086	----------
Resonance Integral, $\int \frac{\sigma_a}{E} dE$	8.33 $(\sigma_s)^{.253}$	(50) ORNL-CF 51-10-110 p. 8
σ_s is defined as $\frac{\Sigma_s}{N_{Th}}$		
Resonance absorption cross section, Σ_{RB}	$\frac{D_{FB} N_{Th}}{\zeta_B \xi_B \Sigma_s} \int \frac{\sigma_a}{E} dE$	(50) ORNL CF 51-10-110 p. 8

3.1.3 Uranium-233

Uranium is not present in the reactor in sufficient quantities that it is necessary to take into account its scattering powers. The thermal (0.025 ev), absorption, capture and fission cross sections are listed below.

Microscopic absorption cross section, $\sigma_a(23)$	560 barns	(50) ORNL CF 51-10-110	
Microscopic capture cross section, $\sigma_c(23)$	52	(50) " " "	
Microscopic fission cross section, $\sigma_f(23)$	508	(50) " " "	
Neutrons per fission, ν	2.57	(50) " " "	
Neutrons per absorption, η	2.33	(50) " " "	
Utilizable energy per fission	184 Mev.	----------	

The fission, parasitic capture and scattering cross sections for U-233 were obtained as functions of energy from four reports (49),(27),(51),(32) which covered different sections of the spectrum. Figure VIII 3-1 shows the variation of fission cross section with neutron energy. The above cross-section curves were integrated graphically to give average values of the cross sections for six energy groups in anticipation of multigroup calculations. Following is a table of those values.

TABLE VIII 3-1
Average Cross Sections of U-233 for Six Energy Groups

Group	Lethargy Range	Energy Range ev	Fission Cross Section Barns	Capture Cross Section Barns	Scattering Cross Section Barns
1	0 - 7.0	10^7 - 9100	2.67	0	3.5
2	7.0 - 12.0	9100 - 60	17.6	2.26	8.0
3	12.0 - 13.7	60 - 11	86	11	8.0
4	13.7 - 16.2	11 - .9	159	20	8.0
5	16.2 - 18.2	.9 - .12	190	24	8.0
Thermal	18.2	.12	230	30	8.0

Drawing # 22890

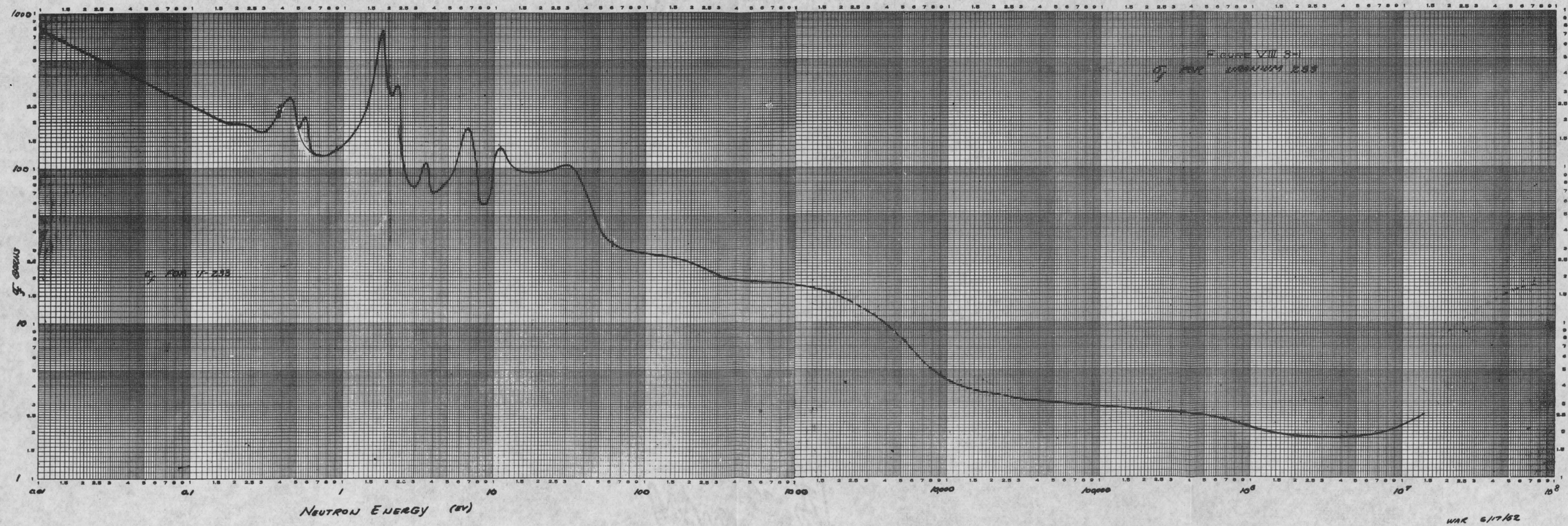

3.1.4 Calculation of Constants from Data

All absorption cross sections were assumed to follow the 1/v law and were corrected on this basis to the temperatures involved.

Macroscopic slowing down cross sections were calculated on the basis of the following formula:

$$\Sigma_F = \frac{\overline{\Sigma_s}}{\ln \frac{E_o}{E_{Th}}}$$

(10)(Glasstone and Edlund, Part III, paragraph 8.12)

where

$$\overline{\Sigma_s} = \frac{\int_{E_{Th}}^{E_o} \Sigma_s(E)\ \phi(E)\ dE}{\int_{E_{Th}}^{E_o} \phi(E)\ dE}$$

(10) Glasstone and Edlund, Part III, paragraph 8.11)

It was assumed that scattering cross sections were sufficiently constant in the area of importance such that $\overline{\Sigma_s}$ could be set equal to Σ_s. E_o was taken as 2.0 Mev. E_{Th} was taken as the energy corresponding to the operating temperature in the region of interest.

Fermi age in the core of the reactor, which is essentially graphite, was calculated using a simple density ratio based on percent voids, Fermi age varies inversely as the square of the density. No attempt was made to correct Fermi age for temperature since this was assumed to be a small correction. Later calculation showed it to amount to about 6-7%.

Fermi age for the blanket was calculated with graphite as a basis and with corrections made for changes in density, macroscopic scattering cross section, macroscopic transport cross section and average logarithmic energy decrement. The formula is as follows:

$$\tau_B = \frac{\tau_o \xi_o \Sigma_{so} \Sigma_{to}}{\Sigma_{sB} \Sigma_{tB} \xi_B}$$ (50) S. Visner- ORNL CF 51-10-110

The subscript zero's indicate properties of pure graphite at the percent voids in question. The subscript B's refer to the actual properties of the blanket.

Fast diffusion coefficients were calculated by taking the product

$\tau \Sigma_F$.

All dissusion lengths were calculated from the formula.

$$L^2 = \frac{1}{3 \Sigma_a \Sigma_t}$$

3.2 Nuclear Calculations:

3.2.1 Introduction

After a survey of literature and many personal consultations it was decided to employ the system of calculations used by the HRE Group at ORNL for the final detailed nuclear calculations in this feasibility study. The theory is essentially a modification of the two-group theory in Part III of the "Elements of Nuclear Reactor Theory", document number ORNL 51-9-127. Dr. S. Visner of ORNL has outlined the method in CF 51-10-110; in addition, the members of this group have received advice and guidance from Dr. Visner in adapting the method to this particular project.

Results obtainable from this method include:

(1) The absorption of resonance neutrons by thorium in the fast group.

(2) The effect on criticality and neutron economy of protactinium, fission products, and higher isotopes.

(3) The absorption of thermal neutrons by the core shell and its effect on neutron economy and criticality.

(4) The effect on criticality and neutron economy of fissioning in the blanket as well as an estimate of the percent of the total power generated in the blanket.

(5) A complete estimate of neutron economy including the fast and slow leakage from the blanket.

Although the derivation presented on the following pages is for the general case of a two-group system with fertile material in both the core and blanket, the method can be readily adapted to systems of more than two regions as well as systems containing fertile material in the blanket only. This section consists of two main parts; the first part discusses the method used by Dr. Visner, the second part presents the simplified method used for the calculations in this report.

A considerable savings in time can be accomplished using the techniques presented in the second part when investigating the effect of the variation of parameters such as core radius, blanket concentrations, etc. A set of curves and a "Modified Welton Method" are used in the simplified calculations to converge the "trial and error solution" for the critical determinant. To illustrate the system of calculations a complete solution by both methods is presented on the following pages, including the tabular forms and curves.

3.2.2 Method Used by Dr. S. Visner

This section is devoted to a detailed treatment of the method of calculation outlined by Dr. S. Visner in CF 51-10-110.

Diffusion Equations

The neutrons are divided into two groups, namely, the slow (thermal) and fast group (energies in excess of thermal). First letters in the subscripts indicate the neutron group, F for fast and S for slow; the second letter indicates the reactor region, C for core and B for blanket. Differential equations for the core are:

$$D_{FC} \nabla^2 \phi_{FC} - (\Sigma_{FC} + \Sigma_{RC}) \phi_{FC} + \frac{K_C}{P_C} \Sigma_{SC} \phi_{SC} = 0 \quad (1)$$

$$D_{SC} \nabla^2 \phi_{SC} - \Sigma_{SC} \phi_{SC} + \Sigma_{FC} \phi_{FC} = 0 \quad (2)$$

For the blanket, the differential equations are:

$$D_{FB} \nabla^2 \varphi_{FB} - (\Sigma_{FB} + \Sigma_{RB}) \varphi_{FB} + \frac{K_B}{P_B} \Sigma_{SB} \varphi_{SB} = 0 \quad (3)$$

$$D_{SB} \nabla^2 \varphi_{SB} - \Sigma_{SB} \varphi_{SB} + \Sigma_{FB} \varphi_{FB} = 0 \quad (4)$$

Notation and Nuclear Constants

It is convenient to define the following nuclear constants to be used in the method as follows:

$$\mathcal{L}^2_{FC} = \frac{\Sigma_{FC}}{D_{FC}} = \frac{1}{\tau_C}$$

$$B^2_{FC} = \mathcal{L}^2_{FC} + \frac{\Sigma_{RC}}{D_{FC}}$$

$$B^2_{SC} = \frac{\Sigma_{SC}}{D_{SC}}$$

$$\mathcal{L}^2_{FB} = \frac{\Sigma_{FB}}{D_{FB}} = \frac{1}{\tau_B}$$

$$B^2_{FB} = \mathcal{L}^2_{FB} + \frac{\Sigma_{RB}}{D_{FB}}$$

$$B^2_{SB} = \frac{\Sigma_{SB}}{D_{SB}}$$

Additional nuclear constants used in this method were estimated by Dr. Visner in the following manner.

$$\tau_B = \frac{1}{3} \int_{\text{thermal energy}}^{\text{fission energy}} \frac{1}{\Sigma_{TRANS\ (Mixture)} \xi \Sigma_{scatt/(mixture)}} \frac{dE}{E} \quad (5)$$

$$\tau_i = \frac{1}{3} \int_{\text{thermal energy}}^{\text{fission energy}} \frac{1}{\Sigma_{Trans.\ (i)} \xi \Sigma_{Scatt.\ (i)}} \frac{dE}{E} \quad (6)$$

Values in equation (5) refer to the properties of the blanket mixture.

Values denoted with the symbol (i) in equation (6) are to be evaluated for an individual element in the mixture (preferably the most abundant material whose properties are reasonably certain). Using average values for the macroscopic cross-sections over the range of integration, the

following relation can be used to estimate the "Fermi age" of the blanket mixture:

$$\tau_B = \frac{\sum_{Trans.\ (i)} \xi \sum_{Scatt.\ (i)}}{\sum_{Trans\ (mixture)} \xi \sum_{Scatt.\ (mixture)}} \tau_i \qquad (7)$$

The "Fermi age" for the core mixture can be estimated in a similar manner.

Diffusion coefficients for the core and blanket mixtures can be estimated as follows:

$$D(mixture) = \frac{1}{3} \sum_{Trans\ (mixture)} \qquad (8)$$

$$\sum_{Trans}(mixture) = \sum_i \sum_{Trans\ (i)} \qquad (9)$$

Because of the addition of thorium to the core and blanket, the resonance escape probability "P" can be considerably less than unity. However, since the ratio "$\frac{K}{P}$" is required, it can be obtained from the four factor formula ($K = \eta \epsilon p f$),

Thorium Macroscopic Resonance Absorption Cross-section

The following relationship was used by Dr. Visner to obtain the macroscopic absorption cross-section of thorium in the resonance region. For the blanket,

$$\sum_{RB} = \frac{D_{FB}\, N(th)}{\tau_B \xi \sum_{Scatt.}} \int_{\text{thermal energy}}^{\text{fission energy}} \sigma_a(E)\, \frac{dE}{E} \qquad (10)$$

Experimental values for $\int_{\text{thermal energy}}^{\text{fission energy}} \sigma_a(E)\, \frac{dE}{E}$ are available for Th-232. Hughes and Eggler[1] determined the values for the resonance absorption integral as:

$$8.33 \left[\sum_i N(i)\, \sigma S(i) / N(th) \right]^{0.253} \qquad (11)$$

$$8.13 \text{ (for infinite dilution)} \qquad (12)$$

(1) CP-3093

where the quantity in brackets is the total macroscopic resonance scattering cross-section per thorium atom.

Solutions of Core Equations

Solutions of the homogeneous parts of the core equations are of the type:

$$\nabla^2 \varphi_F - B^2 \varphi_F = 0 \tag{13}$$

$$\nabla^2 \varphi_S - B^2 \varphi_S = 0 \tag{14}$$

Equations (1) to (4) inclusive, differ from the equations in Part III of the "Elements of Nuclear Reactor Theory", in the fact that the resonance absorption term in the fast group doesn't appear as a source term in the thermal equation. The following derivation will indicate the "B^2" is still the same for both groups.

Solving for φ_{SC} in equation (1) results in

$$\varphi_{SC} = \left[\frac{P_C}{K_C \Sigma_{SC}} (\Sigma_{FC} + \Sigma_{RC}) - D_{FC} \nabla^2 \right] \varphi_{FC} \tag{15}$$

Using this value of φ_{SC} in equation (2) and simplifying, one obtains

$$\left\{ \frac{D_{FC} \nabla^4}{B^2_{SC}} - \left[\frac{(\Sigma_{FC} + \Sigma_{RC})}{B^2_{SC}} + D_{FC} \nabla^2 + (\Sigma_{FC} + \Sigma_{RC}) - \frac{K_C \Sigma_{FC}}{P_C} \right] \right\} \varphi_{FC} = 0 \tag{16}$$

Multiplying by B^2_{SC}/D_{FC} gives

$$\left[\nabla^4 - (B^2_{SC} + B^2_{FC}) \nabla^2 - \left(\frac{K_C B^2_{SC}}{P_C \tau_C} - B^2_{SC} B^2_{FC} \right) \right] \varphi_{FC} = 0 \tag{17}$$

Next, an expression for Σ_{FC} is obtained from equation (2) resulting in

$$\varphi_{FC} = \frac{1}{\Sigma_{FC}} (\Sigma_{SC} - D_{SC} \nabla^2) \varphi_{SC} \tag{18}$$

Substituting this expression into equation (1) and simplifying gives

$$\left\{ \frac{D_{SC}}{\mathcal{L}^2_{SC}} \nabla^4 - \left[(\Sigma_{FC} + \Sigma_{RC}) \frac{D_{SC}}{\Sigma_{FC}} + \frac{\Sigma_{SC}}{\mathcal{L}^2_{FC}} \right] \nabla^2 + \left[(\Sigma_{FC} + \Sigma_{RC}) \frac{\Sigma_{SC}}{\Sigma_{FC}} - \frac{K_C \Sigma_{SC}}{P_C} \right] \right\} \varphi_{SC} = 0 \tag{19}$$

Multiplying the above equation by $FC/D_{FC}D_{SC}$ one obtains

$$\left[\nabla^4 - (B_{SC}^2 + B_{FC}^2)\,\nabla^2 - \left(\frac{K_C\,B_{SC}^2}{P_C\,\tau_C} - B_{SC}^2\,B_{FC}^2\right)\right]\varphi_{SC} = 0 \qquad (20)$$

Examination of the bracketed expression in equations (17) and (20) indicates that the terms are identical, therefore "B^2" in equations (13) and (14) must be equal.

Substituting $B^2\varphi_{FC}$ for $\nabla^2\varphi_{FC}$ in equation (17) and $B^2\varphi_{SC}$ in equation (20) will result in two simultaneous equations containing a quadratic in B^2. The two solutions for B^2 are

$$B_{1C}^2 = \left(\frac{B_{SC}^2 + B_{FC}^2}{2}\right) - \sqrt{\left(\frac{B_{SC}^2 + B_{FC}^2}{2}\right)^2 + \frac{K_C\,B_{SC}^2}{P_C\,\tau_C} - B_{SC}^2\,B_{FC}^2} \qquad (21)$$

$$B_{rC}^2 = \left(\frac{B_{SC}^2 + B_{FC}^2}{2}\right) + \sqrt{\left(\frac{B_{SC}^2 + B_{FC}^2}{2}\right)^2 + \frac{K_C\,B_{SC}^2}{P_C\,\tau_C} - B_{SC}^2\,B_{FC}^2} \qquad (22)$$

Both of these expressions can be evaluated knowing the reactor core properties.

General solutions of the core equations (1) and (2) are linear combinations of X and Y, where X and Y are solutions for the flux when B^2 in the wave equations (13) and (14) has been replaced by B_{1C}^2 and B_{rC}^2 respectively. The core equations canbe written as follows:

$$\nabla^2 X - B_{1C}^2\,X = 0 \qquad (23)$$

$$\nabla^2 Y - B_{rC}^2\,Y = 0 \qquad (24)$$

Flux solutions of these two equations, namely,

$$\varphi_{FC} = A'X + C'Y \qquad (25)$$

$$\varphi_{SC} = A\,Y + C\,Y \qquad (26)$$

involve only two independent constants since inserting these values for φ_{FC} and φ_{SC} back into equations (1) and (2) will result in the following coupling coefficients:

$$\alpha_{1C} = \frac{A'}{A} = \frac{D_{SC}}{D_{FC}} \left(\frac{B^2_{SC} - B^2_{1C}}{\mathcal{L}^2_{FC}} \right) \quad * \tag{27}$$

$$\alpha_{rC} = \frac{C'}{C} = \frac{D_{SC}}{D_{FC}} \left(\frac{B^2_{SC} - B^2_{rC}}{\mathcal{L}^2_{FC}} \right) \tag{28}$$

Values for α_{1C} and α_{rC} can be obtained from the properties of the reactor core materials.

Permissible solutions of X and Y which satisfy the conditions of symmetry and of finite non-negative flux are:

$$X = \frac{\sinh B_{1C} r}{r} \tag{29}$$

$$Y = \frac{\sinh B_{rC} r}{r} \tag{30}$$

Note that if B^2_{1C} is negative, B_{1C} will be an imaginary number; but the sinh of an imaginary number will result in a sine solution as expected. To avoid using imaginary roots, the sinh term in equation (29) has been expressed as a sine term in the tabular form illustrated in this section.

Employing the sine solution for equation (29), the general solutions of the core equations are:

$$\varphi_{SC} = \frac{1}{r} \left\{ A \sin B_{1C} r + C \sinh B_{rC} r \right\} \tag{31}$$

$$\varphi_{FC} = \frac{1}{r} \left\{ \alpha_{1C} A \sin B_{1C} r + \alpha_{rC} C \sinh B_{rC} r \right\} \tag{32}$$

Solution of the Blanket Equations

Equations(3) and (4) for the blanket are identical to the core equations (1) and (2) respectively. Performing operations similar to those indicated for the core equations, it is found that the solutions for B^2 are for the blanket equations:

* Since the solution for B^2_{1C} is negative, it is actually expressed as $- B^2_{1C}$ on the tabular forms to avoid using imaginary roots. Equation (27) is then $\alpha_{1C} = \frac{D_{SC}}{D_{FC}} \left(\frac{B^2_{SC} + B^2_{1C}}{\mathcal{L}^2_{FC}} \right)$

$$B^2_{1B} = \left(\frac{B^2_{SB} + B^2_{FB}}{2}\right) + \sqrt{\left(\frac{B^2_{SB} + B^2_{FB}}{2}\right)^2 + \frac{K_B B^2_{SB}}{P_B \tau_B} - B^2_{SB} B^2_{FB}} \quad (33)$$

$$B^2_{rB} = \left(\frac{B^2_{SB} + B^2_{FB}}{2}\right) + \sqrt{\left(\frac{B^2_{SB} + B^2_{FB}}{2}\right)^2 + \frac{K_B B^2_{SB}}{P_B \tau_B} - B^2_{SB} B^2_{FB}} \quad (34)$$

General solutions for the blanket equations are of the form:

$$\varphi_{SB} = E Z_1 + G Z_2 \quad (35)$$

$$\varphi_{FB} = \alpha_{1B} E Z_1 + \alpha_{rB} G Z_2 \quad (36)$$

where the coupling coefficients α_{1B} and α_{rB} equal

$$\alpha_{1B} = \frac{E'}{E} = \frac{D_{SB}}{D_{FB}} \left(\frac{B^2_{SB} - B^2_{1B}}{\kappa^2_{FB}}\right) \quad (37)$$

$$\alpha_{rB} = \frac{G'}{G} = \frac{D_{SB}}{D_{FB}} \left(\frac{B^2_{SB} - B^2_{rB}}{\kappa^2_{FB}}\right) \quad (38)$$

Using the boundary conditions that the fast and slow neutron fluxes go to zero at the extrapolated boundary, results in the following solutions for Z_1 and Z_2:

$$Z_1 = \frac{\sinh B_{1B} (a'_2 - r)}{r} \quad (39)$$

$$Z_2 = \frac{\sinh B_{rB} (a'_2 - r)}{r} \quad (40)$$

Both B^2_{1B} and B^2_{rB} are positive for the blanket and therefore imaginary roots will not be encountered. In equations (39) and (40), a'_2 refers to the extrapolated radius.

The general solutions of the blanket equations for the flux are:

$$\varphi_{SB} = \frac{1}{r}\left\{E \sinh B_{1B} (a'_2 - r) + G \sinh B_{rB} (a'_2 - r)\right\} \quad (41)$$

$$\varphi_{FB} = \frac{1}{r}\left\{\alpha_{1B} \sinh B_{1B} (a'_2 - r) + \alpha_{rB} G \sinh B_{rB} (a'_2 - r)\right\} \quad (42)$$

Boundary Conditions

Since the differential equations contain four (4) unknowns, namely, A,C,E, and G, four boundary conditions are required. These boundary conditions are that the fast and slow neutron current densities in a direction normal to the core-blanket interface and the fast and slow fluxes at the interface are equal. Expressing these conditions mathematically, one obtains the following equations:

$$\varphi_{FC}(a_1) = \varphi_{FB}(a_1) \tag{43}$$

$$-D_{FC} \nabla \varphi_{FC}(a_1) = -D_{FB} \nabla \varphi_{FB}(a_1) \tag{44}$$

$$\varphi_{SC}(a_1) = \varphi_{SB}(a_1) \tag{45}$$

$$-D_{SC} \nabla \varphi_{SC}(a_1) + D_{SB} \nabla \varphi(a_1) = \Sigma_{a(shell)}\, t\, \varphi_{SC}(a_1) \tag{46}$$

all values are to be evaluated at the core-blanket interface (a_1).

Absorption of thermal neutrons by the core shell of thickness "t" has been introduced into the boundary condition on the slow neutron current density equation (46). However, provision for the scattering and moderating effects of this shell can not be introduced without considering this as a three(3) region problem.

Notation

The following notation has been used to simplify the solution of the boundary condition equations.

$$S_{1C} = \sin B_{1C} a_1 \tag{47}$$

$$S_{rc} = \sinh B_{rC} a_1 \tag{48}$$

$$S_{1B} = \sinh B_{1B} t' \tag{49}$$

$$S_{rB} = \sinh B_{rB} t' \tag{50}$$

$$C_{1C} = (a_1 B_{1C} \cos B_{1C} a_1 - S_{1C}) \tag{51}$$

$$C_{rC} = (a_1 B_{rC} \cosh B_{rC} a_1 - S_{rC}) \tag{52}$$

$$C_{1B} = -(a_1 B_{1B} \cosh B_{1B} t' + S_{1B}) \qquad (53)$$

$$C_{rB} = -(a_1 B_{rB} \cosh B_{rB} t' + S_{rB}) \qquad (54)$$

t' = blanket thickness

Solution of the Boundary Condition Equations

This section will indicate tho solutions to equations (44) and (46).

From equation (44) the following is obtained:

$$-D_{FC}\left\{a_1 \alpha_{1C} \frac{A B_{1c}}{a_1^2} \cos B_{1C} a_1 - \alpha_{1C} \frac{A \sin B_{1C} a_1}{a_1^2} + a_1 \frac{\alpha_{rC} B_{rC} C \cosh B_{rC} a_1}{a_1^2} - \alpha_{rc} \frac{C \sinh B_{rc} a_1}{a_1^2}\right\} = -D_{FB}\left\{-a_1 \alpha_{1B} \frac{E B_{1B}}{a_1^2} \cosh B_{1B} t' - \alpha_{1B} \frac{E \sinh B_{1B} t'}{a_1^2} - a_1 \frac{\alpha_{rB} G B_{rB}}{a_1^2} \cosh B_{rB} t' - \frac{\alpha_{rB} G \sinh B_{rB} t'}{a_1^2}\right\}$$

simplifying, one obtains

$$-D_{FC}\left\{\alpha_{1C} A (a_1 B_{1C} \cos B_{1C} a_1 - \sin B_{1C} a_1) + \alpha_{rc} C(a_1 B_{rc} \cosh B_{rc} a_1 - \sinh B_{rc} a_1)\right\} = -D_{FB}\left\{\alpha_{1B} E(a_1 B_{1B} \cosh B_{1B} t' - \sinh B_{1B} t') + \alpha_{rB} G(a_1 B_{rB} \cosh B_{rB} t' - \sinh B_{rB} t')\right\}$$

$$D_{FC} \alpha_{1C} A C_{LC} + D_{FC} \alpha_{rc} C C_{rC} - D_{FB} \alpha_{1B} E C_{1B} - D_{FB} \alpha_{rB} G C_{rB} = 0 \qquad (55)$$

similarly, equation (46) can be written as

$$-D_{SC}\left\{\frac{A C_{1C} + C C_{rC}}{a_1^2}\right\} + D_{SB}\left\{\frac{E C_{1B} + G C_{rB}}{a_1^2}\right\} = \sum_a t \left\{\frac{A S_{1C} + C S_{rC}}{a_1}\right\}$$

$$-D_{SC}\left\{C_{1C} + \frac{a_1 \sum_a t S_{1c}}{D_{SC}}\right\} A - D_{SC}\left\{C_{rc} + \frac{a_1 \sum_a t S_{rC}}{D_{SC}}\right\} C + D_{SB}\left\{E C_{1B} + G C_{rB}\right\} = 0$$

Letting $\beta = \frac{a_1 \sum a t}{D_{SC}}$, the above equation becomes

$$D_{SC}\left\{C_{1C} + \beta S_{1C}\right\} A + D_{SC}\left\{C_{rC} + \beta S_{rC}\right\} C - D_{SB} E C_{1B} - D_{SB} G C_{rB} = 0 \qquad (56)$$

Final Form of the Boundary Condition Equations

Using the notation listed as (47) to (54) inclusive, the boundary conditions equations reduce to:

$$S_{1C}\,A + S_{rC}\,C - S_{1B}E - S_{rB}G = 0 \quad (57)$$

$$\alpha_{1C}\,S_{1C}\,A + \alpha_{rC}\,S_{rC}\,C - \alpha_{1B}S_{1B}\,E - \alpha_{rB}S_{rB}\,G = 0 \quad (58)$$

$$D_{SC}\,(C_{1C} + \beta\,S_{1C})A + D_{SC}(C_{rC} + \beta\,S_{rC})C - D_{SB}C_{1B}E - D_{SB}\,C_{rB}\,G = 0 \quad (59)$$

$$D_{FC}\,\alpha_{1C}\,C_{1C}\,A + D_{FC}\,\alpha_{rC}C_{rC}\,C - D_{FB}\alpha_{1B}C_{1B}\,e - D_{FB}\alpha_{rB}\,C_{rB}\,G = 0 \quad (60)$$

Critical Equation

For the simultaneous equations (57) to (60) inclusive to have a non-trival solution, the determinant of the coefficients A,C,E, and G must vanish. The critical determinant is

$$\begin{vmatrix} S_{1C} & S_{rC} & -S_{1B} & -S_{rB} \\ \alpha_{1C}\,S_{1C} & \alpha_{rC}\,S_{rC} & -\alpha_{1B}\,S_{1B} & -\alpha_{rB}\,S_{rB} \\ D_{SC}(C_{1C}+\beta\,S_{1C}) & D_{SC}(C_{rC}+\beta\,S_{rC} & -D_{SB}\,C_{1B} & -D_{SB}\,C_{rB} \\ D_{FC}\,\alpha_{1C}\,C_{1C} & D_{FC}\,\alpha_{rC}\,C_{rC} & -D_{FB}\,\alpha_{1B}\,C_{1B} & -D_{FB}\,\alpha_{rB}\,C_{rB} \end{vmatrix} = 0 \quad (61)$$

In simplifying the determinant the following notation will be used.

$$\mu_{1C} = \frac{C_{1C}}{S_{1C}} \qquad \mu_{1B} = \frac{C_{1B}}{S_{1B}} \qquad \sigma_s = \frac{D_{SB}}{D_{SC}}$$

$$\mu_{rC} = \frac{C_{rC}}{S_{rC}} \qquad \mu_{rB} = \frac{C_{rB}}{S_{rB}} \qquad \sigma_F = \frac{D_{FB}}{D_{FC}}$$

Reducing the fourth order determinant (61) to a third order determinant the following intermediate form will be obtained:

$$\begin{vmatrix} 0 & 0 & 0 & -1 \\ \alpha_{1C} - \alpha_{1B} & \alpha_{rC} - \alpha_{rB} & \alpha_{rB} - \alpha_{1B} & -\alpha_{rB} \\ \mu_{1C} - \sigma_S\,\mu_{1B} + \beta & \mu_{rC} - \sigma_S\,\mu_{rB} + \beta & \sigma_S(\mu_{rB}-\mu_{1B}) & -\sigma_S\mu_{rB} \\ \alpha_{1C}\,\mu_{1C} - \sigma_F\,\alpha_{1B}\,\mu_{1B} & \alpha_{rC}\,\mu_{rC} - \sigma_F\,\alpha_{rB}\mu_{rB} & \sigma_F(\alpha_{rB}\mu_{rB}-\alpha_{1B}\mu_{1B}) & -\sigma_F\,\alpha_{rB}\,\mu_{rB} \end{vmatrix} = 0$$

To simplify the above determinant the following notation can be used:

$$a = \alpha_{1C} - \alpha_{1B} \qquad f = \sigma_S (\mu_{rB} - \mu_{1B})$$

$$b = \alpha_{rC} - \alpha_{rB} \qquad g = \alpha_{1C}\,\mu_{1C} - \sigma_F\,\alpha_{1B}\,\mu_{1B}$$

$$c = \alpha_{rB} - \alpha_{1B} \qquad h = \alpha_{rC}\,\mu_{rC} - \sigma_F\,\alpha_{rB}\,\mu_{rB}$$

$$d = \mu_{1C} - \sigma_S\,\mu_{1B} \qquad i = \sigma_F (\alpha_{rB}\,\mu_{rB} - \alpha_{1B}\,\mu_{1B})$$

$$e = \mu_{rC} - \sigma_S\,\mu_{rB}$$

$$r = \alpha_{1B} - \alpha_{rc}$$

$$s = \sigma_F \alpha_{1B} \mu_{1B} - \alpha_{rc} \mu_{rc}$$

Employing the method of expansion by minors, determinant (61) reduces to the following third order determinant

$$\begin{vmatrix} a & b & c \\ d+\beta & e+\beta & f \\ g & h & i \end{vmatrix} = 0 \qquad (62)$$

Expanding and rearranging terms to eliminate "β" from the determinant, results in a convenient expression for the critical determinant.

$$a\,(e+\beta)\,i + (d+\beta)\,hc + g\,b\,f - c\,(e+\beta)\,g - f\,h\,a - i\,b\,(d+\beta) = 0$$

$$a\,i\,e + h\,c\,d + g\,b\,f - c\,g\,e - f\,h\,a - i\,b\,d = -a\,i\,\beta - h\,c\,\beta + c\,g\,\beta + i\,b\,\beta$$

$$\beta\left[(c\,g - a\,i) + (b\,i - c\,h)\right] = \begin{vmatrix} a & b & c \\ d & e & f \\ g & h & i \end{vmatrix} \qquad (63)$$

Expressing the multiplicand of "β" in equation (63) as a sum of two second order determinants one obtains:

$$\beta = \frac{X}{Y+Z} = \begin{vmatrix} a & b & c \\ d & e & f \\ g & h & i \end{vmatrix} \Big/ \left(\begin{vmatrix} b & c \\ h & i \end{vmatrix} + \begin{vmatrix} c & a \\ i & g \end{vmatrix} \right) \qquad (64)$$

Further simplification results in the following equation which is the equation

that must be satisfied if the system is critical.

$$\beta = -\left\{ \frac{d\,Y + e\,Z + f \;\Big|\; \begin{matrix} a & b \\ g & h \end{matrix} \Big|}{Y + Z} \right\} \equiv \frac{a_1 \Sigma a_t}{D_{SC}} \qquad (65)$$

For a specific core shell thickness "t" equation (65) must be satisfied by a trial and error method of solution.

Determination of The Constants In The Flux Equation

The constants for the flux equations are required to evaluate various terms in the neutron balance which is one of the major objectives in breeding calculations. For simplification, it can be assumed that A = 1; this in the final analysis will be equivalent to multiplying each term in the neutron balance by a factor of 1/A. Since the neutron balance lists the relative loss of neutrons to each contributing factor, no adjustment will be required.

The additional three(3) unknowns can be obtained from equations (57), (58) and (60) by using Cramer's Rule to solve for the coefficients. With A = 1 the three (3) simultaneous equations are:

$$S_{rC}C - S_{1B}E - S_{rB}G = -S_{1C} \qquad (66)$$

$$\alpha_{rC} S_{rC} C - \alpha_{1B} S_{1B} E - \alpha_{rB} S_{rB} G = -\alpha_{1C} S_{1C} \qquad (67)$$

$$D_{FC}\alpha_{rC}C_{rC} C - D_{FB}\alpha_{1B}C_{1B} E - D_{FB}\alpha_{rB}C_{rB} G = -D_{FC}\alpha_{1C}C_{1C} \qquad (68)$$

Values obtained for the three unknown coefficients C, E, and G are as follows:

$$C = \frac{M}{Q}\ ; \text{ where } M = \begin{vmatrix} -S_{1C} & -S_{1B} & -S_{rB} \\ -\alpha_{1C} S_{1C} & -\alpha_{1B} S_{1B} & -\alpha_{rB} S_{rB} \\ -D_{FC}\alpha_{1C} C_{1C} & -D_{FB}\alpha_{1B} C_{1B} & -D_{FB}\alpha_{rB} C_{rB} \end{vmatrix} \qquad (69)$$

$$Q = \begin{vmatrix} S_{rC} & -S_{1B} & -S_{rB} \\ \alpha_{rC} S_{rC} & -\alpha_{1B} S_{1B} & -\alpha_{rB} S_{rB} \\ D_{FC}\alpha_{rC} C_{rC} & -D_{FB}\alpha_{1C} C_{1B} & -D_{FB}\alpha_{rB} C_{rB} \end{vmatrix} \qquad (70)$$

$$E = \frac{N}{Q} \text{ ; where } N = \begin{vmatrix} S_{rC} & -S_{1C} & -S_{rB} \\ \alpha_{rC} S_{rC} & -\alpha_{1C} S_{1C} & -\alpha_{rB} S_{rB} \\ D_{FC}\, \alpha_{rC} C_{rC} & -D_{FC}\, \alpha_{1C} C_{1C} & -D_{FB}\, \alpha_{rB}\, C_{rB} \end{vmatrix} \qquad (71)$$

$$G = \frac{P}{Q} \text{ ; where } P = \begin{vmatrix} S_{rC} & -S_{1B} & -S_{1C} \\ \alpha_{rC}\, S_{rC} & -\alpha_{1B}\, S_{1B} & -\alpha_{1C}\, S_{1C} \\ D_{FC}\, \alpha_{rC}\, C_{rC} & -D_{FB}\, \alpha_{1B}\, C_{1B} & -D_{FC}\, \alpha_{1C} C_{1C} \end{vmatrix} \qquad (72)$$

Simplification of Determinants M,N,P, and Q

The determinants used to express the constants in the flux equations can be reduced to second order determinants as illustrated by the simplification of determinant "M". During the operation of simplification, the intermediate form of determinant (69) will be:

$$\frac{M}{S_{1C}\, S_{1B}\, S_{rB}\, D_{FC}} = \begin{vmatrix} 0 & 0 & -1 \\ \alpha_{1B} - \alpha_{1C} & \alpha_{rB} - \alpha_{1B} & -\alpha_{rB} \\ \sigma_F\, \alpha_{1B}\, \mu_{1B} - \alpha_{1C}\, \mu_{1C} & \sigma_F(\alpha_{rB}\, \mu_{rB} - \alpha_{1B} \mu_{1B}) & \sigma_F\, \alpha_{rB}\, \mu_{rB} \end{vmatrix}$$

Using the notation presented previously, the final form of determinant "M" can be expressed as the following second order determinant.

$$M = -D_{FC}\, S_{1C}\, S_{1B}\, S_{rB} \begin{vmatrix} Z \end{vmatrix} \qquad (73)$$

By a similar treatment the remaining determinants can also be simplified. The final form of determinants, N, P, and Q can be expressed as the following equations.

$$N = D_{FC}\, S_{rC}\, S_{1C}\, S_{rC} \begin{vmatrix} b & m \\ h & n \end{vmatrix} \qquad (74)$$

where $m = \alpha_{1C} - \alpha_{rB}$

$n = \alpha_{1C}\, \mu_{1C} - \sigma_F\, \alpha_{rB}\, \mu_{rB}$

$$P = D_{FC}\, S_{rC}\, S_{1B}\, S_{1C} \begin{vmatrix} r & a \\ s & g \end{vmatrix} \qquad (76)$$

Values of The Constants In The Flux Equations

Values for the constants A, C, E and G in the flux equations after simplification are as follows:

$$A = 1 \quad ; \quad C = \frac{M}{Q} = \frac{S_{1C} \mid Z \mid}{S_{rC} \mid Y \mid} \tag{77}$$

$$E = \frac{N}{Q} = - \frac{S_{1C} \begin{vmatrix} b & m \\ h & m \end{vmatrix}}{S_{1B} \mid Y \mid} = \frac{S_{1C} \begin{vmatrix} m & b \\ n & h \end{vmatrix}}{S_{1B} \mid Y \mid} \tag{78}$$

$$G = \frac{P}{Q} = - \frac{S_{1C} \begin{vmatrix} r & a \\ s & g \end{vmatrix}}{S_{rB} \mid Y \mid} = \frac{S_{1C} \begin{vmatrix} a & r \\ g & s \end{vmatrix}}{S_{rB} \mid Y \mid} \tag{79}$$

Slow Flux and Slow Current Density Check

In view of the many numerical manipulations required to evaluate the flux constants, it would be convenient to have some method of checking the results to locate any errors. Two such checks can be readily made at this stage of the calculations; namely, a slow flux check and a slow current density check. It is recommended that these checks be made before continuing with the neutron balance calculations.

The "slow flux check" is obtained from equation (57); noting that A = 1 the check equation is

$$S_{rC}\, C - S_{1B}\, E - S_{rB}\, G = - S_{1C} \tag{80}$$

From equation (59), the "slow current check" equation is obtained; noting that A = 1 and dividing by D_{SC} the check equation is

$$(C_{rC} + \beta\, S_{rC})\, C - \sigma_S\, (C_{1B}\, E + C_{rB}\, G) = - C_{1C} - \beta\, S_{1C} \tag{81}$$

Absorption in Core and Blanket

The absorption of neutrons in the various components of the core and blanket was evaluated as the product of the average flux over the appropriate

region times the macroscopic absorption cross-section for each component.

$$\int_{\text{volume}} \Sigma_i \, \varphi \, d\,V = \text{Absorption in "i"} \qquad (.82)$$

However, since the various components are homogeneously distributed through out the core and blanket respectively, the macroscopic absorption cross-section can be removed from the integral.

$$\Sigma_i \int_{\text{volume}} \varphi \, d\,V = \text{Absorption in "i"} \qquad (83)$$

Volume Integrated Fluxes

The fast and slow-fluxes for the core and blanket can be integrated over the respective volumes to give the following results.

$$\int_{\text{core}} \varphi_{SC} \, dV = \int_0^{a1} \int_0^{\pi} \int_0^{2\pi} \frac{A \sin B_{1c} r + C \sinh B_{rC} r}{r} \, (r^2 \sin\theta \, dr \, d\psi \, d\theta)$$

$$\int_{\text{core}} \varphi_{SC} \, d\,V = 4\pi A \int_0^{a1} \frac{\sin B_{1C} r (r^2)}{r} \, dr + 4\pi C \int_0^{a1} \sinh \frac{B_{rC} r \, (r^2)}{r} \, dr$$

$$= -4\pi A \frac{C_{1C}}{B_{1C}^2} + 4\pi C \frac{C_{RC}}{B_{rC}^2} \qquad (84)$$

Noting that the neutron balance will not be disturbed if each term is multiplied by a constant, it will be convenient to normalize the volume integrated flux by multiplying by $1/4\pi$. Defining this "modified integrated flux" as

$$F_{SC} = \frac{1}{4\pi} \int_{\text{core}} \varphi_{SC} \, dV$$

one obtains for the slow group in the core the value

$$F_{SC} = -\frac{AC_{1C}}{B_{1C}^2} + C \frac{C_{rc}}{B_{rC}^2} \qquad (85)$$

similiarly, for the fast group in the core

$$F_{FC} = -\alpha_{1C} A \frac{C_{1C}}{B_{1C}^2} + \alpha_{rC} C \frac{C_{rC}}{B_{rC}^2} \qquad (86)$$

For the blanket, the integrated flux was calculated as follows:

$$\int_{\text{blanket}} \varphi_{SB}\, dV = \int_{a_1}^{a_2}\int_{o}^{\pi}\int_{o}^{2\pi}\left\{E\,\frac{\sinh B_{1B}(a'_2-r)}{r} + G\,\frac{\sinh B_{rB}(a'_2-r)}{r}\right\}$$

$$(r^2 \sin\theta\, dr\, d\psi\, d\theta)$$

$$\int_{\text{blanket}} \varphi_{SB}\, dV = 4\pi E \int_{a_1}^{a_2} r \sinh B_{1B}(a'_2-r)\, dr + 4\pi G \int_{a_1}^{a_2} r \sinh B_{rB}(a'_2-r)\, dr$$

For the purpose of illustration, the first term in the above equation will be simplified.

$$4\pi E \int_{a_1}^{a_2} r \sinh B_{1B}(a'_2-r)\, dr = 4\pi E \int_{a'_2-a_1}^{ES} (a'_2 - Y) \sinh B_{1B} Y\, (-dY)$$

The following definitions apply to the terms in the above integral.

a_2 = blanket radius

a'_2 = blanket radius plus extrapolation distance

E_s = extrapolation distance for the slow flux

$$\frac{4\pi E}{B_{1B}} \int_{a'_2-a_1}^{E_s} \left\{-a'_2 \sinh B_{1B} Y\,(B_{1B}\, dY) + Y \sinh B_{1B} Y\,(B_{1B}\, dY)\right\} =$$

$$\frac{4\pi E}{B_{1B}^2}\left[-a'_2 B_{1B} \cosh B_{1B} Y + B_{1B} Y \cosh B_{1B} Y - \sinh B_{1B} Y\right]_{a'_2-a_1}^{E_s} =$$

$$\frac{4\pi E}{B_{1B}^2}\Big[-a'_2 B_{1B} \cosh B_{1B} E_s + B_{1B} E_s \cosh B_{1B} E_s - \sinh B_{1B} E_s$$

$$+ a'_2 B_{1B} \cosh B_{1B}(a'_2-a_1) - B_{1B}(a'_2-a_1) \cosh B_{1B}(a'_2-a_1) - \sinh B_{1B}(a'_2-a_1)\Big] \quad (87)$$

To simplify the calculations, the extrapolation distance will be neglected.

$$E_s \tilde{=} 0 \qquad\qquad a'_2 - a_1 \tilde{=} t'$$

Equation (87) will reduce to

$$\frac{4\pi E}{B_{1B}^2}\left[-a_2 B_{1B} + a_1 B_{1B}\cosh B_{1B}(a_2-a_1) + \sinh B_{1B}(a_2-a_1)\right] = -\frac{4\pi E}{B_{1B}^2}\left[a_2 B_{1B} + C_{1B}\right]$$

By similar calculations, it can be shown that the "Modified Integrated Fluxes" for the blanket are:

$$F_{SB} = \frac{1}{4\pi}\int_{\text{blanket}} \varphi_{SB}\, dV = -\frac{E}{B_{1B}^2}\left\{a_2 B_{1B} + C_{1B}\right\} - \frac{G}{B_{rB}^2}\left\{B_{rB} a_2 + C_{rB}\right\} \quad (88)$$

$$F_{FB} = \frac{1}{4\pi}\int_{\text{blanket}} \varphi_{FB}\, dV = -\frac{\alpha_{1B} E}{B_{1B}^2}\left\{a_2 B_{1B} + C_{1B}\right\} - \frac{\alpha_{rB} G}{B_{rB}^2}\left\{a_2 B_{rB} + C_{rB}\right\} \quad (89)$$

Absorption in the Core Shell

Absorption in the core shell is calculated by the following method:

$$\text{Absorption in shell} = \Sigma_a \times \varphi_{SC} \times \text{shell volume} \quad (90)$$

When the shell is fairly thin, the shell volume is essentially $4\pi a_1^2 t$ and the average flux approaches $\varphi_{SC}(a_1)$. Thus, equation (90) can be expressed as:

$$\text{Shell absorption} \tilde{=} 4\pi a_1^2 \Sigma_a t\, \varphi_{SC}(a_1) \quad (91)$$

noting that

$$\Sigma_a t = \beta \frac{D_{SC}}{a_1}$$

$$\varphi_{SC}(a_1) = \frac{S_{1C} + C S_{rC}}{a_1}$$

and inserting these expressions into equation (91) results in the following equation after multiplication by the normalizing factor $1/4\pi$.

$$\frac{1}{4\pi} \text{ x shell absorption} = (S_{1C} + S_{rC}\, C)\, \beta\, D_{SC} \tag{92}$$

Leakage

The total leakage of neutrons from the reactor will consist of leakage from both the slow and fast groups. To calculate this leakage the concept of neutron current density was employed; from theoretical considerations, the number of neutron crossing a unit surface per second in a direction out of the reactor is

$$J - = \left\{ \frac{\varphi}{4} + \frac{\lambda_s}{6} \left(\frac{\partial \varphi}{\partial r} \right) \right\}_{a_2} \tag{93}$$

The assumption will be made that the neutrons leaving the blanket pass into a vacuum; therefore, the neutron current density back into the blanket will be zero.

$$J+ = \left\{ \frac{\varphi}{4} - \frac{\lambda_s}{6} \left(\frac{\partial \varphi}{\partial r} \right) \right\}_{a_2} = 0 \tag{94}$$

The net neutron current density out of the blanket is

$$J = J_- + J_+ \pm \left\{ \frac{\varphi}{4} + \frac{\lambda}{6} \left(\frac{\partial \varphi}{\partial r} \right) \right\}_{a_2} \tag{95}$$

From equation (94) it can be seen that

$$\left(\frac{\varphi}{4} \right)_{a_2} = \left(\frac{\lambda_s}{6} \frac{\partial \varphi}{\partial r} \right)_{a_2}, \text{ and}$$

inserting this value into equation (95) will enable the net neutron current density out of the blanket to be evaluated.

$$J = \left(\frac{\varphi}{4} + \frac{\varphi}{4} \right)_{a_2} = \frac{\varphi}{2} (a_2) \tag{96}$$

It should be noted that all values are to be evaluated at the blanket surface.

The total number of neutrons leaving the blanket surface is

$$\text{Leakage} = \frac{\varphi(a_2)}{2} \; 4\pi a_2^2 \tag{97}$$

Using equation (41) for the slow flux in the blanket, the slow leakage can be expressed as:

$$\text{Slow Leakage} = \frac{4\pi a_2^2}{2a_2} \left\{ E \sinh B_{1B} E_s + G \sinh B_{rB} E_s \right\} \tag{98}$$

In the above equation, E_s is the extrapolation distance for slow neutrons. Multiplying by the normalizing factor of $1/4\pi$, the value for the modified slow leakage is:

$$\frac{\text{Slow Leakage}}{4\pi} = \frac{a_2}{2} \left\{ E \sinh B_{1B} E_s + G \sinh B_{rB} E_s \right\} \tag{99}$$

Similarly, the modified fast leakage can be shown to be equal to:

$$\frac{\text{Fast Leakage}}{4\pi} = \frac{a_2}{2} \left\{ \alpha B_{1B} E \sinh B_{1B} E_F + \alpha_{1B} G \sinh B_{rB} E_F \right\} \tag{100}$$

The extrapolation distance for fast neutrons "E_F" is generally different from "E_s" and can be readily obtained from the diffusion coefficient evaluated earlier.

Neutron Economy

The neutron balance can now be obtained knowing the macroscopic absorption cross sections of each constituent in the core and blanket. It is convenient to evaluate the absorption of neutrons in the various components directly and then normalize to the convenient basis of one (1) neutron absorbed in a key material, namely, the fuel isotope in the core.

Absorption of thermal neutrons in the various constituents of the core and blanket can be calculated directly by multiplying the macroscopic absorption cross section of each constituent by the "modified integrated flux" for the

slow (thermal) group. The absorption of resonance neutrons by thorium can be obtained from the product of the thorium macroscopic resonance absorption cross section (equation 10) and the "modified integrated flux" for the fast group. In addition, the complete neutron balance will provide for the loss of neutrons by absorption in the core shell and leakage from the blanket surface as indicated previously.

A check on the neutron balance can be obtained by noting that in one generation, the loss of neutrons must equal the gain of neutrons if the system is just critical. The loss of neutrons is equal to the sum of all absorptions in the core, blanket, and core shell, plus the slow and fast leakage; whereas, the number of neutrons produced is equal to the sum of fission neutrons produced in both the blanket and core by all fissionable material present. Mathematically, the production of neutrons can be expressed as:

$$\text{Production} = \sum_i \eta^i \Sigma_{fi} \varphi_s$$

For a breeder reactor employing U-233 as the fuel, the effect of the buildup of U-235 during operation must be included.

An examination of the neutron balance will indicate that the arbitrary assignment of unity (1) to "A" and the multiplication by $1/4\pi$ do not effect the final results. Since, these operations are effectively cancelled in the process of normalizing to the convenient basis of one (1) neutron absorbed in the key material in the core.

Breeding Gain

One of the quantities of major interest in a power-breeder reactor is an estimate of the fissionable material produced. The following definitions will prove useful in describing the utilization of fissionable material in a power-breeder reactor.

Net Production = fissionable atoms produced

- fissionable atoms destroyed

$$\text{Breeding Gain} = \frac{\text{fissionable atoms produced}}{\text{fissionable atoms destroyed}} - 1 \qquad (101)$$

Equation (101) gives the gain exclusive of chemical processing, handling, and other losses. A more realist estimate of the gain for the entire system should include these additional losses. The "overall breeding gain" for the entire system can be defined as: (102)

$$\text{Overall Breeding Gain} = \frac{\text{fissionable atoms produced}}{\text{total sum of fissionable atoms destroyed in the entire system}} - 1$$

Blanket Power

The per cent of the total power produced in the blanket of a power-breeder reactor can be calculated as follows. It can be seen that the power of a reactor is equal to

$$P = K \, \varphi_{avg} \, \Sigma_f \, V$$

where the value "K" is a constant to convert the number of fissions per second to megawatts. Using the values for the "modified integrated flux" it is possible to obtain the product of the average flux times the respective volumes.

$$F_{SC} = \frac{\varphi_{SC\,(avg)}}{4\pi} \quad V_C$$

$$F_{SB} = \frac{\varphi_{SB(avg)}}{4\pi} \quad V_B$$

Grouping all constants into a new constant "K", the ratio of the blanket power to the core power is

$$\frac{P_B}{P_C} = \frac{K' \, F_{SB} \, \Sigma_{fB}}{K' \, F_{SC} \, \Sigma_{fC}} = \frac{F_{SB} \, \Sigma_{fB}}{F_{SC} \, \Sigma_{fC}} . \qquad (103)$$

The percent power produced in the blanket can be obtained from equation (103) and is equal to

$$\text{Percent Power In Blanket} = \frac{F_{SB}\,\Sigma_{fB}}{F_{SB}\Sigma_{fB} + F_{SC}\,\Sigma_{fC}} \times 100$$

Explanation of The Sample Calculation

The following sample calculation is included to illustrate the theory presented on the previous pages. Calculations by a "Modified Welton Method" discussed in the next section enabled a preliminary estimate of a reasonable core size to be selected. Strength considerations were the determining factor in establishing the thickness of the core shell. Fluidization properties and heat transfer data were used to determine the percent voids for the core and blanket. Data on fission product poisoning, higher-isotope buildup, and protactinium concentration was obtained by investigation of the chemical processing system.

Because of the high percent voids in the system it is not obvious that there is sufficient moderation to thermalize all the neutrons. An investigation to determine the percent of fissions occuring at thermal energies should be made to check the assumption of this two-group method (i.e., fissions occur at thermal energies only). A document discussing various multi-group methods that can be used to investigate the system is being prepared at present by one of the other groups at ORSORT.

Sketch 1 represents the ideal system used for the sample calculation; whereas, sketch 2 indicates the finite thickness of the core shell. The absorption of thermal neutrons by the core shell has been accounted for, however, the scattering and slowing down properties of the shell were neglected in order to simplify the calculations. Neglecting these properties should have the following physical effects not included in the equations:

(1) Replacing 10 cm. of core material by 10 cm of core shell would provide

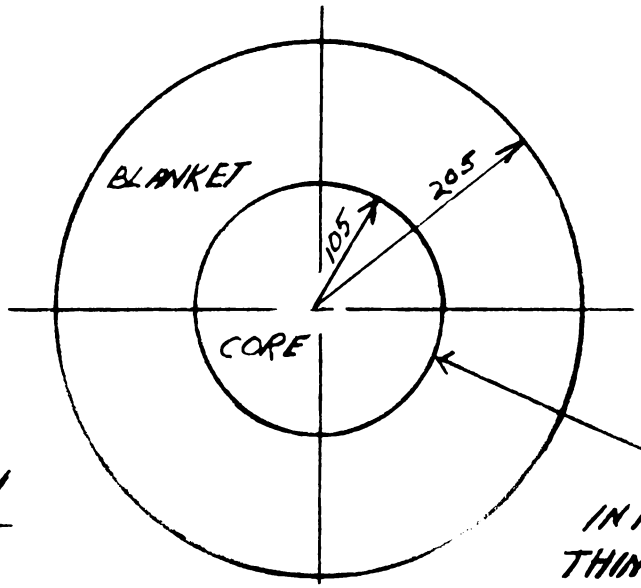

SKETCH 2.1

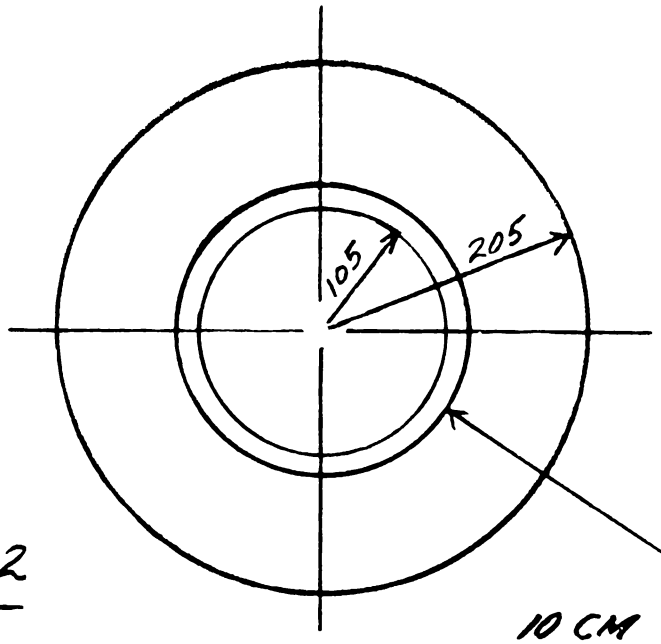

SKETCH 2.2

a "reflector savings"; thereby reducing the critical mass of the core.

(2) The core shell will thermalize part of the fast neutron current from the core, decreasing the probability of leakage from the blanket and also increasing the probability of absorption in thorium.

(3) As for the effect of the core shell on the slow neutrons; it will decrease the net leakage of slow neutrons into the blanket.

Because of these and other effects not apparent at this time, it is not obvious what over-all effect the core shell will have upon the system. However, if the final result is a reduction in the number of neutrons available for breeding the following compensating procedures can be employed.

(1) Decreasing the core size will increase the leakage of neutrons into the blanket.

(2) The same effect can be attained by decreasing the core solids density (i.e., increase the per cent voids).

A three region-two group calculation was not performed because the core shell (third region) is located between a strong source (core) and a strong absorber (blanket) and is only three mean free paths in the thick.

No Breeding in Core
Poisons and Higher Isotopes
also Power in Blanket

Z = 28.097

2% Poisons in Core

21.094 Kg in core

CALCULATION SHEET FOR TWO GROUP - TWO REGIONS

MULTIPLYING CORE, BREEDER BLANKET, SPHERICAL GEOMETRY

$\Sigma_a(FP) = .02\ \Sigma_a(U)$ $\quad$ $\Sigma_a(FP) = .01\ \Sigma_a(U)$

$\Sigma_a(Hl) = .00303\ \Sigma_a(U)$ $\quad$ $\Sigma_a(Hl) = .00303\ \Sigma_a(U)$

Core radius _____ Ft. 105 CM = a_1 $\quad$ Core volume 4.8490 x 10^6 l = V_c

Blanket Radius ____ Ft. 205 Cm = a_2 $\quad$ Blanket Volume 31.2379 x 10^{-6} l = V_B

Core Tank Material Graphite Thermal Abs. Core Tank Mat. 0.0001617 Cm^{-1} = Σ_{sa} @ 1750°F

$\sigma_a(23)$ = 229.36 Core 40% voids		Blanket 45% Voids	
Temp°C =	1093 (.462)	Temp °C =	816 (0.520)
Fuel Compound	(23)	Fertile Compound	(02)
Conc. Fuel Compound	— g/l	Conc. Fertile Isotope	1.0 gm/cm^3
Conc. Fuel Element	— g/l	Mass Fertile Isotope	31,237.9 kg
Enrichment	100%	Conc.	Σ(PA) g/l
Conc. Fuel Isotope	.00435024 gm/cm^3 g/l	Mass.	ΣPA/ΣTH = .0015 kg
Mass Fuel Isotope	21.0943 kg	Conc.	(23) .003190692 gm/cm^3
Mass Fuel Element	— kg	Mass.	100 (99.67083) kg
Mac. Abs. Total Comp.	.002577518 cm^{-1}	Mac. Abs. Total Fert. Comp.	.0083550 cm^{-1}
Mac. Abs. Total Poison	.00005155036 cm^{-1}	Mac. Abs. Total	(PA) .0000125325 cm^{-1}
Mac. Abs. (H.I.) =	.00000780987	Mac. Abs. Total	(23) .002128192 cm^{-1}
Moderator Material	Graphite	Mac. Abs. Total	(C) .00008420 cm^{-1}
Wt. % Impurity - Mod.		Total Mac.Abs.Blanket, Σ_{SB} =	0.010607655 cm^{-1}
Mac. Abs. Total Mod.	.000091300 cm^{-1}	Mac.Res.Abs., Σ_{RB} =	.003963 cm^{-1}
Total Mac. Abs. Core, Σ_{sc} =	.0027286795 cm^{-1}	Res. Escape Prob. p_B =	_____ cm^{-1}
Res. Escape Prob. pc =		η_B =	2.33
η_c =	2.33	k B/P_B =	.467464
k_c =	2.200976	Slow Diff. Coef. D_{sB} =	1.547
Slow Diff. Coef, D_{sc} =	1.488	Fast Diff. Coef. D_{FB} =	2.193
Fast Diff. Coef. D_{Fc} =	2.153	Fermi Age, τ_B =	1204
Fermi Age, τ_c =	958	$\mathscr{L}^2_{FB} = 1/\tau_B$ =	.00083056
$B^2_{Fc} = 1/\tau_c$ =	1.04384 x 10^{-3}	$B^2_{sB} = \Sigma_{sB}/D_{sB}$ =	.00685692
$B^2_{sc} = \Sigma_{sc}/D_{sc}$ =	1.83379 x 10^{-3}	$\mathscr{L}^2_{RB} = \Sigma_{RB}/D_{FB}$ =	.0018071135
$(k_c-1)B^2_{sc}B^2_{Fc}$ =	2.29389 x 10^{-6}	$B^2_{FB} = \mathscr{L}^2_{FB} + \mathscr{L}^2_{RB}$ =	0.00263767
$(B^2_{sc} + B^2_{Fc})/2$ =	1.438815 x 10^{-3}	$(B^2_{FB} + B^2_{sB})/2$ =	.00474729
$[(B^2_{sc}+B^2_{Fc})/2]^2$	2.070188 x 10^{-6}	$[(B^2_{FB}+B^2_{sB})/2]^2$ =	22.5367 x 10^{-6}

NOTE:
Subscript i's Appearing In Table Refer To Subscript l's In Text.

$R^2 = \left[(B_{sc}^2+B_{Fc}^2)/2\right]^2 + (k_c-1)B_{sc}^2B_{Fc}^2 = 4.369078\times10^{-6}$

$R = 2.09023 \times 10^{-3}$

$B_{ic}^2 = R - \left[(B_{sc}^2+B_{Fc}^2)/2\right] = 6.51415 \times 10^{-4}$

$B_{rc}^2 = R + \left[(B_{sc}^2+B_{Fc}^2)/2\right] = 35.29045 \times 10^{-4}$

$B_{ic} = .0255229$

$B_{rc} = .0594058$

$B_{iB} = .04561$

$B_{rB} = .08611$

$D_{sc}/D_{Fc} =$

$\alpha_{ic} = D_{sc}(B_{sc}^2+B_{ic}^2)/D_{Fc}B_{Fc}^2 = 1.64545423$

$\alpha_{rc} = D_{sc}(B_{sc}^2-B_{rc}^2)/D_{Fc}B_{Fc}^2 = -1.1224283$

$t = a_2 - a_1$

$(k_B/P_B)\mathscr{L}_{FB}^2B_{sB}^2 = 2.66226 \times 10^{-6}$

$B_{FB}^2B_{sB}^2 = 18.0863 \times 10^{-6}$

$S^2 = (k_B/P_B)\mathscr{L}_{FB}^2B_{sB}^2 - B_{FB}^2B_{sB}^2 + \left[(B_{FB}^2+B_{sB}^2)/2\right]^2$

$= 7.11266 \times 10^{-6}$

$S = 2.667 \times 10^{-3}$

$B_{iB}^2 = \left[(B_{FB}^2+B_{sB}^2)/2\right] - S = .00208029$

$B_{rB}^2 = \left[(B_{FB}^2+B_{sB}^2)/2\right] + S = .0074142$

Blanket thickness $= a_2 - a_1 = t'$ 100

$D_{sB}/D_{FB} =$

$\alpha_{iB} = D_{sB}(B_{sB}^2-B_{iB}^2)/D_{FB}\mathscr{L}_{FB}^2 = 4.056935$

$\alpha_{rB} = D_{sB}(B_{sB}^2-B_{rB}^2)/D_{FB}\mathscr{L}_{FB}^2 = -.4733146$

$B_{ic}\,a_1 = 2.6799045$ (153°.32.8362)

$B_{iB}\,t' = 4.561$

$B_{rc}\,a_1 = 6.237609$

$B_{rB}\,t' = 8.611$

$B_{iB}\,a_1 = 4.78905$

$B_{rB}\,a_1 = 9.04155$

$S_{ic} = \sin B_{ic}a_1 = .44546$

$S_{iB} = \sinh B_{iB}t' = 47.83929$

$\cos B_{ic}a_1 = -.8952987$

$\cosh B_{iB}t' = 47.83929$

$T_{ic} = B_{ic}a_1 \cos B_{ic}a_1 = -2.39931501$

$C_{ic} = T_{ic} - S_{ic} = -2.844775$

$U_{ic} = C_{ic}/S_{ic} = -6.38621677$

$T_{iB} = B_{iB}a_1 \cosh B_{iB}t' = 229.10475$

$C_{iB} = T_{iB} - S_{iB} = -276.94404$

$U_{iB} = C_{iB}/S_{iB} = -5.78905$

$\sigma_s = D_{sB}/D_{sc} = 1.03965$

$\sigma_s U_{iB} = -6.018585$

$\sigma_s U_{rB} = -10.43969$

$\alpha_{ic}U_{ic} = -10.5082273$

$a = \alpha_{ic} - \alpha_{iB} = -2.4114807$

$b = \alpha_{rc} - \alpha_{rB} = -.6491137$

$c = \alpha_{rB} - \alpha_{iB} = -4.530249$

$d = U_{ic} - \sigma_s U_{iB} = -.367317$

$e = U_{rc} - \sigma_s U_{rB} = 15.677299$

$f = \sigma_s(U_{rB} - U_{iB}) = -4.421111$

$g = \alpha_{ic}U_{ic} - \sigma_F\alpha_{iB}U_{iB} = 13.4137027$

$S_{rc} = \sinh B_{rc}a_1 = 255.81855$

$S_{rB} = \sinh B_{rB}t' = 2745.995$

$\cosh B_{rc}a_1 = 255.81855$

$\cosh B_{rB}t' = 2745.995$

$T_{rc} = B_{rc}a_1 \cosh B_{rc}a_1 = 1595.6960$

$C_{rc} = T_{rc} - S_{rc} = 1339.87745$

$U_{rc} = C_{rc}/S_{rc} = 5.237609$

$T_{rB} = B_{rB}a_1 \cosh B_{rB}t' = 24828.051$

$C_{rB} = T_{rB} - S_{rB} = -27574.046$

$U_{rB} = C_{rB}/S_{rB} = -10.04155$

$\sigma_F = D_{FB}/D_{Fc} = 1.01857$

$\sigma_F\alpha_{iB}U_{iB} = -23.92193$

$\sigma_F\alpha_{rB}U_{rB} = 4.8410719$

$\alpha_{rc}U_{rc} = -5.87884056$

$h = \alpha_{rc}U_{rc} - \sigma_F\alpha_{rB}U_{rB} = -10.719911$

$i = \sigma_F\alpha_{rB}U_{rB} - \sigma_F\alpha_{iB}U_{iB} = 28.763001$

$m = \alpha_{ic} - \alpha_{rB} = 2.1187688$

$n = \alpha_{ic}U_{ic} - \sigma_F\alpha_{rB}U_{rB} = -15.3492992$

$r = \alpha_{iB} - \alpha_{rc} = 5.1793633$

$s = \sigma_F\alpha_{iB}U_{iB} - \alpha_{rc}U_{rc} = -18.043089$

$$x = \begin{vmatrix} a & b & c \\ d & e & f \\ g & h & i \end{vmatrix} = -6.6641068$$

$$M = \begin{vmatrix} m & b \\ n & h \end{vmatrix} = -32.676453 \qquad N = \begin{vmatrix} a & r \\ g & s \end{vmatrix} = -25.963878$$

$$Y = \begin{vmatrix} b & c \\ h & i \end{vmatrix} = -67.234324 \qquad Z = \begin{vmatrix} c & a \\ i & g \end{vmatrix} = 8.59400870 \qquad \beta = X/(Y+Z) = +.113643$$

$$D_{sc}/a_1 = .01417142 \qquad \beta D_{sc}/a_1 = .00161048$$

$$Y + Z = -58.640315$$

Tank thickness = t=

$$\beta D_{sc}/a_1 \, \Sigma_{sa} = 9.9.5967 \text{ cm}$$

$$S_{ic}/Y = -.00662548 \qquad A = 1$$

$$G = \frac{S_{ic}}{S_{rB}} \frac{N}{Y} = 6.26451 \times 10^{-5}$$

$$C = \frac{S_{ic}}{S_{rc}} \frac{Z}{Y} = -.0002225774$$

$$E = \frac{S_{ic}}{S_{iB}} \frac{M}{Y} = 4.52551001 \times 10^{-3}$$

Slow Flux Check:

$$S_{rc}C - S_{iB}E - S_{rB}G = -.4454597427 \qquad -S_{ic} = -.44546$$

Slow Current Check:

$$(C_{rc} + \beta S_{rc})\, C - \sigma_s (C_{iB}E + C_{rB}G) = 2.7941790$$

$$-C_{ic} - \beta S_{ic} = 2.79415159$$

$$F_{sc} = \frac{1}{4\pi} \int \varphi_{sc}\, d\tau = -\frac{A}{B_{ic}^2} C_{ic} + \frac{C}{B_{rc}^2} C_{rc} = 4282.563828$$

$$F_{Fc} = \frac{1}{4\pi} \int \varphi_{Fc}\, d\tau = -\alpha_{ic} \frac{A}{B_{ic}^2} C_{ic} + \alpha_{rc} \frac{C}{B_{rc}^2} C_{rc} = 7280.6662$$

$$F_{sB} = \frac{1}{4\pi} \int \varphi_{sB}\, d = -\frac{E}{B^2_{iB}} (B_{iB}a_2 + C_{iB}) - \frac{G}{B^2_{rB}} (B_{rB}a_2 + C_{rB}) = 814.964714$$

$$F_{FB} = \frac{1}{4\pi} \int \varphi_{FB}\, d = -\alpha_{iB} \frac{E(B_{iB}a_2 + C_{iB})}{B_{iB}^2} - \alpha_{rB} \frac{G(B_{rB}a_2 + C_{rB})}{B_{rB}^2} = 2251.465698$$

$$\frac{F_{Fc}}{F_{sc}} = 1.7000718 \qquad \frac{F_{sB}}{F_{sc}} = .19029832 \qquad \frac{F_{FB}}{F_{sc}} = .525728$$

Absorption in Core

In Compound = F_{sc}(Mac.Abs.Tot.) = 11.03838535

Poisons = .220767707
Higher Isotopes= .033446266

In Moderator = F_{sc}(Mac.Abs.Tot.) = .393139359

Absorption in Blanket

In Th.(fast) = $F_{FB}\Sigma_{rB}$ = 8.92255856

(slow)= $F_{sB}\left(\frac{\quad}{\quad}\right)$ = 6.8090301

Th.(total)= 15.73158866

In C = $F_{sB}\left(\frac{.0686200289}{\quad}\right)$ =

(PA) = .010213545

(23) = 1.73440138

(H1) = .0052552347

(FP) = .0173440138

Absorption in Shell = $(S_{ic} + S_{rc}C)\ \beta D_{sc}$ = .065699132

Leakage Extrapolation Distance

$E_s = 2.13\ D_{sB}$ = 3.29511 $E_f = 2.13\ D_{fB}$ = 4.67109

$B_{iB}E_s$ = .15023996	sinh $B_{iB}E_s$ = .1508534	E sinh $B_{iB}E_s$ = .6828857 x 10^{-3}
$B_{rB}E_s$ = .2837419	sinh $B_{rB}E_s$ = .2875653	G sinh $B_{rB}E_s$ =1.801455 x 10^{-5}
$B_{rB}E_f$ = .40222755	sinh $B_{rB}E_f$ = .4131624	α_{rB}G sinh $B_{rB}E_f$=-1.22506123 x 10^{-5}
$B_{iB}E_f$ = .2130484	sinh $B_{iB}E_f$ = .2146685	α_{iB}E sinh $B_{iB}E_f$= 3.941249 x 10^{-3}

Slow leakage = 1/2 a_2 $\left[E \sinh B_{iB}E_s + G \sinh B_{rB}E_s\right]$ = .0681290921

Fast leakage = 1/2 a_2 $\left[\alpha_{rB} G \sinh B_{rB}E_f + \alpha_{iB}E \sinh B_{iB}E_f\right]$ = .402722334

Total leakage = .470851426

Neutron Economy

Normalizing Factor = .090592459

Core

U-233	1.00000000
(Graphite)	.0356156578
Higher Isotopes	.0030299962
Poisons	.01999999
	1.058645643

Blanket

U-233	.157124553
Thorium	1.42517116648
Pa-233	.00092527526
Graphite	.00621649146
Higher Isotopes	.000476087261
Poisons	.00157124553
	1.591484817

Leakage	.0426558239
Shell Absorption	.00595187877
Total	2.698738162

Check 2.33(1.157124553) = 2.6961002
1.42517116648

Net 23 Production = 1.158049828
+ .267121338

0. Breeding gain = .23085

Power in Blanket = $\frac{.157124}{1.157124}$ = 13.579%

3.2.3 Simplified Method Used By The Authors

It should be apparent that the method presented in the preceding section is laborious and time consuming. Much of the time is devoted to obtaining a critical system; that is, varying the concentration of the fissionable material in the core until the identity(equation 65 section 3.2.2) is satisfied. A considerable savings in time was accomplished by the authors who employed the modifications presented in this section.

The simplification is accomplished by using a "Modified Welton Method" to obtain a preliminary estimate and employing a set of curves to obtain values for B_{1C}, B_{rC}, B_{1B}, and B_{rB}. After the critical system is obtained, the neutron economy is calculated as illustrated in the previous section.

Preliminary Estimate of The Critical Mass

The method presented here is particularly useful for estimating the critical mass of a reflected Homogeneous Thermal Reactor. Notes on the theory associated with this method have been prepared by P. J. Sykes, Jr. (46) of the Oak Ridge School of Reactor Technology. The notes are based on lectures given at ORSORT by Dr. T. A. Welton. By introducing appropriate changes in the derivation presented in the notes by Sykes the method can be applied to cases where the reflector materials differ from the core materials.

The ratio "Z_c" for a reflected homogeneous spherical reactor with dissimilar materials in the core and reflector can be expressed by the following formula:

$$Z_c = \frac{\Sigma_u}{\Sigma_M'} = \frac{1}{R^2} \left\{ \frac{(R^2 + X_1^2 \tau_c)(R^2 + X_2^2 L_M^2)}{\eta\left[R^2 + \frac{\tau_c}{\tau_R}\left(\frac{X_1^2 - X_2^2}{L_R^2 - \tau_R}\right) L_R^2 \tau_R\right] - (R^2 + X_1^2 \tau_c)} \right. \quad (1)$$

where the subscripts C, R, U, and M refer to the core, reflector, uranium and moderator respectively. Values for the functions "X_1" and "X_2" can be

obtained from the core and reflector properties as follows:

$$\frac{X_1}{\tan X_1} = \left(1 - \frac{D_{1R}}{D_{1C}}\right) - \left(\frac{D_{1R}\ R}{D_{1C}\sqrt{\tau_R}}\right) \qquad (2)$$

$$\frac{X_2}{\tan X_2} = \left(1 - \frac{D_{2R}}{D_{2C}}\right) - \left(\frac{D_{2R}\ R}{D_{2C}\ L_R}\right) \qquad (3)$$

Where the subscripts "1" and "2" refer to the fast and slow groups respectively. Values for the function $\frac{\text{"tan X"}}{X}$ can be readily obtained from tabulations such as the "Table of Functions" by Jahnke and Emde.

Additional modification is required to introduce the effect of the thorium resonance upon the reflecting properties of the blanket. This is accomplished by introducing the concept of a "Fictitious Fermi-Age" that is to be substituted for "τ_R" in equations (1) and (2). The "Fictitious Fermi-Age τ'" is evaluated as follows,

$$\frac{1}{\tau'} = \frac{1}{\tau_B} + \frac{\Sigma_{RB}}{D_{FB}} = B^2_{FB}$$

Where the notation is the same as in the previous section. Continuing to use this notation, equation (1), (2), and (3) can be expressed as follows:

$$Z_c = \frac{\Sigma_U}{\Sigma_{moderator}} = \frac{1}{a_1^2}\left\{\frac{(a_1^2 + X_1^2\,\tau_c)(a_1^2 + X_2^2\ L^2_{moderator})}{\eta\left[a_1^2 + \tau_2 B^2_{FB}\left(\frac{X_1^2 - X_2^2}{B^2_{FB} - B^2_{SB}}\right)\right] - (a_1^2 + X_1^2\,\tau_c)}\right\} \qquad (5)$$

$$\frac{X_1}{\tan X_1} = 1 - \sigma_F\ (1 + a_1 B_{FB}) \qquad (6)$$

$$\frac{X_2}{\tan X_2} = 1 - \sigma_S\ (1 + a_1 B_{SB}) \qquad (7)$$

One of the assumptions required to obtain the above equation is that the blanket material is infinite in extent. This results in an underestimation of the critical mass of the system. However, the contribution

of fissioning in the blanket was neglected, resulting in an over-estimation of the critical mass. Each of these factors tend to partially compensate for the effect on critical mass associated with the assumptions.

A calculation to illustrate the method for obtaining a preliminary estimate of the critical mass (i.e., its equivalent "Zc") is included on form sheet # 1. The core and blanket constants in the calculations are for the system illustrated in section (3.2.2).

Using this value of "Zc" in the subsequent form sheets will result in a value for the critical determinant (equation 64 in section 3.2.2). A positive value for this determinant greater than "β" indicates that the critical mass of the system has been over estimated. A negative value indicates that the critical mass has been underestimated. The curve of "Zc" versus the value for the critical determinant for values of Zc approaching the critical system is shown in Figure 1.

Figure 1

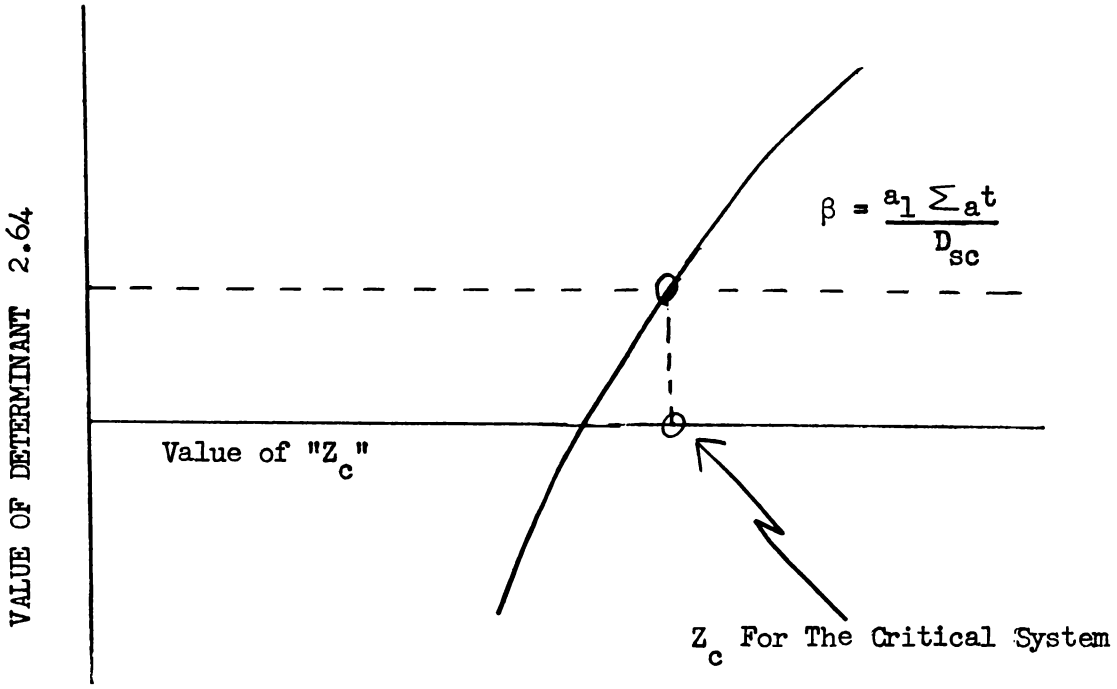

Form Sheet No. 3.7.1

PRELIMINARY ESTIMATE OF CRITICAL MASS

$\frac{X_1}{\tan X_1} = 1 - \sigma_F (1 + a_1 B_{FB})$

$= 1 - 6.5 = -5.5$

$\frac{\tan X_1}{X_1} = -.182$

$X_1 = 2.69 \qquad X_1^2 = 7.23$

$\frac{X_2}{\tan X_2} = 1 - \sigma_s (1 + a_1 B_{SB})$

$= 1 - 10.06 = -9.06$

$\frac{\tan X_2}{X_2} = -.1102$

$X_2 = 2.84 \qquad X_2^2 = 8.07$

$a_1 = 105 \qquad a_1^2 = 11030$

SYSTEM DATA:

$\tau_B = 1204 \qquad \Sigma_{RB} = .003963$

$D_{FB} = 2.193 \qquad D_{FC} = 2.153$

$D_{SB} = 1.547 \qquad D_{SC} = 1.488$

$L_B^2 (C+TH+PA) = 183.04$

$B_{SB}^2 = \frac{Z_B (1 + X_B + Y_B)}{L^2 (C + TH + PA)} = .006857$

$\mathscr{L}_{FB}^2 = 1/\tau_B = .0008306$

$\mathscr{L}_{rB}^2 = RB/D_{FB} = .001807$

$B_{FB}^2 = \mathscr{L}_{FB}^2 + \mathscr{L}_{RB}^2 = .002637$

$B_{FB} = .0513 \qquad B_{SB} = .0828$

$a_1 B_{FB} = 5.39 \qquad a_1 B_{SB} = 8.69$

$\sigma_F = D_{FB}/D_{FC} = 1.0186$

$\sigma_s = D_{SB}/D_{SC} = 1.039$

L_c^2 Graphite $= 16220$

$$Z_c = \frac{1}{a_1^2} \frac{(a_1^2 + X_1^2 \tau_c)(a_1^2 + X_2^2 L_c^2 \text{ graphite})}{\eta_c \left[a_1^2 + \tau_c B_{FB}^2 \left(\frac{X_1^2 - X_2^2}{B_{FB}^2 - B_{SB}^2} \right) \right] - (a_1^2 + X_1^2 \tau_c)}$$

$A = X_1^2 \tau_c = 6930$

$C = a_1^2 = A = 17960$

$E = \tau_c B_{FB}^2 = 2.53$

$F = X_1^2 - X_2^2 = -.84$

$G = B_{FB}^2 - B_{SB}^2 = -.004219$

$\eta_c J = 26900$

$B = X_2^2 L_c^2$ graphite $= 131000$

$D = a_1^2 + B = 142030$

$H = \frac{(E)(F)}{G} = 504$

$J = a_1^2 + H = 11534$

$K = \eta_c J - C = 8940$

$$Z_c = \frac{(C)(D)}{(a_1^2)(K)} = 25.8$$

Nomenclature

The following equations will apply to systems where fertile material is present only in the blanket. If systems are investigated where both the core and blanket contain fertile material, then the equations derived here for the blanket also apply to the core.

For the core containing no fertile material:

$$\frac{K_c}{P_c} = \eta_f = \eta_c \frac{\Sigma_a(u)}{\Sigma_a(u) + \Sigma_a(M) + \Sigma_a(Hl) + \Sigma_a(FP)} \qquad (8)$$

where the subscripts U, M, Hl, and FP refer to the uranium, moderator, higher isotopes, and fission products respectively. Simplification of equation (8) is possible by letting

$$Zc = \Sigma_a(U)/\Sigma_a(M)$$

$$\Sigma_a(Hl) = X_c \Sigma_a(U)$$

$$\Sigma_a(FP) = Y_c \Sigma_a(U)$$

Employing the above notation, equation (8) reduces to

$$\frac{K_c}{P_c} = \eta_c \frac{Z_c}{Z_c (1 + X_c + Y_c) + 1} \qquad (9)$$

Similarly, it can be shown that the square of the diffusion length for the system can be expressed as follows:

$$\frac{1}{B^2_{SC}} \cong \frac{L_M^2}{Zc\ (1 + Xc + Yc) + 1} \qquad (10)$$

In the derivation of equation (10) it was assumed that the concentration of uranium was low enough that its effect upon the diffusion coefficient could be neglected. For the blanket containing fertile material, it can be shown that corresponding equations for the blanket are:

$$\frac{K_B}{P_B} = \eta_B \frac{Z_B}{Z_B (1 + X_B + Y_B) + 1} \qquad (11)$$

$$Z_B = \frac{\Sigma_a(U)}{\Sigma_a(th) + \Sigma_a(PA) + \Sigma_a(M)} \qquad (12)$$

$$\Sigma_a(PA) = W_B \Sigma_a (TH)$$

$$\Sigma_a(Hl) = X_B \Sigma_a (U)$$

$$\Sigma_a(FP) = Y_B \Sigma_a(U)$$

The additional subscripts TH and PA refer to thorium and protactinium respectively.

$$\frac{1}{B^2_{SB}} = \frac{L^2 (M + TH + PA)}{Z_B(1 + X_B + Y_B) + 1} \qquad (13)$$

Curves for Blanket and Core Data

Curves for B_{lC}, B_{rC}, B_{lB}, and B_{rB} can be calculated for the system after obtaining the values indicated in the two previous paragraphs. The curves should include values of Zc and Z_B ranging from zero to values which correspond to reasonable inventory of fissionable material. The accuracy of subsequent calculations will depend on the number of points used to draw the curves and on the scale used to plot the data.

Form sheets (2) and (3) are used to obtain values for B_{lB}, B_{rB}, B_{lC} and B_{rC}. The Z_B and Z_c correspond to inventories of fissionable material used in the sample calculation in section 3.2.2. Curve (1) is to be used in conjunction with form sheet (4); after determining the desired concentration of fissionable material in the blanket, values for B_{lB} and B_{rB} can be obtained for the equivalent of Z_B. Form sheet (5) is to be used in conjunction with curve (2). A preliminary estimate of Zc is obtained as illustrated on form sheet (1) and subsequent estimates of Zc determined by using the information pertaining to figure (1).

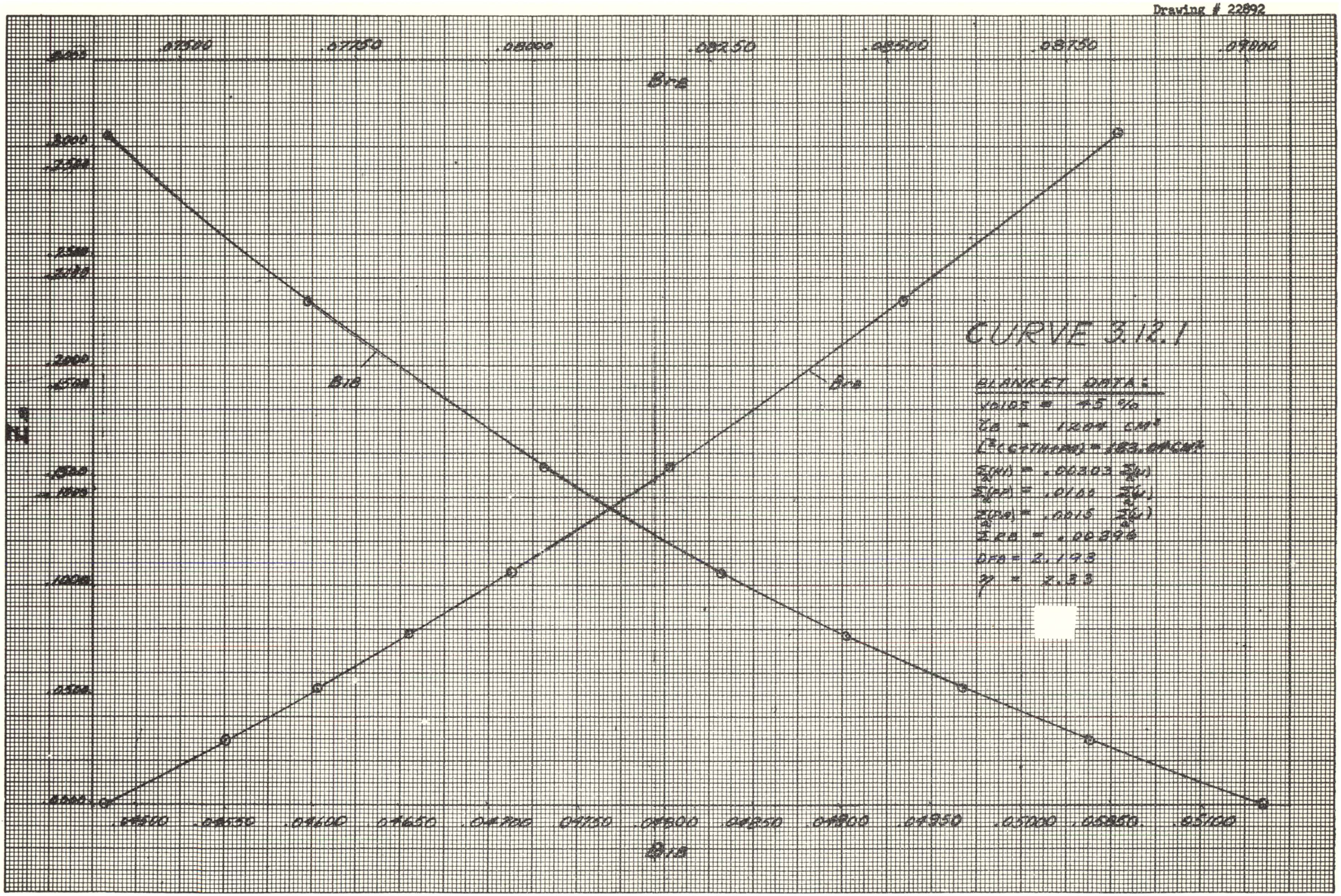
.07500
.07750
.08000
.08250
.08500
.08750
.09000
.04500
.04600
.04650
.04700
.04750
.04800
.04850
.04900
.04950
.05000
.05100
CURVE 3.12.1
BLANKET DATA:
VOIDS = 45 %
DFB = 2.193

Drawing # 22893

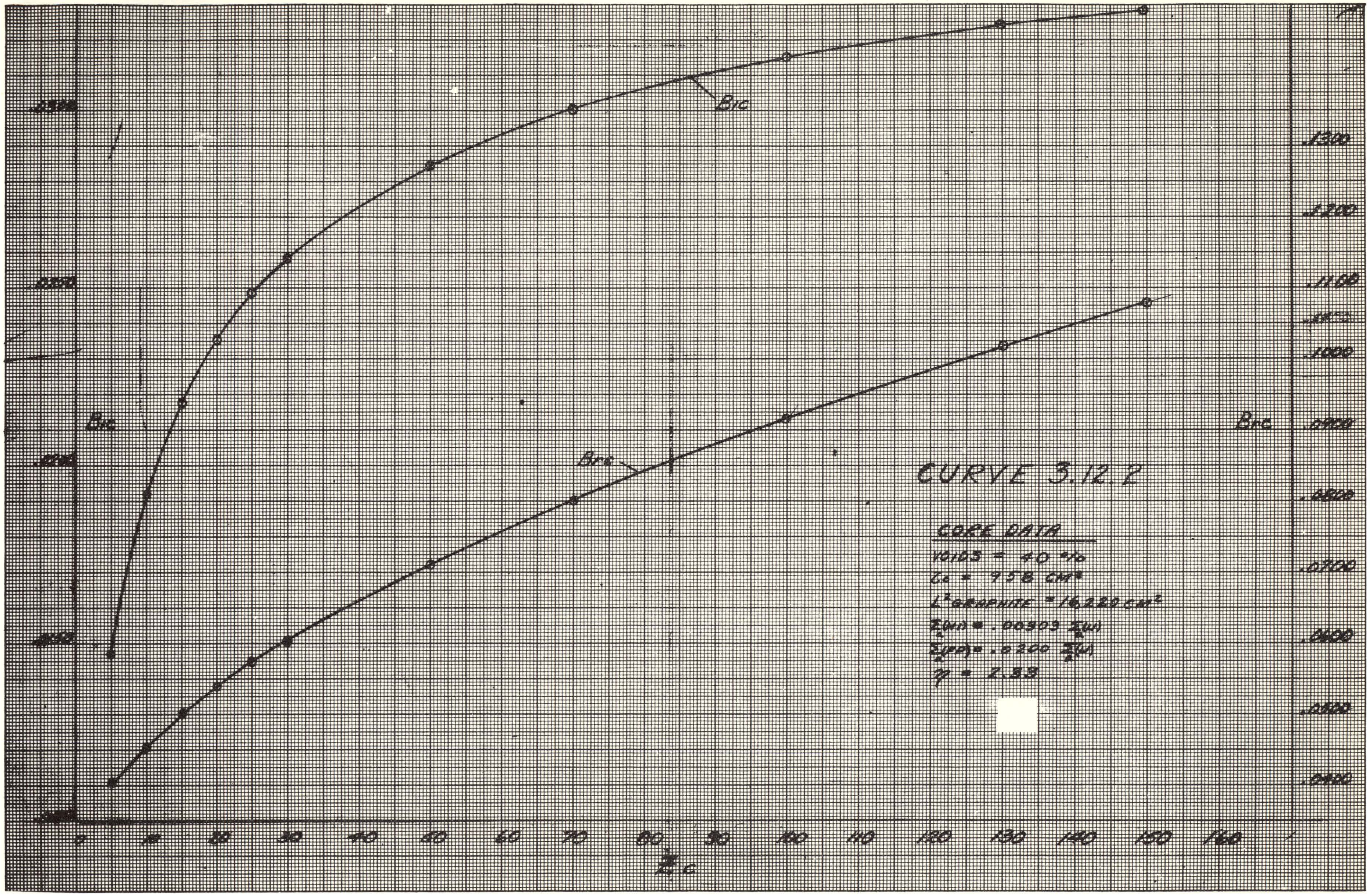

Various values of Zc are used until the identity, equation (65) in section 3.2.2 is satisfied. Curve (3) illustrates the behavior of the critical determinant for actual values of Zc.

After completing form sheet (4) for the blanket, the critical system can be determined using only form sheet (5). Examination of this form sheet will indicate that only six terms in the determinant are dependent on Zc; the additional terms are dependent on the blanket data.

After the critical system has been determined, the neutron balance is obtained as indicated in section 3.2.2. Form sheet (6) can be used to obtain the remaining information.

Form Sheet No. 3.13.2

CALCULATIONS FOR B_{1c} AND B_{rc}

SYSTEM DATA:

$X_c = \Sigma_a(H1)/\Sigma_a(U) = .00303$ $\quad\quad$ $\tau_c = 958$

$Y_c = \Sigma_a(FP)/\Sigma_a(U) = .0200$ $\quad\quad$ L_c^2 graphite $= 16{,}220$

$\eta_c = 2.33$ $\quad\quad$ $P_c = 1.0$

Z_c	Case: 1 28.10	Case: 2	Case: 3	Case: 4
$Z_c\ (1+X_c+Y_c) =$	28.74			
$K_c = \eta_c \dfrac{Z_c}{Z_c(1+X_c+Y_c)+1} =$	2.201			
$B_{sc}^2 = \dfrac{Z_c\ (1+X_c+Y_c)+1}{L_c^2 \text{ graphite}} =$	.001834			
$B_{FL}^2 = 1/\tau_c =$	1.044×10^{-3}			
$B_{FC}^2\ B_{sc}^2 =$	1.914×10^{-6}			
$A = \left[(B_{sc}^2 + B_{Fc})/2\right] =$	.001437			
$A^2 =$	2.066×10^{-6}			
$B = (K_c-1)\ B_{sc}^2\ B_{Fc}^2 =$	2.295×10^{-6}			
$R^2 = A^2 + \beta =$	4.361×10^{-6}			
$R =$	2.088×10^{-3}			
$B_{1c}^2 = R - A =$	6.509×10^{-4}			
$B_{1c} =$	.02551			
$B_{rc}^2 = R + A =$	35.29×10^{-4}			
$B_{rc} =$	.05937			

Form Sheet No. 3.13.1

CALCULATIONS FOR B_{1B} AND B_{rB}

SYSTEM DATA:

$X_B = \Sigma_a(H1)/\Sigma_a(U) = .00303$ $\quad \tau_B = 1204$

$Y_B = \Sigma_a(FP)/\Sigma_a(U) = .0100$ $\quad L_B^2 (C + TH + PA) = 183.04$

$W_B = \Sigma_a(PA)/\Sigma_a(TH) = .0015$ $\quad \Sigma_{RB} = .00396$

$\eta_B = 2.33$ $\quad D_{FB} = 2.193$

Z_B	Case: 1 .252	Case: 2	Case: 3	Case: 4
$Z_B (1 + X_B + Y_B) =$	.2551			
$\frac{K_B}{P_B} = \eta_B \frac{Z_B}{Z_B (1+X_B+Y_B) + 1} =$	.4675			
$B_{sB}^2 = \frac{Z_B(1 + X_B + Y_B) + 1}{L_B^2 (C + TH + PA)} =$	.006857			
$\ell_{FB}^2 B_{SB}^2 = \frac{B_{SB}^2}{\tau_B} =$	5.68×10^{-6}			
$\Sigma_{RB} / D_{FB} =$	.001807			
$B_{FB}^2 = \frac{1}{\tau_B} + \frac{\Sigma_{RB}}{D_{FB}} =$	.002638			
$A = \left[(B_{FB}^2 + B_{SB}^2)/2 \right] =$	.004743			
$A^2 =$	22.54×10^{-6}			
$B = \left(\frac{K_B}{P_B}\right) \ell_{FB}^2 B_{SB}^2 =$	2.662×10^{-6}			
$C = B_{FB}^2 B_{SB}^2 =$	18.08×10^{-6}			
$S^2 = \left[A^2 + B - C \right] =$	7.112×10^{-6}			
$S =$	2.667×10^{-3}			
$B_{1B}^2 = A - S =$	.002080			
$B_{1B} =$	.04561			
$B_{rB}^2 = A + S =$	.007414			
B_{rB}	.08611			

Drawing # 22894

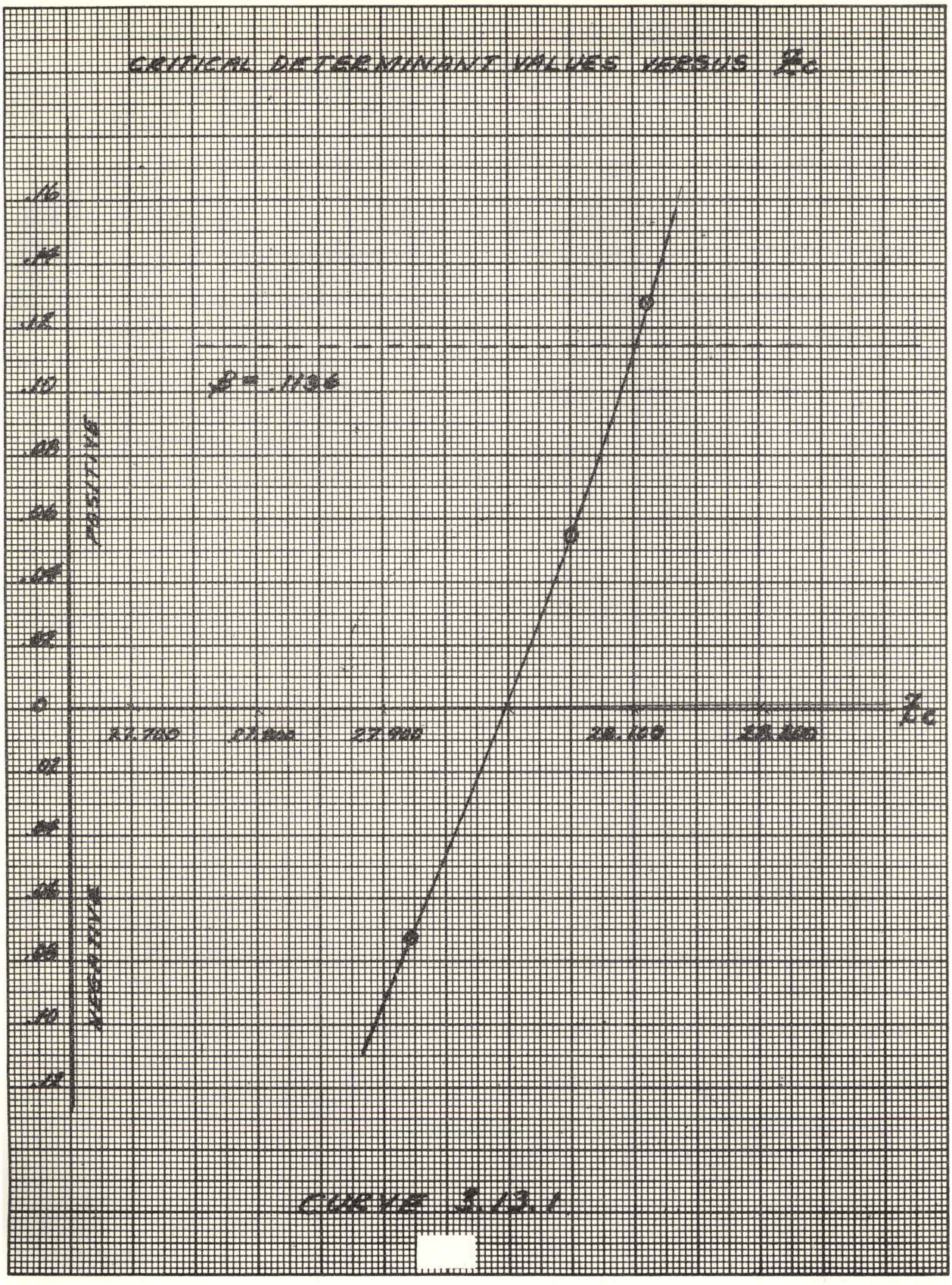

Form Sheet No. 3.14.1

CALCULATION OF DETERMINANT VALUES
(Blanket Values)

a_1 = 105	$L_B^2(C + TH + PA) = 183.04$	$\sigma_s = D_{SB}/D_{SC} = 1.039$
t' = 100	$\mathscr{H}_{FB}^2 = 1/\tau_B = 8.306 \times 10^{-4}$	$\sigma_F = D_{FB}/D_{FC} = 1.018$
τ_B = 1204	$(1 + X_B + Y_B) = 1.01302$	$D_{SB}/D_{FB}\mathscr{H}_{FB}^2 = 849.3$

Z_B	Case: 1 .2551	Case: 2	Case: 3	Case: 4
From Curve				
B_{1B} =	.04561			
B_{rB} =	.08611			
B_{1B}^2 =	.00208			
B_{rB}^2 =	.007414			
$B_{1B}\, a_1$ =	4.789			
$B_{1B}\, t'$ =	4.561			
$B_{rB}\, a_1$ =	9.042			
$B_{rB}\, t'$ =	8 .611			
$B_{SB}^2 = \dfrac{Z_B(1 + X_B + Y_B) + 1}{L_B^2(C + PA + TH)}$ =	.006857			
$(B_{SB}^2 - B_{1B}^2)$ =	.004777			
$\alpha_{1B} = \dfrac{D_{SB}}{D_{FB}\mathscr{H}_{FB}^2}(B_{SB}^2 - B_{1B}^2)$ =	4.057			
$(B_{SB}^2 - B_{rB}^2)$ =	-.0005573			
$\alpha_{rB} = \dfrac{D_{SB}}{D_{FB}\mathscr{H}_{FB}^2}(B_{SB}^2 - B_{rB}^2)$ =	-.4733			
* Coth $B_{1B}\, t'$	1			
$U_{1B} = -B_{1B} a_1 \text{ Coth } B_{1B} t' - 1$ =	-5.789			
* Coth $B_{rB}\, t'$	1			
$U_{rB} = -B_{rB}\, a_1 \text{ coth } B_{rB} t' - 1$ =	-10.04			
$\sigma_S\, U_{1B}$ =	-6.019			
$\sigma_S\, U_{rB}$ =	-10.44			
$\sigma_S(U_{rB} - U_{1B})$ =	-4.421			
$\sigma_F\, \alpha_{1B}\, U_{1B}$ =	-23.92			
$\sigma_F\, \alpha_{rB}\, U_{rB}$ =	4.841			

* Coth (4) = 1

Form Sheet 3.14.2

SOLUTION OF CRITICAL DETERMINANT

Sheet 1 of 2

System Data:

a_1 = 105 $\quad L_c^2$ Graphite = 16220

τ_c = 958 $\quad (1 + X_c + Y_c)$ =

$B_{FC}^2 = 1/\tau_c$ = .001044 $\quad D_{SC}/D_{FC}\, B_{FC}^2$ = 662.1

Z_c	Case: 1 28.10	Case: 2	Case: 3	Case: 4
From Curve				
B_{1c} =	.02552			
B_{rc} =	.05941			
B_{1c}^2 =	6.514×10^{-4}			
B_{rc}^2 =	35.29×10^{-4}			
$B_{1c}\, a_1$ =	2.680			
$B_{rc}\, a_1$ =	6.238			
$B_{SC}^2 = \dfrac{Z_c\,(1+X_c+Y_c) + 1}{L_c^2 \text{ graphite}}$ =				
$(B_{SC}^2 + B_{1C}^2)$ =				
$\alpha_{1C} = \dfrac{D_{SC}}{D_{FC}\, B_{FC}^2}\,(B_{SC}^2 + B_{1C}^2)$	= 1.645			
$(B_{SC}^2 - B_{FC}^2)$ =				
$\alpha_{rc} = \dfrac{D_{SC}}{D_{FC} B_{FC}^2}\,(B_{SC}^2 - B_{rC}^2)$ =	-1.122			
Cot $B_{1C}\, a_1$ =	-2.009			
$U_{1C} = B_{1C} a_1$ Cot $B_{1C} a_1$ =	-6.386			
Coth $B_{rC}\, a_1$ =	1			
$U_{rC} = B_{rC} a_1$ coth $B_{rC} a_1 - 1$ =	5.238			
$\alpha_{1C}\, U_{1C}$ =	-10.51			
$\alpha_{rC}\, U_{rC}$ =	-5.879			
Determinant Values:				
$a = \alpha_{1C} - \alpha_{1B}$ =	-2.411			
$b = \alpha_{rC} - \alpha_{rB}$ =	-.6491			
$C = \alpha_{rB} - \alpha_{1B}$ =	-4.530			
$d = U_{1C} - \sigma_S\, U_{1B}$ =	-.3676			
$e = U_{rC} - \sigma_S\, U_{rB}$ =	15.68			
$f = \sigma_S\,(U_{rB} - U_{1B})$ =	-4.421			

Form Sheet 3.14.2

SOLUTION OF CRITICAL DETERMINANT

Sheet 2 of 2

$g = a_{1C}U_{1C} - \sigma_F a_{1B}U_{1B} =$	13.41			
$h = a_{rC}U_{rC} - \sigma_F a_{rB}U_{rB} =$	-10.72			
$i = \sigma_F a_{rB}U_{rB} - \sigma_F a_{1B}U_{1B} =$	28.76			
Determinant Solution:				
bi =	-18.67			
Ch =	48.56			
Y = bi - Ch =	-67.23			
Cg =	-60.77			
ai =	-69.36			
Z = cg - ai =	8.594			
ah =	25.85			
bg =	-8.707			
T = ah - bg =	34.56			
dy =	24.72			
eZ =	134.7			
fT =	-152.8			
dY + eZ + fT =	6.664			
Y + Z =	-58.64			
$\beta = -\left\{\frac{dY + eZ + FT}{Y + Z}\right\} =$	.1141			
Core Shell Data:				
Σa =	.0001617			
t =	10			
$\beta = \frac{a_1 \Sigma a t}{D_{SC}} =$	.1141			

Form Sheet 3.15.1

NEUTRON BALANCE

Sheet 1 of 2

Z_C = 28.10

$\Sigma_{graphite}$ = 9.180×10^{-5}

$\Sigma_a(U) = Z_C \Sigma_{graphite}$ = .002577

$\Sigma_a(H1) = X_C \Sigma_a(U)$ = 7.81×10^{-6}

$\Sigma_a(FP) = Y_C \Sigma_a(U)$ = 5.155×10^{-5}

$S_{1C} = \text{Sin } B_{1C} a_1$ = .4455

$S_{rC} = \text{Sinh } B_{rC} a_1$ = 255.8

$C_{1C} = U_{1C} S_{1C}$ = -2.845

$C_{rC} = U_{rC} S_{rC}$ = 1339

$m = \alpha_{1C} - \alpha_{rB}$ = 2.119

$m = \alpha_{1C} U_{1C} - \sigma_F \alpha_{rB} U_{rB}$ = -15.35

$r = \alpha_{rB} - \alpha_{rC}$ = 5.179

$s = \sigma_F \alpha_{1B} U_{1B} - \alpha_{rC} U_{rC}$ = -18.04

$M = mh - bn$ = -32.67

S_{1C}/Y = -.006625 $\quad A = 1$

$C = \frac{S_{1C}}{Y} \frac{Z}{S_{rC}}$ = -2.226×10^{-4}

Z_B =

$\Sigma_{graphite}$ = 8.42×10^{-5}

$\Sigma_a(TH)$ = 835.5×10^{-5}

$\Sigma_a(PA) = W_B \Sigma_a(TH)$ = 1.253×10^{-5}

Sum ' = 845.1×10^{-5}

$\Sigma_a(W) = Z_B$ ' = .00319

$\Sigma_a(H1) = X_B \Sigma_a(U)$ = 6.448×10^{-6}

$\Sigma_a(FP) = Y_B \Sigma_a(U)$ = 2.128×10^{-5}

$S_{1B} = \text{Sinh } B_{1B} t'$ = 47.83

$S_{rB} = \text{Sinh } B_{rB} t'$ = 2745

$C_{1B} = U_{1B} S_{1B}$ = -276.9

$C_{rB} = U_{rB} S_{rB}$ = -27575

$N = aS - rg$ = -25.96

$G = \frac{S_{1C}}{Y} \frac{N}{S_{rB}}$ = 6.264×10^{-5}

$E = \frac{S_{1C}}{Y} \frac{M}{S_{1B}}$ = 4.525×10^{-3}

Slow Flux Check

$S_{rC} C - S_{1B} E - S_{rB} G$ = -.4454 $\qquad -S_{1C}$ = -.4454

Slow Current Check

$(C_{rC} + \beta S_{rC}) C - \sigma_S (C_{1B} E + C_{rB} G)$ = 2.794

$-C_{1C} - \beta S_{1C}$ = 2.794

$F_{SC} = \frac{1}{4\pi} \int \varphi_{SC} \, dV = -\frac{A}{B_{1C}^2} C_{1C} + \frac{C}{B_{rC}^2} C_{rC}$ = 4282

$F_{SC} = \frac{1}{4\pi} \int \varphi_{FC} \, dV = -\alpha_{1C} \frac{A}{B_{1C}^2} C_{1C} + \alpha_{rC} \frac{C}{B_{rC}^2} C_{rC}$ = 7280

$F_{SB} = \frac{1}{4\pi} \int \varphi_{SB} \, dV = -\frac{E}{B_{1B}^2} (B_{1B} a_2 + C_{1B}) - \frac{G}{B_{rB}^2} (B_{rB} a_2 + C_{rB})$ = 814.9

$F_{FB} = \frac{1}{4\pi} \int \varphi_{FB} \, dV = -\alpha_{1B} E \frac{(B_{1B} a_2 + C_{1B})}{B_{1B}^2} - \alpha_{rB} G \frac{(B_{rB} a_2 + C_{rB})}{B_{rB}^2}$ = 2251

$\frac{F_{FC}}{F_{SC}}$ = 1.700	$\frac{F_{SB}}{F_{SC}}$ = .1903	$\frac{F_{FB}}{F_{SC}}$ = .5257

Form Sheet No. 3.15.1

NEUTRON BALANCE

Sheet 2 of 2

Absorption in Core: In fuel isotope = F_{SC}(Mac.Abs.Tot.)= 11.04	In Moderator = .3931 In Poisons = .2208 In Higher Isotopes = .03345
Absorption in Blanket In Thorium (Fast) = $F_{FB\ rB}$ = 8.923 (Slow) = F_{SB}(Mac.Abs.Tot.) = 6.809 Total = 15.73	In Moderator = = .06862 In (PA) = .01021 In (23) = 1.734 In Poisons = .01734 In Higher Isotopes = .005255

Absorption in Shell = $(S_{1C} + S_{rC}\ C)\ \beta\ D_{SC}$ = .06569

Leakage:

E_S = 2.13 D_{sB} = 3.295 E_f = 2.13 D_{fB} = 4.671

$B_{1B}\ E_S$ = .1503	Sinh $B_{1B}\ E_S$ = .1508	E Sinh $B_{1B}\ E_S$ = 6.826×10^{-4}
$B_{rB}\ E_S$ = .2837	Sinh $B_{rB}\ E_S$ = .2876	G Sinh $B_{rB}\ E_S$ = 1.801×10^{-5}
$B_{rB}\ E_f$ = .4022	Sinh $B_{rB}\ E_f$ = .4132	α_{rB} G Sinh $B_{rB}\ E_f$ = -1.225×10^{-5}
$B_{1B}\ E_f$ = .2130	Sinh $B_{1B}\ E_f$ = .2147	α_{1B} E Sinh $B_{1B} E_f$ = 3.941×10^{-3}

Slow Leakage = 1/2 a_2 [E Sinh $B_{1B}\ E_S$ + G Sinh $B_{rB}\ E_S$] = .06812

Fast Leakage = 1/2 a_2 [α_{rB} G Sinh $B_{rB}\ E_f$ + α_{1B} E Sinh $B_{1B}\ E_f$] = .4027

Leakage (Total) = .4709

NEUTRON BALANCE:

Core:	Fuel Isotope	=	1.0000000	Normalizing Factor
	Moderator	=	.035620	.0906
	Higher Isotopes	=	.003029	Check
	Poisons	=	.019990	2.33(1.157) = 2.696
Blanket:	Thorium	=	1.4252	
	U-233	=	.1571	Net 23 Production
	Protactinium	=	.0009253	.2671
	Moderator	=	.006216	
	Higher Isotopes	=	.0004761	
	Poisons	=	.001571	Breeding Gain
Shell:			.005952	.2309
Leakage:			.04266	
Total			2.6987	

3.2.4 Modification of The Standard Two-Group Method To Incorporate The Effect Of Thorium Resonance Absorption

The notation employed by Glasstone and Edlund (10) in "Elements of Nuclear Reactor Theory", Part III, will be used to facilitate comparisons. The thorium resonance effects directly only the fast and slow blanket fluxes hence only the following two equations need be considered.

$$D_{1R} \nabla^2 \phi_{1R} - \Sigma_{1R} \phi_{1R} - \Sigma_{RR} \phi_{1R} = 0 \qquad (1)$$

$$D_{2R} \nabla^2 \phi_{2R} - \Sigma_{2R} \phi_{2R} + \Sigma_{1R} \phi_{1R} = 0 \qquad (2)$$

Σ_{RR} is the macroscopic resonance absorption cross section of thorium as calculated from experimental equations reported in ORNL CF- 51-10-110. Dividing equation (1) by D_{1R} and combining the last two terms.

$$\nabla^2 \phi_{1R} - \left(\frac{\Sigma_{1R} + \Sigma_{RR}}{D_{1R}} \right) \phi_{1R} = 0 \qquad (3)$$

Define $\frac{\Sigma_{1R} + \Sigma_{RR}}{D_{1R}} \equiv \mathcal{H}_{1R}^2$.

This differs from the usual definition by the addition of $\frac{\Sigma_{RR}}{D_{1R}}$. The equation becomes

$$\nabla^2 \phi_{1R} - \mathcal{H}_{1R}^2 \phi_{1R} = 0 \qquad (4)$$

The solutions of this equation for a spherical system are

$$\phi_{1R} = \frac{P \sinh \mathcal{H}_{1R} r}{r} + \frac{Q \cosh \mathcal{H}_{1R} r}{r}$$

Upon applying the boundary condition that the flux must vanish at the extrapolated boundary, a_2, the equation reduces to:

$$\phi_{1R} = \frac{F \sinh \mathcal{H}_{1R} (a_2 - r)}{r}$$

Dividing equation (2) by D_{2R}

$$\nabla^2 \phi_{2R} - \frac{\Sigma_{2R}}{D_{2R}} \phi_{2R} - \frac{\Sigma_{1R}}{D_{2R}} \phi_{1R} = 0 \qquad (5)$$

Define: $\frac{\Sigma_{2R}}{D_{2R}} \equiv \mathcal{H}_{2R}^2$

The solutions of the homogeneous part of this equation are:

$$\phi_{2R} = \frac{P' \sinh \mathcal{H}_{2R} r}{r} + \frac{Q' \cosh \mathcal{H}_{2R} r}{r}$$

Applying the same boundary condition as above

$$\phi_{2R} = \frac{G' \sinh \mathcal{H}_{2R} (a_2 - r)}{r} .$$

The solution of the inhomogeneous part of equation (5) is merely ϕ_{1R} with some constant of proportionality, S_3. The complete solutions then are:

$$\phi_{2R} = \frac{G \sinh \mathcal{H}_{2R} (a_2 - r)}{r} + \frac{S_3 F \operatorname{Sinh} \mathcal{H}_{1R} (a_2 - r)}{r}$$

S_3 may be determined by substituting the inhomogeneous solution, $S_3 F \frac{\operatorname{Sinh} \mathcal{H}_{1R} (a_2 - r)}{r} = S_3 \phi_{1R}$, into equation (5)

$$S_3 \nabla^2 \phi_{1R} - S_3 \mathcal{H}_{2R}^2 \phi_{1R} + \frac{\Sigma_{1R}}{D_{2R}} \phi_{1R} = 0 .$$

But $\nabla^2 \phi_{1R} = \mathcal{H}_{1R}^2$ by equation (4).

Hence, $S_3 \mathcal{H}_{1R}^2 \phi_{1R} - S_3 \mathcal{H}_{2R}^2 \phi_{1R} + \frac{\Sigma_{1R}}{D_{2R}} \phi_{1R} = 0$

$$S_3 = \frac{\Sigma_{1R}}{D_{2R}} \left(\frac{1}{\mathcal{H}_{2R}^2 - \mathcal{H}_{1R}^2} \right) .$$

The only difference between this coupling coefficient and the usual one is the value of $\mathcal{H}_{1R}^2$ which is greater.

3.3.1 Fission Product Poisoning

All the fission products produced have a finite absorption cross section for neutrons. Schuman (1) has tabulated the yields and cross sections of a limited number of fission products and the effect of each on neutron economy. Stoughton (2) has lumped all the fission products, formed during fission of U-235, into three groups, using an average cross section for each group:

Group	Yield	Cross Section (Barns)	
1	1.5 %	50,000	
2	158.5 %	50	(about 100°C)
3	40 %	—	(Gases)

It is assumed that group 3, consisting of those elements which are gases at normal pressures and temperatures is removed from the core and causes only a small amount of poisoning.

In the present analysis, Stoughton's estimate was assumed to hold for U-233 and for the fluidized solids system. Data by Smith and Young (1') on the diffusion of barium and strontium out of graphite impregnated with uranium indicates that many of the group 1 and 2 elements would also be removed by the gas stream at the 2000° F operating temperatures. However, in order to obtain a conservative estimate of the poisoning, all members of each of group 1 and 2 were assumed to remain in the fuel until removed in processing. It wasfurther assumed that the 50,000 barns value for group 1 would hold even at 2000° F but that the cross section of group 2 follows the 1/v variation and becomes approximately 25 barns in the 1500-2000° F range. Elements in group 1 are assumed to fall into g roup 2 after neutron capture; group 2 elements remain in the group 2 even after absorption of one or more neutrons and are removed only in chemical processing.

(1) KAPL-634, R. P. Schuman
(2) R. W. Stoughton - Lecture on 12-28-51
(1') C. A. Smith andC. T. Young- NAA-SR-72

The differential equation for the buildup of these fission products and the equivalent poisoning are:

1. $\frac{dN_1}{dt} = Y_1 \Sigma_f (23) \phi V_R - c N_1 - \sigma_1 N_1 \phi V_R$

2. $\frac{dN_2}{dt} = Y_2 \Sigma_f (23) \phi V_R - c N_2 + \sigma_1 N_1 \phi V_R$

where: Subscript 1 and 2 refers to group 1 and 2

c = processing rate = $\frac{\text{vol. processed/sec}}{\text{total* fuel-solids volume}}$

V_R = Yield of fission product

*Total volume includes material in core plus heat exchanger plus connecting transfer lines.

From the preceding equation one gets:

3. $N_1 = \frac{Y_1 \Sigma_f(23) \phi V_R}{c + \sigma_1 \phi V_R} \left\{ 1 - e^{-(c+\sigma_1 \phi R) t} \right\}$

4. $\frac{\Sigma(P_1 1)}{\Sigma_a(23)} = Y_1 \left(\frac{\Sigma_c(23)}{\Sigma_a(23)} \right) V_R \left(\frac{\sigma_1 \phi V_R}{c + \sigma_1 V_R} \right) \left\{ 1 - e^{-(c+\sigma_1 \phi V_R) t} \right\}$

5. $N_2 \approx (Y_1 + Y_2) \frac{\Sigma_f(23) \phi V_R}{c} (1 - e^{-ct})$

6. $\frac{\Sigma(P_1 2)}{\Sigma_a(23)} \approx (Y_1 + Y_2) \frac{\Sigma_c(23)}{\Sigma_a(23)} \left(\frac{\sigma_2 \phi V_R}{c} \right) (1 - e^{-ct})$

Then total poisoning, $\Sigma(P)/\Sigma_a(23)$, = $\frac{\Sigma(P,1)}{\Sigma_a(23)} + \frac{\Sigma(P_1 2)}{\Sigma_a(23)}$.

For the purposes of calculations, V_R for the core was taken as equal to 4. This represents, approximately, a median for the several designs proposed in the engineering studies. The blanket material is not circulated through external vessels and V_R for the blanket thus equals unity.

Using the above basis and equations, values were obtained for poisoning due to fission products, as a function of flux, processing rate, and time of

operation. Tables VIII 3-3, VIII 3-4 and Figure VIII 3-2 show the calculated poisoning effects in the core and Table VIII 3-6 shows the effects in the blanket.

The poisoning effect for the hypothetical case of no circulation of the fuel-solids material through external units (i.e., for V_R = 1 for the core) and for the apparently highly conservative value of 50 barns cross section for group 2 at 2000° F are shown in Table VIII 3-3. This latter set of values showed a poisoning about 5 times that of the preceeding analysis.

TABLE VIII 3 - 2

SOME FISSION PRODUCTS YIELDS AND CROSS SECTIONS

(From KAPL 634 by R. P. Schuman)

Mass	Important Element	σ (barns)	Yield U-233	U-235	Less Important Elements
83	Kr	205	.77	.58	
95	Mo	13.4	5.7	6.0	Zr, Nb
103	Rh	149	.85	3.7	Ru
108	Pd	11	.09	.09	
109	Ag	99	.047	.028	Pd
113	Cd	20,000	.015	.014	
115	In	197	.017	.011	Cd
127	I	6.3	.17	.20	Te
129	I	15	.7	1.0	Te
131	I	600	2.7	2.8	
"	Xe	120	2.7	2.8	
133	Cs	26	5.6	6.29	Xe
135	Xe	2×10^6	6.7	5.9	
139	La	8.4	6.4	(1.9)	
141	Pr	13	5.4	6.3	Ce
143	Nd	240	4.0	5.7	Ce,Pr
147	Pm	60	1.2	2.6	Nd
149	Sm	65,000	.55	1.4	Pm
151	Sm	2,000	.24	.5	
152	Sm	135	.14	.3	
153	Eu	240	.078	.15	Sm
155	Eu	7,900	.03	.031	
157	Gd	240,000	.009	.015	Eu

TABLE VIII 3-3

EQUILIBRIUM VALUES FOR FISSION PRODUCTS POISONING IN CORE

Basis:
Group 1 --- 1.5% yield --- 50,000 barns
Group 2 --- 160% yield ---- 25 barns(2000°F)
Total volume fuel to core volume --- 4

Flux	10^{13}			10^{14}			5×10^{14}			10^{15}		
	$\frac{\Sigma P,1}{\Sigma 23}$	$\frac{\Sigma P,2}{\Sigma 23}$	$\frac{\Sigma P}{\Sigma 23}$	$\frac{\Sigma P,1}{\Sigma 23}$	$\frac{\Sigma P,2}{\Sigma 23}$	$\frac{\Sigma P}{\Sigma 23}$	$\frac{\Sigma P,1}{\Sigma 23}$	$\frac{\Sigma P,2}{\Sigma 23}$	$\frac{\Sigma P}{\Sigma 23}$	$\frac{\Sigma P,1}{\Sigma 23}$	$\frac{\Sigma P,2}{\Sigma 23}$	$\frac{\Sigma P}{\Sigma 23}$
10 day process cycle	.0013	.0001	.0014	.0070	.0008	.0028	.0115	.0040	.0155	.0124	.0080	.0204
30 day process cycle	.0033	.0002	.0035	.0104	.0023	.0127	.0128	.0117	.0245	.0132	.0234	.0366
100 day process cycle	.0070	.0008	.0078	.0124	.0078	.0202	.0134	.0390	.0524	.0135	.0780	.0915
1 year process cycle	.0109	.0028	.0137	.0133	.0284	.0417	.0136	.1420	.1556	.0136	.2840	.2976

TABLE VIII 3 - 4

MAXIMUM EQUILIBRIUM VALUES FOR FISSION PRODUCTS POISONING

Basis: same as Table except
$\sigma_a = 50$
$V_R = 1$

Flux	10^{12}	10^{13}	10^{14}	10^{15}
$\Sigma P/\Sigma 23$ for:				
15 day process cycle	.0010	.0065	.0217	.110
30 day process cycle	.0018	.0097	.032	.208
60 day process cycle	.0032	.0139	.052	.40
100 day process cycle	.0048	.0177	.078	.65

TABLE VIII 3 - 5

FISSION PRODUCTS POISONING BUILDUP IN CORE

Basis:
Group 1 --- 1.5% Yield --- σ = 50,000 b.
Group 2 --- 160% Yield --- σ = 25 b (1)
Total Volume active fuel to core volume --- 4
Processing Time Cycle ---------- 30 days
Fissionable fuel ------------ U-233

Ave. flux,	10^{13}			10^{14}			5×10^{14}			10^{15}		
	$\Sigma_{P,1}/\Sigma_{23}$	$\Sigma_{P,2}/\Sigma_{23}$	Σ_P/Σ_{23} (2)	$\Sigma_{P,1}/\Sigma_{23}$	$\Sigma_{P,2}/\Sigma_{23}$	Σ_P/Σ_{23}	$\Sigma_{P,1}/\Sigma_{23}$	$\Sigma_{P,2}/\Sigma_{23}$	Σ_P/Σ_{23}	$\Sigma_{P,1}/\Sigma_{23}$	$\Sigma_{P,2}/\Sigma_{23}$	Σ_P/Σ_{23}
1 day after startup	.0002	.0001	..0003	.0014	.0001	.0015	.0056	.0004	.0060	.0089	.0008	.0097
30 days after startup	.0021	.0001	.0022	.0103	.0015	.0118	.0128	.0075	.0203	.0132	.0150	.0282
100 days after startup	.0033	.0002	.0035	.0104	.0022	.0126	.0128	.0113	.0241	.0132	.0226	.0358
1 year after startup			.0035	.		.0127			.0245			.0366
Equilibrium values	.0033	.0002	.0035	.0104	.0023	.0127	.0128	.0117	.0245	.0132	.0234	.0366

(1) Assuming approximately 50 b at 100°F, 25 b, @ 2000° F

(2) Σ_P = sum of $\Sigma_{P,1}$ and $\Sigma_{P,2}$

TABLE VIII 3 - 6

EQUILIBRIUM VALUES FOR FISSION PRODUCTS POISONING IN BLANKET

Basis:

Group 1 ---- 1.5% yield - 50,000 barns
Group 2 ---160 % yield -- 25 barns (1500°F)
Equilibrium values.

Flux		10^{12}	3×10^{12}	10^{13}	10^{14}
Σ_p/Σ_{23}^a	for 10 day cycle	.0006	.0017	.0044	.0141
	30 day cycle	.0017	.0041	.0085	.0220
	60 day cycle	.0030	.0065	.0117	.0320
	100 day cycle	.0044	.0086	.0141	.0447
	365 day cycle	.0095	.0150	.0243	.1285
	1000 day cycle	.0141	.0231	.0447	.3180

Drawing # 22895

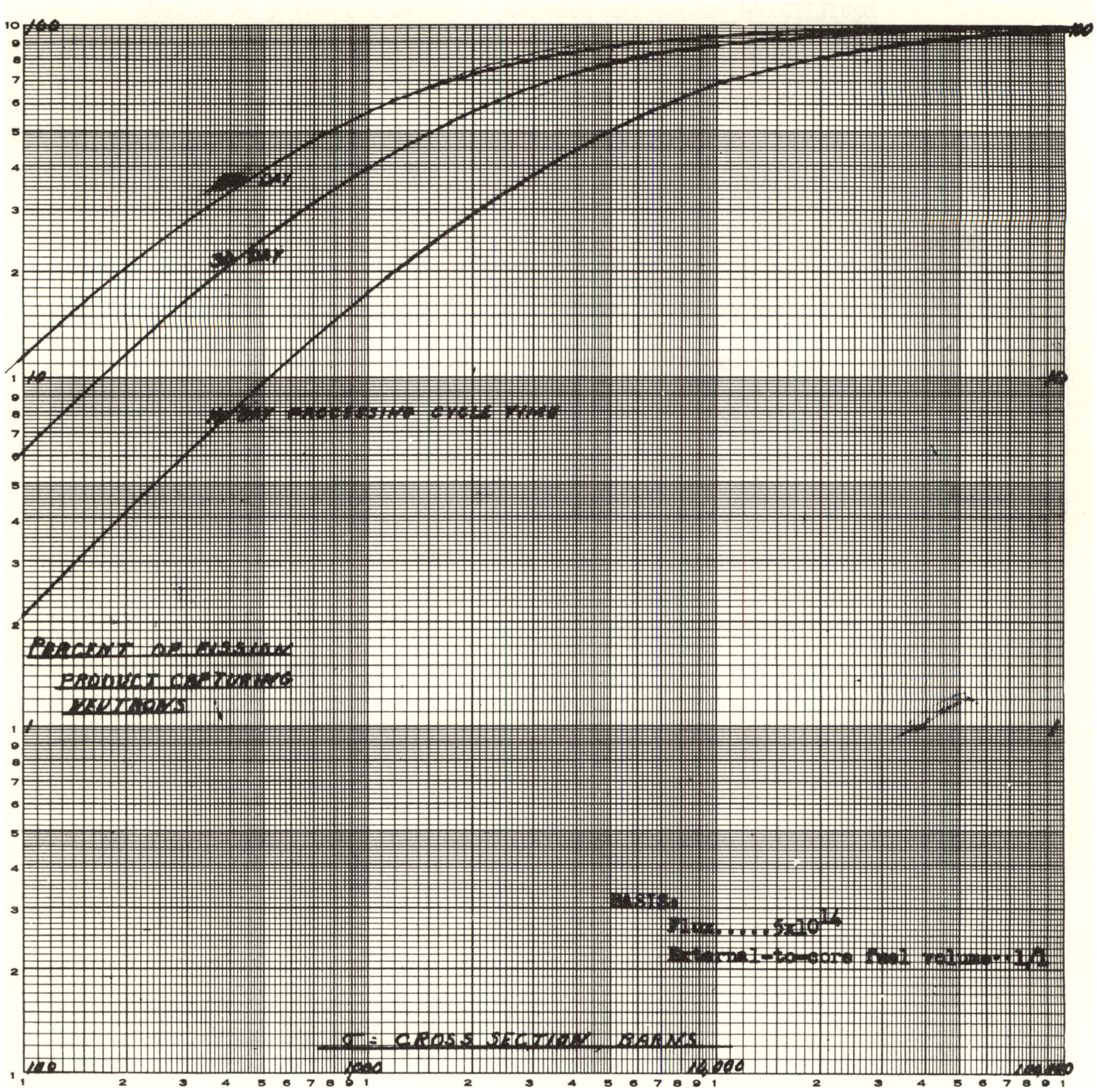

FIGURE VIII 3-2

PERCENT OF FISSION PRODUCT CAPTURING NEUTRONS: FUNCTION OF CROSS SECTION AND PROCESSING RATE

3.3.2 Buildup of Higher Uranium Isotopes In Blanket

The higher isotope buildup is usually expressed either as the N/N_{23} ratio or as the $\Sigma / \Sigma_{a(23)}$ ratio. The latter will be used in this report.

The differential equation for this buildup are:

for U-234: $$\frac{d N_{24}}{dt} = N_{23}\sigma^{c}_{23}\phi + N_{13}\sigma_{13}\phi - N_{24}\sigma_{24}\phi - N_{24}\, c$$

for U-235: $$\frac{d N_{25}}{dt} = N_{24}\sigma_{24}\phi - N_{25}\sigma^{a}_{25}\phi - N_{25}\, c$$

for U-236: $$\frac{d N_{26}}{dt} = N_{25}\sigma^{c}_{25}\phi - N_{26}\sigma_{26}\phi - N_{26}\, c$$

where:

ϕ = average flux (in the blanket)

t = time seconds

N = atoms per cc.

c = processing rate, equals fraction of blanket volume processed externally(for uranium removal) per second.

These equations can be readily integrated but one must choose the appropriate boundary conditions. In a breeder of the type proposed in this report, this could be any one of the following:

(1) No U-233 or U-235 blanket at start of operation. No processing the blanket until the desired concentration of U-233 has been produced.

(2) Same as (1) but processing may start at any desired time.

(3) A predetermined amount of U-233 is charged to blanket at start of operation. This may or may not be the same as the final operating concentration.

(4) A predetermined amount of U-235 is charged to blanket at start of operation.

In each case, the total poisoning effect is very small and is caused almost entirely by the first isotope above the fissionable isotope present.

Assuming that U-233 is charged to the system before start of operation (assumption # 3) the integrated equations become :

$$\Sigma_{(24)}/\Sigma_{a(23)} = \frac{\Sigma_c(23)}{\Sigma_a(23)} \frac{(\sigma_{24}\phi)}{(c+\sigma_{24}\phi)} \left(1 - e^{-(c+\sigma_{24}\phi)t}\right)$$

$$\Sigma_{a(25)}/\Sigma_a(23) \approx \frac{\Sigma_c(23)}{\Sigma_a(23)} \left(\frac{\sigma^a_{25}\phi}{c+\sigma^a_{25}\phi}\right)\left(\frac{\sigma_{24}\phi}{c+\sigma_{24}\phi}\right)\left(1 - e^{-(c+\sigma_{24}\phi)t}\right)$$

$$\left(1 - e^{-(c+\sigma^a_{25}\phi)t}\right)$$

$$\Sigma_{(26)}/\Sigma_a(23) \approx \frac{\Sigma_c(23)}{\Sigma_a(23)} \left(\frac{\sigma_{24}\phi}{\sigma_{24}\phi+c}\right)\left(\frac{\sigma^c_{25}\phi}{\sigma^a_{25}\phi+c}\right)\left(\frac{\sigma_{26}\phi}{\sigma_{26}\phi+c}\right)$$

$$\times \left[1 - e^{-(\sigma_{24}\phi+c)t}\right]\left[1 - e^{-(\sigma^a_{25}\phi+c)t}\right]\left[1 - e^{-(\sigma_{26}\phi+c)t}\right]$$

In the above equation, the U-234 production from the protactinium was omitted since this would be a small part of the total when the U-233 concentration is high. The maximum poisoning occurs at equilibrium and becomes as follows:

	$\phi = 10^{12}$		$\phi = 10^{13}$	
Processing cycle time (days	100	365	100	365
$\Sigma_{(24)}/\Sigma_a(23)$	.000292	.00106	.00292*	.0106
$\Sigma_{a(25)}/\Sigma_a(23)$	8.4×10^{-7}		8.4×10^{-6}	
$\Sigma_{(26)}/\Sigma_a(23)$	7.5×10^{-11}		7.5×10^{-10}	

*The protactinium contribution would have been .00006 or approximately 2% of total.

At small values of t, the above approximate equations for 25 and 26 give values somewhat larger than the true values. Since even these approximate values are so small, it is unnecessary to use any greater precision. The net poisoning effect of the three isotopes, expressed as $\Sigma_{(H1)}/\Sigma_a(23)$, is shown in Figure as a function of time.

3.3.3 Protactinium Losses

The differential equation describing the material balance for protactinium is:

$$\frac{dN}{dt} = \Sigma(TH)\ \phi - \lambda N - \sigma_{13}\ \phi N - c N$$

where: λ = decay constant --- sec^{-1}

c = removal rate - fraction per sec.

At equilibrium one gets:

1. Fraction decaying to 23 : $\dfrac{\lambda}{\lambda + \sigma_{13}\phi + c} = F_\lambda$

2. Fraction removed to processing plant: $\dfrac{c}{\lambda + \sigma_{13}\phi + c} = F'_c$

3. Fraction lost to neutron capture $\dfrac{\sigma_{13}}{\lambda + \sigma_{13}\ \phi + c} = F$

Using the constants $\lambda = 2.94 \times 10^{-7}\ sec^{-1}$, $\sigma_{13} = 17 \times 10^{-24}\ cm^2$, and $\phi = 10^{13}$, one gets the following results:

	30 day ($c = 3.87 \times 10^{-7}$)	100 day ($c = 1.16 \times 10^{-7}$)	1 year cycle ($c = .318 \times 10^{-7}$)
F_λ	.4318	.7166	.902
F_c	.568	.283	.0975
F_σ (loss)	.00025	.00042	.00052
Similarly at $\phi = 4 \times 10^{12}$			
F_σ (loss)	.00010	.00016	.00021

The chemical processing losses are expected to be small, presumably less than 0.1% of the Pa still present. Since this is the same order of magnitude as losses of U-233 during processing, one does not gain in yield by holding the blanket effluent material over a long cooling period. Thus this cooling period can be dictated entirely by the activity of the materials

and whether it is desirable to isolate the Pa from the U-233.

In nuclear calculations, a convenient way of expressing the neutron capture by Pa is through the term $\Sigma(13)/\Sigma(TH)$. From the differential equation:

$$\frac{dN(13)}{dt} = \Sigma_{(TH)}\,\phi - N(13)\,(c + \lambda + \sigma_{13}\,\phi)$$

one gets the solution:

$$\Sigma(13)/\Sigma(TH) = \frac{\sigma_{13}\,\phi}{c + \lambda + \sigma_{13}\phi}\,(1 - e^{-(c+\lambda+\sigma_{13}\phi)t}),$$

From the above equation, one gets the following equilibrium values:

Processing cycle time, days	60	100	365	∞
$\Sigma_{(13}/\Sigma_{(TH)}$ at $\phi = 10^{13}$	.00040	.00047	.00059	.00065
at $\phi = 3 \times 10^{13}$	.0012	.0014	.0018	.0020
at $\phi = 4 \times 10^{12}$	.00016	.00018	.00024	.00026

3.4 CONTROL AND SAFETY

Fine Control:

Material : Thorium Plate (m.p. 1845° C)

Density ρ: 11.2 gm/cm^3

σ_a(thermal) : 7.0 barns

Temperature Factor: 0.52 0

σ_a(1500 °F) = 7.0 x 0.520 = 3.64 barns

$$\Sigma_a = \frac{3.64}{1.128} \times \frac{0.602 \times 11.2}{232} = 0.0945 \text{ cm}^{-1}$$

Calculation of Resonance Absorption by Thorium Plate

σ_S = 12.7 barns

$$* \int \sigma_a \frac{dE}{E} = 8.33\,(12.7)^{0.253} = 8.33\,(1.902) = 15.85$$

$$\Sigma_{RB} = \frac{D_{1R}}{\tau_R \xi_R} \frac{N_{TH}}{\Sigma_S} \int \sigma_a \frac{dE}{E}$$

$$= \frac{\Sigma_{1R}\,\tau_R}{\tau_R\,\xi_R} \frac{N_{TH}}{\Sigma_S} \int \sigma_a \frac{dE}{E} \qquad \text{but} \quad \Sigma_{1R} = \frac{\Sigma_S\,\xi_R}{\ell N \frac{E_o}{E_{TH}}}$$

$$\Sigma_{RB} = \frac{N_{TH}}{\ell n \frac{E_o}{E_{TH}}} \int \sigma_a \frac{dE}{E} = \frac{0.0291 \times 15.85}{\ell n\, 21.56 \times 10^6}$$

$\Sigma_{RB} = 0.0301$

Using the Exponential Intensity Attenuation

$$I = I_o\, e^{-\Sigma_a t}$$

where t = thickness of the absorber, we obtain the plot shown in Figure III 4-2 It can be seen from this graph that a 7.3 cm plate is only 50% effective in cutting thermal neutron intensity and 20% effective in cutting fast neutron intensity.

Determination of The Effectiveness of Such A Plate On The Reactivity Of The Reactor

Using the constants derived in the critical 120 cm system with $k_{eff} = 1$ we obtain the equivalent, simplified relationship

$$k_c\, e^{-B^2 L_c^2} = 1 + L^2 B^2$$

where $\tau_c = 958$

$L^2 = 844.25$

$k_\infty = k_c = 2.15892$

From this transcendental equation a material buckling B_m^2 is derived which satisfies the equation such that $k_{eff} = 1$. This value was found to be $B_m^2 = 4.6052 \times 10^{-4}\ cm^{-2}$. On the other hand the geometrical buckling, for a bare sphere is $B_G^2 = \left(\frac{\pi}{R}\right)^2 = 6.85387 \times 10^{-4}\ cm^{-2}$. Consider now two

* (18)

reactor cores of equal radii with the peculiar properties that one allows only fast neutron leakage the other only thermal neutron leakage. The equations defining these reactors are:

$$k_{eff}\Big)_f = \frac{k_c\, e^{-B^2 G \tau}}{1 + L^2 B_m^2}$$ "all" fast leakage

and

$$k_{eff}\Big)_s = \frac{k_c\, e^{-B_m^2 \tau}}{1 + L^2 B_G^2}$$ "all" slow leakage

from which

$$k_{eff}\Big)_f = 0.90821, \qquad \Delta k = -0.1938$$

$$k_{eff}\Big)_s = 0.87973, \qquad \Delta k = -0.12027.$$

Assuming then that 10% of the surface area of the core is covered by 7.3 cm thorium plate we find.

$$\Delta_{k_s} = (0.5)(0.1)(.12027) = 0.006013$$

$$\Delta_{k_f} = (0.2)(0.1)(.1938) = 0.003818$$

$$\Delta_{k_{total}} = 0.009831 \approx 1\%.$$

The results obtained from this method of calculation of control effectiveness are in fair agreement with experimental data obtained from the HRE wherein a similar method was used in calculating control effectiveness.

Reactivity Temperature Coefficient

We shall assume 1/v dependence of the absorption cross sections of the core materials in the operating range of 20° C to 1093° C.

Then: $\sigma_a = \sigma_{a_o}\sqrt{\frac{T_o}{T}}$ where, in our case $\begin{cases} \sigma_a = \sigma_{a_o} \times 0.462 \text{ in core} \\ \sigma_a = \sigma_{a_o} \times 0.520 \text{ in blanket} \end{cases}$

The σ_s's on the other hand are fairly constant in both core and reflector so that

$$\sigma_s = \sigma_{s_o}\left(\frac{T_o}{T}\right)^x \qquad \text{where} \quad |x| < 0.1$$

Define $\theta \equiv \frac{T}{T_o}$ so $\sigma_s = \sigma_{s_o}\,\theta^{-x}$.

The change in reactivity for small changes in temperature due to variation of cross section only is given by

$$* \left(\frac{\partial \rho}{\partial T}\right)_{\substack{\text{dens.}\\ \text{const.}}} = -\frac{B^2}{K_c T_o} - \left[\left(\frac{1}{3\xi\Sigma_s\Sigma_t}\right)_o \theta^{-1} + (x+\tfrac{1}{2})\,\theta^{x-\frac{1}{2}}\,L_o^2\right].$$

Then at the operating temperature the change in reactivity per °C will be,

$$\left(\frac{\partial \rho}{\partial T}\right)_d = -\frac{B^2}{k_c T_o} - \left[\left(\frac{D_{SC}}{\xi\,\Sigma_s}\right) + \frac{1}{2}\,L_o^2\right]$$

where:

B^2 = material buckling for the critical reactor

$K_c = K_\infty$

$T_o = 2000°\ F = 1093\ °C$

$D_{SC_o} = 1.488$

$\xi = 0.158$

$\Sigma_s = 0.237$

$L_o^2 = 830$

$\theta \cong 1$ and $x = 0$ for small ΔT

α = linear expansion coefficient

$M_o = L_o^2 + \tau_o = 1.780$.

Fixing the microscopic cross section and the buckling but varying the density of the core material yields

*Reactor Theory Pa rt IV.(11)

$$\left(\frac{\partial \rho}{\partial T}\right)_{\sigma_a \sigma_s B^2} = - \frac{6 \alpha B^2 M_o}{K_c} .$$

Finally fixing the macroscopic cross sections and varying the buckling only, yields,

$$\left(\frac{\partial \rho}{\partial T}\right)_{\Sigma_a \Sigma_s} = \frac{2(k-1)}{K} \alpha .$$

Tabulating The Results We Have

$$\left(\frac{\partial \rho}{\partial T}\right)_d = - 7.32 \times 10^{-5} \text{ per } ^\circ C$$

$$\left(\frac{\partial \rho}{\partial T}\right)_{\sigma_a \sigma_s B^2} = - 1.59 \times 10^{-5} \text{ per } ^\circ C$$

$$\left(\frac{\partial \rho}{\partial T}\right)_{\Sigma_a \Sigma_s} = + 0.75 \times 10^{-5} \text{ per } ^\circ C$$

So the total $\frac{\partial \rho}{\partial T} = -8.16 \times 10^{-5}$ per °C

Thus it is seen that the temperature coefficient is rather strongly negative so that the reactor will be stable, tending to hold itself at a constant power level. It should be noted that the decrease in Xenon resonance absorption with increasing temperature has been omitted from these calculations since it is assumed that Xenon will be constantly removed as a gas from the reactor system.

Calculation of Total $\Delta \rho$ over temperature range of 1093° C to 20°C

Method # 1

1093°C $k_{eff} = 1 = \frac{K_c e^{-B_m^2 \tau}}{1 + L^2 B_m^2}$, $B_m^2 = 4.6 \times 10^{-4} \text{ dm}^{-2}$

20° C $\tau = 958 \text{ cm}^2$

$L_o^2 = 16{,}220 \times 0.462 \text{ cm}^2$

$B_m^2 = 4.6 \times 10^{-4} \text{ cm}^{-2}$ (assumed constant)

Thus: $k_{eff} = \frac{1.38879}{1 + (.462)(.38879)} = 1.18$

$\Delta k = 18\%$

Method # 2

In general: $\rho = \frac{k-1}{k} - \frac{B^2}{k} \left[\tau_o - \left\{ \frac{D_{SC}}{\xi_s} \ell n\, \theta \right\} + L_o^2 \right]^{1/2} \theta$

1093° C : $\theta = 4.662$

$$\rho = \frac{1.159}{2.159} - \frac{4.6 \times 10^{-4}}{2.159} \left\{ 958 - (39.8\, \ell n\, 4.662) + 830 \cdot 4.66 \right\}^{1/2}$$

$\rho = -0.0372$

20° C : $\theta = 1$

$\rho = 0.5368 - .3810$

$\rho = 0.1558$

In going from 1093°C to 20°C therefore

$\Delta \rho = 0.1558 - (-0.0372) = + 0.1930$

or $\Delta k = 19.3\%$

APPENDIX

Criticality of Transfer Lines and Heat Exchanger

Transfer Lines

Infinite cylinder 5' diameter, infinite water reflected, 60% voids, system at room temperature.

Core Constants:

$R = 2.5' = 76.2$ cms

$\tau_c = 2{,}156\ cm^2$

$D_{1c} = 3.05$ cm

$D_{2c} = 2.234$ cm

$\Sigma_{a_{Mod}} = 3.31 \times 10^{-4} \times 0.4 = 1.324 \times 10^{-4}$ cms

$$L^2_{Mod} = \frac{1}{3\Sigma_a \Sigma_t} = \frac{1 \times 10^4}{3 \times 1.324 \times 0.1492} = 16{,}850\ cm^2$$

Reflector Constants: (H_2O)

$L_R^2 = 7.13\ cm^2$

$\tau_R = 33\ cm^2$

$D^2_R = 0.135$ cm

$D_{1R} = 0.9$ cm (ORNL CF 49-3-90)

Welton Equations Used in Calculation

$$\frac{x_1 J_1(x_1)}{J_o(x_1)} = \frac{D_{1R}}{D_{1c}} \frac{R}{\sqrt{\tau_R}} \frac{K_1(R/\sqrt{\tau_c})}{K_o(R/\sqrt{\tau_R})}$$

$$\frac{x_2 J_1(x_2)}{J_o(x_2)} = \frac{D_{2R}}{D_{2c}} \frac{R}{L_c} \frac{K_1(R/L_R)}{K_o(R/L_R)}$$

Solving for x_1 and x_2 we get

$x_1 = 1.9$, $x_2 = 1.55$

Then with $Z = \frac{\sum u}{\sum_{Mod}}$,

$$Z = \frac{1}{R^2} \left\{ \frac{(R^2 + x_1^2 \tau_c)(R^2 + x_2^2 \tau_c)}{\eta \left(R^2 + \frac{L_R^2 (x_1^2 - x_2^2) \tau_c}{L_R^2 - \tau_R} \right) - (R^2 + x_1^2 \tau_c)} \right\} .$$

The numerator will always be positive, so that if the denominator is negative we most certainly have a subcritical system (i.e., the denominator must pass through zero before z can become positive). Anticipating that the system is sub-critical we solve the denominator,

$$\eta \left(R^2 + L_R^2 \frac{(x_1^2 - x_2^2) \tau_c}{L_R^2 - \tau_R} \right) - R^2 + x_1^2 \tau_c \quad .$$

and find that it is negative,

Heat Exchanger:

Assumed equivalent to a 3' radius sphere upon bed collapse to 60% voids. Worst spacing of tubing considered so that only 30% of total volume is steel. Also considered as infinitely water reflected, with entire system at room temperature.

Core Constants:

R = 3' = 91.5 cms.

τ_c = 2.56

D_{1c} = 3.05

D_{2c} = 2.234

347 Stainless M-B σ's/gram S.S. *

Iron	= 1.69 x 10^{-5}	cm^2
Chromium	= 1.36 x 10^{-5}	cm^2
Nickel	= 2.00 x 10^{-5}	cm^2
Manganese	= 2.48 x 10^{-5}	cm^2
Total	38 7.7 x 10^{-5}	cm^2/gram S.S.

*(37)

The density of stainless steel in the heat exchanger is 0.268 g/cm^3.

$$\overline{\Sigma_a}\,(S.S.) = 38.8 \times 10^{-4} \times 0.268 \quad g/cm^3$$

so $$\overline{\Sigma_a}(\text{Total Mod.}) = \Sigma_a\,(\text{Graphite}) + \Sigma_a(S.S.) = 10.53 \times 10^{-4}\ cm^{-1}$$

$$L^2_{o_{Mod.}} = 2{,}120\ cm^2.$$

Reflector constant are identical with those of the transfer lines.

Welton Equations Used In Calculation

$$\frac{\text{Tan } x_1}{x_1} = \frac{D_{1c}}{D_{1c} - D_{1R}\left(R/\sqrt{\gamma R} + 1\right)}$$

$$\frac{\text{Tan } x_2}{x_2} = \frac{D_{2c}}{D_{2c} - D_{2R}\,(R/L_R + 1)}$$

Solving we find

$$x_1 = 2.575$$

$$x_2 = 2.05.$$

Again anticipating that the system is subcritical we solve the denominator of an equation identical with that used previously. It is found negative so the system is sub-critical.

VIII - 4 BIBLIOGRAPHY

1. Agron, Paul - Personal communication July 7, 1952

1a. Broodley, P. R. and Buckley, F. D. - POWER (June and August 1951)

2. Bruce, F. R. - TID-73

3. Cesler, W. L. - Electrical World 138, No. 6 - 107 (1952)

4. Colburn, A. - Ind. Eng. Chem. 33 , 910 (1931)

5. Detroit Edison Co. and Dow Chemical Co. report to A.E.C. upon feasibility of power from a nuclear reactor (1952)

6. Dow and Jakob - Chemical Engineering Progress 47, No. 12 - 637 (1951)

7. Eister, W. K. - ORNL-663, ORNL-721, ORNL-763

8. Forsythe, W. L., et al - Ind. Eng. Chem. 41 No. 6 - 1200 (1949)

9. Gamson, B. W. - Chemical Engineering Progress 47, No. 1 - 19 (1951)

10. Glasstone and Edlund - ORNL CF-51-9-127 Part III

11. Glasstone and Edlund - ORNL CF-51-9-128 Part IV

12. Goring, Curran, Tarbox and Garin - Ind. Eng. Chem. 44 - 1051-1057 (1952)

13. Gresky, A. T. - ORNL CF-51-11-65

14. Gulbranson and Andrew - Ind. Eng. Chem. 44 - 1048 (1952)

15. Haines and Way - ORNL-86

16. Hodgman, C. D. - Handbook of Chemistry and Physics

17. Holmes, D. K. - ANP-58, Lectures to the Oak Ridge School of Reactor Technology on February 25, 1952 and February 28, 1952

18. Hughes and Eggler - CP-3093

19. Kent, W. - Mechanical Engineers' Handbook (1945) p. 3-32

20. Lapple, C. E. - Fluid and Particle Mechanisms - University of Delaware (1951)

21. Leuze, R. - Personal communication June 19, 1952

22. Leva and Grumman, Chemical Engineering Progress 48, No. 6 - 307 (1952)

23. Leva, M. et al - Bulletin 504, Bureau of Mines (1951)

24. Malm, J. G. - ANL-4411

25. Malmstrom and Miller - NAA-SR-151

25a. Malmstrom, Keen and Green - NAA-SR-79

26. McAdams, W. H. - Heat Transmission (1942 p. 230

27. McDaniel, B. D. - LA-190

28. McPherson, R. G. - M-3448

29. Mickley and Trilling - Ind. Eng. Chem. 41 No. 6 - 1135 (1949)

30. Miller and Logwinuk - Ind. Eng. Chem. 43 No. 5 -1220 (1951)

31. Morse, R. D. - Ind. Eng. Chem. 41, No. 6 -1117 (1949

32. Myer, W. - LA-994

33. Ott, H. C. - CL-RWS-31

34. Power Magazine, Steam Turbines, December 1945

35. Roe, F. C. - Blast Furnace and Steel Plant Design, April 1952

36. Schuman, R. P. - KAPL-634

37. Segaser - ORNL CF-52-2-12

38. Siegel, S. - TID-72

39. Sinclair Research Laboratories - unpublishes data

40. Smith and Young - NAA-SR-72

41. Spiers, H. M. - Technical Data on Fuel, The British National Committee World Power Conference, 1952 p. 252.

42. Steele, G. N. - NAA-SR-36

43. Stokes, C. A. - Chemical Engineering Progress 46, No. 8 - 423 (1950)

44. Stokes, R. L. - Ind. Eng. Chem. 41, No. 6 - 1196 (1949)

45. Stoughton, R. W. - Lecture to the Oak Ridge School of Reactor Technology December 28, 1951

46. Sykes, P. J. - Notes on Simplified Two-group Method

47. Thompson, A. S. - Engineering Lectures Notes from the Oak Ridge School of Reactor Technology (1952)

48. Tucker and Brooks - TID-66

49. Tunnicliffe, P. R. - CRPG-458

50. Visner, S. - ORNL- CF-51-10-110

51. Wattenberg and Hoyt - ANL-4397

52. Wilhelm and Kwauk - Chemical Engineering Progress 44, No. 3 - 201 (1948)

53. Wood, S. A. Proc. of Inst. of Mech. Eng. (London) 142, 149-164 (1939)

54. Putnam, Palmer, "Energy in the Future." A series of three lectures given at Oak Ridge, Tennessee, August 14, 15 and 16, 1951. (To be published)

55. Menke, J. R., "Nuclear Fission as a Source of Power," MDDC-1104, June 30, 1947.

☆ U. S. GOVERNMENT PRINTING OFFICE : 1957 O - 428072